Universidade do Minho
Escola de Engenharia

Andreia Filipa Ferreira Salvador

Functional analysis of syntrophic LCFA-degrading microbial ecosystems

outubro de 2013

Andreia Filipa Ferreira Salvador **Functional analysis of syntrophic LCFA-degrading microbial ecosystems**
UMinho | 2013


FCT Fundação para a Ciência e a Tecnologia
MINISTÉRIO DA CIÊNCIA, TECNOLOGIA E ENSINO SUPERIOR
Portugal
COMPETE
POPH
PROGRAMA OPERACIONAL FACTORES DE COMPETITIVIDADE
PROGRAMA OPERACIONAL POTENCIAL HUMANO
QREN
QUADRO DE REFERÊNCIA ESTRATÉGICO NACIONAL
PORTUGAL 2007.2013
UNIÃO EUROPEIA
Fundo Social Europeu

Universidade do Minho
Escola de Engenharia

Andreia Filipa Ferreira Salvador

Functional analysis of syntrophic LCFA-degrading microbial ecosystems

Tese de Doutoramento em Engenharia Química e Biológica

Trabalho realizado sob a orientação da
Doutora Diana Zita Machado de Sousa
e da
Doutora Maria Madalena dos Santos Alves

outubro de 2013

Autor Andreia Filipa Ferreira Salvador

email asalvador@deb.uminho.pt

Título da tese

Functional analysis of syntrophic LCFA-degrading microbial ecosystems

Orientadores

Doutora Diana Zita Machado de Sousa

Doutora Maria Madalena dos Santos Alves

Ano de conclusão 2013

Doutoramento em Engenharia Química e Biológica

Universidade do Minho, 1 de outubro de 2013

_____

AGRADECIMENTOS

São muitos aqueles a quem devo um profundo agradecimento por me terem acompanhado e apoiado durante este percurso quer profissionalmente como pessoalmente.

Agradeço em primeiro lugar às minhas orientadoras Diana Sousa e Madalena Alves. O optimismo, a força e o rigor com que agarram a investigação são inspiradores. Foi um privilégio ter desenvolvido este projecto convosco.

Também merecem um agradecimento especial o Théodore Bouchez e a Ariane Bize do Irstea (França) que se envolveram neste tema e colaboraram sempre com dedicação e entusiasmo.

A todos os co-autores deste trabalho um muito obrigado, nomeadamente à Ana Julia Cavaleiro, à Ana Guedes, à Sónia Barbosa, à Juliana Ramos, à Alcina Pereira, ao Alfons Stams, ao Théodore Bouchez, à Ariane Bize, à Madalena Alves e à Diana Sousa pelo trabalho, dedicação e discussões que promoveram.

Também gostaria de agradecer a todos aqueles que se foram cruzando comigo no laboratório e nos corredores no Departamento de Engenharia Biológica, em especial aos meus colegas do BRIDGE, e também do Irstea. Um especial agradecimento à Madalena Vieira, à Tânia Ferreira, à Chrystelle Bureau, à Celine Madigou e à Laëtitia Cardona por toda a ajuda técnica. Aos meus colegas de doutoramento com quem partilhei o gabinete e com os quais se geraram conversas muito interessantes num espírito de entreajuda e partilha de conhecimentos.

Um agradecimento muito especial às colegas e grandes amigas do “Clube secreto das amigas cientistas”. Sem vocês, não teria sido tão agradável!

Ao Bruno por toda a atenção, carinho, companheirismo e interesse no meu trabalho e pelo grande apoio nas alturas mais difíceis.

E por último um grande agradecimento à minha família, em especial à minha mãe pelo amor e apoio incondicionais.

Sem vocês esta tese não existiria. Muito obrigada!

The work presented in this thesis was financially supported by a research grant (SFRH/BD/48960/2008) from the Portuguese Foundation for Science and Technology (FCT) and European Social Fund (POPHQREN), and by the project FCOMP-01-0124-FEDER-014784, financed by the FEDER funds through the Operational Competitiveness Programme (COMPETE) and by national funds through the Portuguese Foundation for Science and Technology (FCT).

ABSTRACT

Anaerobic degradation of long-chain fatty acids (LCFA), is not yet completely understood. Previous studies suggest that different microorganisms might be involved in the degradation of saturated and unsaturated LCFA and that these compounds inhibit severely the microbial activity, especially the methanogenic activity. In this study, the toxic effect of saturated- (palmitate (C16:0) and stearate (C18:0)) and unsaturated-LCFA (oleate (C18:1)), towards pure cultures of hydrogenotrophic methanogens was evaluated by measuring cells viability and methanogenic activity of *Methanospirillum hungatei* and *Methanobacterium formicicum*. The presence of hydrogenotrophic (*M. formicicum* and *M. hungatei*) and acetoclastic (*Methanosaeta concilii* and *Methanosarcina. mazei*) methanogens in oleate and palmitate enrichment cultures was detected by PCR-DGGE fingerprinting techniques. Acetoclastic methanogens and *M. formicicum* grew in oleate and palmitate enrichment cultures but *M. hungatei* only grew in the palmitate's enrichment. *M. hungatei* was more sensitive than *M. formicicum* particularly to unsaturated LCFA. The later was also the most abundant hydrogenotroph detected during the continuous treatment of a synthetic wastewater composed mainly by oleate, as determined by PCR-DGGE. In the same study*, M. concilii* was identified as the most representative acetoclast. In order to investigate differences between the proteins expressed during the degradation of saturated and unsaturated LCFA, a metaproteomics experiment was designed, in which an anaerobic sludge was incubated with palmitate, stearate and oleate. The same COGs functional categories were identified in the different conditions. The majority of the proteins were assigned to functional categories, energy production and conversion, posttranslational modification and lipid metabolism. Most of the proteins identified belong to *Methanosaeta concilli*, *Syntrophobacter fumaroxidans*, *Pelobacter propionicus* and *Pelotomaculum thermopropionicum*. *Methanosaeta concilii* was indeed the most abundant archaea detected by pyrosequencing analysis of the 16S rRNA gene, but the other microorganisms were not even detected by pyrosequencing. Studying metaproteomes of complex microbial communities is still a big challenge especially because most of their genomes are not sequenced which difficult proteins identification. Likewise, when analyzing the proteome of the co-culture, *Syntrophomonas zehnderi* and *M. formicicum*, specialized on the degradation of LCFA, *M. formicicum*'s proteome could be much better characterized compared to *S. zehnderi*'s, since the genome of a very close related strain of the former is available in public databases and the genome of *S. zehnderi* is not. *S. zehnderi* was a dominant microorganism in oleate degrading enrichment cultures under methanogenic and non-methanogenic conditions, stablishing close relationships with hydrogenotrophic methanogens and homoacetogenic bacteria, respectively.

RESUMO

Os ácidos gordos de cadeia longa (AGCL) podem ser convertidos a metano por digestão anaeróbia. Contudo, aspectos relacionados com a microbiologia desta conversão ainda não estão completamente compreendidos. Estudos anteriores sugerem que diferentes microrganismos possam estar envolvidos na degradação de AGCL saturados e insaturados e ainda que os AGCL inibem a actividade microbiológica e de forma mais severa a actividade metanogénica. Neste trabalho foi avaliado o efeito toxico dos ACGL saturados (palmitato (C16:0) e estearato (C18:0)) e insaturados (oleato (C18:1)) sobre culturas puras de *Methanobacterium formicicum* e *Methanospirillum hungatei* monitorizando a sua viabilidade celular e actividade metanogénica. A presença destes organismos hidrogenotróficos bem como de dois organismos acetoclásticos, *Methanosaeta concilii* e *Methanosarcina mazei*, em culturas mistas enriquecidas em degradadores de palmitato e de oleato, foi determinada por PCR-DGGE. Todos permaneceram nos dois enriquecimentos com excepção do *M. hungatei* que não foi capaz de crescer no enriquecimento com oleato. Este microrganismo mostrou ser mais sensível do que o *M. formicicum* aos AGCL insaturados, segundo os resultados de viabilidade celular e actividade metanogénica. Em reactores anaeróbios alimentados com um efluente sintético, composto maioritariamente por ácido oleico, *M. formicicum* e *M. concilii* foram identificados como os metanogénicos predominantes. Foi efectuado um estudo de metaproteómica com o objectivo de detectar diferenças na expressão de proteínas por parte de uma cultura mista a crescer em AGCL saturados e insaturados. A maioria das proteínas identificadas nos vários ensaios estava relacionada com processos metabólicos de produção de energia, incluindo o metabolismo dos lípidos, e modificação pós-traducional. A maioria das proteínas identificadas corresponde a proteínas dos seguintes microrganismos: *Methanosaeta concilli*, *Syntrophobacter fumaroxidans*, *Pelobacter propionicus* e *Pelotomaculum thermopropionicum*. Estas amostras foram paralelamente classificadas taxonomicamente com base nos resultados de pirosequenciação do gene que codifica para a subunidade 16S do rRNA. Segundo esta análise a *Methanosaeta concilii* foi identificada como o organismo metanogénico mais dominante, contudo, não foram detectadas sequências correspondentes a *S. fumaroxidans*, *P. propionicus* ou *P. thermopropionicum*. A falta de informação genética/proteica sobre os microrganismos envolvidos na degradação de AGCL dificulta a identificação de proteínas que poderão ser relevantes neste processo. Analisou-se também a expressão proteica de dois organismos sintróficos, *Syntrophomonas zehnderi* and *M. formicicum*, que convertem os AGCL a metano. Neste caso particular foi possível obter uma melhor caracterização do proteoma de *M. formicicum* do que de *S. zehnderi*, consequência do facto de apenas o genoma de uma estirpe próxima do primeiro se encontrar sequenciado. A *S. zehnderi* foi identificada como uma bactéria dominante em culturas especializadas na degradação de oleato quer em condições metanogénicas, estabelecendo relações de sintrofia com microorganismos metanogénicos hidrogenotróficos, quer em condições não metanogénicas onde a interacção como organismos homoacetogénicos terá sido favorecida.

TABLE OF CONTENTS

LIST OF FIGURES

LIST OF TABLES

LIST OF SYMBOLS AND ABBREVIATIONS

ARISA	automated ribosomal intergenic spacer analysis
ARDRA	amplified ribosomal DNA-restriction analyse
ATP	adenosine triphosphate
BLAST	Basic Local Alignment Search Tool
bp	base pair
BrES	2-bromoethanesulfonate
CH_4	methane
CO_2	carbon dioxide
CoA	coenzyme A
COD	chemical oxygen demand
COGs	clusters of orthologous groups
DGGE	denaturing gradient gel electrophoresis
DNA	desoxyribonucleic acid
DSMZ	German Collection of Microorganisms and Cell Cultures
EDTA	ethylene-diamine-tetraacetic acid
EGSB	expanded granular sludge bed
ENA	European Nucleotide Archive
FAD/$FADH_2$	oxidized/reduced forms of flavin adenine dinucleotide
FISH	fluorescence in situ hybridization
GC	gas chromatography
H_2	hydrogen
H_2O	water
HPLC	high-performance liquid chromatography
KEEG	Kyoto Encyclopedia of Genes and Genomes
LCFA	long chain fatty acid
LC-MS	liquid chromatography–mass spectrometry
LPS	lipopolysaccharides
NAD^+/NADH	oxidized/reduced forms of nicotinamide adenine dinucleotide

N_2	nitrogen
NCBI	National Center for Biotechnology Information
OL	oleic acid
OLR	organic loading rate
OTU	operational taxonomic unit
PA	palmitic acid
PCR	polymerase chain reaction
RDP	ribossomal database project
RFLP	estriction fragment length polymorphism
RNA	ribonucleic acid
mRNA	messenger ribonucleic acid
rRNA	ribossomal ribonucleic acid
rpm	revolutions per minute
SDS-PAGE	sodium dodecyl sulfate polyacrylamide gel electrophoresis
SMA	specific methanogenic activity
ST	stearic acid
TCD	thermal conductivity detector
TCA	cycle tricarboxylic acid cycle
UNIPROT	Universal Protein Resource
VFA	volatile fatty acids
Vol, v	volume
Wt	weigth
WTA	wall teichoic acids
$\Delta G0'$	standard free energy change

Chapter 1

Context, Aim and Thesis Outline

1.1 Context and motivation

Lipids are organic molecules which are present in various types of wastewater such as dairy wastewater (Alves et al., 2009; Sousa et al., 2007b). Those effluents can be treated by anaerobic digestion coupling wastewater treatment to the production of renewable energy, in the form of biogas. However, anaerobic treatment of lipid-rich wastewater is associated with technical operational problems such as biomass flotation and washout (Alves et al., 2001). Furthermore, compounds generated during anaerobic degradation of lipids namely, long-chain fatty acids (LCFA) cause microbial inhibition which compromises the efficiency of the treatment. Research has been done during the last years in order to develop new reactor configurations and to improve anaerobic digestion of lipid rich wastewater. Recently, a patent for a reactor specifically designed to overcome those technical problems was created (Alves et al., 2009).

LCFA with increasing chain length and more double bonds exert the most adverse effect towards anaerobic microbial communities (Demeyer and Henderic, 1967; Prins et al., 1972). Not all microorganisms show the same sensitivity to these organic compounds. Gram negative bacteria might be less sensitive than gram-positive, and methanogenic archaea are usually reported as the most sensitive (Hwu and Lettinga, 1997; Kuang et al., 2006; Roy et al., 1985). Nevertheless, microbial communities can adapt to LCFA and convert it to methane (Alves et al., 2009; Cavaleiro et al., 2009; Pereira et al., 2004). The way microbes adapt to LCFA loads in continuous or batch reactors, the identification of the most abundant microorganisms in the communities as well as the ones directly related to LCFA

consumption are some of the microbiology questions that scientists are trying to answer. Indeed, there are some studies characterizing anaerobic communities degrading LCFA (Baserba et al., 2012; Grabowski et al., 2005; Hatamoto et al., 2007b; Hatamoto et al., 2007c; Menes et al., 2001; Palatsi et al., 2010; Pereira et al., 2002b; Shigematsu et al., 2006; Sousa et al., 2007a; Sousa et al., 2007b). These studies resulted in interesting findings, namely the identification of main players in anaerobic LCFA degradation, but also the differences in microbial community composition of cultures exposed to saturated- or to unsaturated-LCFA (Sousa et al., 2007a; Sousa et al., 2007b). In anaerobic reactors microbial communities are very diverse and, in these ecosystems, microbial predominance and activity do not go always together. Microbial activity and specificity for LCFA can be better studied using enrichment approaches. For example, *Syntrophomonadaceae* members are known as syntrophic fatty acid degraders (from enrichment studies and physiological properties of isolated bacteria), but in bioreactors they are always found in lower numbers probably because they are very slow growing microbes (Stams et al., 2012). Fatty acids are likely degraded via β-oxidation but the mechanism by which saturation of (unsaturated) fatty acids occurs is still not yet well understood (Sousa et al., 2009a). Another intriguing feature is that oleate does not seem to undergo directly β-oxidation. During oleate (C18:1) anaerobic degradation by complex microbial communities, palmitate (C16:0) accumulates outside of the cells forming macroscopic whitish matter; this accumulated substrate can be consumed after fairly extended incubation (Pereira et al., 2002a). The microbiology and biochemical mechanisms behind the anaerobic degradation LCFA, special the differential properties of saturated- and unsaturated-LCFA degradation, need to be further

investigated in order to provide a complete picture of LCFA conversion in anaerobic environments.

1.2 Aim

The aim of this research is to get more insights in the microbial communities that are actively degrading LCFA anaerobically. Experiments were designed aiming the identification of important players involved in LCFA degradation in complex microbial communities and the investigation of metabolic differences between the degradation of saturated- and unsaturated-LCFA. For this propose, a combination of cultivation based methodologies and molecular biology approaches based on 16S rRNA gene analysis, as well as comparative metaproteomics was used.

1.3 Thesis outline

In this chapter the contextualization and motivation for the development of further research on anaerobic LCFA degradation is presented. An overview of the current knowledge on anaerobic microbial communities degrading LCFA and of the methodologies utilized for studying those communities is given in **Chapter 2**. The next two chapters focus on the identification of methanogenic archaea that are able to tolerate and maintain methanogenic activity in a bioreactor continuously loaded with LCFA-rich wastewater (**Chapter 3**), or in batch LCFA-degrading enrichment cultures (**Chapter 4**). In chapter 4, the effect of LCFA on the methanogenic activity and cell viability of pure cultures of hydrogenotrophic methanogens was also investigated. In **Chapter 5**, an anaerobic complex microbial community was enriched in specialized LCFA degrading microorganisms. These consortia were

characterized physiologically and some predominant microorganisms could be detected and identified by using molecular biology methods. Finally, two different proteomic studies are presented in chapters 6 and 7. In **Chapter 6** a comparative characterization of the proteome of a complex microbial community during the degradation of three different LCFA (palmitate, stearate and oleate) is presented. In **Chapter 7** the proteome of a co-culture of two syntrophic microorganisms, *Syntrophomonas zehnderi* and *Methanobacterium formicicum*, which are able convert stearate and oleate to methane was also investigated.

Chapter 2

General introduction to syntrophic LCFA-degrading ecosystems

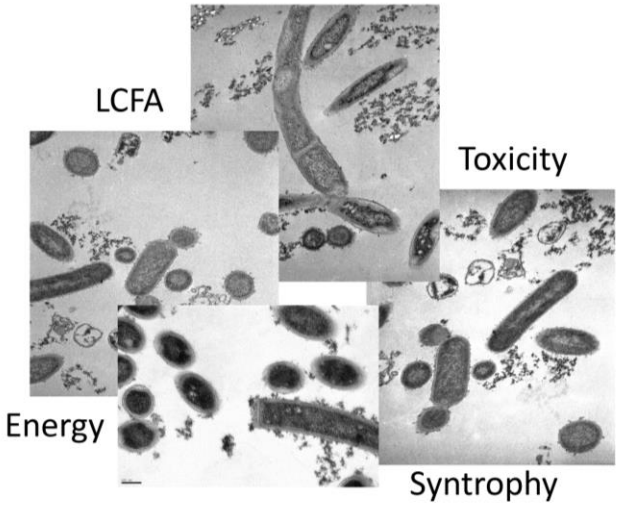

Long-chain fatty acids (LCFA) can be degraded anaerobically by means of syntrophic associations between bacteria and hydrogen consuming microorganisms.

Under methanogenic conditions, i.e., in the absence of external electron acceptors others than CO_2, such as oxygen, nitrate or sulfate, hydrogenotrophic methanogens are the syntrophic partners, who keep the hydrogen partial pressure low enough to allow LCFA conversion to methane. The energy conserved in methane molecules can be utilized afterwards.

In this chapter, an overview of the current knowledge about anaerobic LCFA conversion is presented, with emphasis on the microbial communities involved.

Molecular biology tools and especially recent “omics” technologies opened new perspectives for the study of such complex microbial communities and some relevant examples will be given.

2.1 A brief introduction to long-chain fatty acids

Long-chain fatty acids are carboxylic acids with chain lengths longer than 12 carbon atoms that are obtained from lipids hydrolysis. LCFA can be found in the protonated form but at neutral pH they appear in the ionized form. They are composed by a hydrophobic hydrocarbon chain and by a hydrophilic carboxylate group which confer an amphiphilic character and partial water solubility. LCFA can be classified as saturated if they have no double bonds and unsaturated if one (monounsaturated) or more double bonds (polyunsaturated) are present in the hydrocarbon chain. Saturated- and unsaturated-LCFA present different molecule conformations caused by the presence of double bonds. Saturated-LCFA molecules are straight while unsaturated-LCFA molecules show a bend conformation. Most natural occurring LCFA have even number of carbons (Table 2.1).

Table 2.1 Carbon chain length and degree of saturation of most natural occurring LCFA.

Common name	Systematic name	Number of carbons	Number of double bonds	Position of double bonds
Miristic acid	Tetradecanoic	14	0	-
Palmitic acid	Hexadecanoic	16	0	-
Palmitoleic acid	cis-9-hexadecanoic	16	1	C9
Stearic acid	Octadecanoic	18	0	-
Oleic acid	cis-9-octadecanoic	18	1	C9
Linoleic acid	cis-9,12- octadecadienoic	18	2	C9; C12

LCFA are widespread in nature being found in animals, plants and microorganisms (Rustan and Drevon, 2005). LCFA can be found in wastewater, i.e. dairy wastewater, where palmitate (C16:0) and oleate (C18:1) are abundant (Alves et al., 2009; Sousa et al., 2007b).

2.2 Anaerobic LCFA conversion to methane: biochemical and thermodynamic considerations

It is assumed that anaerobic degradation of LCFA occurs via classical β-oxidation (Weng and Jeris, 1976). Enzymology of LCFA β-oxidation is well reported in *Escherichia coli* (Black and DiRusso, 2003; DiRusso et al., 1999; DiRusso and Nystrom, 1998). Studies on the regulation of fatty acid metabolism were conducted in different bacteria namely *E. coli*, *Bacillus subtilis* and *Streptococcus pneumonia* (Fujita et al., 2007). The main steps of fatty acids degradation via β-oxidation are exemplified in Figure 2.1. Briefly, transport of fatty acids into the cells is mediated by a membrane transport protein (FadL). An acyl-CoA synthetase (FACS, which is encoded by the *fadD* gene) activates long-chain fatty acid to long-chain fatty acyl-CoA. Details on the transport of exogenous LCFA are given by Black and DiRusso (2003). Activated LCFA can enter the β-oxidation cycle. Acyl-CoA dehydrogenase, enoyl-CoA hydratase, 3-hydroxyacyl-CoA dehydrogenase and 3-ketoacyl-CoA thiolase are the enzymes catalyzing the β-oxidation reactions, i.e., two dehydrogenations, one hydration and one thiolytic cleavage (Figure 2.1). Proteins homologous to those operating under aerobic conditions were identified in *E. coli* and associated to LCFA metabolism under anaerobic conditions when nitrate was the electron acceptor (Campbell et al., 2003). At the end of each β-oxidation cycle, the LCFA loses two carbon atoms forming one acetyl-CoA, and the remaining LCFA chain is submitted to another β-oxidation cycle. Acetyl-CoA produced at the end of each β-oxidation cycle can be converted to acetate by acetate kinase activity.

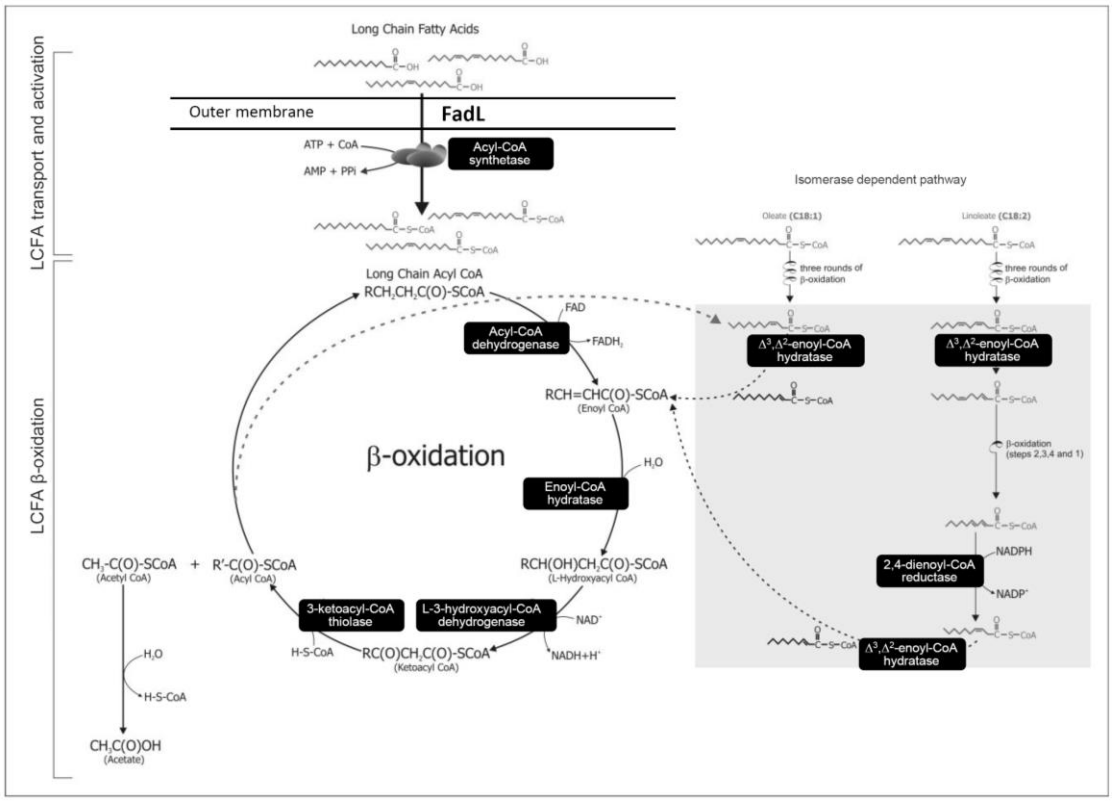

Figure 2.1 Activation and β-oxidation of even numbered LCFA in *E. coli*. The enzymes involved are indicated in the black boxes. Isomerase-dependent pathway for the degradation of unsaturated-LCFA is represented on the grey box (adapted from Sousa et al. (2009a)).

Unsaturated-LCFA degradation is suggested to occur via β-oxidation isomerase-dependent pathway even though a thioesterase-dependent pathway may occur to a smaller extent in *E. coli* (Ren et al., 2004). Other authors suggested a preliminary hydrogenation of unsaturated-LCFA prior β-oxidation (Novak and Carlson, 1970; Roy et al., 1986; Weng and Jeris, 1976). As a consequence of a preliminary hydrogenation of the unsaturated-LCFA oleate (C18:1), stearate (C18:0) should be formed. However, in anaerobic bioreactors palmitate (C16:0) is the fatty acid accumulating outside the cells when oleate (C18:1) is the sole substrate (Pereira et al., 2002a). This recurrent experimental observation suggests that the first steps of unsaturated LCFA degradation in methanogenic communities is still an open research question. Sousa et al. (2009b)

hypothesized that conversion of oleate to palmitate in anaerobic bioreactors might not be syntrophic. These authors observed that in bioreactors where methanogenesis was inhibited and no hydrogen scavengers were present, oleate was still converted to palmitate but palmitate was not further degraded. If this is a two-step process one can wonder whether in complex methanogenic anaerobic communities the same or different microorganisms are catalyzing those reactions (first the conversion of oleate to palmitate and secondly the complete β-oxidation of palmitate) (Sousa et al., 2009a).

Under methanogenic conditions, LCFA degradation occurs by a strict cooperation between LCFA-consuming syntrophic bacteria and hydrogenotrophic methanogens, who utilize the hydrogen formed by bacteria to produce methane. This relationship between syntrophic bacteria and methanogens is of utmost importance to achieve LCFA degradation anaerobically. Nor the bacteria nor the methanogen alone could degrade LCFA. In the absence of a hydrogen scavenger, hydrogen molecules tend to accumulate and, at high hydrogen partial pressure, LCFA conversion is not thermodynamically feasible (McInerney et al., 2008; Sieber et al., 2012; Sousa et al., 2009a). The reason behind is that high hydrogen concentrations inhibit hydrogenase activity (Garcia et al., 2000). When hydrogen partial pressure is maintained high (>10 Pa) hydrogen can no longer be produced from NADH (Schink, 1997; Sieber et al., 2012; Stams and Plugge, 2009). Gibbs free energy changes for LCFA degradation reactions decrease significantly when hydrogen partial pressure is kept low as it is shown in Table 2.2.

Table 2.2 Anaerobic conversion reactions to methane of some LCFA with different carbon atoms and different number of double bonds (adapted from Sousa et al. (2007b).

LCFA	Equation	$\Delta G^{0'}$ (kJ reaction^{-1})[a]	$\Delta G^{0'}$ (kJ reaction^{-1})[b]
Palmitate	$C_{16}H_{31}O_2^- + 14H_2O \rightarrow 8C_2H_3O_2^- + 14H_2 + 8H^+$	+419	−81
Oleate	$C_{18}H_{33}O_2^- + 16H_2O \rightarrow 9C_2H_3O_2^- + 15H_2 + 7H^+$	+391	−131
Methanogenic substrate	**Equation**	$\Delta G^{0'}$ (kJ reaction^{-1})[a]	$\Delta G^{0'}$ (kJ reaction^{-1})[b]
Acetate	$C_2H_3O_2^- + H_2O \rightarrow HCO_3^- + CH_4$	−31	−19
Hydrogen and CO_2	$4H_2 + HCO_3^- + H^+ \rightarrow CH_4 + 3H_2O$	−136	−20

[a] Gibbs free energies (at 25°C) calculated under standard conditions (solute concentrations of 1 M and gas partial pressure of 105 Pa).

[b] Gibbs free energies (at 25°C) for LCFA concentration of 1 mM, acetate concentration of 10 mM, and H_2 partial pressure of 1 Pa.

The little energy obtained by LCFA conversion to methane (the majority of energy is stored in methane molecules produced) is available for cell maintenance, growth and cell division and has to be divided between the microorganisms involved in the syntrophic relationship (McInerney et al., 2008; Schink, 1997; Sieber et al., 2012).

To achieve complete conversion of LCFA to methane, bacterial and both aceticlastic and hydrogenotrophic activities should be guaranteed. Note that 9 moles of methane are produced from 1 mole of oleate via aceticlastic pathway (~70% of total theoretical methane produced) and 3.75 moles of methane are produced via hydrogenotrophic pathway. Nevertheless, from the thermodynamic viewpoint only the absence of hydrogen consuming microorganism hinders LCFA oxidation by syntrophic bacteria.

Instead of hydrogen, formate can be formed and exchanged between syntrophic bacteria and formate consuming methanogens (Sieber et al., 2012; Stams and Plugge, 2009) but formate was never quantified during anaerobic LCFA conversion (Sousa et al., 2009a).

2.3 Methanogenic communities degrading LCFA: Diversity and toxicity considerations

Valorization of LCFA-rich wastewater can be accomplished by the conversion of LCFA to methane gas. Despite the high energetic potential of LCFA, some problems are associated to the treatment of wastewater with high LCFA content. These problems are related with operational problems (LCFA adsorb onto the biomass causing its flotation and consequent washout from the bioreactors, hampering the anaerobic treatment) and with microbial activity inhibition. Suspended sludge is considered more susceptible to LCFA inhibition than granular sludge (Hwu et al., 1996) and methanogenic archaea more sensitive than bacteria (Hwu and Lettinga, 1997; Kuang et al., 2006). The most sensitive methanogens to oleate (C18:1 LCFA) reported in the literature belong to *Methanosarcinaceae* family (Kuang et al., 2006).

It is accepted that LCFA interfere with microbial activity primarily by interacting with the plasma membrane (Hook et al., 2010; Koster and Cramer, 1987; Soliva et al., 2004). It may affect energy production mechanisms (i.e. oxidative phosphorylation and electron transport chain), avoid nutrients uptake and inhibit enzymatic activity or even cause cell lysis (Desbois and Smith, 2010). However, behavior of different groups of microorganisms in the presence of LCFA is not the same. For instance, Gram-positive bacteria are more sensitive than Gram-negative bacteria and this difference might be related with the different structure of cell membranes which is also responsible for the different response to Gram staining. The major difference between Gram-positive and Gram-negative bacteria is that the later contain an outer membrane (Figure 2.2). The outer membrane of Gram-negative bacteria is composed of phospholipids, in the inner part of the outer membrane, glycolipids in the outer part of the outer membrane and several lipoproteins. The protective function of the outer membrane is related with the presence of

lipopolysaccharides. Lipopolysaccharides (LPS) are the major components of the outer membrane and represent an important barrier for hydrophobic molecules. No correlation was found between the lower susceptibility of Gram-negative bacteria to LCFA inhibition and their ability to metabolize these molecules. Instead, tolerance to LCFA appears to be linked to the presence of LPS, since cells lacking part of their LPS are inhibited by LCFA whereas cells with intact LPS are not (Sheu and Freese, 1973). Large hydrophilic molecules entrance inside gram-negative cells is also limited by the presence of outer membrane porins. Likewise, Gram-positive bacteria are more susceptible to the effect of antibiotics than gram-negative bacteria. Nevertheless, Gram-positive bacteria contain structures in their envelope which can protect the cells against LCFA inhibition. The wall teichoic acids (WTA) are cell surface glycopolymers only found in gram-positive bacteria envelopes which confer them antimicrobial LCFA resistance (Swoboda et al., 2010) (Kohler et al., 2009). The loss of WTA in mutants of *Staphylococcus aureus*, a gram-positive bacterium, causes an increase of the cell surface hydrophobicity which allows LCFA to penetrate easily the cell wall and bind to the plasma membrane (Kohler et al., 2009).

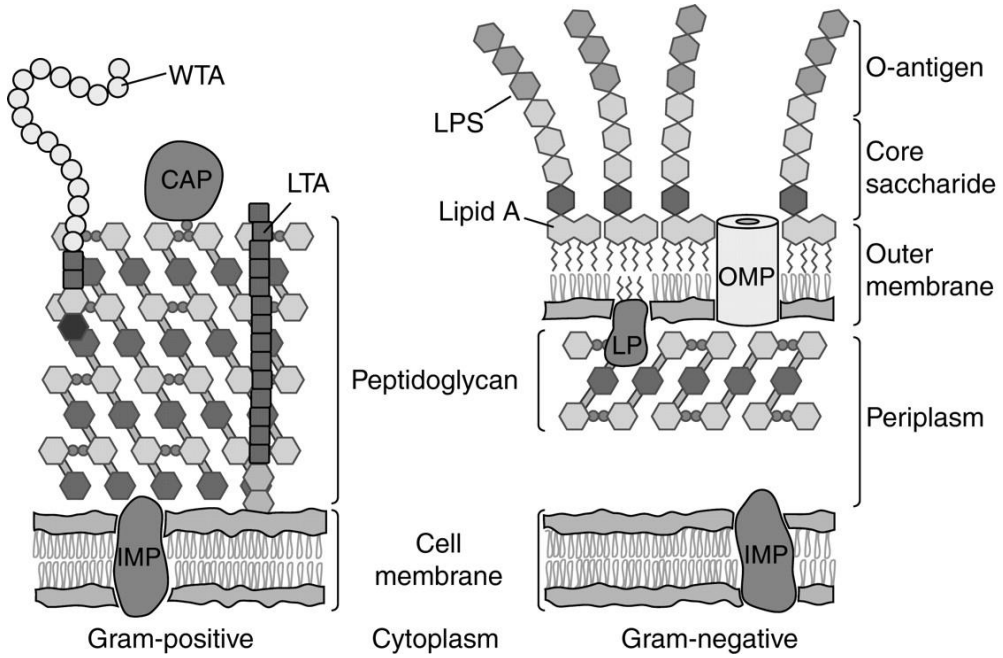

Figure 2.2 Differences between gram-positive and gram-negative cell envelopes. CAP: covalently attached protein; IMP: integral membrane protein; LP: lipoprotein; LPS: lipopolysaccharide; LTA: lipoteichoic acid; OMP: outer membrane protein; WTA: wall teichoic acid (in Silhavy et al. (2010)).

Most known syntrophic LCFA degraders exhibit a negative response to Gram staining (Table 2.3). The majority of the syntrophic-LCFA oxidizers belong to genus *Syntrophomonas*. Some *Syntrophomonas* species show a variable response to gram-staining and others stain gram-negative (Table 2.3). Cell wall ultrastructure of *Syntrophomonas* species is complex and indicative of the presence of an outer membrane but unlike gram-negative bacteria *Syntrophomonas* cells do not contain lipopolysaccharides (Sieber et al., 2010; Wu et al., 2006a). Furthermore, the genome of *Syntrophomonas wolfei* does not include genes necessary for LPS biosynthesis (Sieber et al., 2010). Other strategies might be behind the tolerance of certain bacteria to LCFA. It is known that humans produce LCFA for protection against pathogenic bacteria. Some of those bacteria developed strategies for dealing with the antimicrobial activity of LCFA such as the use of efflux pumps to expel LCFA out of the cells. Those efflux systems are well reported for *Escherichia coli*, *Neisseria gonorrhoeae* and *Pseudomonas aeruginosa*

(Long et al., 2008; Martinez et al., 2013; Schielke et al., 2010). Another example is that of the gram-positive bacterium, *Staphylococcus aureus*, which responds to free LCFA by increasing the expression of genes related to membrane stabilization, peptidoglycan synthesis and by reducing the hydrophobicity of cell surface (Kenny et al., 2009).

Table 2.3 Substrate specificity and response to gram-staining of syntrophic LCFA-degrading bacteria.

LCFA degrading bacteria	Gram staining	Fatty acids	Reference
Syntrophomonas zehnderi	variable	C4:0 – C18:0; C16:1; C18:1; C18:2	Sousa et al. (2007c)
Syntrophomonas sapovorans	negative	C4:0 – C18:0; C18:1; C18:3	Roy et al. (1986)
Syntrophomonas palmitatica	negative	C4:0 – C18:0	Hatamoto et al. (2007a)
Syntrophomonas wolfei subsp. *saponavida*	negative	C4:0 – C18:0	Lorowitz et al. (1989)
Syntrophomonas curvata	variable [a]	C4:0 – C18:0; C18:1	Zhang et al. (2004)
Thermosyntropha lipolytica	negative [b]	C4:0 – C18:0; C18:1; C18:2; Triacylglycerides; olive oil	Svetlitshnyi et al. (1996)
Thermosyntropha tengcongensis	negative [b]	C4:0 – C18:0; C18:1	Zhang et al. (2012)
Syntrophus aciditrophicus	negative	C4:0 – C8 (some unsaturated); C16:0 – C18:0; Benzoate	Jackson et al. (1999)

[a] Cells present a gram-negative cell wall ultrastructure.

[b] Cells stained gram-negative but present a gram-positive ultrastructure.

Methanogens are another group of microorganisms reported as very susceptible to LCFA inhibitory effect (Angelidaki and Ahring, 1995; Demeyer and Henderic, 1967; Hanaki et al., 1981; Koster and Cramer, 1987; Lalman and Bagley, 2001; Lalman and Bagley, 2000). However, methanogenic activity can be high in anaerobic bioreactors treating LCFA containing wastewaters. In fact, methanogenic activity as well as the numbers of methanogenic archaea (determined by quantification of archaea sequences by real-time PCR) increased in samples, previously loaded with LCFA during continuous bioreactors operation, that were incubated in batch to promote the degradation of the accumulated LCFA (Pereira et al., 2004; Sousa et al., 2007a). Pereira et al. (2005) attributed the transient decrease of methanogenic activities to transport limitations of products and

substrates caused by the adsorption of LCFA onto microbial cells, rather than to a bactericidal or an irreversible toxicity. Adsorption of LCFA onto the sludge is necessary to allow LCFA degradation by bacteria (Hwu et al., 1998). Furthermore, high rate continuous treatment of LCFA-rich wastewater can be feasible if the microbial community is adapted by sequencing cycles of LCFA feeding and degradation in which the contact between LCFA and biomass is promoted (Cavaleiro et al., 2009).

It is accepted that the mechanism of inhibition towards methanogens involves LCFA binding to the cell envelope hindering membrane functions (Hook et al., 2010; Soliva et al., 2004). Nevertheless, to our knowledge only one study explored the effect of LCFA on the membranes of pure cultures of methanogenic archaea (Zhou et al., 2013). Cell membrane permeability increased when the ruminal methanogen *Methanobrevibacter ruminantium* was exposed to medium- or to long-chain saturated fatty acids. According to Koster and Cramer (1987) the cell walls of methanogens resembles those of gram-positive bacteria, the most LCFA-sensitive group of bacteria. However, cell envelopes of methanogens are distinct from those of bacteria and differ among methanogenic groups, both chemically and structurally (Garcia et al., 2000). Some methanogens stain gram-negative, others gram-positive and some others show a variable response to gram-staining (Table 2.4). Besides, the composition and organization of methanogens cell envelope is not the same of gram-positive or gram-negative bacteria. Instead, cell membranes of methanogenic archaea contain C20 and/or C40 isopranyl glycerol ethers (Balch et al., 1979; Garcia et al., 2000) and the cell walls can consist of pseudomurein (found in orders *Methanobacteriales* and *Methanopyrales*), methanochondroitin (found in family *Methanosarcinaceae*), being proteinaceous (orders *Methanococcales, Methanomicrobiales* and also in *Methanosarcinales*) or even being covered by a sheath like members of *Methanospirillaceae* family (Garcia et al., 2000; Sprott et al., 1983; Whitman et al., 2006).

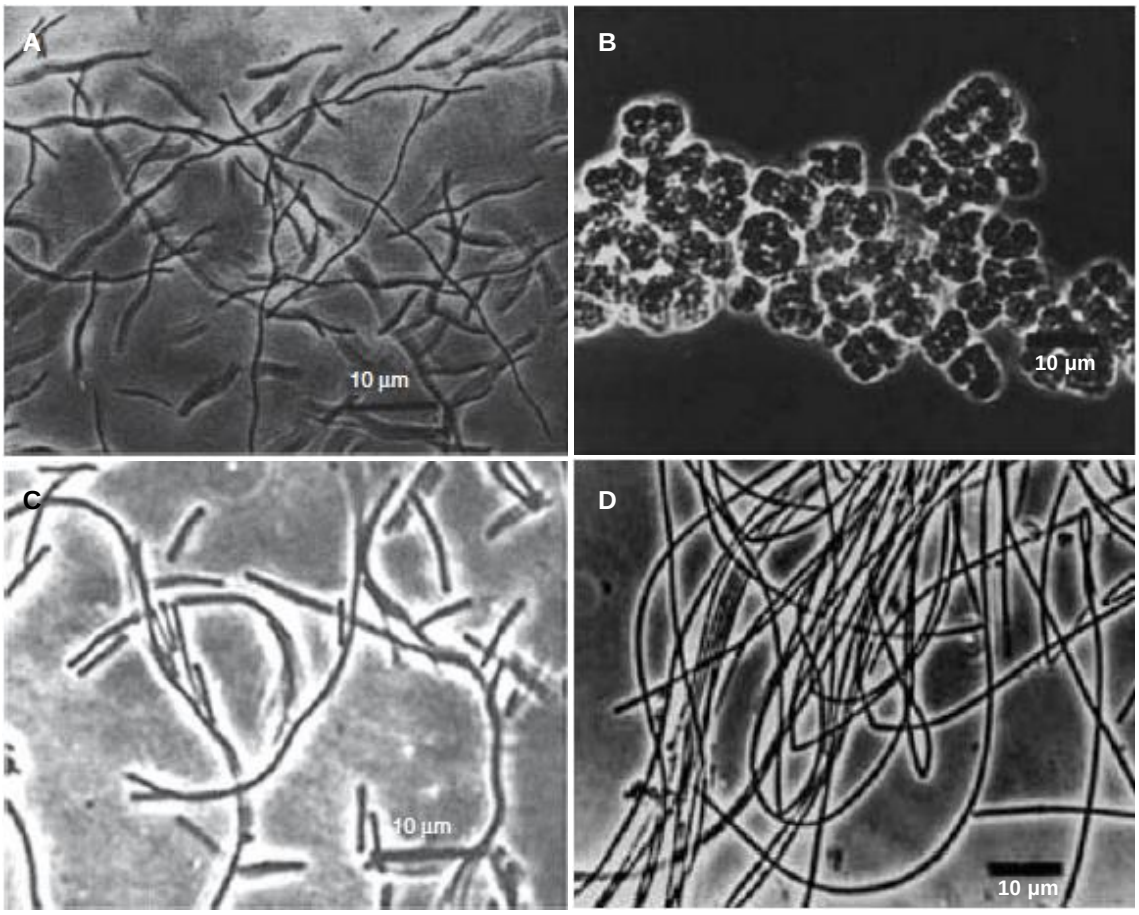

Figure 2.3 Phase contrast photomicrographs of the most common methanogenic archaea genera in anaerobic bioreactors treating LCFA-rich wastewater (*Methanobacterium*, *Methanospirillum*, *Methanosarcina* and *Methanosaeta*). (A) *Methanobacterium formicicum*; (B) *Methanosarcina barkeri*; (C) *Methanospirillum hungatei*; (D) *Methanosaeta concilii* (adapted from Whitman et al. (2006)).

Most common methanogens found in anaerobic bioreactors fed with LCFA belong to the genera *Methanosaeta*, *Methanosarcina*, *Methanospirillum* and *Methanobacterium* (Pereira et al., 2002b; Shigematsu et al., 2006; Sousa et al., 2007a). Despite the fact that this archaea are all methane producers, several differences between these genera can be addressed. Apart from the structural differences of the cell envelopes mentioned above, they also exhibit metabolic differences. Microorganisms from genera *Methanobacterium* and *Methanospirillum* are hydrogenotrophic methanogens able to utilize both hydrogen and formate for methane production (Table 2.4). Because they are hydrogen scavengers

they are often used as partners for the isolation of syntrophic fatty acid degrading bacteria (Hatamoto et al., 2007a; Roy et al., 1986; Sousa et al., 2007c; Wu et al., 2006a; Wu et al., 2007; Wu et al., 2006b; Zhang et al., 2004; Zhao et al., 1990). On the other hand, *Methanosarcina* and *Methanosaeta* share the ability to use acetate for growth and methane production and are called aceticlastic methanogens. Acetate is the only substrate utilized by *Methanosaeta* while *Methanosarcina* microorganisms are more versatile and can utilize methylated C1 compounds or even hydrogen (Table 2.4). The first step of methanogenesis from acetate (acetate activation to acetyl-CoA) is catalyzed by different enzymes in *Methanosaeta* (AMP-forming acetyl-CoA synthetase) and in *Methanosarcina* (acetate kinase plus phosphotransacetylase) (Smith and Ingram-Smith, 2007). Only these two genera utilize acetate for methane production (Smith and Ingram-Smith, 2007) but they usually do not co-exist in LCFA environments (Sousa et al., 2007a). Due to the higher affinity for acetate, *Methanosaeta* are more abundant when acetate concentration is low (Jetten et al., 1992; Smith and Ingram-Smith, 2007). The filamentous nature of *Methanosaeta* cultures made them important microorganisms for granules formation in anaerobic bioreactors (Baloch et al., 2008).

In continuous bioreactors fed with LCFA, *Methanosaeta* was identified as the most abundant acetoclastic methanogen whereas when the same sludge was incubated in batch, to degrade the accumulated substrate, *Methanosarcina* become dominant (Sousa et al., 2007a).

Table 2.4 Taxonomy, morphology and physiological characteristics of methanogenic archaea.

Order/Genus	Morphology	Gram stain	Temperature	Substrates	References
Methanobacteriales					
Methanobacterium	rod	+; –; v	m; t	H_2/CO_2 ; some: formate, isopropanol, isobutanol	Boone et al. (1993b)
Methanothermobacter	rod	+	t	H_2/CO_2	Smith et al. (1997)
Methanobrevibacter	short rod	+	m	H_2/CO_2 ; formate	Boone et al. (1993b)
Methanosphaera	cocci	+	m	H_2 plus methanol	Biavati et al. (1988); Fricke et al. (2006)
Methanothermus	rod	+	t	H_2/CO_2	Boone et al. (1993b)
Methanococcales					
Methanocaldococcus	cocci	–	t	H_2/CO_2 ; formate	Boone et al. (1993b)
Methanotorris	cocci	–	t	H_2/CO_2	Boone et al. (1993b)
Methanococcus	cocci	–	m; t	H_2/CO_2 ; formate	Boone et al. (1993b)
Methanothermococcus	cocci	–	t	H_2/CO_2 ; formate	Boone et al. (1993b)
Methanomicrobiales					
Methanocorpusculum	irregular cocci	–	m	H_2/CO_2 ; formate; some: isopropanol, isobutanol	Boone et al. (1993b)
Methanoculleus	irregular cocci	–	m; t	H_2/CO_2 ; formate; some: isopropanol, isobutanol	Boone et al. (1993b)
Methanofollis	irregular cocci	?	m	H_2/CO_2 ; formate	Boone et al. (1993b)
Methanogenium	irregular cocci	–	p; m; t	H_2/CO_2 ; formate; some: isopropanol, isobutanol, isopentanol, cyclopentanol, 1-propanol, ethanol	(Boone et al. (1993b); Frimmer and Widdel (1989); Romesser et al. (1979)
Methanolacinia	pleomorphic rods	–	m	H_2/CO_2 ; isopropanol; isobutanol, isopentanol, cyclopentanol	Boone et al. (1993b)
Methanomicrobium	rod	–	m	H_2/CO_2 ; formate	Boone et al. (1993b)
Methanoplanus	irregular disc/plate	–	m	H_2/CO_2 ; formate; some: isopropanol	Boone et al. (1993b); Brambilla et al. (2010)
Methanolinea	Rod-shaped with blunt-ends	–	m	H_2/CO_2 ; formate	Imachi et al. (2008)
Methanoregula	dimorphic: thin rods or irregular cocci	–	m	H_2/CO_2	Brauer et al. (2011)
Methanosphaerula	cocci		m	H_2/CO_2 ; formate	Cadillo-Quiroz et al. (2009)
Methanospirillum	spirillum	–	m	H_2/CO_2 ; formate; some: isopropanol, isobutanol	Boone et al. (1993b)
Methanocalculus	irregular cocci; some with flagella	–	m	H_2/CO_2 ; formate	Lai et al. (2002); Lai et al. (2004); Ollivier et al. (1998)

Table 2.4 (Continued)

Order/Genus	Morphology	Gram stain	Temperature	Substrates	References
Methanosarcinales					
Methanosaeta	rod, filaments	–	m; t	Acetate	Patel and Sprott (1990)
Methanimicrococcus	irregular cocci	?	m	methanol + H_2	Sprenger et al. (2000)
Methanococcoides	irregular cocci	–	m; p	trimethylamine	Singh et al. (2005)
Methanohalobium	flat polygons	?	m; t	Me	Boone et al. (1993b)
Methanohalophilus	irregular cocci	–	m	Me	Boone et al. (1993a)
Methanolobus	irregular cocci	–	m; p	Me; some: dimethylsulfide, methanethiol	Boone et al. (1993b); Zhang et al. (2008)
Methanomethylovorans	irregular cocci	–	m; t	methanol, methylamines; some: methanethiol, dimethyl sulfide	Jiang et al. (2005); Lomans et al. (1999)
Methanosalsum	irregular cocci	–	m; t (45°C)	Me; dimethylsulfide, methanethiol	Boone and Baker (2001); Boone et al. (1993b)
Methanosarcina	cocci; forming	+; –; v	p; m; t	Acetate; Me; some: H_2 + CO_2	Boone et al. (1993b); Maestrojuán and Boone (1991)
Methermicoccus	cocci	+	t	methanol, methylamine and trimethylamine	Cheng et al. (2007)
Methanopyrales					
Methanopyrus	rod	+	ht	H_2/CO_2	Kurr et al. (1991)

v = gram variable

p = psychrophilic; m = mesophilic; t = thermophilic; ht = hyperthermophilic

Me = methylated C1 compounds (methanol, trimethylamine, dimethylamine, monomethylamine)

Unlike methanogenic communities, bacterial communities inhabiting bioreactors treating LCFA-rich wastewater are very diverse. As it was mentioned before, known syntrophic LCFA degraders belong to *Deltaproteobacteria*, family *Syntrophaceae* and to *Firmicutes*, family *Syntrophomonadaceae* (Table 2.3) (Sousa et al., 2009a). However, culture independent methods applied to LCFA degrading environments revealed the presence of other groups of microorganism with different taxonomic classifications. Table 2.5 summarizes the phylogenetic identification of microorganisms detected in bioreactors or in enrichment cultures degrading LCFA, using molecular biology tools based on 16S rRNA gene analysis. With the exception of the work from Grabowski and her colleagues (Grabowski et al., 2005) sequences from *Syntrophomonas* genus or *Syntrophomonadaceae* family were always detected in LCFA environments. Other members from phylum *Firmicutes*, particularly microorganisms close related to *Clostridium* species, and from phylum *Proteobacteria* were also detected in several studies. The ability of some *Clostridium* species to degrade LCFA in co-culture with hydrogenotrophic methanogens was investigated but none of them succeeded (Sousa et al., 2009a). Members of phyla *Bacteroidetes*, *Synergistetes* and *Spirochaetes* between others were also detected, even though their direct involvement in LCFA degradation was never demonstrated. Anaerobic microbial communities degrading oleate (unsaturated-LCFA) and palmitate (saturated-LCFA) in bioreactors and in enrichment cultures were studied and differences were observed between the composition of communities degrading saturated- and unsaturated-LCFA (Sousa et al., 2007a; Sousa et al., 2007b). Although *Syntrophomonas*-like organisms were present in all situations, 16S rRNA gene sequences exhibit low similarity between them suggesting that different *Syntrophomonas* species were dominant in saturated- and unsaturated-degrading environments. In fact, to our knowledge, only few *Syntrophomonas* species are able to

degrade unsaturated-LCFA with more than 18 carbon atoms, namely *S. sapovorans*, *S. curvata* and *S. zehnderi*, (Table 2.3). Moreover, oleate degrading enrichment cultures were able to degrade palmitate but the opposite was only possible after extended contact with palmitate and required microbial community composition changes (Sousa et al., 2007b).

Table 2.5 Phylogenetic composition of microbial communities present in LCFA-degrading bioreactors or enrichment cultures.

Substrate and culture conditions	**Techniques applied**	**Bacterial community**	**Archaeal community**	**Reference**
Thermophilic oleate degrading enrichment cultures	Culture dependent; ARDRA; sequencing	*Firmicutes* (*Clostridia*) *Synergistetes* (*Sinergistia*)	*Methanobacterium thermoautotrophicum* (added to the enrichment culture)	Menes et al. (2001)
Bioreactors with granular and suspended sludge fed with oleate	PCR-DGGE, sequencing, FISH	*Firmicutes* (*Syntrophomonas* and others) *Proteobacteria* *Synergistetes*	*Methanobacterium* sp. *Methanobacterium formicium* *Methanosaeta concilii*	Pereira et al. (2002b)
Stearate degrading enrichment cultures	Culture dependent; RFLP; FISH; sequencing	*Deltaproteobacteria* (*Syntrophus gentianae*) *Bacteroidetes* (*Cytophaga* sp. BHI60-95B)	*Methanocalculus taiwanensis* *Methanosaeta concilii*	Grabowski et al. (2005)
Synthetic LCFA wastewater containing oleate and palmitate (chemostat cultivation)	Real-time PCR; FISH; DGGE; cloning; sequencing	*Firmicutes* (*Syntrophomonadaceae* and others) *Proteobacteria* *Bacteroidetes* *Spirochaetes*	*Methanosarcina* *Methanosaeta* *Methanospirillum*	Shigematsu et al. (2006)
Batch degradation of oleate or palmitate accumulated during continuous feeding	DGGE; real-time PCR; sequencing; FISH	*Firmicutes* (*Clostridiaceae*, *Syntrophomonadaceae*, uncultured) *Proteobacteria* *Bacteroidetes*	*Methanobacterium aarhusense* *Methanobacterium formicicum* *Methanosaeta concilii* *Methanosarcina mazei*	Sousa et al. (2007a)
Oleate or palmitate enrichment cultures	Culture dependent; DGGE; sequencing	*Syntrophomonas* – in both enrichments *Bacteroidetes/Chlorobi* group (*Chlorobium*) – in oleate enrichment *Proteobacteria* (*Desulfovibrio*)- in oleate enrichment *Proteobacteria* (*Syntrophobacter*, *Halothiobacillus*) – in palmitate enrichment	Archaeal community was not studied	Sousa et al. (2007b)

Table 2.5 (continued)

Substrate and culture conditions	Techniques applied	Bacterial community	Archaeal community	Reference
Thermophilic or mesophilic palmitate, stearate, oleate or linoleate enrichment cultures	Culture dependent; PCR; RFLP; cloning	*Firmicutes* (*Syntrophomonas*, *Syntrophothermus*, others) *Proteobacteria* (*Deltaproteobacteria*)	Archaeal community was not studied but *Methanosaeta* was detected by microscopic observation	Hatamoto et al. (2007b)
Incubations with palmitate under mesophilic or thermophilic conditions	RNA-SIP; RFLP sequencing	*Bacteroidetes* *Firmicutes* (*Clostridium; Syntrophomonas; Syntrophothermus; Tepidanaerobacter; Desulfotomaculum; Coprothermobacter*) *Deltaproteobacteria* (*Syntrophaceae; Geobacteraceae*) *Synergistetes; Deferribacteres; Bacteroidetes/Chlorobi group; Thermotogae; Acidobacteria; Spirochaetes;* candidate division OP11; Others	Archaeal community was not studied	Hatamoto et al. (2007c)
Thermophilic bioreactor fed with manure with successive pulses of a LCFA mixture (oleate, stearate, palmitate)	PCR-DGGE; sequencing	*Firmicutes* (*Clostridium; Syntrophomonadaceae*) *Synergistetes*	*Methanosarcina*	Palatsi et al. (2010)
Thermophilic bioreactor fed with manure with continuous addition of oleate	PCR-DGGE; sequencing	*Firmicutes* (*Syntrophomonas* and others) *Bacteroidetes* *Proteobacteria* *Thermotogae*	*Methanococcus* *Methanosarcina* *Methanobacterium* *Methanosaeta*	Baserba et al. (2012)

Target gene for fingerprinting analysis, FISH and sequencing was always the 16S rRNA gene.

2.4 Culture independent methods for the study of LCFA-degrading microbial communities

In the last decades, advances and development of new methodologies for the detection and identification of microorganisms in their natural environments have changed our idea about the diversity of the microorganisms, their functions and interactions in complex communities.

The major percentage of microorganisms in their natural environment are thought to be non-cultivable microorganisms or very difficult to cultivate or isolate (80 to 99%) (VerBerkmoes et al., 2009) and individual microbial activities might change when microorganism are cultivated outside their natural environment (Siggins et al., 2012b). Using culture independent methodologies it is possible to detect and to identify many of these microorganisms whose function and importance in their niche should not be ignored. Molecular biology methods always have a molecular biology target. Common targets include genes, mRNA, proteins or even lipids. Biological information of living organisms is stored in genomes which are made of DNA molecules organized by genes; the DNA can be transcribed to mRNA that in turn can be translated to proteins (Figure 2.4). Microbial ecologists make use of these biomolecules to explore microbial diversity and activity in a variety of environments.

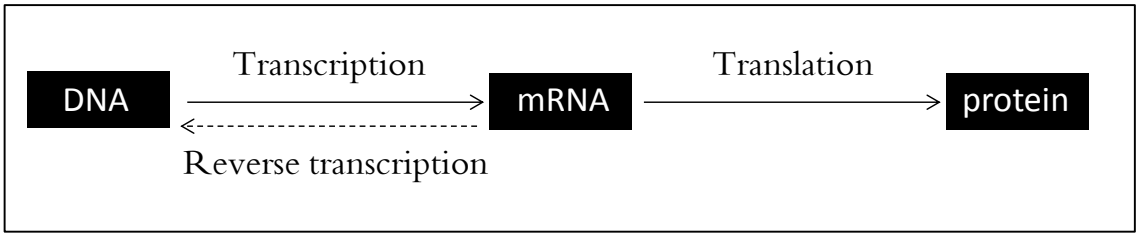

Figure 2.4 The central dogma of molecular biology.

2.4.1 PCR-dependent methods in molecular ecology

Polymerase chain reaction (PCR) is one of the most used techniques in laboratories since its discovery by Kary Mullis in 1983. Most of fingerprinting methods in microbial ecology require a first PCR step in which desirable a target gene of the entire community is amplified in order to increase the number its of copies to allow further analysis.

Prokaryotic phylogenetic studies often use the 16S rRNA gene (coding for the small subunit of the ribosome). Several reasons exist for the choice of the 16S rRNA gene: it is present in all prokaryotic microorganisms, and so it is universal; it contains high conserved regions as well as highly variable regions, which facilitates universal primers design; exhibits minimum lateral gene transfer; databases for 16S rRNA gene sequences information are growing rapidly, which facilitates taxonomic comparisons (Amann and Ludwig, 2000; Delong and Pace, 2001).

Other genes may be chosen to study specific groups inside complex communities, e.g. the amoA gene to identify ammonia oxidizers (Nicolaisen and Ramsing, 2002) or the mcrA gene to identify methanogens (Luton et al., 2002).

Fingerprinting methods namely, DGGE, ARDRA, ARISA, RFLP are widely used in molecular ecology of anaerobic LCFA degrading communities (Table 2.6). These methods rely on the differences in the sequences of 16S rRNA genes observed between species. Fingerprinting techniques are useful to estimate the diversity of microbial communities, although they do not allow identifying directly the microorganisms present. Nevertheless, these fingerprinting techniques, particularly DGGE, can be coupled to other methods in order to obtain microbial identification. DGGE bands can be directly excised from the DGGE gel, submitted

to DNA sequencing and DNA sequences analyzed for taxonomic assignment. Alternatively, clone libraries can be constructed followed by 16S rRNA gene sequencing.

Table 2.6 Some PCR-dependent fingerprinting techniques used for the study of the structure and dynamics of LCFA degrading microbial communities.

		Short description
ARDRA	Amplified Ribosomal DNA Restriction Analysis	16S rRNA genes are first PCR-amplified and secondly digested using restriction enzymes. Fragments are separated in an agarose or polyacrylamide gel and patterns obtained are compared between samples.
T-RFLP	Terminal restriction fragment length polymorphism	16S rRNA genes are first PCR-amplified using primers fluorescently-labeled at the 5'-end. Amplicons are digested using restriction enzymes and separated by electrophoresis. Only the terminal labeled restriction fragment will be detected. An electropherogram is obtained. Each peak corresponds to a specific fragment length and the intensity is proportional to the abundance of the fragment in the sample. Fragments profiles are compared between samples.
ARISA	Automated Ribosomal Intergenic Spacer Analysis	Intergenic spacer region (16S-23S) of the rRNA operon is amplified. PCR fragments are separated and obtained profiles are compared between samples.
DGGE	Denaturing Gradient Gel Electrophoresis	PCR-amplified DNA molecules with an attached GC clamp are separated in a gel containing a denaturing gradient composed by urea and formamide. Different DNA sequences will denature in different positions in the DGGE gel. DGGE profiles obtained are compared between samples.

DGGE has been extensively used to study LCFA-degrading microbial communities usually coupled to sequence analysis (Table 2.5). The common approach was to select the most prominent bands in the DGGE profile for further 16S rRNA genes sequences identification. DGGE profiles from DNA samples collected from the top (floating sludge: encapsulated by LCFA) and in the bottom (settled sludge) layers of anaerobic bioreactors treating LCFA-rich wastewater revealed a clear shift in the bacterial communities but not in archaeal communities (Pereira et al., 2002b).

Similar results were obtained from EGSB bioreactors loaded in continuous with oleate or palmitate in which the bacterial communities diverged from each other and from the communities present in the inoculum sludge whereas the archaeal community was much less affected, given by DGGE profiles comparison (Sousa et al., 2007a). Nevertheless, in the same study, archaeal communities suffered major changes after degrading the accumulated LCFA in batch. DGGE was also used to follow the shifts in bacterial communities during enrichment of saturated- or unsaturated-LCFA degraders and revealed that bacterial diversity decreased in both situation and furthermore that the two enrichments diverged significantly from each other (Sousa et al., 2007b). On the other hand, by comparing DGGE profiles, Palatsi et al. (2010) did not detect major differences in both bacterial and archaeal communities after two pulses of LCFA in an anaerobic thermophilic bioreactor fed with manure. Another thermophilic bioreactor fed with manure received continuous addition of oleate and, in this case, the bacterial community diverged significantly from the one before oleate addition (Baserba et al., 2012). In these studies, DGGE fingerprinting was coupled to cloning and sequencing of 16S rRNA genes or to direct sequencing of excised bands from the DGGE gel, in order to better interpret DGGE results and to obtain information on the composition of microbial communities (Table 2.5).

Fingerprinting techniques are qualitative or semi-quantitative and therefore, the relative abundance of a given microorganism in a biological sample cannot be easily estimated based on these techniques. Other methods can be used for that propose. Real-time quantitative PCR had been used to estimate the abundance of archaeal and bacterial microorganisms in a mesophilic microbial consortium degrading a LCFA-based wastewater. Bacterial 16S rRNA genes were 10 fold more abundant

than archaeal's. Specifically, *Methanosaeta*, *Methanospirillum* and *Methanosarcina* genera could be detected and quantified using real-time quantitative PCR, although *Methanosarcina* was not detected in the same samples using a DGGE couple to cloning library and 16S rRNA gene sequencing approach (Shigematsu et al., 2006). During continuous load of oleate or palmitate in anaerobic bioreactors, relative abundance of archaeal microorganisms was not significantly affected, given by quantitative PCR analysis. However, after degradation of the accumulated LCFA in batch the numbers of archaeal 16S rRNA genes increased considerably (Sousa et al., 2007a).

2.4.2 PCR-independent and *in situ* methods in molecular ecology

Fluorescence *in situ* hybridization (FISH) is a quantitative technique dependent on microscopic observation. Biological samples are fixed and specific oligonucleotide probes will be hybridizing with the complementary sequence in the ribosome. Usually the ribosome is chosen by the reasons already explained above but also because ribosomes exist in high numbers inside the cells (Amann and Ludwig, 2000), even higher when the cells are active, which increases the signal of the probe.

FISH was applied to anaerobic degrading LCFA environments to detect and quantify specific groups of archaea and bacteria. *Methanosaeta*-like microorganisms were relatively abundant in granular sludge and were detected but much less abundant in suspended sludge during anaerobic treatment of oleic acid-based wastewater (Pereira et al., 2002b). *Methanosaeta*-like archaea were also detected,

using FISH probes, in bioreactors continuously fed with LCFA while *Methanosarcina*-like organisms become more abundant during batch operation and after LCFA depletion from the medium (Sousa et al., 2007a). Grabowski et al. (2005) observed that archaeal microorganisms were distributed spatially close to syntrophic LCFA degrading bacteria, and that abundant bacteria belong to class *Deltaproteobacteria*, using FISH observation as quantification method.

More advanced techniques were recently developed for *in situ* identification of microorganism in complex samples. So far, there are no studies applying such techniques (e.g., NanoSIMS, CARD-FISH or Raman-FISH), to LCFA degrading communities.

2.4.3 The "omics" in molecular ecology

Phylogenetic identification of microorganisms in complex microbial communities is not the only aim of microbial ecologists. Linking microbial identification to microbial function became the goal of more recent investigations. Metagenomics, metatranscriptomics, metaproteomics and metabolomics study respectively collective microbial genomes, transcriptomes, proteomes or even the produced metabolites by microorganisms within an environmental sample. These approaches aim to address important environmental questions. The objective is to have a global idea of how the microbial communities behave, what are the principal activities, who is performing those activities and how microorganism interact with each other and with the environment. While metagenomics gives insights on the potential of a given microbial community based on the microbial genomic information,

transcriptomics retrieves information on communities activities. In metatranscriptomics studies, the analysis of messenger RNA (mRNA) instead of DNA gives information on the activity of the community in the way that only the expressed genes will be detected (Prakash and Taylor, 2012). Because mRNA is not obligatory transcribed to proteins and is also more unstable than proteins, metaproteomics approaches, which deal with direct analysis of the proteins expressed, gives a more accurate functional scenario of the microbial community (Prakash and Taylor, 2012; Schneider and Riedel, 2010). Metaproteomics data analysis and consequently functional information retrieved from metaproteomics studies is determined by the metagenomics information available. In turn, metagenomics data functional assignment depends on whole genomes information available as well as on the sequencing technology and on bioinformatics tools used to analyze, interpret the data and to overcome sequencing errors and other limitations (Prakash and Taylor, 2012). A typical metagenomics approach begins by total community DNA extraction followed by the generation and screening of clone libraries (Handelsman, 2004). Some metagenomics studies target specific genes or functions (e.g. 16S rDNA clone libraries) while others rely on whole genome sequencing (Chen and Pachter, 2005). The development of second generation sequencing, such as 454-pyrosequencing and Illumina (sequencing by synthesis), allowed retrieving much more sequences from complex microbial communities than with Sanger sequencing (chain-termination method) although shorter reads can be obtained (Ahmadian et al., 2006; Ronaghi, 2001; Wooley et al., 2010). As a result, short sequences from a variety of different microorganism are collected and the analysis of these complex data is still a challenge particularly when sequences belong to unsequenced genomes (Sharma et al., 2012). Almost complete

genomes could be obtained from environmental samples using metagenomic approaches (Tyson et al., 2004; Venter et al., 2004). However, in many cases, assembly of metagenomic reads is a challenge, primarily because the genomes are only partially sampled, which is even more drastic for less abundant microorganisms and secondly, because of the incomplete genomic information in databases which difficult the correct taxonomic assignment and contributes for the high percentage of unknown sequences in metagenomic data (Prakash and Taylor, 2012; Wooley et al., 2010). Taxonomic assignment of metagenomic sequences can be achieved based on sequence composition, using TETRA, TACOA, NBC or PhyloPythia software, or based on sequence homology using MEGAN, MetaBin between other tools, by searching against a reference database like NCBI non redundant database (Sharma et al., 2012). Although metagenomics data analysis still require further development, the fact that the amount of genomic sequences are increasing every day in databases, make these approaches very promising for the interpretation of microbial community potential. More detailed information about recent advances on metagenomics can be found in the literature (Chen and Pachter, 2005; Prakash and Taylor, 2012; Sharma et al., 2012; Simon and Daniel, 2011; Valenzuela et al., 2006; Wooley et al., 2010).

Metaproteomics appeared as a field that allows retrieving functional information of the active fraction of the microbial communities without need of cultivation. In a typical metaproteomics study, proteins are extracted, purified, concentrated, denatured and reduced, prior to protein separation by gel electrophoresis or by "off gel" isoelectric focusing, although some approaches do not require a previous separation step (Ros et al., 2002; Schneider and Riedel, 2010; VerBerkmoes et al., 2009; Wilmes and Bond, 2009). After enzymatic digestion of proteins, peptides are

separated and analyzed by mass spectrometry (MS) or by liquid chromatography coupled to mass spectrometry (Figure 2.5). Protein identification is based on mass spectra analysis using bioinformatics tools. Sample preparation protocols include mainly the following steps: (1) cell lysis, which can be mechanical (e.g. bead beating, French press, vortex, and sonication) or using detergents (e.g. CHAPS, Tryton X-series) or even a combination of both methods; (2) protein purification and concentration, usually by precipitation with acetone, ethanol or trichloroacetic acid; (3) protein denaturation and reduction, accomplished using buffers containing chaotropes (e.g. urea, thiourea), ionic (e.g. SDS) or non-ionic detergents (e.g. CHAPS, Tryton X-series); reducing agents (e.g. DTT, DTE); and protease inhibitors (e.g. PMSF) (Canas et al., 2007; Schneider and Riedel, 2010). Digestion of proteins with trypsin or other enzymes (usually Glu-C, Lys-C, Asp-N and chymotrypsin) can be made in solution or in gel to reduce the complexity of peptide mixtures. In gel digestion is much less susceptible to interfering substances than digestion in solution but total peptide recovery from the gel might be difficult (Schneider and Riedel, 2010). Peptides are analyzed by reversed-phase chromatography couple to a mass spectrometer where peptide parent ions are fragmented to obtain tandem mass spectra. Sequest, Mascot, OMSSA, Sonar and X! Tandem are algorithms that match MS/MS spectra to peptide sequences, by searching against a protein sequence database (Balgley et al., 2007; Craig and Beavis, 2003; Field et al., 2002; Perkins et al., 1999; Yates, III, 1998). There are also *de novo* algorithms for generation of peptide sequences based on MS/MS spectra without the need of comparison with a FASTA protein database (e.g. PEAKS, Lutefish and GutenTag) (Khalsa-Moyers and McDonald, 2006).

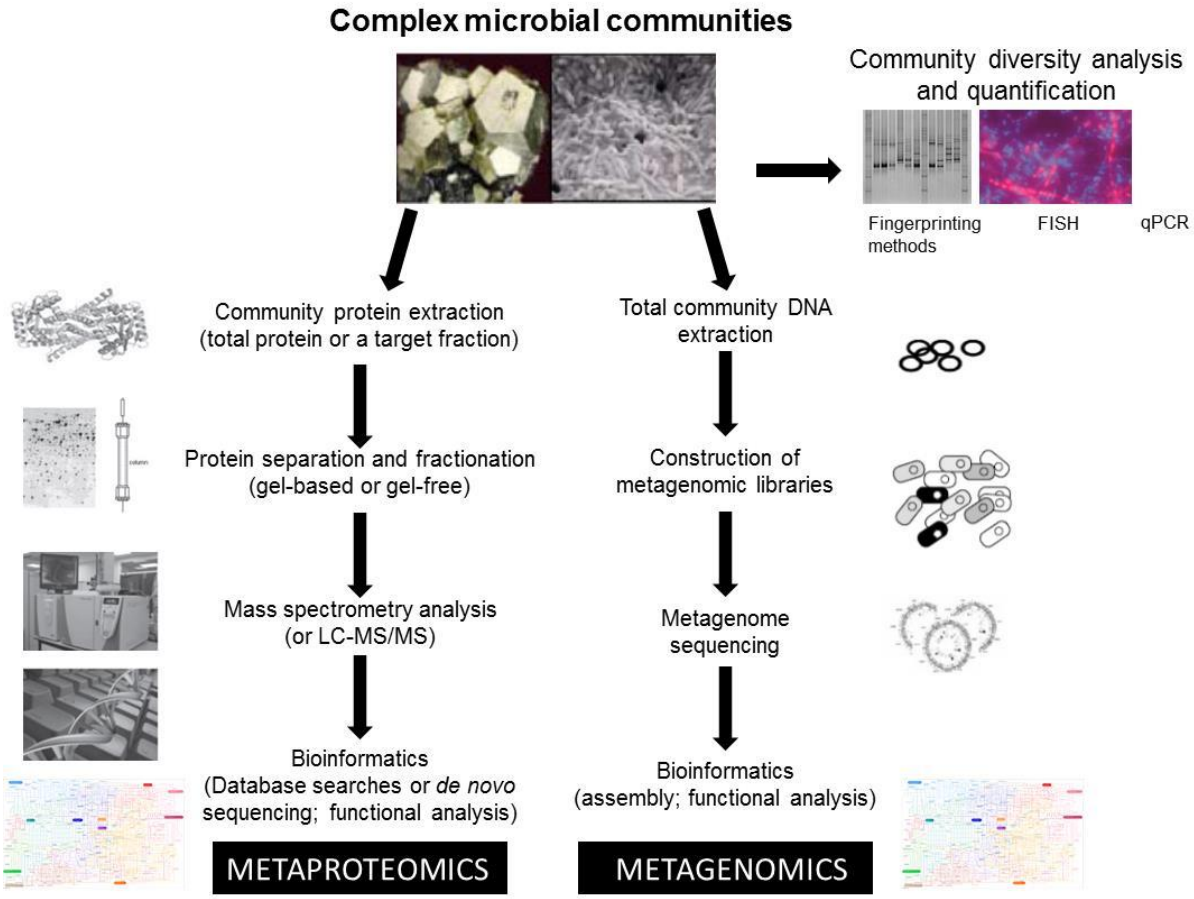

Figure 2.5 General steps of metagenomics and metaproteomics methodologies and other molecular biology techniques for the study of complex microbial communities (adapted from Valenzuela et al. (2006) and Siggins et al. (2012)).

To our knowledge, there is only one proteomics study involving mesophilic syntrophic fatty acid-degrading bacteria (Schmidt et al., 2013). The protein pool expressed by *Syntrophomonas wolfei* growing on butyrate (C4:0), in co-culture with the hydrogen/formate utilizing methanogen *Methanospirillum hungatei*, was compared with the one obtained when this bacterium was grown non-syntrophically in crotonate (C4:1). Formate dehydrogenases and hydrogenases were most abundant during butyrate and crotonate degradation, respectively. The electron flow during butyrate utilization by *S. wolfei* could be described and involved a membrane bound EtfAB:quinone oxidoreductase, a menaquinone, a b-

type cytochrome and a formate dehydrogenase (Schmidt et al., 2013). Another comparative proteomics study was carried out with the thermophilic methanogen *Methanothermobacter thermautotrophicus* growing in axenic culture or in syntrophy with the butyrate-degrading bacterium *Syntrophothermus lipocalidus*. Proteins related to RNA/DNA metabolisms, amino acid synthesis and carbon fixation were down-regulated when the methanogen was growing in syntrophy. Also, acylation of alpha-subunits of the proteasome was different when *M. thermautotrophicus* was growing alone or in co-culture (Enoki et al., 2011).

A combination of genomic and proteomic analysis of the syntroph thermophilic propionate-oxidizer *Pelotomaculum thermopropionicum* pointed out for the importance of fumarase on the energy conservation of the bacterium. Many of the genes required for propionate oxidation were organized in an operon-like cluster containing several promoter sequences and a transcriptional regulator (Kosaka et al., 2006). Syntrophic growth of *Dehalococcoides ethenogenes*, a specialist in the dechlorination of tetrachloroethene and trichloroethene, was investigated by a transcriptomic couple to a proteomic approach when the bacterium was grew together with *Desulfovibrio vulgaris* and *Methanobacterium congolense* or only with *Desulfovibrio vulgaris*. *D. ethenogenes* grew better and exhibited a faster dechlorination in syntrophic cultures than in pure cultures. This was due to the degradation of lactate by *D. vulgaris* which resulted on the formation of hydrogen and acetate that were then utilized by *D. ethenogenes* as electron donor and carbon source, respectively (Men et al., 2012). Adaptation of mesophilic *Methanosarcina barkeri* to low temperatures was reflected in the proteome of this methanogen. Several proteins associated to substrate utilization for methane production and also

proteins with chaperon activity, among others, were differential expressed when growing at 15ºC (Gunnigle et al., 2013).

The examples showed above correspond to proteomic studies using defined cultures, which facilitate data analysis and interpretation.

The effect of trichloroethylene exposure in the structure and function of complex microbial communities was investigated by 16S rRNA gene analysis and metaproteomics (Siggins et al., 2012a). Although major differences in the communities' structure and composition could not be addressed based on 16S rRNA gene analysis, changes in the metaproteome of microbial communities between reactors supplemented and non-supplemented with trichloroethylene were more evident, with several proteins being differentially expressed in the presence of trichloroethylene (Siggins et al., 2012a).

Recently, Wu and colleagues (2013) identified *Pelotomaculum*, *Methanolinea* and *Methanosaeta* as the most abundant microorganisms present in terephthalate degrading complex microbial community based on 16S rDNA analysis. Metaproteomics analysis of this community confirmed that *Pelotomaculum* spp. were actively degrading TA via the decarboxylation and benzoyl-coenzyme A dependent pathway producing acetate, H_2/CO_2 and butyrate that were subsequently utilized by methanogens and other bacteria within the community (Wu et al., 2013).

Siggins et al. (2012b) reviewed the advances of metaproteomics in various microbiology environments namely, soil, freshwater and marine, bioengineered systems and human microbiome. Due to the complexity of such environments only few studies gave answer to specific questions regarding the behavior of microbial communities (Siggins et al., 2012b). Advances on metagenomics and

metaproteomics approaches hopefully will allow increasing our knowledge on microbial community activities and functions in natural environments.

Chapter 3

Endurance of methanogenic archaea in anaerobic bioreactors treating oleate based wastewater

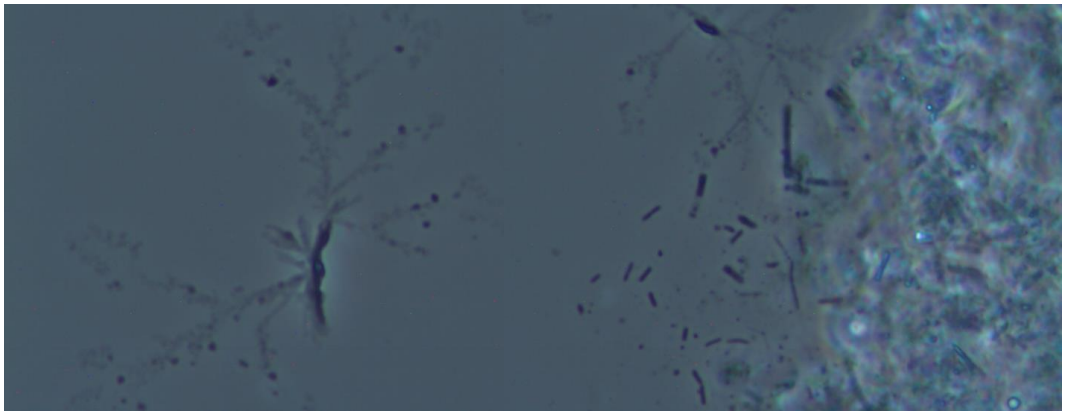

Methanogenic archaea are reported as very sensitive to lipids and long chain fatty acids (LCFA). Therefore, in conventional anaerobic processes, methane recovery during LCFA-rich wastewater treatment is usually low. By applying a start-up strategy, based on a sequence of step feeding and reaction cycles, an oleate-rich wastewater was efficiently treated at an organic loading rate of 21 kg COD m^{-3} day^{-1} (50% as oleate), showing a methane recovery of 72%. In the present work, the archaeal community developed in that reactor is investigated using a 16S rRNA gene approach. This is the first time that methanogens present in a bioreactor converting efficiently high loads of LCFA to methane are monitored. DGGE profiling showed that major changes on the archaeal community took place during the bioreactor start-up, where phases of continuous feeding were alternated with batch phases. After a start-up, a stable archaeal community (similarity higher than 84%) was observed and maintained throughout continuous operation. This community exhibited high LCFA-tolerance and high acetoclastic and hydrogenotrophic activity. Cloning and sequencing results showed that *Methanobacterium*- and *Methanosaeta*-like microorganisms prevailed in the system and were able to tolerate and endure during prolonged exposure to high LCFA loads, despite the previously reported LCFA-sensitivity of methanogens.

Salvador AF, Cavaleiro AJ, Sousa DZ, Alves MM and Pereira MA (2013) Endurance of methanogenic archaea in anaerobic bioreactors treating oleate-based wastewater. Appl Microbiol Biotechnol 97:2211-2218

3.1 Introduction

Long chain fatty acids (LCFA) conversion to methane involves the activity and syntrophic collaboration of acetogenic bacteria, oxidizing LCFA to hydrogen and acetate, and methanogenic archaea, responsible for consuming hydrogen and acetate with the production of methane and carbon dioxide (Schink, 1997). Hydrogen interspecies transfer is obligatory as it renders LCFA oxidation exergonic (Sousa et al., 2009a). To guarantee a maximum methane production, acetate conversion to methane is crucial as well. Therefore, acetoclastic and hydrogenotrophic methanogenic activity should be maximized to achieve high methane yields in anaerobic digesters. However, it has been suggested that LCFA can exert inhibitory effect towards anaerobic microorganisms, in particular methanogens (Hwu and Lettinga, 1997; Koster and Cramer, 1987; Lalman and Bagley, 2001; Perle et al., 1995). Adsorption of LCFA onto the microbial cell wall (Koster and Cramer, 1987) and binding of LCFA to cell membranes with interference in transport functions (Hook et al., 2010; Soliva et al., 2004a) have been suggested as potential mechanisms underlying inhibition by LCFA. Nevertheless, some authors documented only a transient inhibition and suggest that adaptation of microbial communities to LCFA may occur after extended exposure (Alves et al., 2001; Broughton et al., 1998; Kim et al., 2004; Pereira et al., 2004). Transport limitations, due to the accumulation of LCFA onto the sludge, could also contribute to the generally observed lag phases ascribed to microbial inhibition (Pereira et al., 2005). A sequential process, in which a first step of LCFA accumulation was promoted, followed by batch degradation of the biomass-associated substrate, was found to be a possible solution for the treatment of this type of wastewaters (Cavaleiro et al.,

2008; Pereira et al., 2004). More recently, (Cavaleiro et al., 2009) showed that continuous treatment of high LCFA loads can also be achieved after a start-up in cycles, alternating continuous feeding with batch phases. Based on these findings, a novel high rate anaerobic reactor specifically designed for the treatment of lipids/LCFA wastewaters has been developed (Alves et al., 2007; Alves et al., 2009). (Sousa et al., 2007a) used FISH and real-time PCR for quantifying methanogens during fed-batch degradation of LCFA. Results showed that the relative abundance of archaea increased during degradation of biomass-accumulated LCFA. Two major groups of methanogens were identified: hydrogen- and formate-utilizing organisms, closely related to *Methanobacterium*, and acetoclastic organisms closely related to *Methanosaeta* and *Methanosarcina*. Methanogenic communities in high-rate continuous reactors efficiently degrading LCFA were never studied. In this work, we focused on the composition and dynamics of the archaeal community that colonized the anaerobic bioreactor described in the work of Cavaleiro et al. (2009), which was fed with a synthetic wastewater mainly composed of oleic acid (mono-unsaturated C18 LCFA).

3.2 Materials and methods

3.2.1 Sludge source

A total of fifteen sludge samples were collected during the operation of a mesophilic (37°C) up-flow anaerobic column reactor fed with an oleate-rich wastewater as described by Cavaleiro et al. (2009). Table 3.1 shows sludge sampling times and a summary of the operating conditions and the performance data of the reactor.

The reactor was inoculated with anaerobic suspended sludge collected from a municipal sludge digester and its concentration was maintained stable around 20 gVS L-1. Reactor feed consisted of a mixture of skim milk and sodium oleate (50:50% COD) supplemented with macro- and micronutrients and bicarbonate, as previously described by Alves et al. (2001).

Five cycles of continuous feeding phases (F), alternated with batch reaction phases (R), were applied during the first 213 days of operation (Period I). During feeding phases LCFA accumulation inside the bioreactor was favored, whereas degradation of the accumulated LCFA was promoted during reaction phases. Length of feeding and reaction phases was established based on the methane production efficiency and LCFA accumulation/degradation in the bioreactor mixed liquor (Cavaleiro et al., 2009). Period I corresponded to the system start-up and was followed by a continuous feeding period (Period II, days 243-665). Reactor operation was interrupted from days 213 to 243. Detailed description on bioreactor operation conditions can be found in the paper by Cavaleiro et al. (2009).

Table 3.1 Sludge sampling times and summary of corresponding operating conditions and performance data (Cavaleiro et al. 2009)

Period Operation mode	Phase [a]	Time (days)	Sampling day	OLR (kg COD m^{-3} day^{-1})	Methane yield [b] (%)
	F-1	0-17	0	4.4 ± 0.6	n.d.
	R-1	17-45	17	n.a.	
	F-2	45-62	45	4.4 ± 0.6	66.7
Period I	R-2	62-100	62	n.a.	
	F-3	100-117	100	4.4 ± 0.6	72.7
Cycles	R-3	117-138	-	n.a.	
	F-4	138-166	138	4.4 ± 0.6	n.d.
	R-4	166-181	-	n.a.	
	F-5	181-203	181	8.2 ± 0.6	90.7
	R-5	203-213	213	n.a.	
stop phase		216-243			
(sludge at 4ºC)					
	C-1	243-277	-	5.0 ± 0.4	81.5
	C-2	277-333	-	7.8 ± 1.0	79.5
Period II	C-3	333-389		9.8 ± 2.2	86.0
	C-4	389-437	389	11.5 ± 2.2	98.4
Continuous	C-5	437-571	437; 494;544	20.6 ± 4.0	71.5
	C-6	571-608	584; 599	26.1 ± 4.2	60.9
	C-7	608-665	665	31.2 ± 7.9	57.0

[a] F, Feeding; R, Reaction; C, Continuous.

[b] Methane yield (%) = $g_{COD\text{-}CH4\ produced}$ / $g_{COD\ removed}$ * 100

n.a., not applicable; n.d., not determined.

3.2.2 DNA extraction and amplification

Aliquots of well-homogenized sludge were immediately frozen at the time of sampling and stored at -20ºC. Total genomic DNA was extracted using a FastDNA SPIN Kit for Soil (Qbiogene, Carlsbad, CA, USA) according to manufacturer's instructions. 16S rRNA-genes were amplified by polymerase chain reaction (PCR) using a Taq DNA Polymerase kit (Life Technologies, Gaithersburg, MD, USA). Primer sets A109(T)-f/515-r and Uni1492-r/Arch109-f (Grosskopf et al., 1998; Lane, 1991; Nübel et al., 1996) were used for 16S rRNA gene amplification for DGGE and sequencing purposes, respectively; primer 515-r for DGGE analysis was modified by the addition of a 40 bp GC clamp at the 5' end of the sequence. A description of PCR programs and primers sequences can be found in the paper by (Sousa et al., 2007a). All primers used were synthesized commercially by Invitrogen (Life Technologies). Size and yield of PCR products were estimated using a 100 bp DNA ladder (MBI Fermentas, Vilnius, Lithuania) via 1% (wt/vol) agarose gel electrophoresis and ethidium bromide staining.

3.2.3 DGGE analysis

DGGE analysis of the amplicons was performed as previously described by Zoetendal et al. (2001) by using the Dcode system (Bio-Rad, Hercules, CA, USA) with 8% (vol/vol) polyacrylamide gels and a denaturant gradient of 30 to 60%. A 100% denaturing solution was defined as 7 M urea and 40% formamide. Electrophoresis was performed for 16 h at 85 V in 0.5X TAE buffer at 60°C. DGGE gels were stained with $AgNO_3$ according to the procedure previously described by Sanguinetti et al. (1994). DGGE profiles were scanned at 400 dpi and

compared using the BioNumerics™ software package (version 5.0; Applied Maths BVBA, Sint-Martens-Latem, Belgium). Similarity between DGGE profiles was determined by calculating similarity indices of the densitometric curves of the compared profiles, using the Pearson product-moment correlation (Hane et al., 1993). Peak heights in the densitometric curves were used to determine the diversity indices based on the Shannon Wiener diversity index, calculated as follows:

$$H = - \Sigma (P_i \ln(P_i))$$

where, H is the diversity index and P_i is the importance probability of the bands in a lane ($P_i=n_i/n$, *where* n_i is the height of an individual peak and n is the sum of all peak heights in the densitometric curves).

3.2.4 Cloning and sequencing of PCR-amplified products

PCR products obtained from DNA samples corresponding to the final time of Period I and II (days 213 and 665, respectively) were purified with Nucleo Spin Extract II kit (Clontech Laboratories) and cloned into E. coli® 10G Electrocompetent Cells (Lucigen® Corporation) by using Promega pGEM-T Easy vector system (Promega, Madison, WI, USA). PCR was performed on cell lysates of ampicillin-resistant transformants by using pGEM-T specific primers PG1-f and PG2-r to confirm the size of the inserts. Clones with the correct size insert were further amplified with primer set A109(T)-f/515r for DGGE comparison with original sample profiles. PCR products of transformants resolving at the same

position of predominant bands in the DGGE community fingerprint were chosen for further analysis. Selected clones were amplified with using pGEM-T vector-targeted primers SP6/T7, purified using the Nucleo Spin Extract II kit (Clontech Laboratories), and subjected to DNA sequence analysis. Sequencing reactions were performed at Biopremier (Lisboa, Portugal). Consensus sequences obtained were checked for potential chimera artifacts using Mallard v1.02 (Ashelford et al., 2006) and Pintail v1.1 (Ashelford et al., 2005) software.

3.2.5 Phylogenetic analysis

Similarity searches for the 16S rRNA gene sequences derived from the sludge clones were performed using the NCBI BLAST search program within the GenBank database (http://www.ncbi.nlm.nih.gov/blast/) (Altschul et al., 1990). Alignment of 16S rRNA sequences was performed by using FastAligner V1.03 tool of the ARB program package (Ludwig et al., 2004). The resulting alignments were manually checked and corrected when necessary, and unambiguously aligned nucleotide positions were used for construction of the archaea 16S rRNA gene based phylogenetic tree, using the neighbour joining method (Saitou and Nei, 1987). Phylogenetic placement was performed in comparison with reference sequences with Felsenstein correction and application of archaeal filter.

Nucleotide sequences obtained in this study have been deposited in the European Nucleotide Archive (ENA) under accession numbers **HE648042** to **HE648052**.

3.3 Results

3.3.1 Analysis of methanogenic communities during bioreactor start-up

Microbial diversity and shifts in archaeal communities present in the anaerobic bioreactor during the intermittent feeding start-up were estimated by 16S rRNA gene PCR-DGGE (Figure 3.1). Analysis of eight sludge samples withdrawn from the reactor during start-up period (Table 3.1) revealed a shift in the archaeal communities overtime, with samples grouping in three main clusters (Figure 3.1b). The inoculum sludge (t=0 days) showed the lowest diversity (Shannon diversity index of 0.67) and shared only 47% similarity with the other sludge samples; there was a fast shift in the archaeal community after contacting with oleate and skim milk (reactor sludge sample withdrawn on day 17 is only 67% similar to the inoculum sludge). Similarity between samples collected during the 1st and 2nd cycle of sludge acclimation (until day 100 of bioreactor operation) and samples from subsequent cycles (from day 138 to 213) is 58%. On the other hand, samples collected on days 138, 181 and 213 are 88% similar and almost no variation on the archaeal communities structure was observed between samples collect during the 5th cycle (corresponding to samples from days 181 and 213) as they share 98% similarity (Figure 3.1b). This means that major shifts in the archaeal community took place during the first 2 cycles of the start-up operation.

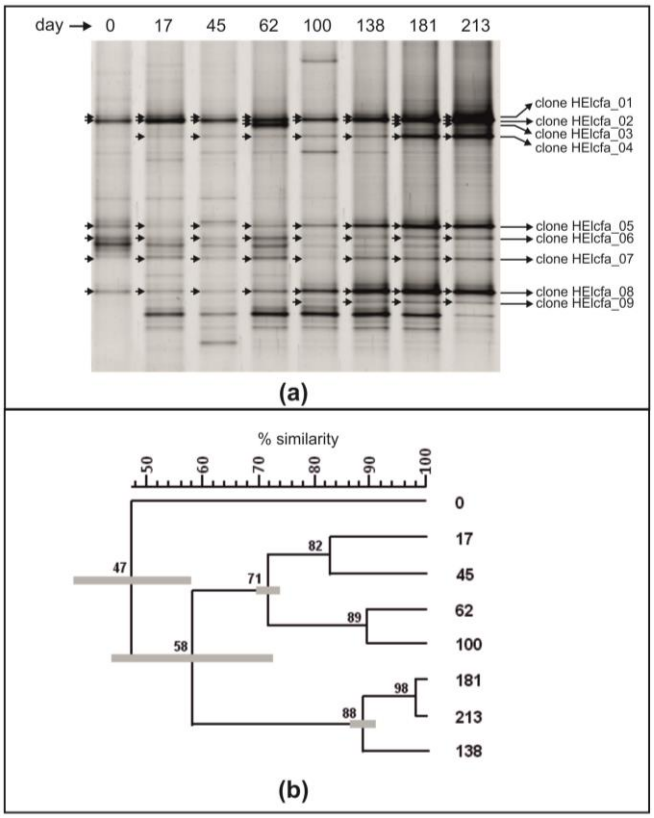

Figure 3.1 DGGE pattern (a) and cluster analysis (b) of archaeal 16S rRNA gene fragments obtained from samples collected during reactor start-up (Period I). Cluster analysis was performed using the unweighted pairwise grouping method with mathematical averages (UPGMA). Numbers 0 to 213 correspond to sampling days during Period I and DGGE bands analyzed by cloning and sequencing are identified.

3.3.2 Endurance of methanogenic communities in continuous high-rate bioreactor

Period II of operation corresponds to continuous reactor feeding with an increasing OLR of up to 32 kg COD m^{-3} day^{-1} (50% COD as sodium oleate) (Table 3.1). Figure 3.2 shows the DGGE profiles of archaeal 16S rRNA fragments obtained from seven different sludge samples collect during that period (from day 389 to 665) as well as the corresponding similarity index dendrogram. Similarity between the obtained profiles was always higher than 84% and fluctuated between 89 to 98% within the five last samples. Shannon diversity indices (H) decreased 28% from the

sample collected on day 389 to day 437, and from this moment on, the variation of the diversity indices was very low (less than 12% of variation) showing the stability of the archaeal community diversity during the continuous bioreactor operation.

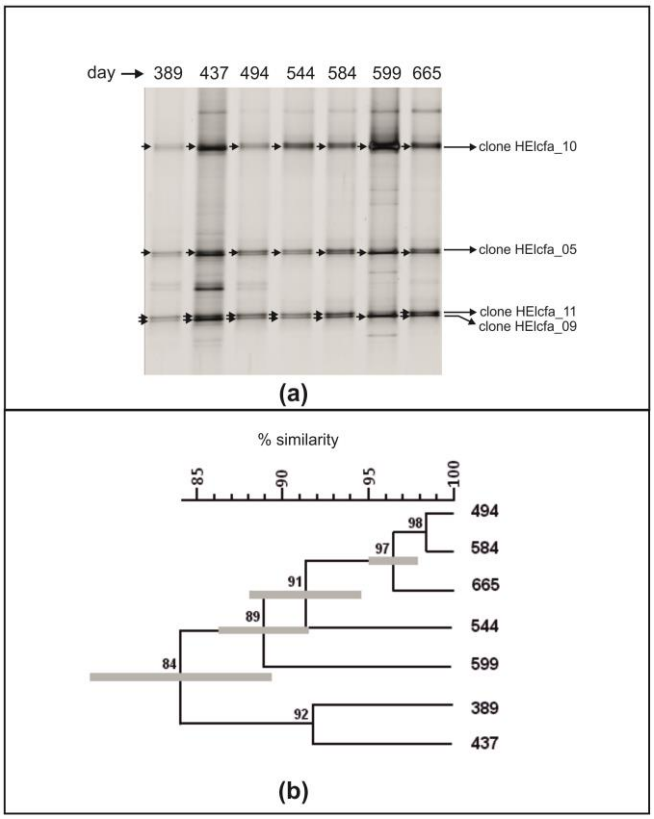

Figure 3.2 DGGE pattern (a) and cluster analysis (b) of archaeal 16S rRNA gene fragments obtained from samples collected during reactor continuous operation (Period II). Cluster analysis was performed using the unweighted pairwise grouping method with mathematical averages (UPGMA). Numbers 389 to 665 correspond to sampling days during Period II and DGGE bands analyzed by cloning and sequencing are identified.

3.3.3 Phylogenetic analysis of predominant bands in the archaeal DGGE patterns

To assign the composition of the predominant community visualized in the DGGE-patterns, nearly full-length archaeal 16S rRNA gene fragments, retrieved from the sludge sample collected at the end of the start-up period (day 213) and at the end of the continuous period (day 665), were used to construct clone libraries. Clones with the same electrophoretic mobility as that of predominant bands of

archaeal DGGE-patterns were selected for further sequence analysis. Phylogenetic affiliation of sequences was initially assessed by BLAST similarity searches and RDP Classifier, and confirmed by secondary structure-assisted alignment and phylogenetic analysis (Figure. 3.3). Clones 5 and 9 were originated from the sample collected on day 213 (end of Period I). Their correspondence to bands present in the sample collected on day 665 was made by comparing the electrophoretic mobility of the PCR products.

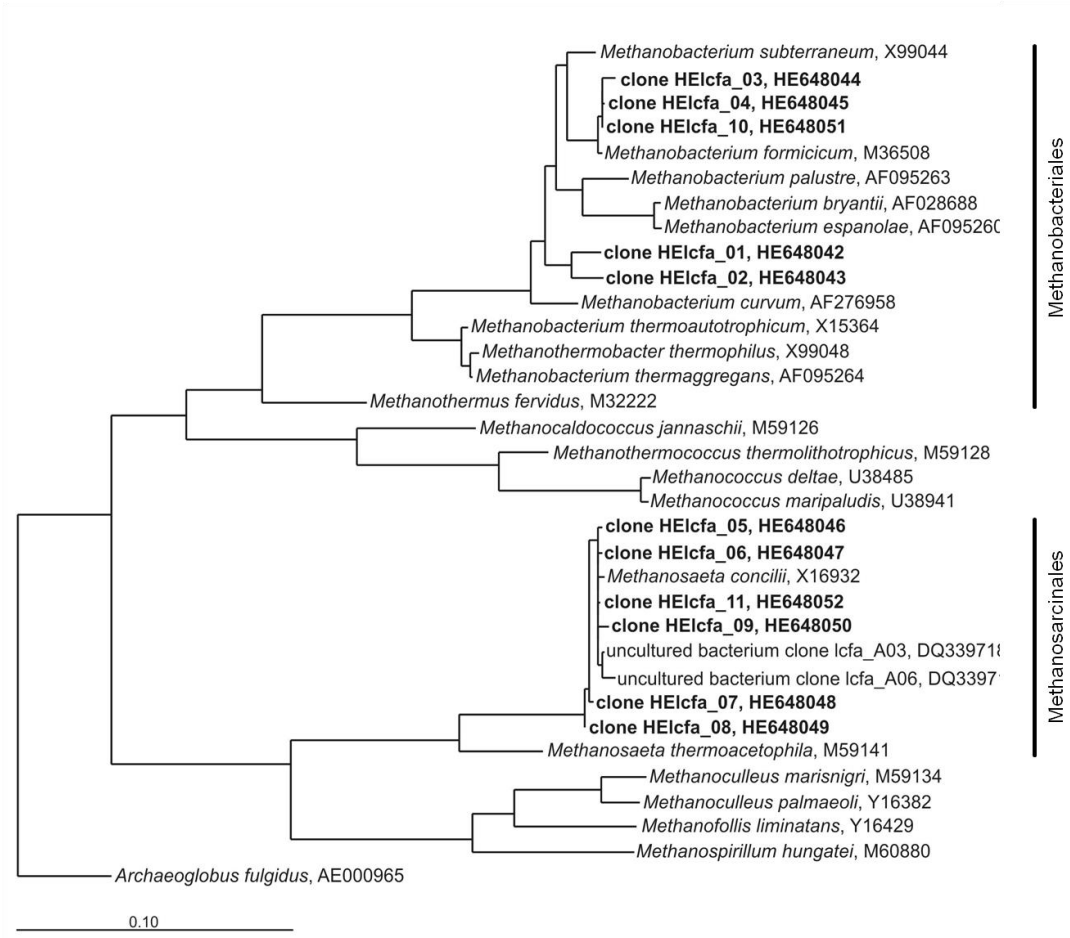

Figure 3.3 Phylogenetic tree of archaeal 16S rRNA gene sequences retrieved from the sludge samples collected at the end of both operational periods, Period I and Period II. Trees were calculated using the ARB software package (Ludwig et al. 2004) and applying the neighbor-joining method (Saitou and Nei 1987). Closely related sequences, with the respective ENA accession number, are shown as reference. *Archaeoglobus fulgidus* (AE000965) was used as outgroup for archaea tree. Reference bars indicate 10% sequence divergence.

The retrieved 16S rRNA sequences were affiliated with methanogenic archaea belonging to the phylum *Euryarchaeota* and to the orders *Methanobacteriales* and *Methanosarcinales* (Figure 3.3). At the end of the start-up period, retrieved sequences showed higher similarity to those of *Methanobacterium* sp. OM15 (99%) (clones HElcfa_03 and HElcfa_04), *Methanobacterium beijingense* 8-2 (98%) (clones HElcfa_01 and HElcfa_02) and *Methanosaeta concilii* GP-6 (99%) (clones HElcfa_05 to HElcfa_09), according to BLAST searches. The analysis of 16S rRNA sequences obtained at the end of Period II revealed the presence of the same genera, namely *Methanosaeta* and *Methanobacterium* (Figure 3.3). Retrieved sequences were most related with the sequences of the following methanogens: *Methanosaeta concilii* GP-6 (99% of similarity) (clones HElcfa_05, HElcfa_09 and HElcfa_11) and *Methanobacterium* sp. OM15 (99% of similarity) (clone HElcfa_10).

3.4 Discussion

Key methanogenic groups showing high LCFA-tolerance and high methanogenic activity were identified through molecular characterization of the archaeal community present in the anaerobic bioreactor. *Methanobacterium*- and *Methanosaeta*-like microorganisms prevailed in the system (Figure 3.3) during alternating feeding and batch cycles (period I) and continuous operation (period II), and likely contributed to the high methane production observed. Maximum specific methane production rates around 1000 mg COD-CH_4 gVS^{-1} day^{-1} were achieved in the bioreactor when OLR of 26-31 kg COD m^{-3} day^{-1} were applied, showing that LCFA were not inhibiting the methanogens (Cavaleiro et al. 2009). Moreover, the specific methanogenic activity of this consortia increased considerably, i.e. from non detectable values to 497±19 mL CH_4 g VS^{-1} day^{-1} in

acetate and from 56±6 to 1322±174 mL CH_4 g VS^{-1} day^{-1} in hydrogen (Cavaleiro et al., 2009).

Although the presence of *Methanobacterium*- and *Methanosaeta*-like microorganisms has been previously reported in anaerobic bioreactors fed with LCFA (Bertin et al., 2004; Grabowski et al., 2005; Ince et al., 2003; Pereira et al., 2005; Rizzi et al., 2006; Sousa et al., 2007a), this is the first study in which the two methanogenic genera are shown to tolerate and endure during extended contact with LCFA loads higher than 10 kg COD m^{-3} day^{-1}.

LCFA accumulation inside the bioreactor reached a maximum concentration of 44 mM (23 mM palmitate and 21 mM stearate) at the end of the second cycle (period I). These concentration values are much higher than reported IC_{50} (concentration that causes a 50% relative methanogenic activity loss). At mesophilic temperatures, IC_{50} values for oleate towards acetoclastic methanogens ranges 0.1–4.35 mM (Alves et al., 2001; Hwu and Lettinga, 1997; Koster and Cramer, 1987; Pereira et al., 2005). This wide range of IC_{50} values is justified by the different parameters than can influence oleate toxicity, namely (i) the type of anaerobic sludge (Hwu and Lettinga, 1997), (ii) presence of divalent cations in the medium (Koster and Cramer, 1987; Roy et al., 1985), and (iii) potential biomass adaptation (Alves et al., 2001). IC_{50} values towards the acetoclastic methanogens were also reported for linoleate (C18:2), stearate (C18:0) and palmitate (C16:0), i.e. 0.8 mM, 5.4 mM, and 4.3-6 mM, respectively (Pereira et al., 2005; Shin et al., 2003).

Bioreactor feeding strategy changed drastically from Period I (cycles) to Period II (continuous) but methanogenic community composition did not, since the same archaeal groups were identified (Figure 3.3). According to the DGGE profile (Figure 3.1), the most relevant changes on the methanogenic community occurred

during cycles 1 and 2 of Period I. Archaeal community diversity remained stable until the end of the experiment, i.e. diversity indices varied less than 12% and similarity between profiles was higher than 84% (Figure 3.2). Only during the first 100 days of the bioreactor operation LCFA accumulation was observed, and was efficiently biodegraded by the anaerobic consortium thereafter (Cavaleiro et al., 2009). This dynamics of LCFA accumulation/degradation probably contributed to the establishment of a methanogenic community adapted to the presence of high oleate concentrations. Besides acclimation of archaeal cells, high efficiency of the LCFA-degrading bacteria might also have contributed to the endurance of the prevailing methanogens.

The results obtained in this work emphasize that a correct equilibrium between LCFA adsorption and biodegradation can trigger microbial community adaptation, as previously suggested by Alves et al. (2001) and Pereira et al. (2004). The results also suggest that methanogenic microorganisms belonging to *Methanobacterium* and *Methanosaeta* genera are important to achieve efficient LCFA conversion to methane in continuous high rate anaerobic bioreactors treating LCFA rich wastewater.

Chapter 4

Activity and viability of methanogens in anaerobic digestion of unsaturated and saturated LCFA

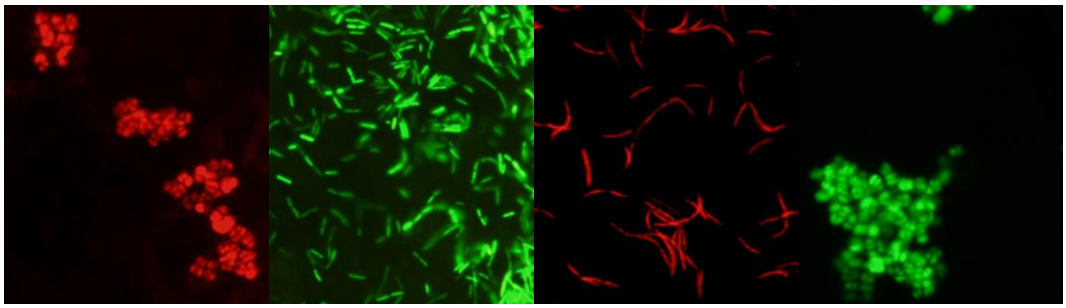

Lipids can be anaerobically digested to methane, but methanogens are often considered as highly sensitive to the long-chain fatty acids (LCFA) deriving from lipids hydrolysis. In this work, the effect of unsaturated (oleate, C18:1) and saturated (stearate, C18:0, and palmitate, C16:0) LCFA towards methanogenic archaea was studied in batch enrichments and in pure cultures. Overall, oleate had a more stringent effect on methanogens than saturated LCFA and the degree of tolerance to LCFA was different amongst distinct species of methanogens. *Methanobacterium formicicum* was able to grow in both oleate and palmitate-degrading enrichments, OM and PM cultures, while *Methanospirillum hungatei* only survived in PM culture. The two acetoclastic methanogens tested, *Methanosarcina mazei* and *Methanosaeta concilii*, could be detected in both enrichment cultures, with better survival in PM than in OM cultures. Viability tests using live/dead staining further confirmed that exponential growth phase cultures of *M. hungatei* are more sensitive to oleate than *M. formicicum* cultures; exposure to 0.5 mM of oleate damaged 99 ± 1 % of the cell membranes of *M. hungatei* and 53 ± 10 % of *M. formicicum*. In terms of methanogenic activity, *M. hungatei* was inhibited for 50% by 0.3, 0.4 and 1 mM of oleate, stearate and palmitate, respectively. *M. formicicum* was more resilient, since 1 mM of oleate and more than 4 mM of stearate or palmitate was needed to cause 50% inhibition on methanogenic activity.

Salvador AF, Sousa DZ, Ramos J, Guedes AP, Barbosa S, Stams AJM, Alves MM and Pereira MA (2013) Activity and viability of methanogens in anaerobic digestion of unsaturated and saturated long-chain fatty acids. Applied and Environmental Microbiology. doi:10.1128/AEM.00035-13

4.1 Introduction

Anaerobic degradation of long-chain fatty acids (LCFA) is essential for efficient biogas production from complex lipid-containing wastewaters (Alves et al., 2009; Pereira et al., 2004). However, there is still concern regarding the potential toxic effect of LCFA towards methanogenic communities. Toxicity of LCFA is the main reason for insufficient treatment results of LCFA-containing wastewaters (Angelidaki and Ahring, 1992; Hanaki et al., 1981; Hwu and Lettinga, 1997; Koster and Cramer, 1987; Rinzema et al., 1994). Studies of methanogenic inhibition in the rumen confirm the toxicity of these compounds. Soliva *et al.* (2004b) showed the anti-methanogenic potential of saturated fatty acids of medium chain length, specifically myristate (C14:0) and laurate (C12:0). The adverse effect of fatty acids towards methanogens appears to be more pronounced at longer chain length and more unsaturated bonds (Demeyer and Henderic, 1967; Prins et al., 1972). Besides, methanogens inhibition by fatty acids is a rapid phenomenon with long recuperation time, as shown by Koster (1987): 50% loss of methanogenic activity was observed after exposing methanogenic sludge to 7.5 mM laurate for only 7.5 minutes.

Sensitivity of microorganisms to LCFA seems to be related to their cell wall structure, with Gram-positive bacteria and methanogens being more easily inhibited than Gram-negative bacteria (Roy et al., 1985). Inhibition of pure cultures of methanogens by fatty acids is reported in literature (Prins et al., 1972) (Soliva CR et al., 2009). Nevertheless, methanogens are ubiquitous in anaerobic bioreactors treating LCFA-rich wastewaters, even over prolonged continuous

LCFA loading (Salvador et al., 2013; Sousa et al., 2007a). Sousa *et al.* (2007) identified three predominant genera of methanogens in LCFA-degrading sludges: *Methanobacterium*, *Methanosaeta* and *Methanosarcina*. *Methanobacterium*-related species were the predominant hydrogenotrophs in continuous bioreactors, together with acetoclastic methanogens closely related to *Methanosaeta concilli*. Batch incubation of sludges containing high concentrations of LCFA, stimulated the development of *Methanosarcina*, while *Methanosaeta* did not develop. The hydrogenotrophic methanogen, *Methanospirillum hungatei*, was identified in LCFA enrichment cultures (Roy et al., 1985). Recently, Salvador et al. (2013) reported the endurance of methanogenic archaea in continuously fed reactors treating oleate-based effluent, with *Methanobacterium* and *Methanosaeta* being the predominant genera of hydrogenotrophic and acetoclastic methanogens, respectively.

Understanding the effects of LCFA on growth of methanogens may provide insight to overcome potential problems occurring during the anaerobic digestion of lipid-rich wastewater. Both hydrogenotrophic and acetoclastic methanogens are essential for methane formation from complex lipid-containing wastewaters. If methanogenesis is inhibited LCFA conversion by anaerobic bacteria is no longer possible due to the syntrophic nature of LCFA conversion (McInerney et al., 2008; Schink and Stams, 2006). In this work the effect of unsaturated- and saturated-LCFA on methanogenic archaea was studied in two different experiments. First, the prevalence of pure cultures of acetoclastic and hydrogenotrophic methanogens in enrichment cultures degrading oleate (C18:1, unsaturated LCFA) or palmitate (C16:0, saturated LCFA) was investigated. In a second experiment, the effect of LCFA on methanogenic activity and membrane integrity of pure cultures of the

hydrogenotrophic methanogens, *Methanobacterium formicicum* and *Methanospirillum hungatei*, was studied.

4.2 Materials and methods

4.2.1 Source of enrichment cultures and microorganisms

Methanospirillum hungatei (DSM 864^T), *Methanobacterium formicicum* (DSM 1535^T) and *Methanosarcina mazei* (DSM 2053^T) were obtained from the Deutsche Sammlung von Mikroorganismen und Zellkulturen (DSMZ), Braunschweig, Germany. *Methanosaeta concilii* strain GP-6 (DSM 3671^T) was kindly provided by Caroline Plugge, Laboratory of Microbiology, Wageningen University, The Netherlands.

Oleate- and palmitate-degrading enrichment cultures (OM and PM cultures, respectively) used in this work have been previously described by Sousa *et al.* (19). OM and PM cultures were anaerobically grown in mineral medium containing 1 mM of oleate (C18:1, unsaturated LCFA) or 1 mM of palmitate (C16:0, saturated LCFA), as the sole carbon and energy sources. Both enrichment cultures were started from the same inoculum sludge originating from an anaerobic lab-scale reactor fed with LCFA-based effluent (Sousa et al., 2007b).

4.2.2 Medium composition and cultivation

Methanogenic pure cultures and enrichment cultures were cultivated under strictly anaerobic conditions in a bicarbonate-buffered mineral salt medium (Stams et al., 1993). The medium was dispensed into serum bottles that were subsequently sealed with butyl rubber septa and aluminum crimp caps. The headspace of serum bottles was flushed with a mixture of H_2/CO_2 or N_2/CO_2 (80:20; $1.7x10^5$ Pa): bottles used

for growing hydrogenotrophic methanogens (*M. hungatei* and *M. formicicum*) were flushed with H_2/CO_2; bottles for growing acetoclastic methanogens (*M. concilii* and *M. mazei*) and the enrichment cultures were flushed with N_2/CO_2. The bottles were autoclaved for 20 minutes at 121°C. Before inoculation, mineral medium was reduced with 0.8 mM sodium sulfide ($Na_2S.7\text{-}9H_2O$). For growing the acetoclastic methanogens, sodium acetate was added to the medium to a final concentration of 50 mM. Oleate and palmitate (sodium salts) were added to the enrichment cultures to a final concentration of 1 mM. All the inoculations and transfers were done aseptically using sterile syringes and needles. Cultures were incubated statically at 37°C and in the dark.

4.2.3 Selection of methanogenic partners in LCFA enrichments

To evaluate the selection of hydrogenotrophic partners in the enrichments, *M. hungatei* (Mh) and *M. formicicum* (Mf) (5%, v/v) were separately added to OM and PM enrichments as hydrogen scavengers. Cultures OM-Mh/PM-Mh and OM-Mf/PM-Mf were sub-cultured five times with 1 mM oleate/palmitate. Subsequently, to study the selection of acetoclastic methanogens in the enrichment cultures, OM-Mf and PM-Mh cultures were amended with *M. concilii* (Mc) and *M. mazei* (Mm) in four independent enrichment series: OM-Mf-Mc, PM-Mh-Mc, OM-Mf-Mm, and PM-Mh-Mm. These cultures were incubated with 1 mM oleate/palmitate and sub-cultured two successive times. Culture samples (10 mL) were withdrawn from all the enrichments before each transfer to evaluate the prevalence of methanogens by Denaturing Gradient Gel Electrophoresis (DGGE).

4.2.4 Methane production by pure cultures of hydrogentrophic methanogens in the presence of LCFA

Batch toxicity assays were performed to study the effect of unsaturated- and saturated-LCFA on pure cultures of *M. hungatei* and *M. formicicum*. Pure cultures of *M. hungatei* and *M. formicicum* were grown in 50 mL basal medium using 120 mL serum bottles. Headspace was flushed and pressurized to $1.7x10^5$ Pa with a mixture of H_2/CO_2 (80:20). After autoclaving, medium was inoculated with 10 mL of active methanogenic strains. Oleate, stearate (C18:0, saturated LCFA), and palmitate were added to exponentially growing cultures of *M. hungatei* and *M. formicicum* at different final concentrations (0.5, 1.0, 2.0 and 4.0 mM). Before LCFA addition, methane accumulated in the headspace was aseptically replaced by H_2/CO_2 (80:20; $1.7x10^5$ Pa) in order to guarantee no substrate limitations during exposure to LCFA. A control assay with no LCFA addition was also performed. Experiments were conducted in triplicates. The vials were incubated at 37°C without agitation. Methane production was measured over time. Inhibition caused by the LCFA was measured by comparing the differences in methane production rate (R_m) between cultures with LCFA (R_{m-LCFA}) with that of control cultures ($R_{m-control}$). Inhibition of different concentrations of the LCFA was defined as the percentage of the methane production rate of cultures with LCFA compared to control cultures without LCFA addition.

$$Inhibition\,(\%) = \frac{R_{m-LCFA}}{R_{m-control}} \times 100 \qquad \text{Eq. (1)}$$

Relative methane production rates were plotted against the concentration of the LCFA for calculation of the concentration of LCFA leading to 50% inhibition on methane production rate (inhibitory concentration, IC_{50}).

4.2.5 Effect of unsaturated-LCFA on membrane integrity of hydrogenotrophic methanogens

Membrane integrity of *M. hungatei* and *M. formicicum* grown with H_2/CO_2 in the presence of 0.5 and 1 mM oleate was analyzed using the LIVE/DEAD® BacLight™ bacterial viability kit (Invitrogen Molecular Probes). Oleate was added to cultures growing on H_2/CO_2, at the beginning of the exponential growth phase; bottles' headspace was flushed with H_2/CO_2 (80:20, 1.7×10^5 Pa) before oleate addition. A control assay in the absence of oleate was performed. Cells were stained by dual fluorescent dyes, a green-fluorescent nucleic acid stain, SYTO®9, and a red-fluorescent nucleic acid stain, propidium iodide (PI). SYTO®9 stains all cells but PI only stains those with damaged membranes. For this reason, microorganisms with intact cell membranes stain green fluorescent, whereas microorganisms with damaged membranes stain red fluorescent. One mL of culture sample was mixed in an eppendorf tube with 500 µl NaCl 0.85% and 0.5 µl of each stain, SYTO®9 and PI, and incubated for 15 minutes at room temperature and in the dark. The mixture was then filtered through 0.2 µm polycarbonate black filters (Whatman, Kent, UK). Filters were mounted with low-fluorescence immersion oil on glass microscope slides and observed on an epifluorescence microscope (Olympus BX51, x 60 magnification oil immersion objective) using FITC and Cy3 long pass filters. FITC filter reveals SYTO9 stained cells, corresponding to all cells, and Cy3 filter reveals those which are stained by both dyes and are thus damaged. From each membrane

10 to 20 randomly selected microscopic fields, each of 0.0158 mm^2, were photographed with a CCD camera (Olympus DP71) using an image acquisition software (Olympus Cell B). Images obtained with both filters, and corresponding to the same microscopic fields, were superposed and cells with damage and intact membranes were counted. All experiments were done in duplicate. Percentage of membrane-damaged cells was calculated in relation to the total number of cells.

4.2.6 Analytical methods

Methane was measured using a Pye Unicam GC-TCD gas chromatograph (Cambridge, England), with a Porapack Q (100-180 mesh) column. Helium was the carrier gas (30 mL min^{-1}) and the temperatures of the injection port, column and detector were 110, 35 and 110ºC, respectively. VFA were analyzed by high-pressure liquid chromatography from centrifuged (10,000xg, 10 min) samples of the culture media. VFA were measured with a Polyspher OA HY column (300 by 6.5 mm; Merck, Darmstadt, Germany) and an RI SE-61 refractive index detector (Shodex, Tokyo, Japan). The mobile phase was 0.01 N H_2SO_4 at a flow rate of 0.6 mL min^{-1}. The column temperature was 60ºC.

4.2.7 DNA extraction and amplification

Inoculum sludge used to start up the enrichment series OM and PM (5 mL), pure cultures of methanogens (10 mL) and enrichment cultures OM and PM amended with methanogens (10 mL) were concentrated by centrifugation (10,509×g, 10 min) at the time of sampling, frozen and stored at -20ºC. Total genomic DNA was extracted using a FastDNA SPIN kit for soil (MP Biomedicals, USA) in accordance with the manufacturer's instructions. Archaeal 16S rRNA genes were amplified by PCR using a Taq DNA polymerase kit (Invitrogen, Carlsbad, CA, USA); reaction

mixtures and PCR programs used were as described elsewhere (Sousa et al., 2007a). Primer set A109(T)-f/515-r (Grosskopf et al., 1998) was used for archaea 16S rRNA gene amplification for denaturing gradient gel electrophoresis (DGGE). A 40 bp GC-clamp was added at the 5' end sequence of the primer 515-r (Muyzer et al., 1993). Archaeal 16S rRNA genes were selectively amplified for cloning using the primer set Arch109-f/ Uni1492-r (Grosskopf et al., 1998; Lane, 1991). Size and yield of PCR products were estimated using a 100 bp DNA ladder (MBI Fermentas, Vilnius, Lithuania) via 1% (w/v) agarose gel electrophoresis and ethidium bromide staining.

4.2.8 DGGE analysis

DGGE analysis of the PCR products was performed with the DCode system (Bio-Rad, Hercules, CA, USA). Gels containing 8% (wt/vol) polyacrylamide (37.5:1 acrylamide/bis-acrylamide) were used with a linear denaturing gradient of 30–50%, with 100% of denaturant corresponding to 7 M urea and 40% (vol/vol) formamide. Electrophoresis was performed for 16 h at 85 V and 60 °C in a 0.5x Tris-acetate–EDTA buffer. DGGE gels were stained with silver nitrate (Sanguinetti et al., 1994) and scanned at 400 dpi.

4.2.9 Cloning and sequencing

A 16S rRNA gene PCR-based clone library was constructed using the DNA extracted from the enrichments inoculum sludge. The PCR product was purified with Nucleo Spin Extract II kit (Clontech Laboratories) and cloned into *E. coli* JM109 (NZYTech, Lisbon, Portugal) by using the Promega pGEM-T Easy vector

system (Promega, Madison, WI, USA) as previously described (Sousa et al., 2007a). Clones with the correct size insert were further amplified for DGGE comparison with the inoculum sample profile and enrichment cultures amended with methanogens. Plasmids of transformants (corresponding to predominant bands in the DGGE community fingerprint) were purified using the Nucleo Spin Extract II kit (Clontech Laboratories) and subjected to DNA sequence analysis. Sequencing reactions were performed at Macrogene (Amsterdam, The Netherlands). Consensus sequences obtained were checked for potential chimera artifacts using Pintail v1.1 software (Ashelford et al., 2005).

4.2.10 Phylogenetic analysis

Similarity searches for the 16S rRNA gene sequences were performed using the NCBI BLAST search program within the GenBank database (http://www.ncbi.nlm.nih.gov/blast/) (Altschul et al., 1990).

Nucleotide sequences obtained in this study have been deposited in the European Nucleotide Archive (ENA) under accession numbers HF955499 to HF955506.

4.2.11 Statistical analysis

The modified Gompertz equation was used to describe the progress of cumulative methane production by pure culture methanogens (Lay et al., 1998). Equation (Eq. 2) was used to calculate the maximum methane production rate in the toxicity assays.

$$M(t) = P\exp\left[-\exp\left[\frac{R_m e}{P}(\lambda - t) + 1\right]\right] \qquad \text{(Eq. 2)}$$

where $M_{(t)}$ = cumulative methane production at time t (mM), P = maximum methane production (mM), R_m = maximum methane production rate (mM day^{-1}),

e = 2.7182818, λ = lag-phase time (days). For each assay, all the individual measurements performed in the three replicates were utilized independently. R^2 values and the standard errors for each variable were calculated.

Significant differences between biological samples, during exposure to different concentrations of oleate, were determined using SPSS 19.0 statistic software.

Mann-Whitney U or Kruskal-Wallis tests were applied to non-viable cell counting data if two or more samples were compared at a time, respectively. Significant threshold was set at $p < 0.05$.

4.3 Results

4.3.1 Selection of methanogenic partners in LCFA enrichments

Predominant methanogens in the inoculum sludge used in OM and PM were identified by 16S rRNA gene cloning and sequencing (Table 4.1). Hydrogenotrophic community was dominated by microorganisms clustering within the *Methanobacteriales* and *Methanomicrobiales* orders. *Methanosaeta*- and *Methanosarcina*-related species were the acetoclastic predominant methanogens.

LCFA conversion relies on syntrophic interactions between acetogenic LCFA degraders and hydrogenotrophic methanogens (Sousa et al., 2009a). To guarantee high numbers of hydrogen-consuming methanogens in the enrichment procedure, it is current practice to supplement the enrichment cultures with pure cultures of hydrogenotrophs upon transfers. *Methanospirillum hungatei* and *Methanobacterium formicicum* are normally chosen as hydrogenotrophic partners for the enrichment and isolation of fatty acids-degrading bacteria (Stams et al., 2012). In this study the prevalence of *M. hungatei* DSM 864^T and *M. formicicum*

DSM 1535^T in cultures OM and PM was studied during five subsequent transfers of the LCFA-degrading enrichments. Presence or absence of these methanogens in enrichment cultures, after the degradation of 1 mM of oleate or palmitate, was assessed by 16S rRNA gene PCR-DGGE (Figure 4.1).

Table 4.1 Affiliation of the archaeal clones retrieved from the OM and PM enrichments inoculum sludge.

Band ID	Clone	Closest relative [1]	% Identity
1	C8-lcfa	*Methanobacterium* sp. OM15	99
		Methanobacterium formicicum MG-134	99
2	G1-lcfa	*Methanosaeta concilii* GP-6	99
3	A9-lcfa	Uncultured archaeon clone MCSArc_B6	98
		Methanoculleus bourgensis MS2	98
4	A5-lcfa	*Methanosaeta concilii* GP-6	99
5	A1-lcfa	Uncultured *Methanospirillum* sp. clone sagar115	99
		Methanospirillum hungatei JF-1	99
6	A6-lcfa	*Methanosarcina mazei* Tuc01	96
7	A2-lcfa	*Methanosarcina mazei* Tuc01	100
8	G2-lcfa	*Methanosarcina mazei* Tuc01	99

[1] Closest relative species of the selected clones determined by NCBI blast search. In cases where the first closest database hit was an uncultured microorganism the first hit of a cultured microorganism is also given.

M. hungatei succeeded to co-exist with *M. formicicum* in the PM enrichment culture, even when *M. formicicum* was the amended methanogenic partner (Figure. 4.1B, lanes PM-Mf(1) to PM-Mf(4)). However, in OM enrichments, *M. hungatei* did not prevail following its repeated addition to the enrichment cultures (Figure 4.1A, lanes OM-Mh(1) to OM-Mh(5)). *M. formicicum* sustained in the presence of oleate and grew in the OM enrichment cultures, as revealed by the

presence of a predominant DGGE-band corresponding to this methanogen after the second transfer in oleate (Figure 1A, lanes OM-Mf(2) to OM-Mf(5)).

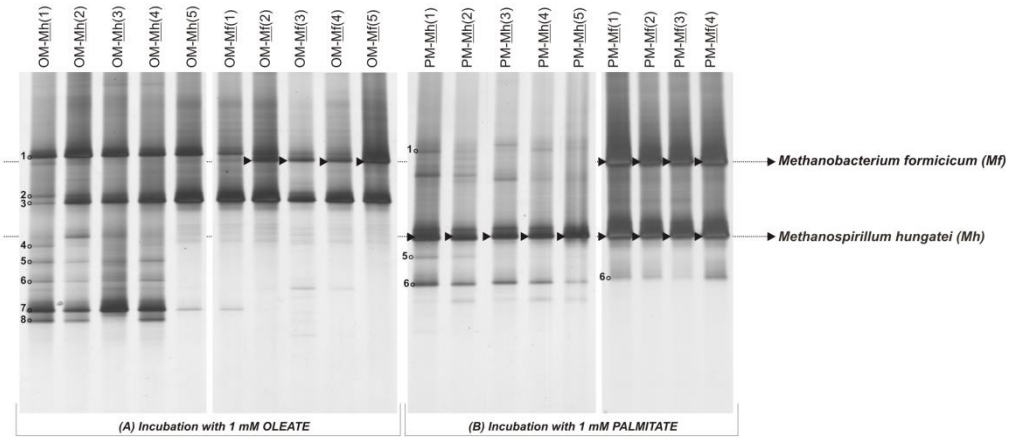

Figure 4.1 DGGE pattern of archaeal 16S rRNA gene fragments present in OM and PM enrichment cultures during successive transfers with addition of *Methanospirillum hungatei* (Mh) or *Methanobacterium formicicum* (Mf) as hydrogen consumers. Arrows indicate the presence of added methanogens in the enrichment cultures. Numbers from 1 to 8 indicate the DGGE bands identified by cloning and sequencing (phylogenetic affiliation in Table 4.1); clones were retrieved from the inoculum sludge used to start-up enrichment series OM and PM.

A similar approach was used to investigate the prevalence of the acetoclastic methanogens *M. concilii* and *M. mazei* in cultures OM and PM. The hydrogenotrophic methanogens *M. formicicum* and *M. hungatei* were also added to the OM and PM enrichments, respectively (and in view of the previous results), to guarantee efficient hydrogen consumption. *M. concilii* and *M. mazei* were detected in OM and PM cultures as shown in Figure 4.2. Nevertheless, DGGE bands corresponding to *M. concilii* and *M. mazei* showed higher relative intensity (compared with other bands in the same samples) in the PM than in the OM culture DGGE profile, which suggests that these methanogens were more abundant in the PM culture than in the OM culture (Figure 4.2). No acetate was detected in PM cultures amended with *M. concilii*, which shows that this acetoclast could

efficiently consume acetate derived from palmitate oxidation. *M. mazei* was not as efficient in maintaining acetate at low concentrations, likely due to its higher half-saturation coefficient (Ks) for acetate (Jetten et al., 1992), which accumulated in the medium of cultures PM-Mh-Mm at a ratio of 6.6 mol acetate/mol palmitate added. In OM cultures acetate accumulated both in the presence of *M. concilii* and *M. mazei* in amounts of 6.5-8.0 mol acetate/mol oleate added, which are close to stoichiometric values considering complete oleate oxidation. This indicates that acetoclastic activity was affected by oleate, which is coherent with the DGGE results. Methane production in OM cultures, 1.7 ± 0.2 mol CH_4 / mol oleate added, could be justified just by hydrogenotrophic activity.

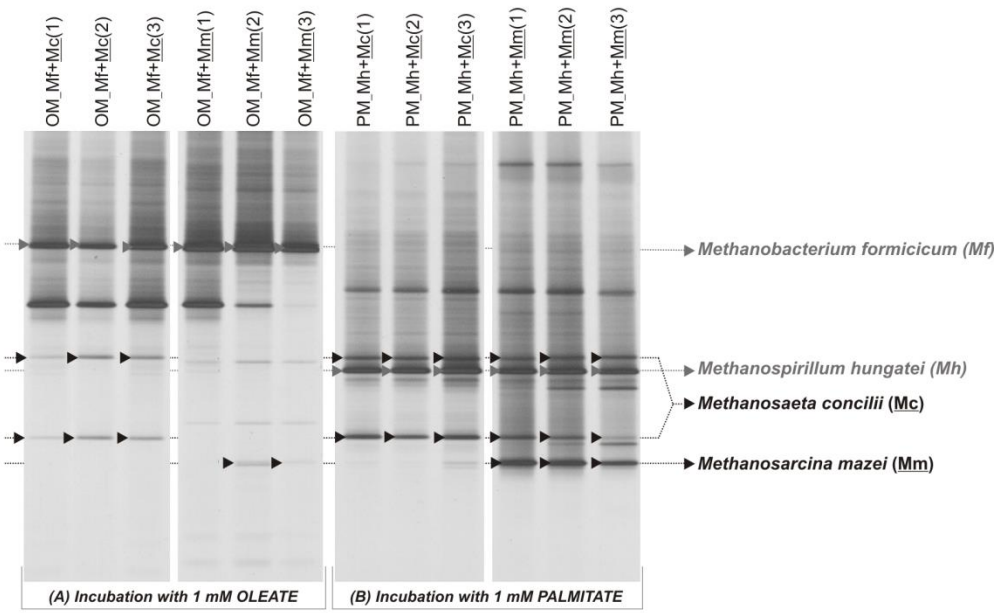

Figure 4.2 DGGE pattern of archaeal 16S rRNA gene fragments present in OM and PM enrichment cultures during successive transfers with addition of *Methanosaeta concilii* (Mc) or *Methanosarcina mazei* (Mm) as acetate consumers. *Methanospirillum hungatei* (Mh) and *Methanobacterium formicicum* (Mf) were added to PM and OM cultures, respectively, to ensure low hydrogen concentration during LCFA degradation. Arrows indicated the presence of added methanogens in the enrichment cultures.

4.3.2 Methane production by pure cultures of hydrogenotrophic methanogens in the presence of LCFA

The hydrogenotrophic methanogens, *M. hungatei* and *M. formicicum*, were selected to further evaluate the differential toxic effect of unsaturated and saturated LCFA. For comparison, two C18 LCFA with different degree of saturation were used: oleate (unsaturated LCFA, C18:1) and stearate (saturated LCFA, C18:0). Palmitate (saturated LCFA, C16:0) was also selected to evaluate the potential effect of the hydrocarbon chain length. Methane production rate from H_2/CO_2 by pure cultures of *M. hungatei* and *M. formicicum*, in the presence of unsaturated and saturated LCFA, and respective half inhibitory concentrations (IC50), are shown in Table 4.2. Overall, LCFA affected both *M. hungatei* and *M. formicicum,* as translated by a decrease in methane production rate in the presence of LCFA, even for LCFA concentrations as low as 0.5 mM (Figure. S4.1 in the supplementary material). Effect of oleate on *M. hungatei* was severe, with only 0.5 mM oleate causing a decrease of approximately 60% in methane production rate from H_2/CO_2. The same oleate concentration had no major effect on the methane production rate of *M. formicicum*, but concentrations above 1 mM had a strong effect on this methanogen as well. A reduction in methane production rate of 84-93% was observed in the presence of oleate concentration $\geq$ 2 mM (i.e. from 1.81 ± 0.13 mM CH_4 d^{-1} (in control assay) to 0.29 ± 0.06 and 0.12 ± 0.01 mM CH_4 d^{-1} in the presence of 2 and 4 mM oleate, respectively – Table 4.2). Stearate and palmitate were less inhibitory to *M. formicicum* than to *M. hungatei* cultures. Stearate or palmitate concentration of 4 mM caused less than 50% inhibition of *M. formicicum* pure cultures, while *M. hungatei* IC_{50} values were 0.4 and 1 mM for stearate and palmitate, respectively.

Table 4.2 Methane production rate by hydrogenotrophic methanogens in the presence of different concentrations of LCFA and inhibitory concentration (IC50) required for 50% inhibition of hydrogenotrophic methanogens exposed to LCFA.

		Methanospirillum hungatei		*Methanobacterium formicicum*	
	LCFA concentration (mM)	Methane production rate[1] (mM CH_4 d^{-1})	IC_{50} (mM)	Methane production rate[1] (mM CH_4 d^{-1})	IC_{50} (mM)
no LCFA	-	4.24 ± 0.27	-	1.81 ± 0.13	-
oleate	0.5	1.58 ± 0.12	0.3	1.82 ± 0.10	1.0
	1.0	1.49 ± 0.18		0.86 ± 0.04	
	2.0	1.31 ± 0.13		0.29 ± 0.06	
	4.0	1.01 ± 0.15		0.12 ± 0.01	
stearate	0.5	1.81 ± 0.35	0.4	1.78 ± 0.12	> 4.0
	1.0	2.38 ± 0.33		1.79 ± 0.15	
	2.0	2.04 ± 0.20		1.44 ± 0.16	
	4.0	1.11 ± 0.14		1.05 ± 0.09	
palmitate	0.5	2.69 ± 0.32	1.0	1.62 ± 0.13	> 4.0
	1.0	2.39 ± 0.27		1.08 ± 0.17	
	2.0	0.67 ± 0.07		0.95 ± 0.04	
	4.0	0.50 ± 0.07		1.05 ± 0.09	

[1] Values calculated by fitting experimental data (triplicates) to the Gompertz model (Lay et al 1998); $0.901 < R^2 < 0.987$

4.3.3 Effect of unsaturated-LCFA on membrane integrity of hydrogenotrophic methanogens

The effect of oleate on membrane integrity of *M. hungatei* and *M. formicicum* was studied in order to further evaluate the resistance of these two microorganisms towards the presence of unsaturated LCFA (Figure 4.3).

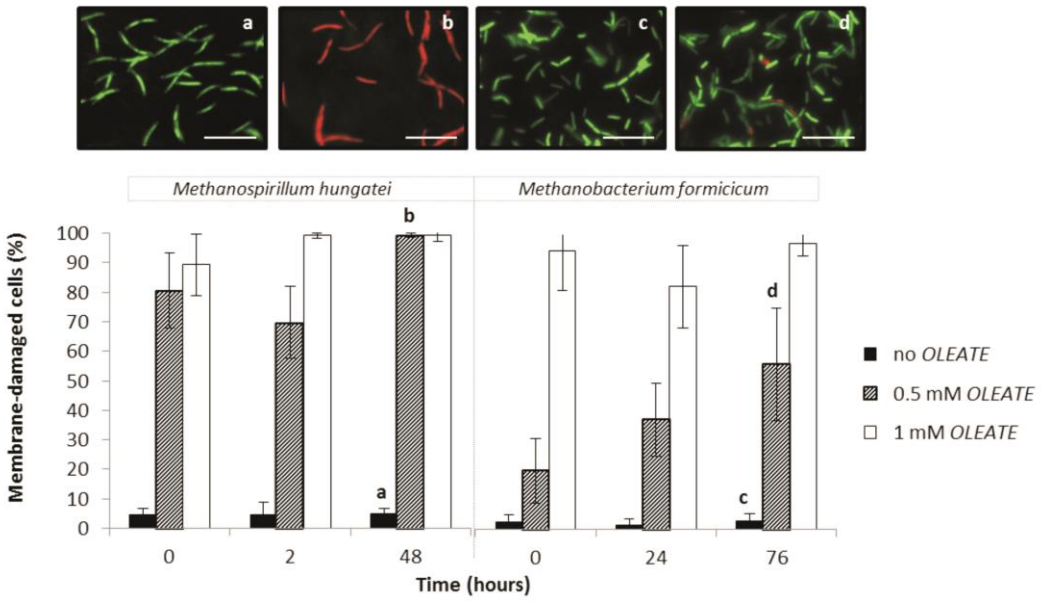

Figure 4.3 Percentage of membrane-damage cells of *M. hungatei* and *M. formicicum* in pure cultures when growing on H_2/CO_2, without LCFA addition and in the presence of 0.5 and 1 mM of oleate. Live/dead staining images of *M. hungatei* and *M. formicicum* – leters (a,b,c,d) correlate images with assay and sampling time in the graph. Scale bar, 10 μm.

Membrane integrity of *M. hungatei* and *M. formicicum* cells was affected by the presence of oleate. The adverse effect of oleate on membrane integrity of *M. hungatei* is obvious, even for the lowest oleate concentration tested and immediately after LCFA addition. Percentage of *M. hungatei* damaged cells just after the supplementation of 0.5 mM oleate to the medium was as high as 81 ± 13 %, compared to 5 ± 2 % of cells damaged in the control assay ($p=0.003$). After 48 h of exposure of this microorganism to 0.5 mM or 1 mM oleate about 99% of the cells were damaged, while in the control assay damaged cell membranes represented less than 7 % of all the cells ($p<0.001$). *M. formicicum* could endure better the lower concentration of oleate (0.5 mM), with just 56 ± 19 % cells damaged after 76 hours of incubation (this value is highly significantly different from the percentage of *M. hungatei* damaged cells measured after 48 h contact with 0.5 mM oleate,

$p<0.001$). Nevertheless, oleate at a final concentration of 1 mM had a similar fast and severe injuring effect on the cell membranes of both methanogens with around 90% of the cells damaged just after the addition of the inhibitor.

4.4 Discussion

This research shows that the response of methanogens to saturated- and unsaturated-LCFA is diverse. Prevalence of *M. hungatei* and *M. formicicum* in LCFA-degrading enrichments was dependent on the saturation degree of the fatty-acids (Figure 4.1). *M. formicicum* could prevail in OM and PM enrichments, but *M. hungatei* was only detected in PM enrichments (Figure 4.1). Considering the absolute methane production rate, H_2/CO_2 conversion to methane by *M. hungatei* is faster than by *M. formicicum*, even in the presence of LCFA (Table 4.2). However, the decrease on the methane production rate in the cultures incubated with LCFA, when compared with the control assays (without LCFA), is noticeable sharper in *M. hungatei* cultures. As a consequence lower IC50 for oleate were obtained for *M. hungatei* (0.3 mM) than for *M. formicicum* (1 mM). OM enrichments were amended with 1 mM oletate, which can partially explain the endurance of *M. formicicum* in the OM enrichments. Other factors might affect the structure and methanogenic composition of LCFA-degrading enrichment mixed cultures; the existence of syntrophic interactions likely has an important role in the selection of certain methanogens. *M. hungatei* has been isolated from sewage sludge (Ferry et al., 1974) and, although frequently detected in anaerobic reactors, *Methanobacterium* species seem to have highest predominance in digesters sludge (Leclerc et al., 2004). Moreover, *Methanobacterium*-related microorganisms have been detected as the predominant hydrogen scavengers in oleate-contacting sludges

(Pereira et al., 2002b; Salvador et al., 2013; Sousa et al., 2007a). Microorganisms closely related to both of these species were also detected in the inoculum sludge used in OM and PM enrichments (Table 4.1), which has previously been in contact with LCFA in continuous-batch reactor indicating their importance during the degradation of these substrates. *M. hungatei* and *M. formicicum* are metabolically similar, but their cell envelope properties are different (Whitman et al., 2006). Cells of *M. formicicum* have a rigid pseudomurein wall, while *M. hungatei* cells have a proteinaceous cell surface structure and are normally covered by a sheath that encloses several cells and make the cells in the middle of the filament less permeable (Beveridge et al., 1991; Koga et al., 1993). Membrane lipid-composition in *M. hungatei* and *M. formicicum* membranes is also different (Koga et al., 1993; Koga et al., 1998; Koga and Morii, 2005). *M. formicicum* has four different phospholipids (inositol, ethanolamine, serine and aminopentanetetrol) compared with only two in *M. hungatei* (glycerol and aminopentanetetrol). Differences in membrane composition between the two tested hydrogenotrophs may be related to the differential vulnerability to LCFA. In fact, membrane damage in *M. hungatei* was more severe than in *M. formicicum*, as evidenced in the cell viability assays performed in this study (Figure 4.3). Jarrell et al. (1987) verified that, when exposed to ammonia, butyrate and propionate, *M. hungatei* was more sensitive than *M. formicicum*, which is in line with the higher susceptibility of *M. hungatei* to LCFA as observed in our work. It should be noted that toxicity and live-dead assays were performed using pure cultures of methanogens; in a bioreactor, and as part of complex syntrophic communities, methanogens might have extra protection to endure higher LCFA concentrations.

The acetoclastic methanogens, *M. mazei* and *M. concilii*, were both successfully integrated in PM cultures (Figure 4.2), but in OM cultures acetate accumulated to almost stoichiometric concentrations to the corresponding complete oleate oxidation. Also for the tested acetoclasts, oleate seems to have a more stringent effect than palmitate. This could be related to a higher susceptibility of acetoclastic methanogens to oleate, as happens with hydrogenotrophic methanogens. The study by Sousa *et al.* (2007a) describes OM and PM enrichments. Throughout a 2-years period, OM and PM cultures were transferred to enrich for oleate- and palmitate degraders; at the moment of the transfers no acetoclastic methanogens were supplemented. Stable OM enrichments could convert oleate, but acetate accumulated in the medium and was no further converted to methane. Conversely, microbial communities in PM enrichments could convert acetate completely to methane. This indicates that acetoclasts were eliminated from OM cultures over the enrichment process, which can be due to low growth rates of these microorganisms in the presence of oleate. Live-dead assays could give further insights on membrane damage of acetoclasts by LCFA. However, both *Methanosaeta* and *Methanosarcina* species form dense aggregates and we did not succeed to perform single cell counting. Nevertheless, it was clear from the OM and PM incubations that oleate is more toxic than palmitate to both *M. concilii* and *M. mazei*. It is reported that toxicity of fatty acids increases with the degree of unsaturation of the molecule (Prins et al., 1972). Prins *et al.* (1972) determined the IC50 values for pure cultures of rumen methanogens in the presence of linolenate (C18:3) and linoleate (C18:2), observing IC50 values of about 1.8 fold higher for linolenate. However, the mechanisms underlying this differential effect are not completely understood. The bent conformation of unsaturated and poly-unsaturated LCFA might influence the

way that these acids interact with cell membranes, potentiating their toxicity. Results in this work show that LCFA have an effect on membrane integrity of methanogens, and this effect is more pronounced when considering unsaturated LCFA. These findings should stimulate further investigation on the mechanisms of methanogenic inhibition by LCFA.

Chapter 5

Physiological and molecular characterization of methanogenic and non-methanogenic oleate-degrading enrichment cultures

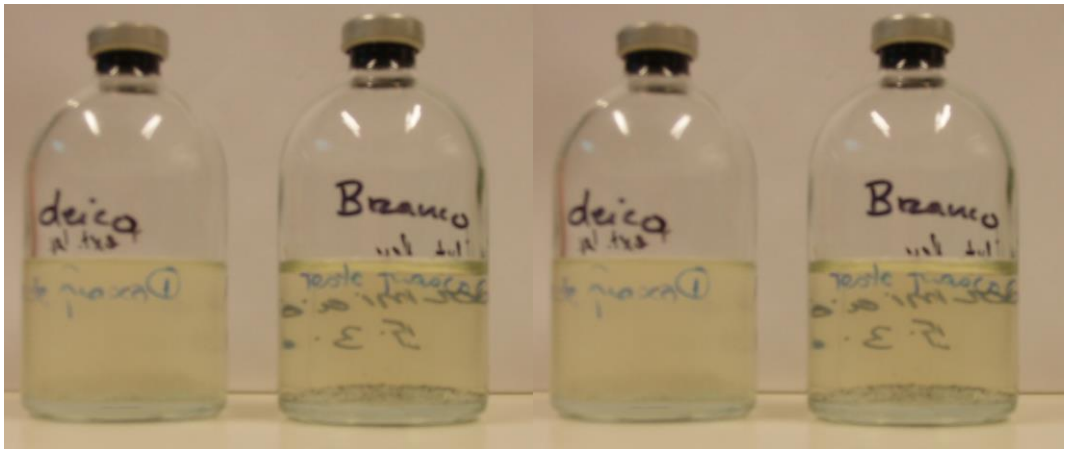

Syntrophic degradation of long-chain fatty acids (LCFA) relies on the close cooperation of syntrophic bacteria with hydrogen scavengers, usually hydrogenotrophic methanogens. In this work methanogenic and methanogenic-inhibited enrichment cultures degrading unsaturated-LCFA (oleate – C18:1) were obtained and physiologically characterized. Oleate degradation by the methanogenic enrichment resulted on methane production via hydrogenotrophic methanogenesis and on acetate accumulation, caused by the loss of acetoclastic activity. Acetate was also the main product of oleate conversion by methanogenic-inhibited enrichment cultures, most likely produced by the activity of hydrogen consuming homoacetogens. In a third assay both methanogenic and homoacetogenic activities were prevented and oleate was still converted to acetate, although reactions and microbial interactions remain unclear. Diversity of enrichment cultures was assessed by 16S rRNA gene PCR-DGGE, cloning and sequencing. Bacterial sequences were assigned to *Syntrophomonas zehnderi*, *Sporanaerobacter acetigenes*, *Mycobacterium frederiksbergense* and to *Desulfovibrio* species whereas archaeal sequences corresponded to hydrogenotrophs belonging to *Methanobacterium* and *Methanoculleus* genera. *S. zehnderi* is a LCFA-utilizing bacterium that was identified in all oleate incubations, likely converting oleate to hydrogen and acetate in both methanogenic and non methanogenic enrichments either by cooperating respectively with methanogens or with other hydrogen scavengers.

5.1 Introduction

Long-chain fatty acids (LCFA) can be converted to methane by the cooperation of syntrophic acetogenic bacteria with hydrogenotrophic and acetoclastic methanogens (Sousa et al., 2009a). Acetoclastic activity is needed to achieve complete conversion of LCFA to methane but hydrogenotrophic activity is mandatory to keep low levels of hydrogen that are necessary to allow the continuity of LCFA degradation by bacteria, otherwise LCFA degradation is thermodynamically unfavorable (Table 5.1, reaction 1) (Schink, 1997; Sieber et al., 2012).

Table 5.1 Possible reactions involved in the syntrophic conversion of oleate (adapted from (Schink, 1997; Sousa et al., 2007b; Thauer et al., 1977)).

Reaction		Equation	$\Delta G^{0'}$ (kJ reaction^{-1})[(a)]
1	Oleate degradation	$C_{18}H_{33}O_2^- + 16\ H_2O \rightarrow 9\ C_2H_3O_2^- + 15\ H_2 + 8\ H^+$	+338
2	Acetoclastic methanogenesis	$C_2H_3O_2^- + H_2O \rightarrow HCO_3^- + CH_4$	-31
3	Hydrogenotrophic methanogenesis	$4H_2 + HCO_3^- + H^+ \rightarrow CH_4 + H_2O$	-136
4	Homoacetogenesis	$4\ H_2 + 2\ HCO_3^- + H^+ \rightarrow C_2H_3O_2^- + 2\ H_2O$	-105

[(a)] Gibbs free energy changes (at 25°C) calculated at standard conditions (solute concentrations of 1 M and gas partial pressure of 10^5 Pa).

Acetoclastic methanogens are somehow sensitive to oleate (C18:1), and acetate tends to accumulate during oleate degradation by specialized oleate-degrading enrichment cultures, even after extended incubation (Sousa et al., 2007b). Moreover, hydrogenotrophic methanogens are also more sensitive to oleate than to other LCFA, namely palmitate (C16:0) and stearate (C16:0) (Sousa et al., 2013) (Chapter 4). Hydrogen scavengers, other than hydrogenotrophs, may contribute for oleate degradation in anaerobic systems. For example, homoacetogenic bacteria can

grow autotrophically on hydrogen together with carbon dioxide, being acetate the sole metabolic end product (Table 5.1, reaction 4) (Diekert and Wohlfarth, 1994). The collaboration between LCFA degrading bacteria and homoacetogenic bacteria in anaerobic treatment systems could be an interesting alternative for elevated acetate production, which is also a building block of interest for biotechnological applications. Most common hydrogen oxidizing methanogens in mesophilic LCFA degrading environments include *Methanobacterium* and *Methanospirillum* species (Pereira et al., 2002b; Salvador et al., 2013; Shigematsu et al., 2006; Sousa et al., 2007a) (Table 2.5). LCFA degradation under sulfate reducing conditions favors the growth of hydrogen utilizing sulfate reducing bacteria related to *Desulfovibrio*, *Desulfohabdus* and *Desulfomicrobium* genera (Sousa et al., 2009c). However, there is no information about non-methanogenic hydrogen consuming microorganisms in anaerobic LCFA degrading systems in the absence of external electron acceptors such as sulfate or nitrate.

In this work, we aim to get more insights into anaerobic oleate conversion promoting the cooperation of oleate degraders with methanogens or with alternative hydrogen scavengers. Oleate degrading enrichment cultures growing under methanogenic or non-methanogenic conditions were physiologically characterized and microbial composition of well-established communities was investigated by PCR-DGGE fingerprinting and 16S rRNA gene sequencing.

5.2 Materials and methods

5.2.1 Inoculum source and characterization of oleate-degrading enrichment cultures

Suspended anaerobic sludge (ETAR do Freixo, Porto, Portugal) was acclimated to LCFA in a continuous anaerobic bioreactor (2.8 L) operated at 37°C during 15 days. The substrate was a mixture of LCFA at a final concentration of 1 mM (41% as oleate, 44% as stearate and 15% as a mixture of myristate and palmitate). The organic loading rate applied was 1g COD L^{-1} day^{-1} and the hydraulic retention time was 1 day. This substrate was supplemented with macronutrients, micronutrients, and $NaHCO_3$, as described elsewhere (Alves et al., 2001). The acclimated sludge was washed once with anaerobic medium to remove part of the accumulated substrate and incubated at 37°C and in batch during 25 days, for complete substrate consumption, until methane production stabilized.

Enrichment series were performed in 120 ml serum bottles, sealed with butyl rubber septa and aluminum crimp caps, and containing 50 ml of anaerobic bicarbonate-buffered mineral salt medium (Sousa et al., 2007b). The headspace of serum bottles was flushed with a mixture of N_2/CO_2 (80:20; $1.7x10^5$ Pa) and sterilized by autoclaving. The medium was subsequently reduced with 0.8 mM sodium sulfide ($Na_2S.7-9H_2O$) and supplemented with a vitamins solution (Stams et al., 1993).

Two distinct enrichment series were started by adding oleate (methanogenic enrichments, cultures OL-M) or oleate plus bromoethanesulfonate (methanogenic inhibited enrichments, cultures OL-MI) to the serum bottles (Figure 5.1). Sodium oleate was added sterile to a final concentration of 1 mM and bromoethanesulfonate

(BrES) was used as methanogenic inhibitor (Zinder et al., 1984), at a final concentration of 20 mM. Enrichments were performed in duplicate. Methanogenic and methanogenic-inhibited oleate-degrading enrichment cultures were obtained after 5 successive transfers of active cultures (10% v/v) into new medium containing oleate and oleate plus BrES, respectively, during approximately one year. Stable methanogenic and non-methanogenic enrichments were transferred one more time for further characterization. A control assay (OL-MI-P) was done to avoid homoacetogenesis and for that propose, phosphate buffered medium (20 mM, pH 7.0, pressurized with 100 % N_2 at 1.7 x 10^5 Pa) instead of bicarbonate buffered medium was used (Figure 5.1). All the assays were performed in triplicate. The inoculation and the addition of sterile solutions were made using syringes and needles under sterile conditions. All bottles were incubated at 37°C, without shaking and in the dark.

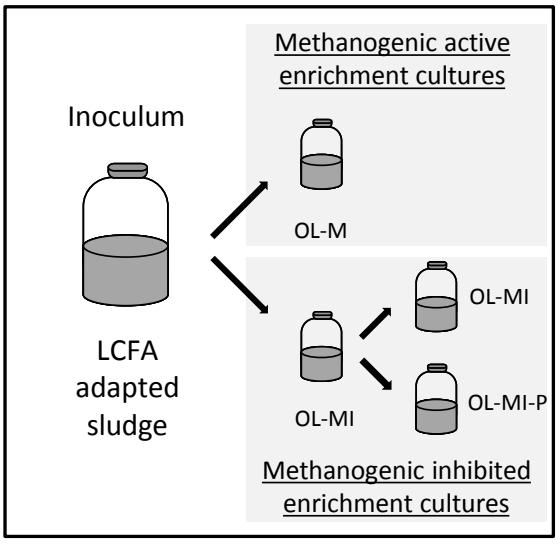

Figure 5.1 Different enrichment series for obtaining oleate degrading cultures under methanogenic active and methanogenic-inhibited conditions. A common inoculum was used to begin the enrichment series OL-M and OL-MI. Stable OL-MI enrichment culture was used to inoculate the OL-MI-P enrichment culture.

Physiological characterization of stable enrichment cultures was performed through LCFA, volatile fatty acids (VFA) and methane quantification during oleate degradation. Microbial communities' composition established after 28 days of incubation was investigated by PCR-DGGE and 16S rRNA gene cloning and sequencing.

5.2.2 Analytical methods

Methane concentration in the serum bottles headspace was measured by gas chromatography (Chrompack CP 9000), using a Porapak Q column and a flame ionization detector. N_2 was used as gas carrier. Injection port, column and detector temperatures were 100, 35 and 220 °C, respectively. Mixed liquor samples were periodically withdrawn from the bottles for VFA and LCFA quantification. VFA were analyzed by HPLC (Jasco, Japan) using a Chrompack organic analysis column (30×6.5 mm) with a mobile phase of 5 mM H_2SO_4 at a flow rate of 0.6 mL min^{-1}. The column temperature was set at 60°C and the detection was made spectrophotometrically at 210 nm. LCFA were extracted and quantified as described elsewhere (Neves et al., 2009). Esterification of free fatty acids was performed with propanol, in acid medium (3.5 hours at 100°C). Propyl esters were further extracted with dichloromethane and analyzed in a gas chromatograph (Varian 3800) equipped with a flame ionization detector and a eq.CP-Sil 52 CB 30 m x 0.32 mm x 0.25 μm capillary column (Teknokroma, TR-WAX). Helium was used as carrier gas at a flow rate of 1.0 mL min^{-1}. Initial oven temperature was set at 50 °C for 2 min and final temperature of 225 °C was attained with a ramp rate of 10°C min^{-1}. Injector and detector temperatures were 220°C and 250°C, respectively.

5.2.3 Molecular methods

10 ml of well-homogenized enrichment cultures OL-M, OL-MI and OL-MI-P were concentrated by centrifugation (10,509×g, 10 min) and stored at -20ºC. RNA latter was added, at the time of sampling, to stabilize and protect cellular RNA. RNA was extracted using a FastRNA Pro Soil-Direct Kit (MP Biomedicals, USA) in accordance with the manufacturer's instructions. cDNA was produced using SuperScript® Reverse Transcriptase III (Life Tecnologies) and random primers.

16S rRNA genes were amplified by PCR using a Taq DNA polymerase kit (Invitrogen, Carlsbad, CA, USA). Primer sets U968-f/1401-r (Nübel et al., 1996) and A109(T)-f/515-r (Grosskopf et al., 1998; Lane, 1991) were used respectively for bacterial and archaeal 16S rRNA gene amplification for denaturing gradient gel electrophoresis (DGGE) and for cloning. A 40 bp GC-clamp was added at the 5' end sequence of primers U968-f and 515-r (Muyzer et al., 1993). Reaction mixtures and PCR programs are described elsewhere (Sousa et al., 2007a). Size and yield of PCR products were estimated using a 100 bp DNA ladder (MBI Fermentas, Vilnius, Lithuania) via 1% (w/v) agarose gel electrophoresis and safe green staining.

DGGE analysis of the PCR products was performed with the DCode system (Bio-Rad, Hercules, CA, USA). Gels containing 8% (wt/vol) polyacrylamide (37.5:1 acrylamide/bis-acrylamide) were used with a linear denaturing gradient (30–60% for the separation of bacterial amplicons and 30-50% for archaeal amplicons), with 100% of denaturant corresponding to 7 M urea and 40% (vol/vol) formamide. Electrophoresis was performed for 16 h at 85 V and 60 °C in a 0.5x Tris-acetate–EDTA buffer. DGGE gels were stained with silver nitrate (Sanguinetti et al., 1994) and scanned at 400 dpi.

PCR products previously purified with Nucleo Spin Extract II kit (Clontech Laboratories) were cloned into *E. coli* JM109 (NZYTech, Lisbon, Portugal) by using the Promega pGEM-T Easy vector system (Promega, Madison, WI, USA) as previously described (Sousa et al., 2007a). Clones with the correct size insert were further amplified for DGGE comparison with original sample profiles (OL-M, OL-MI, OL-MI-P and OL-MA, with OL-MA corresponding to the characterization of archaeal community from OL-M enrichment culture). Plasmids of transformants, corresponding to predominant bands in the DGGE community fingerprint, were purified using the Nucleo Spin Extract II kit (Clontech Laboratories) and subjected to DNA sequence analysis. Sequencing reactions were performed at Macrogene (Amsterdam, The Netherlands). DNA sequences obtained were compared with those in the NCBI database using nucleotide BLAST (http://blast.ncbi.nlm.nih.gov/Blast.cgi). Phylogenetic assignment of 16S rDNA sequences was confirmed with the ribosomal database project (RDP) classifier (Wang et al., 2007).

5.3 Results

5.3.1 Physiological characterization of oleate-degrading enrichment cultures

Oleate concentration in OL-M cultures decreased to undetectable levels after 70 days of incubation (Figure 5.2). Oleate degradation was followed by acetate accumulation in the medium at a maximum concentration of 7.6 ± 0.2 mM (Figure 5.2), a value close to the stoichiometry of oleate β-oxidation to acetate and hydrogen (Table 5.1, reaction 1). Further conversion of acetate to methane and carbon dioxide did not occur during the 113 days of incubation. No other VFA

neither intermediary LCFA were detected in the liquid. Cumulative methane production (2.9 ± 0.4 mM) was low when compared with the theoretical methane production that could be expected from complete oleate conversion to methane, i.e. 12.75 mM (Table 5.2, reactions 1, 2 and 3). This can be explained as methane was produced exclusively from hydrogen by hydrogenotrophic archaea.

Methanogenesis was successfully inhibited by the addition of BrES in OL-MI enrichment culture, since no methane was detected during the assay. Acetate accumulated faster than in the methanogenic enrichment (OL-M), achieving its maximum value after 17 days of incubation (Figure 5.2, b) and higher acetate concentrations were obtained, i.e. 10.3 ± 0.3 mM. This value agrees well with the stoichiometry of oleate conversion to acetate under non-methanogenic conditions giving place for homoacetogenic activity (Table 5.1, reactions 1 and 4). Palmitate was transiently quantified in the medium at concentrations lower than 0.24 ± 0.01 mM. Shorter chain fatty acids, butyrate (C4:0) and hexanoate (C6:0) accumulated in the medium (up to 0.4 mM) after 13 days of incubation and further degradation did not occur during the time course of the experiment (Figure 5.2, b). OL-MI-P enrichment cultures succeed to degrade oleate (Figure 5.2, c) and after approximately 40 days of incubation oleate was no longer detected in the medium. Acetate accumulated in the medium from the first days of incubation on and reached its maximum concentration (7.7 ± 0.7 mM) after 113 days (Figure 5.2, c). Hexanoic (C6:0) and decanoic acids (C10:0) concentrations (approximately 0.3 mM each) were detected from day 70 on and further degradation did not occur until the end of the experiment.

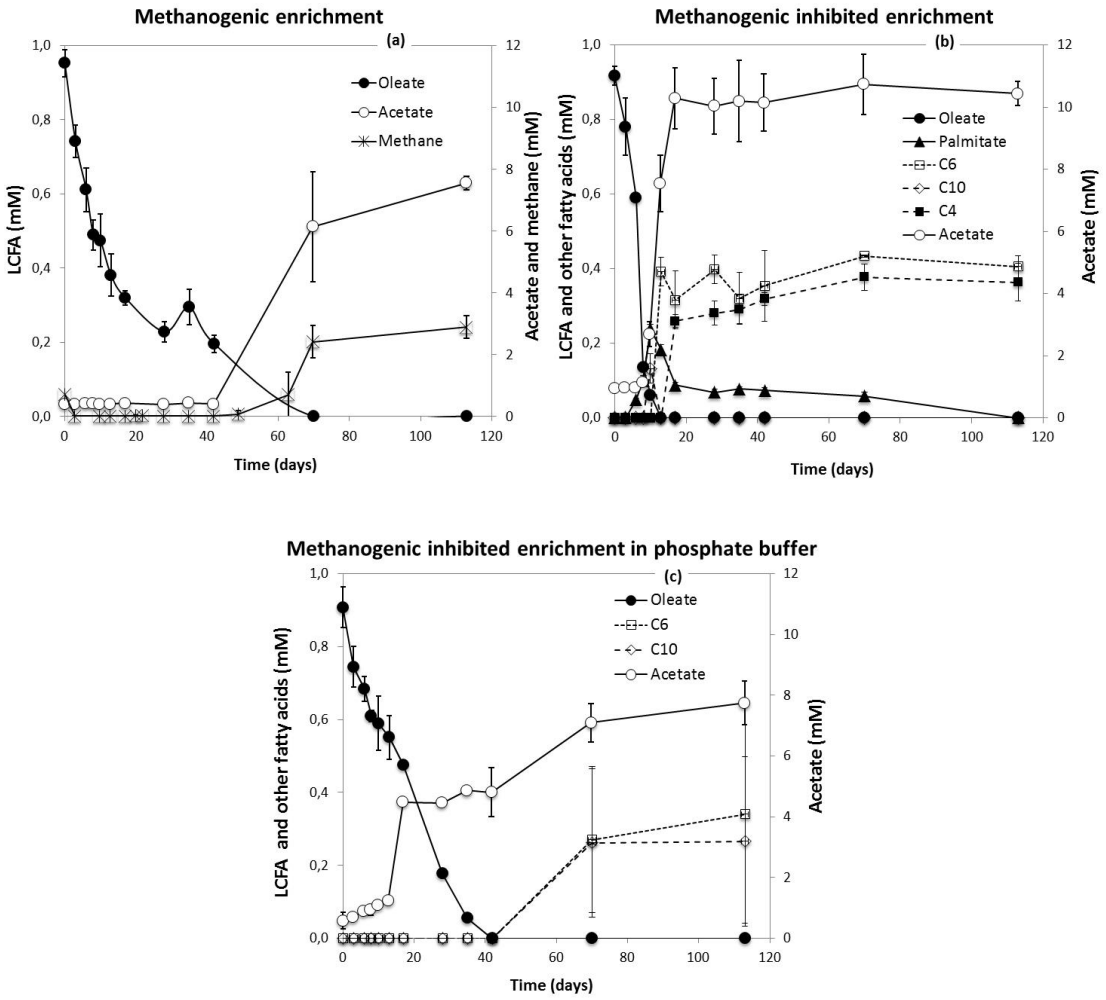

Figure 5.2 Formation, degradation and accumulation of products during oleate utilization by methanogenic (a) and methanogenic-inhibited (b and c) enrichment cultures. Non-methanogenic enrichment cultures were grown in bicarbonate buffered medium (b) or in phosphate buffered medium (c).

5.3.2 Molecular characterization of oleate-degrading enrichment cultures

Bacterial communities from cultures OL-M, OL-MI and OL-MI-P diverged from the original inoculum sludge community (I) (Figure 5.3, a). Besides, differences between DGGE profiles of the three different enrichments were also evident.

Samples M, MI and MI-P, corresponding to methanogenic- (OL-M) and methanogenic inhibited-enrichment cultures (OL-MI and OL-MI-P) were selected for 16S rRNA gene cloning and sequencing. Archaeal community (sample

MA, corresponding to incubation OL-M) was less diverse than bacterial, with three major bands in the DGGE profile (Figure 5.3, b). Clone sequences corresponding to most prominent bands of the DGGE profiles were compared with those in the NCBI nucleotide database. Table 5.2 shows the most similar sequences to the clones' sequences obtained from samples OL-M, OL-MI and OL-MI-P.

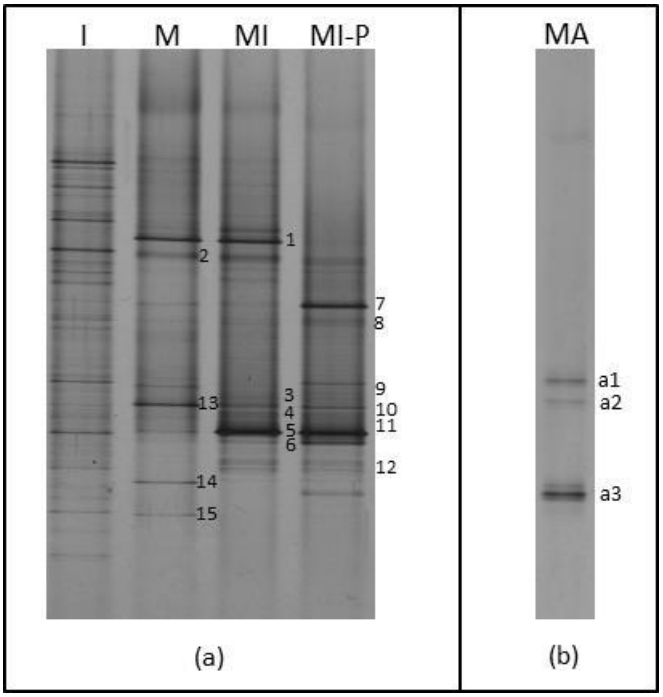

Figure 5.3 DGGE patterns of bacterial (a) and archaeal (b) 16S rRNA gene fragments obtained from the different oleate enrichment cultures. I - inoculum sludge; M – methanogenic enrichment culture; MA – methanogenic enrichment culture (archaeal community); MI – methanogenic inhibited enrichment culture; MI-P – methanogenic inhibited enrichment culture in phosphate buffer. Numbers 1 to 15 and designations a1 to a3 correspond to DGGE bands whose 16S rRNA sequences were obtained by cloning and sequencing.

Table 5.2 Affiliation of bacterial and archaeal clones retrieved from oleate degrading enrichment cultures obtained by BLAST search.

Band	Clone ID	Closest relatives [a]	Sequence ID	Identity (%)
1	OLBES_E1; OL_A10; OL_D7; OL_E10	*Syntrophomonas zehnderi* OL-4 strain OL-4	NR_044008.1	99
2	OL_A11; OL_B5	*Syntrophomonas zehnderi* OL-4 strain OL-4	NR_044008.1	99
3	OLBES_C3	Uncultured *Desulfovibrio* sp. clone NSBac23	JX462541.1	99
		Desulfovibrio aminophilus strain ALA-3	NR_024916.1	98
4	OLBES_A4	Uncultured *Desulfovibrio* sp. clone NSBac23	JX462541.1	99
		Desulfovibrio aminophilus strain ALA-3	NR_024916.1	98
5	OLBES_D7	Uncultured *Desulfovibrio* sp. clone NSBac23	JX462541.1	99
		Desulfovibrio aminophilus strain ALA-3	NR_024916.1	98
6	OLBES_B2	Uncultured *Desulfovibrio* sp. clone NSBac23	JX462541.1	99
		Desulfovibrio aminophilus strain ALA-3	NR_024916.1	98
7	OLBESPO_A7	*Sporanaerobacter acetigenes* strain DSM 13106	GQ461827.1	95
8	OLBESPO_B11	*Sporanaerobacter acetigenes* strain DSM 13106	GQ461827.1	99
9	OLBESPO_A11	Uncultured *Desulfovibrio* sp. clone NSBac23	JX462541.1	99
		Desulfovibrio aminophilus strain ALA-3	NR_024916.1	98
10	OLBESPO_A5	*Desulfovibrio alcoholovorans* strain SPSN	NR_037130.1	99
11	OLBESPO_A6	Uncultured *Desulfovibrio* sp. clone NSBac23	JX462541.1	99
		Desulfovibrio aminophilus strain ALA-3	NR_024916.1	98
12	OLBESPO_E2	Uncultured *Desulfovibrio* sp. clone NSBac23	JX462541.1	99
		Desulfovibrio aminophilus strain ALA-3	NR_024916.1	98
13	OL_F2	Uncultured *Desulfovibrio* sp. clone NSBac23	JX462541.1	99
		Desulfovibrio aminophilus strain ALA-3	NR_024916.1	98
14	OL_B3	*Mycobacterium frederiksbergense* strain CP78b	KF057957.1	100
15	OL_G6; OL_G9	*Mycobacterium frederiksbergense* strain CP78b	KF057957.1	99
a1	OL_Arch_A6; OL_Arch_C1	Uncultured euryarchaeote clone ZW-M-11	KF360017.1	100
		Methanobacterium beijingense strain 4-1	AY552778.3	99
a2	OL_Arch_B6; OL_Arch_C8	Uncultured archaeon	AB820003.1	100
		Methanobacterium formicicum strain MG-134	HQ591420.1	99
a3	OL_Arch_B4; OL_Arch_B12	Uncultured archaeon	AB084243.1	100
		Methanoculleus bourgensis MS2	AF095269.1	97

[a] In cases where the first NCBI BLAST hit was an uncultured microorganism, the first hit of a cultured microorganism was also given.

The majority of bacterial clones' sequences retrieved were assigned to *Desulfovibrio* genus (DGGE bands 3 to 6 and 9 to 13). Sequences were closely related to those of uncultured *Desulfovibrio* species but also to *Desulfovibrio alcoholovorans* strain

SPSN and *Desulfovibrio aminophilus* strain ALA-3. Beyond *Desulfovibrio* genus, retrieved sequences were similar to those of *Syntrophomonas zehnderi* (DGGE bands 1 and 2), *Sporanaerobacter acetigenes* (DGGE bands 7 and 8) and *Mycobacterium frederiksbergense* (DGGE bands 14 and 15). *Syntrophomonas zehnderi*-like organisms were dominant not only in culture OL-M but also in sample OL-MI. The development of these bacteria was favored during the enrichment process under methanogenic and non-methanogenic conditions.

Nonetheless, when OL-MI culture was transferred to phosphate buffered anaerobic medium those microorganisms became less dominant according to the DGGE profile, since band 1 is not predominant in sample MI-P (Figure 5.3, a). On the other hand, *Sporanaerobacter acetigens*-like organisms became apparently more predominant in enrichment culture OL-MI-P given by the increase of band 6 intensity in sample MI-P (Figure 5.3, a). Three clones whose sequences could be assigned to *Mycobacterium frederiksbergense* were obtained from methanogenic oleate degrading enrichment (OL-M) (Table 5.2).

Bands a1 to a3 correspond to 16S rRNA gene sequences retrieved from OL-M enrichment and are close related to genes from the hydrogenotrophic methanogens *Methanobacterium beijingense*, *Methanobacterium formicicum* and *Methanoculleus bourgensis* (Table 5.2). No aceticlastic methanogens could be detected by 16S rDNA DGGE, cloning and sequencing during degradation of oleate under methanogenic conditions.

5.4 Discussion

Oleate was successfully degraded by methanogenic and non-methanogenic enrichment cultures. 16S rRNA gene based analyses reveled *Syntrophomonas zehnderi*-like organisms as a predominant bacterium in OL-M and OL-MI enrichment cultures (Figure 5.3 and Table 5.2). Indeed, *S. zehnderi* was the only bacterium identified in this experiment which is known as an oleate degrader (Sousa et al., 2007c). *Syntrophomonas* activity depends on syntrophic interactions with hydrogen utilizing microorganisms (Lorowitz et al., 1989). Cooperation with hydrogenotrophic methanogens was observed in the methanogenic enrichment culture (OL-M culture) given by the production of methane (Figure 5.2, a) and the identification of 16S rRNA gene sequences close related to *Methanobacterium* and *Methanoculleus* sequences. The presence of *Methanobacterium* and specifically *M. formicicum* in LCFA-degrading microbial communities had been reported in previous studies (Table 2.5 and Chapter 3) and *S. zehnderi* was isolated together with *M. formicicum* as a syntrophic partner for oleate degradation (Sousa et al., 2007c). *Methanoculleus bourgensis* was detected in the inoculum sludge used to start-up oleate and palmitate enrichments described in Chapter 4 but its presence was not reported in other LCFA-degrading consortia (Table 2.5). Other *Methanoculleus* species were identified in LCFA containing bioreactors, namely *M. palmolei* which was isolated from a bioreactor treating palm oil mill wastewater (Zellner et al., 1998). Both *Methanobacterium*- and *Methanoculleus*-like microorganisms utilize hydrogen and formate for methane production (Table 2.4) and were likely the methanogenic partners in the syntrophic conversion of oleate to methane in OL-M enrichment.

In the methanogenic inhibited culture (OL-MI) homoacetogenic activity was promoted. Even though no known homoacetogenic bacteria could be identified by cloning and sequencing of the 16S rRNA genes retrieved from culture OL-MI, acetate accumulated in the medium at concentrations higher than 10 mM (Figure 5.1, b) and this reflects the production of acetate via oleate β-oxidation plus via hydrogen oxidation by homoacetogenic bacteria (Table 5.1). Complete oleate degradation produces 9 moles of acetate and 15 moles of hydrogen. Those 15 moles of hydrogen can be used by homoacetogenic bacteria to produce 3.75 moles of acetate which makes 12.75 moles of acetate expected from the complete conversion of oleate to acetate and this value is higher than the 10.4 mM obtained experimentally. However, other compounds were formed during oleate degradation by the OL-MI culture. Butyrate (C4) as well as hexanoate (C6) accumulated in the medium at a concentration of approximately 0.4 mM each (Figure 5.2). Carbon balance closed in OL-M, OL-MI and OL-MI-P enrichments with an error of 3 %, 5 % and 16 %, respectively. The highest value (obtained for OL-MI-P enrichment) results from the errors associated with the experimental determination of C6- and C10-fatty acids concentrations in OL-MI-P enrichment culture. Whether the formation of these fatty acids, higher than acetate (i.e. C4, C6 and C10), resulted from incomplete β-oxidation of oleate or were constructed by using acetate and hydrogen molecules available in the medium is still not possible to be explained with the available data.

These results show that oleate degradation is possible when methanogenesis is inhibited although collaboration between oleate-degrading syntrophic bacteria and other microorganisms, most likely homoacetogenic bacteria, would be necessary to decrease hydrogen partial pressure, allowing continuous oleate degradation. *S.*

zehnderi-like microorganisms were dominant in OL-M and OL-MI enrichment cultures but much less abundant in OL-MI-P cultures (Figure 5.3, a). When homoacetogenic activity was inhibited in culture OL-MI-P (in which no CO_2 was available for the formation of acetate by homoacetogens (Table 5.1, reaction 4) oleate conversion was observed but microorganisms consuming hydrogen could not be identified using this approach. *Sporanaerobacter acetigens* was detected in OL-MI-P enrichment culture but its function on this enrichment is unclear. *S. acetigens* is reported as a fermenter of substrates such as peptone, glucose, peptides and amino acids to acetate, hydrogen and carbon dioxide (Hernandez-Eugenio et al., 2002). Likewise, *Mycobacterium* species involvement in methanogenic communities degrading LCFA is difficult to establish, particularly because mycobacteria are reported as obligate aerobes. Ribosomal sequences (DGGE bands 14 and 15) were assigned to *M. frederiksbergense*, a soil polycyclic aromatic hydrocarbon-degrading bacterium not associated to anaerobic environments (Willumsen et al., 2001). This bacterium degrades polycyclic aromatic hydrocarbons, is able to hydrolyze Tween 80 (a non-ionic detergent composed by oleic (~70 %), linoleic, palmitic and stearic acids) and also utilizes compounds such as gluconate and succinate between others (Willumsen et al., 2001), but its involvement in LCFA degradation has never been reported.

Despite the differences between microbial communities composition of OL-MI and OL-MI-P cultures they have some physiological similarities since oleate was converted mainly to acetate but also to residual amounts of other short- to medium-chain fatty acids in both incubations (Figure 5.2, b and c). Acetate was one of the final products of oleate degradation in OL-M enrichment too (Figure 5.2, a), meaning that the acetate formed from oleate β-oxidation was not being converted

to methane by acetoclastic methanogens. The loss of acetoclastic activity was observed before in methanogenic oleate-degrading enrichment cultures but not in methanogenic palmitate-degrading enrichment cultures in which acetate could be converted to methane (Sousa et al., 2007b), which suggest that prolonged exposure to oleate causes severe inhibition of this group of methanogens.

Several 16S rRNA gene sequences retrieved from samples OL-MI and OL-MI-P were assigned to *Desulfovibrio* species (Figure 5.3 and Table 5.2). Detection of *Desulfovibrio*-related organisms have been detected before in methanogenic oleate-degrading enrichment cultures (Sousa et al., 2007b) but their function remains unclear. *Desulfovibrio* species are known as hydrogen utilizers but only when sulfate is the electron acceptor (Carepo et al., 2002; Walker et al., 2009). Under non-sulfate reducing conditions, *Desulfovibrio* species function as hydrogen producers instead of hydrogen oxidizers (Carepo et al., 2002) establishing syntrophic associations with hydrogen consuming microorganisms (Walker et al., 2009). Nevertheless, growth of *Desulfovibrio* species might have been supported by the small quantities of sodium sulfide that are supplemented to the medium (~ 0.8 mM) and thus, probably some of the hydrogen formed during oleate degradation could have been used by these microorganisms. On the other hand, the abundance of *Desulfovibrio* species in these enrichments, based on DGGE analysis, might have been overestimated because these microorganisms have on average 4.5 copies of the 16S rRNA gene in their genomes (Christophersen et al., 2011). Thus, *Desulfovibrio* species, although present, might not be as abundant in oleate-degrading enrichment cultures as they might seem by a simple DGGE profile observation.

This study shows that *S. zehnderi*, a known syntrophic LCFA degrader, had an important role on the utilization of oleate, in methanogenic and non-methanogencic oleate-degrading enrichments. Under methanogenic conditions oleate could be converted to methane and acetate, most likely by the activity of *S. zehnderi* and by its cooperation with *Methanobacterium*- and *Methanoculleus*-related microorganisms. On the other hand, the results obtained in this study do not allow inferring about specific functions of *Sporanaerobacter*-like, *Mycobacterium*-like and *Desulfovibrio*-like microorganisms in oleate-degrading enrichment cultures. Because acetate was the ultimate product of anaerobic oleate degradation, the utilization of these acetate-producing cultures could be an option of biotechnology interest. Further investigation on the microbial interactions in oleate degrading environments, especially in non-methanogenic environments, is needed to understand the dynamics of oleate degradation by mixed anaerobic microbial communities.

Chapter 6

Comparative metaproteomics and diversity of LCFA-degrading microbial communities

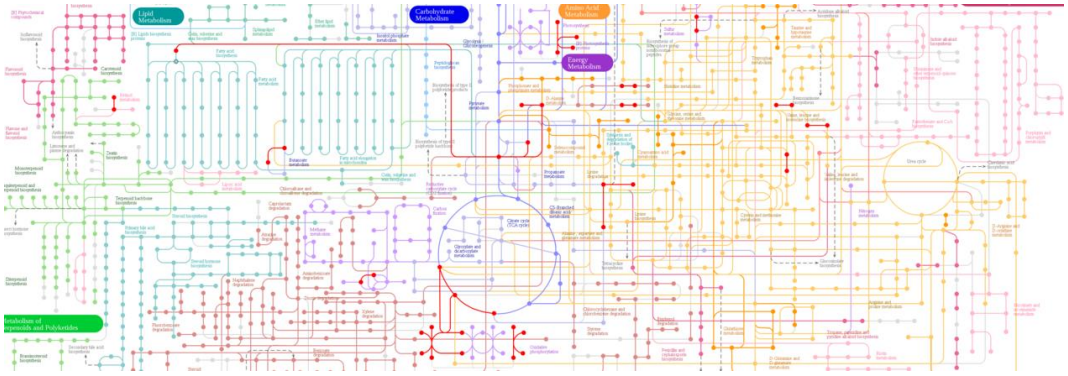

A combination of shotgun metaproteomics and 16S rRNA gene pyrosequencing was used to identify potential functional pathways and key microorganisms involved in long-chain fatty acids (LCFA) anaerobic conversion. Microbial communities degrading saturated- and unsaturated-LCFA were compared. Archaeal communities were mainly composed of *Methanosaeta*, *Methanobacterium* and *Methanospirillum* species, both in stearate (saturated C18:0) and oleate (mono-unsaturated C18:1) incubations. Over 80% of the 16S rRNA gene sequences clustered within the *Methanosaeta* genus, which is in agreement with the high number of proteins assigned to this group (94%). Archaeal proteins related with methane metabolism were highly expressed. Bacterial communities were rather diverse and the composition dissimilar between incubations with saturated- and unsaturated-LCFA. Stearate-degrading communities were enriched in *Deltaproteobacteria* (34% of the assigned sequences), while microorganisms clustering within the *Synergistia* class were more predominant in oleate incubation (25% of the assigned sequences). Bacterial communities were diverse and active, given by the high percentage of proteins related with mechanisms of energy production. Several proteins were assigned to syntrophic bacteria, emphasizing the importance of the interactions between acetogens and methanogens in energy exchange and formation in anaerobic LCFA-rich environments.

.

Salvador AF, Bize A, Alves MM, Bouchez T and Sousa DZ. Comparative metaproteomics and diversity of LCFA degrading microbial communities.

6.1 Introduction

Methane production from long-chain fatty acids (LCFA)-rich wastewaters is a feasible and cost effective way of merging wastewater purification with renewable energy production (Alves et al., 2009). Microbial community composition in anaerobic bioreactors fed with LCFA, or in enrichment cultures consuming saturated- or unsaturated- LCFA, have been studied by 16S rRNA gene-based molecular techniques (Hatamoto et al., 2007b; Pereira et al., 2002b; Shigematsu et al., 2006; Sousa et al., 2007a; Sousa et al., 2007b; Sousa et al., 2008). Bacterial communities in bioreactor LCFA-degrading sludges were widely distributed over a number of different taxa, with predominance of microorganisms from the *Clostridiaceae* and *Syntrophomonadaceae* families (Pereira et al., 2002b; Sousa et al., 2007a; Sousa et al., 2007b). Methanogenic communities were mainly composed by *Methanobacterium*, *Methanosaeta* and *Methanosarcina* species (Pereira et al., 2002b; Salvador et al., 2013; Sousa et al., 2007a). Upon enrichment, members of the *Syntrophomonas* genus are normally detected together with hydrogenotrophic methanogens (Hatamoto et al., 2007b; Sousa et al., 2007a; Sousa et al., 2013). Nevertheless, a distinct bacterial profiling seems to occur in saturated and unsaturated-LCFA degrading enrichments (Sousa et al., 2009a), which strongly suggests differences in their degradation pathways. Phylogenetic studies provide information on the composition of microbial communities but do not allow to infer the function and/or activity of microorganisms. Metaproteomics approaches offer such a possibility and have been applied to various complex environments, such as the human gut and oral microbiota, soil and marine ecosystems, activated sludge and anaerobic digestion processes (Siggins et al., 2012b). Abram et al. (2011) were the first to report metaproteomics data from anaerobic bioreactor sludge. Eighteen

protein functions were identified from the sludge of the glucose-fed reactor, mainly linked to methanogenesis, glycolysis and pentose phosphate pathway. A minimum overlap was observed between phylogenetic and metaproteomics data which was attributed to the fact that microbial composition was studied using a DNA-based approach, therefore not directly targeting microbial activity. Low number of protein identification were reported by Hanreich et al. (2012), when analysing the metaproteome of a thermophilic microbial community in a biogas reactor fed with agricultural biomass. This is mainly due to the fact that genomic data from biogas communities is rather limited. Again, proteins related to methanogenesis were identified, but also proteins of members of the potentially syntrophic *Synergistales*. In this work we want to target syntrophic interactions present in LCFA-degrading communities from a functional point of view. We have used a shotgun metaproteomics approach combined with total community diversity analysis characterization by 16S rRNA gene pyrosequencing in order to get more insights into the composition, activity and function of anaerobic microbial communities degrading saturated- and unsaturated- LCFA. The major goals of this study were: (i) to link structure and function of microbial communities involved in LCFA degradation, and (ii) to investigate potential differences in the degradation of saturated- and unsaturated-LCFA.

6.2 Materials and methods

6.2.1 Anaerobic incubations with LCFA

Anaerobic sludge was collected from a brewing industry anaerobic bioreactor (Lisbon, Portugal) and incubated with saturated- or unsaturated-LCFA. The sludge and the anaerobic medium, which consisted in a bicarbonate-buffered mineral salt

medium (Sousa et al., 2007b), were dispensed into serum bottles that were then sealed with butyl rubber septa and aluminum crimp caps. The headspace of serum bottles was flushed with a mixture of N_2/CO_2 (80:20; $1.7x10^5$ Pa) and the medium was subsequently reduced with 0.8 mM sodium sulfide ($Na_2S.xH_2O$, x=7-9). The assays were designated by PA, ST and OL that correspond to the incubations where palmitate (C16:0), stearate (C18:0), oleate (C18:1) were added at a final concentration of 2 mM, respectively. All bottles were incubated at 37ºC, without shaking and in the dark. Aliquots were sampled, during LCFA degradation, for DNA and protein extraction as well as for LCFA, VFA and methane concentration determination.

6.2.2 Analytical methods

Methane, volatile fatty acids (VFA) and long-chain fatty acids (LCFA) were analyzed as described in section 5.2.2.

6.2.3 DNA extraction and fingerprinting analyses

At day 5 of biomass incubation, 2 mL aliquots of well-homogenized mixed cultures were collected, concentrated by centrifugation (10,000×g, 10 min), frozen and stored at -20ºC. Total genomic DNA was extracted using UltraClean® Soil DNA Isolation Kit (MO BIO Laboratories, Inc.) in accordance with the manufacturer's instructions. Automated ribosomal intergenic spacer analysis (ARISA) was used to estimate the diversity of mixed microbial communities. Primers sets ITSF/ITSR and 1389F/71R were used to amplify the intergenic spacer region of bacterial and archaeal rRNA operons, respectively (Table S6.5). PCR products were separated on a chip (Agilent DNA 7500 Kit) using Agilent 2100 Bioanalyzer, according to the manufacturer's instructions.

6.2.4 454 - Pyrosequencing of 16S rRNA genes

Taxonomic composition of microbial communities developed in OL and ST incubations was assessed by 16 rRNA gene pyrosequencing as described by Smith et al. (2010) (Research and Testing Laboratory, Texas, USA), using the primer sets 28F/519R and Arch349F/Arch806R for *Bacteria* and *Archaea* amplification, respectively. The sequences obtained were processed with the Quantitative Insights Into Microbial Ecology (QIIME) software (Caporaso et al., 2010). 16S DNA sequence reads were trimmed according to the quality scores at a 25 threshold in a 50 bp sliding window. Reads shorter than 150 bp, longer than 600 bp, with the longest homopolymer greater than 6 nucleotides, or containing an ambiguous base were then discarded. The remaining reads were aligned with PyNAST (Caporaso et al., 2010) using as a template the Silva 108 database core-aligned set formatted for QIIME. Putative chimeric sequences identified with ChimeraSlayer were discarded. UCLUST was used for clustering sequences into Operational Taxonomic Units (OTUs) according to their sequence similarity (set at 97%) (Edgar, 2010). The taxonomic classification was obtained by using RDP classifier (Cole et al., 2003; Wang et al., 2007), at a 0.8 bootstrap cut-off, using the longest sequence in each OTU as the representative sequence. OTUs not corresponding to the expected phylogenetic domain were discarded. The relative abundance of different taxa within a sample was estimated by the relative number of reads corresponding to each taxon.

6.2.5 Protein extraction and purification

Proteins were extracted from sludge samples as described by Wilmes and Bond (2004) with some modifications. Briefly, cells were resuspended in urea-thiourea-CHAPS (UTCHAPS) buffer containing dithiothreitol (DTT), Tris and EDTA. PMSF was added every 30 minutes during 2 h of vortex and ice cycles. Cells were lysed by bead beating (using zirconia/silica beads with a diameter of 0.1 mm). The suspension was centrifuged at 22000 x g, 4 °C, 45 min to remove cell debris and proteins present in the supernatant were subsequently precipitated with cold acetone (1/2 v/v) and TCA (1/10 v/v) followed by overnight incubation at -20 °C. After centrifugation (22000 x g, 4 °C, 30 min) protein pellet was washed with acetone and centrifuged several times in order to remove all remaining TCA. Pellet was air dried and resuspended in UTCHAPS buffer (without Tris and EDTA) by vortexing during 2 h at 10 °C. The supernatant collected after centrifugation (22000 x g, 10 °C, 45 min) contained the purified proteins. Protein concentration was determined by using the 2-D Quant Kit (Amersham Biosciences), according to manufacturer's instructions.

6.2.6 SDS-PAGE protein electrophoresis and LC-MS/MS analysis

Proteins were separated by SDS-PAGE electrophoresis using NuPAGE Novex Bis-Tris Mini Gels (Invitrogen). For each sample, 12 gel fractions were collected along the protein profile and were subsequently digested with trypsin prior to LC-MS/MS analysis. Liquid chromatography coupled to tandem mass spectrometry (LC-MS/MS) analysis was performed with an Ultimate 3000 LC system (Dionex) connected by a nanoelectrospray interface to a linear ion trap mass spectrometer coupled to an Orbitrap detector (LTQ-Orbitrap, Thermo Fisher, Waltham, MA,

USA; PAPPSO proteomic platform, INRA, Jouy-en-Josas) as described elsewhere (Ibrahim et al., 2007).

6.2.7 Database searching, protein identification and functional annotation

Protein identification was made by matching tandem mass spectra against model spectra created from each peptide present in a protein database by using X!Tandem software (Craig and Beavis, 2004). Two specific protein databases, one for archaeal and another for bacterial proteins identification were downloaded from the Uniprot website (http://www.uniprot.org) and combined prior analysis of MS/MS spectra with X!Tandem. *Euryarchaeota* database (taxon ID: 28890) comprise 265758 entries at the date of database download (10/12/2012). The bacterial protein database was composed of proteins allocated to families detected by pyrosequencing of the 16S rRNA gene from sludge samples collected from ST and OL incubations (taxa: 649777, 292628, 558415, 186817, 815, 424536, 31979, 89373, 194924, 186806, 136, 213422, 188709, 213423, 171551, 213468, 213465, 186814, 543310, 1106, 186807, 972, 41294, 453228, 213121, 84642, 543, 75682, 203494 entries: 7104112, downloaded on 12/12/2012).

Scaffold software (version 4.0.4) (Searle, 2010) was used to group, visualize and validate the identified proteins. Peptide and protein probability thresholds were set to higher than 90% and 95%, respectively, with a minimum of 2 identified peptides per protein. In order to increase the number of identified proteins, a less stringent analysis was performed, with only 1 identified peptide per protein. Functional annotation of proteins was obtained by scanning protein sequences against the Cluster of Orthologous Groups database (COG database) (Marchler-Bauer et al., 2011). The relative abundance of proteins was estimated based on the number of

spectra assigned to each protein. Normalized spectral counts obtained from Scaffold (given by the Quantitative Value) were used to allow a semi-quantitative comparison between biological samples.

6.3 Results

6.3.1 Anaerobic LCFA degradation and methane production

Saturated or unsaturated LCFA were successfully converted to methane by the anaerobic mixed cultures (Figure 6.1). After 8 days of incubation LCFA concentration OL, ST and PA incubations dropped from approximately 1.8 mM to non-detectable concentrations. In OL and ST incubations there was a transient accumulation of palmitate that was ultimately converted to methane. The only VFA detected during LCFA degradation was acetic acid, but in low amounts (less than 1.4 mM).

6.3.2 Diversity and taxonomic characterization of LCFA degrading communities

ST and PA ARISA fingerprints were identical, but microbial communities diverged when incubated with oleate (Figure S6.1). Based on these results, samples from ST and OL incubations were selected for phylogenetic characterization by 16S rRNA gene pyrosequencing, in order to investigate differences on the composition of microbial communities incubated with saturated- or unsaturated-LCFA.

Bacterial sequences were distributed over 20 phyla inside Bacteria domain (Table S6.2). *Proteobacteria*, *Synergistetes, Firmicutes*, *Bacteroidetes*, *Chloroflexi* and *Spirochaetes* were the most abundant phyla but their relative abundance was not the same in samples ST and OL. The biggest difference was found for class *Synergistia* that was represented by 8 % of the sequences in ST incubation and 28 % in OL incubation, and also for Delta*proteobacteria*, that in turn was represented by 33 %

of the sequences in ST and 6 % in OL incubations (Figure 6.2; Table S6.2). A significant amount of sequences could only be affiliated to the Domain *Bacteria* suggesting that a considerable part of the microbial community (7% in ST and 16 % in OL) is unknown so far.

Archaeal diversity was investigated as well. The majority of the 16S rRNA gene sequences were assigned to *Methanosaeta* genus in both incubations (96% in ST and 82% in OL), which suggests that microorganisms from this group might have an important role in the acetate utilization during LCFA degradation (Figure 6.2). Hydrogenotrophic methanogens were also present, even though less abundant than acetoclasts according to pyrosequencing results, and the most represented genera were *Methanobacterium*, *Methanospirillum* and *Methanolinea* (Figure 6.2). Although those taxa were detected in both incubations, they were all more abundant in OL incubation. For example, *Methanobacterium* accounted for 8 % of the total sequences obtained in OL incubation and only 1 % in ST incubation.

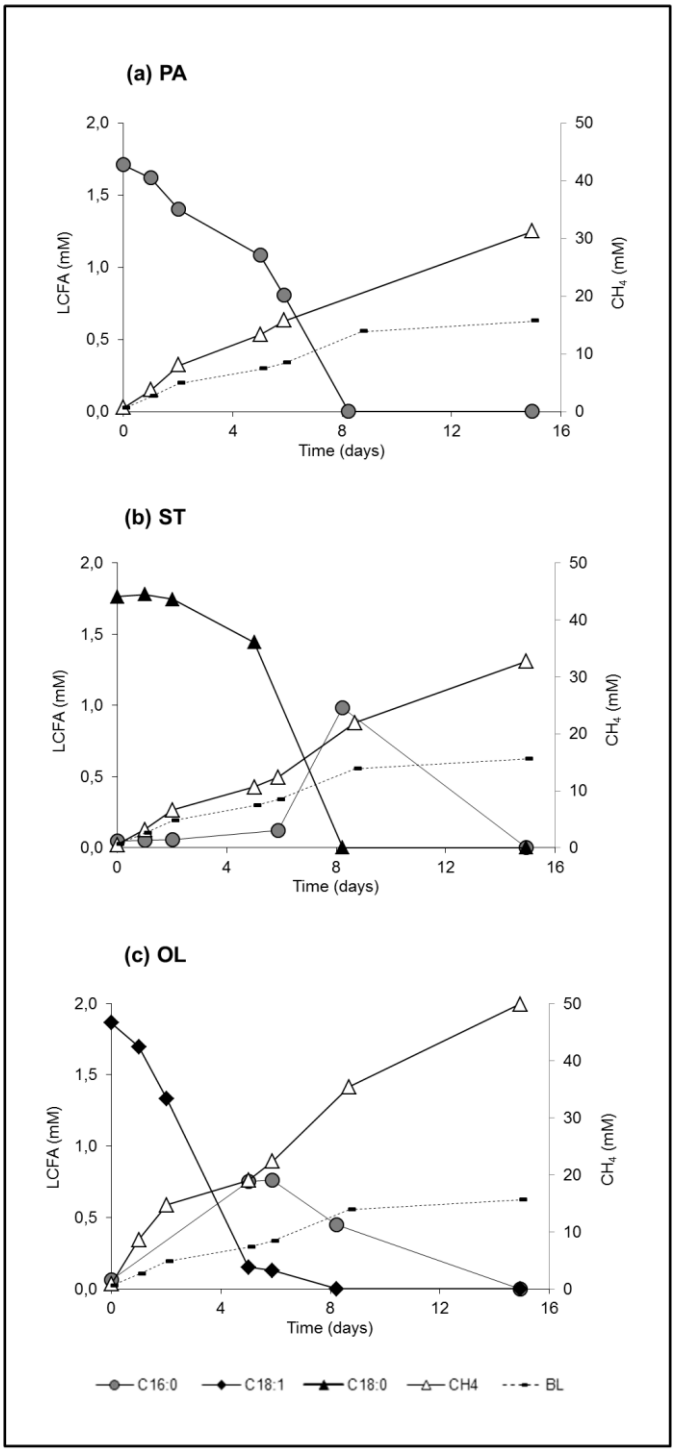

Figure 6.1 Palmitate (a), stearate (b) and oleate (c) conversion to methane. Methane production in the blank assay (BL), in which no LCFA were added, is represented.

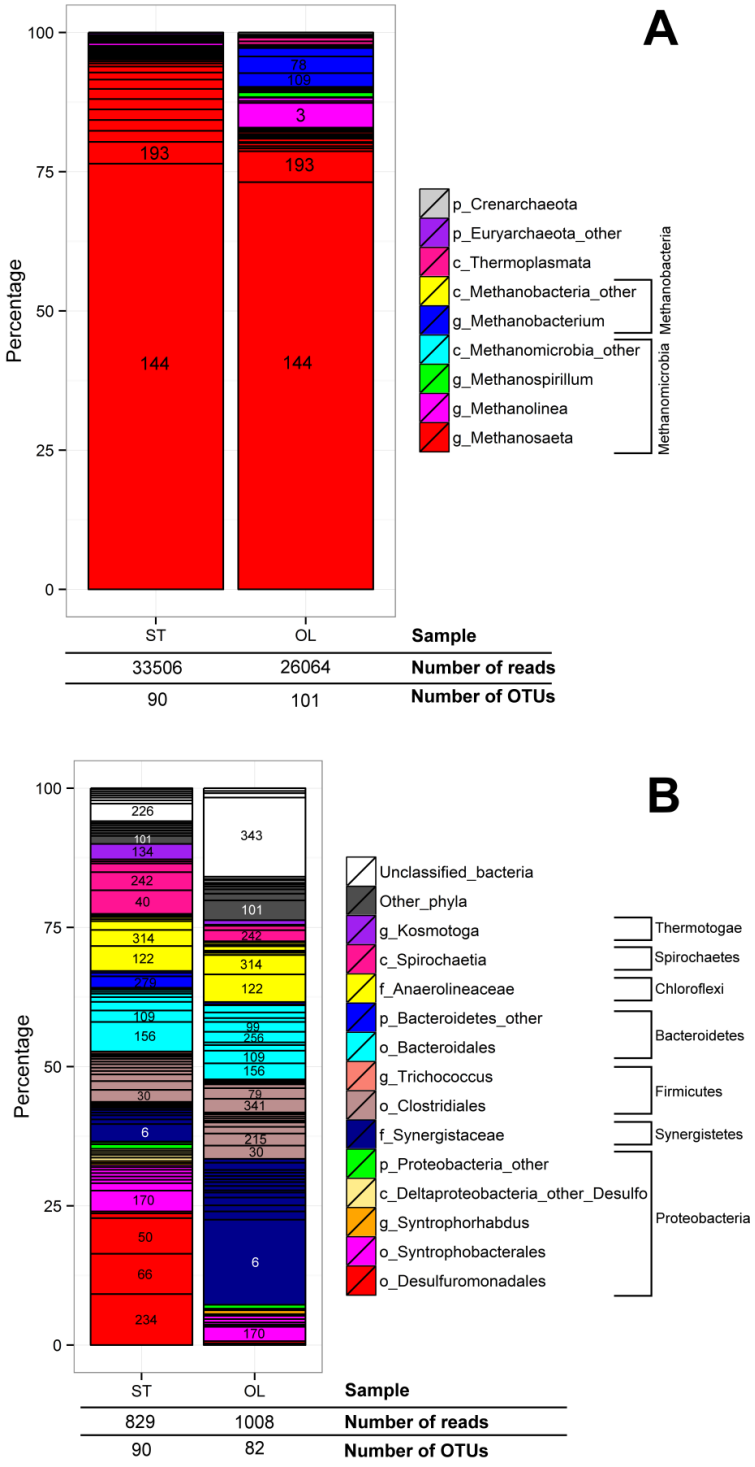

Figure 6.2 Taxonomic distributions of microbial communities degrading stearate (ST) and oleate (OL) obtained by 16S rRNA gene pyrosequencing. A: archaeal primer set: 107 OTUs were obtained including 84 retrieved in both ST and OL. B: bacterial primer set: 102 OTUs were obtained including 70 retrieved in both ST and OL samples. For the most abundant groups, the arbitrary OTU number is indicated.

OTU: Operational Taxonomic Unit. Only the OTUs with more than 3 reads for at least one of the samples were used; p_: phylum; c_: class; o_: order; f_: family; g_: genus; C_Deltaproteobacteria_other_Desulfo includes the OTUs affiliated to the genera *Desulfolobus*, *Desulfomicrobium* and *Desulfovibrio*.

6.3.3 Metaproteomics characterization of LCFA degrading communities

6.3.3.1 Metaproteomics of bacterial communities

A total of 39 bacterial proteins could be identified in the experiments. Nearly the same proteins could be identified in incubations PA, ST and OL but their relative abundances were different (Table 6.1). Proteins were assigned to 9 different COG functional categories (Table 6.1). The most represented COG functional categories were category C (Energy production and conversion), category O (Posttranslational modification, protein turnover, chaperones) and category I (Lipid transport and metabolism) (Table 6.1). The majority of the spectra were matching to proteins assigned to microorganisms within *Clostridia* and *Deltaproteobacteria* classes. From those, proteins related to *Pelotomaculum thermopropionicum*, *Pelobacter propionicus*, and *Syntrophobacter fumaroxidans* were the most abundant (Table1). The major number of proteins and also the most abundant ones are involved in energy production mechanisms. These include oxidation-reaction proteins that are part of membrane complexes involved in electron or hydrogen atoms transport namely: NADH dehydrogenase (EC:1.6.5.3), which receives hydrogen atoms from NADH and transfer them to flavoproteins; succinate dehydrogenase (EC:1.3.5.1) and succinate dehydrogenase or fumarate reductase, flavoprotein subunit (EC:1.3.99.1) that catalyzes succinate oxidation or fumarate reduction; and ATP synthase (EC:3.6.3.14) which catalyzes the interconversion of ATP and ADP+P_i. Succinate dehydrogenase or fumarate reductase (EC:1.3.99.1) belong to the protein pool of TCA cycle. Other two proteins detected in this study are also related to incomplete reductive TCA cycle, succinyl-CoA ligase (EC:6.2.1.5), catalyzing the reversible reaction of succinate to succinyl-CoA, and pyruvate carboxylase

(EC:6.4.1.1), catalyzing the formation of oxaloacetate from pyruvate. Iron-containing alcohol dehydrogenase (A1AME6) from *Pelobacter propionicus* and alcohol dehydrogenase (A5D4P0) from *Pelotomaculum thermopropionicum,* which catalyze the oxidation of primary alcohols to aldehydes or secondary alcohols to ketones, are among the most abundant bacterial proteins detected when the biomass was exposed to palmitate, stearate or oleate.

Proteins related to lipid metabolism were also abundant, representing 5% of total amount of proteins expressed by microbial communities PA and ST and 7% by OL. These proteins are carboxyl transferase that participates in fatty acid biosynthetic process, and glutaconate CoA-transferase which participates in styrene degradation and butanoate metabolism. A significant percentage of the proteins (44%) were assigned to those of syntrophic bacteria and they also corresponded to the most abundant bacterial proteins (Table S6.4).

Table 6.1 Identification, functional assignment and relative abundance of bacterial proteins identified in PA, ST and OL incubations.

				Normalized Spectrum Counts			
COG Functional Category	**Protein name**	**Uniprot ID**	**Organism**	**LCFA**	**PA**	**ST**	**OL**
Energy production and conversion					152	137	69
	ATP synthase subunit beta	A0LLF8	*Syntrophobacter fumaroxidans*		1	2	2
	Glycerol kinase	A9WJ21	*Chloroflexus aurantiacus*		2	1	0
	Glycerol kinase	A5UU55	*Roseiflexus sp.*		1	0	1
	AprA (Fragment)	A6YCY7	*Desulforhabdus sp. DDT*		7	2	2
	Aldehyde oxidase and xanthine dehydrogenase molybdopterin binding	E1JYE0	*Desulfovibrio fructosovorans JJ*		1	2	1
	Iron-containing alcohol dehydrogenase	E8RC61	*Desulfobulbus propionicus*		7	1	0
	Aldehyde dehydrogenase, molybdenum-binding subunit apoprotein	A1AP96	*Pelobacter propionicus*		10	7	0
	NADH dehydrogenase subunit E	A1AUU0	*Pelobacter propionicus*		1	3	0
	Iron-containing alcohol dehydrogenase	A1AME6	*Pelobacter propionicus*		34	35	31
	Succinate dehydrogenase subunit A	A0LJT0	*Syntrophobacter fumaroxidans*		5	6	6
	Succinyl-CoA ligase [ADP-forming] subunit alpha	A0LIY7	*Syntrophobacter fumaroxidans*		11	11	4
	Pyruvate carboxylase subunit B	A0LFF9	*Syntrophobacter fumaroxidans*		3	5	0
	Succinate dehydrogenase or fumarate reductase, flavoprotein subunit	C6BYJ6	*Desulfovibrio salexigens*		4	1	2
	Dissimilatory adenylylsulfate reductase alpha subunit	E8RDT8	*Desulfobulbus propionicus*		5	1	0
	NAD-dependent aldehyde dehydrogenase, CoA-acylating	Q3A0W4	*Pelobacter carbinolicus*		4	6	0
	Molybdopterin-binding aldehyde oxidoreductase	Q3A811	*Pelobacter carbinolicus*		5	7	0
	Succinate dehydrogenase or fumarate reductase, flavoprotein subunit	Q312T8	*Desulfovibrio desulfuricans*		12	13	13
	Aldehyde dehydrogenase, molybdenum-binding subunit apoprotein	A5GB32	*Geobacter uraniireducens*		11	7	0
	Alcohol dehydrogenase	A5D4P0	*Pelotomaculum thermopropionicum*		28	29	6

Table 6.1 (continued)

COG Functional Category	Protein name	Uniprot ID	Organism	Normalized Spectrum Counts			
				LCFA	PA	ST	OL
Posttranslational modification, protein turnover, chaperones					11	21	13
	60 kDa chaperonin 2	A0LKS4	*Syntrophobacter fumaroxidans*		1	2	0
	Chaperone protein DnaK (HSP70)	B5EC42	*Geobacter bemidjiensis*		2	2	0
	60 kDa chaperonin	D2Z8X1	*Dethiosulfovibrio peptidovorans*		0	0	5
	60 kDa chaperonin	E1QE82	*Desulfarculus baarsii*		2	3	1
	Chaperone protein DnaK (HSP70)	D7ALW9	*Geobacter sulfurreducens*		2	2	0
	60 kDa chaperonin	D7AG51	*Geobacter sulfurreducens*		4	7	1
	Thioredoxin	A4WG29	*Enterobacter sp.*		0	5	7
Translation, ribosomal structure and biogenesis					0	1	0
	Elongation factor Tu (EF-Tu)	A9WFP3	*Chloroflexus aurantiacus*		0	1	0
Amino acid transport and metabolism					4	2	0
	Extracellular ligand-binding receptor	A0LMX6	*Syntrophobacter fumaroxidans*		2	1	0
	Ketol-acid reductoisomerase	D7AKA6	*Geobacter sulfurreducens*		2	1	0
Lipid transport and					9	10	7
	Carboxyl transferase	A0LHL3	*Syntrophobacter fumaroxidans*		4	6	1
	Glutaconate CoA-transferase	A0LHC3	*Syntrophobacter fumaroxidans*		5	4	6
Carbohydrate transport and metabolism					4	2	1
	Maltoporin (Maltose-inducible porin)	A0KHF6	*Aeromonas hydrophila subsp. hydrophila*		0	0	1
	Pyruvate, phosphate dikinase	B1BIK5	*Clostridium perfringens C*		2	1	0
	Pyruvate phosphate dikinase	A4YPR5	*Bradyrhizobium sp.*		2	2	0
Secondary metabolites biosynthesis, transport and catabolism					0	0	4
	Microcompartments protein	E4RM95	*Halanaerobium hydrogeniformans*		0	0	4
Cell wall/membrane/envelope biogenesis					0	0	1
	Omp38 protein	Q7X589	*Aeromonas veronii*		0	0	1
General function prediction only					13	9	3
	RNA-binding protein Hfq	A1AT91	*Pelobacter propionicus*		3	3	2
	ACT domain protein	A0LIW7	*Syntrophobacter fumaroxidans*		1	2	2
	Molybdopterin oxidoreductase Fe4S4 region	A0LE81	*Syntrophobacter fumaroxidans*		9	4	0

6.3.3.2 Metaproteomics of archaeal communities

The analysis of archaeal metaproteome resulted in the identification of 183 proteins. Those proteins were distributed for 18 different COG functional categories as it is shown in Table 6.2. The best represented categories were category H (Coenzyme transport and metabolism), category C (Energy production and conversion) and category I (Lipid transport and metabolism). About 12%, 7% and 6% of the proteins showed uncharacterized conserved domains in ST, PA and OL incubations, respectively. Proteins highly expressed were related to methane metabolism, lipid metabolism and energy production, namely V-type ATP synthase, acetyl-CoA decarbonylase/synthase complex, CO dehydrogenase/acetyl-CoA synthase complex, acetyl-coenzyme A synthetase, methyl-coenzyme M reductase and tetrahydromethanopterin S-methyltransferase (Table S6.1). More than 83% of the identified proteins were attributed to *Methanosaeta concilii*. Once again, the majority of the identified proteins were common to the three incubations although small differences in estimated protein abundances could be detected. The proteins assigned to *Methanospirillum hungatei* and to *Methanobacterium* species were related to methane metabolism. Proteins from *Methanobacterium formicicum, Methanobacterium subterraneum* and *Methanobacterium* sp. seem to be more expressed in OL incubation than in PA and ST incubations (Table S6.1). This observation is consistent with pyrosequencing results which revealed *Methanosaeta* as the most abundant microorganism in all incubations while *Methanobacterium, Methanolinea and Methanospirillum* were more abundant in OL incubation than in PA and ST incubations (Figure 6.2).

Table 6.2 Relative abundance of archaeal proteins identified in PA, ST and OL incubations and COG functional categories assignment.

	Normalized Spectrum Counts			
COG Functional Category	**LCFA**	**PA**	**ST**	**OL**
Energy production and conversion		722	758	674
Posttranslational modification, protein turnover, chaperones		35	38	56
Translation, ribosomal structure and biogenesis		31	39	17
Nucleotide transport and metabolism		9	9	11
Transcription		49	21	8
Amino acid transport and metabolism		17	7	28
Lipid transport and metabolism		245	204	177
Carbohydrate transport and metabolism		14	10	16
Secondary metabolites biosynthesis, transport and catabolism		1	1	1
Coenzyme transport and metabolism		713	665	667
Cell wall/membrane/envelope biogenesis		13	8	34
Inorganic ion transport and metabolism		12	11	34
Cell cycle control, cell division, chromosome partitioning		2	0	0
Signal transduction mechanisms		34	38	86
Intracellular trafficking, secretion, and vesicular transport		0	0	5
Replication, recombination and repair		3	5	1
General function prediction only		31	17	58
Function unknown		10	8	29
No COG		144	119	263

6.3.4 Comparison of taxonomic groups detected by metaproteomics and 16S rRNA gene pyrosequencing

Methanogenic communities established in PA, ST and OL incubations were dominated by *Methanosaeta*-like organisms since these organisms were abundantly detected by 16S rRNA gene pyrosequencing and by the proteomics approach (Figure 6.2, Table S6.1). Also consistent between the two approaches was the detection of hydrogenotrophic methanogens in all LCFA incubations, although more abundant in OL incubation than in PA or ST. On the other hand, microorganisms from the domain *Bacteria* distributed differently among taxonomic groups when considering DNA sequencing analyses or proteomic analyses. Clearly differences are detected at phylum level. From the 6 more abundant phyla detected by 16S rRNA pyrosequencing (Figure S6.2), only microorganisms belonging to

Proteobacteria, *Firmicutes*, *Synergistetes* and *Chloroflexi* were present according to metaproteomics results. Furthermore, relative abundance of those phyla is markedly different when considering the results obtained by the two methods (Figure S6.2). At the genus level, only 5 genera were simultaneously detected by pyrosequencing and metaproteomics namely, *Syntrophobacter*, *Geobacter*, *Desulfovibrio*, *Desulfobulbus* and *Clostridium*, which means that a significant number of genera were only detected by one or another approaches (Figure S6.2). Besides, proteins could be assigned to 10 genera that were not detected by 16S rRNA pyrosequencing. Among those is *Pelobacter* genus with 15% of the total proteins detected (Figure S6.2).

6.4 Discussion

Anaerobic sludge short incubation (15 days) with saturated- and unsaturated-LCFA resulted in the differentiation of bacterial communities. A high percentage of 16S rRNA gene sequences assigned to the family *Synergistaceae* and order *Clostridiales* were found in OL incubation, while bacteria belonging to the class *Deltaproteobacteria*, including *Syntrophobacterales* members, were predominant in ST incubation. The presence of *Deltaproteobacteria* in saturated-LCFA degrading communities has been previously remarked, although *Syntrophus aciditrophicus* is the only bacterium of this group that is known to convert LCFA (Sousa et al., 2009a). Syntrophic bacteria belonging to the *Syntrophomonadacea* family (*Clostridiales*) are known LCFA-degraders (Sousa et al., 2009a). They normally occur in low amount in anaerobic reactors but are considered important players in the degradation of both saturated- and unsaturated-LCFA (Stams et al., 2012). This might be one of the reasons why no proteins from the *Syntrophomonadacea* family

could be identified in OL or ST incubations. It has been referred that a microorganism must represent at least few percent of the community to allow proteins identification (Wilmes and Bond, 2009) and *Syntrophomonas* sequences corresponded only to 0.1% of the total 16S rRNA gene sequences obtained by pyrosequencing in ST and in OL incubations. Another cause for the low level of protein identification from syntrophs might be the lack of genomic information. Presently there is only one genome available from a medium-chain fatty acid degrader (*Syntrophomonas wolfei*). The conversion of fatty acids with different carbon chain length might require different enzymes activities. For instance, the genome of *E. coli* encodes two different acyl-CoA dehydrogenases, one specific for medium-chain acyl-CoA and another specific for medium- and long-chain acyl-CoA (Sousa et al., 2009a). In this study, proteins associated to lipid metabolism were among the most abundant bacterial proteins, although identified in a variety of bacterial genera, including the *Nitrobacter* (*Alphaproteobacteria*), *Syntrophobacter* (*Deltaproteobacteria*) and *Pelotomaculum* (*Firmicutes*) (Table 6.1, Table S6.5). Proteins identified in ST and OL incubations were analogous, despite the differences in microbial composition. An abundant protein was annotated as acetyl-CoA synthetase; this protein is involved in fatty acid activation prior to its degradation. Beta-oxidation enzymes, namely acyl-CoA dehydrogenase, enoyl-CoA hydratase, 3-hydroxyacyl-CoA dehydrogenase and acetyl-CoA acetyltransferase (DiRusso et al., 1999) were not identified. Interestingly, 44% of the bacterial proteins detected in this study, which were also among the most abundant proteins, were identified as belonging to syntrophic microorganisms from the families *Desulfovibrionaceae*, *Geobacteraceae*, *Pelobacteraceae*, *Peptococcaceae* and *Syntrophobacteraceae* (Table S6.4). Although these syntrophic microorganisms

are not described as LCFA consumers, this finding highlights the importance of syntrophic relationships in LCFA degrading environments. Acetate and hydrogen molecules are likely to be exchanged between bacteria and methanogens for the production of methane, allowing the energy recovery from LCFA. *De Novo* sequencing strategies were applied in order to evaluate the possibility of increasing bacterial protein identification but no relevant additional identifications were obtained (data not shown).

Methanogenic community was dominated by *Methanosaeta*-like populations. *Methanosaeta* species were the only acetate utilizers whose proteins were identified (with exception of a methyl-coenzyme M reductase from *Methanosarcina barkeri*) (Table S6.1), which indicates that acetoclastic methanogenesis was almost exclusively carried out by this group of archaea. Concerning hydrogen utilizing methanogens, *Methanobacterium* and *Methanospirillum* genera are the most active. Nevertheless, much less proteins were identified when comparing with *Methanosaeta*, probably because hydrogenotrophic microorganisms were less abundant as told by pyrosequencing results (Table S6.3). Furthermore, 16S rRNA gene sequences matching within the *Methanobacterium* genus were most similar to those of uncultured microorganisms, with exception of *Methanobacterium kanagiense* (genome sequencing data not available), which makes the target protein database less specific for the identification of proteins expressed by those species. *Methanosaeta* and *Methanobacterium* species are often identified in LCFA rich environments (Pereira et al., 2002b; Salvador et al., 2013; Shigematsu et al., 2006; Sousa et al., 2007a). Therefore the presence and activity of these microorganisms in PA, ST and OL incubations is consistent with previous data. Hydrogenotrophic methanogens in this study were more abundant and active in unsaturated-LCFA

incubation than in saturated-LCFA incubations (Figure 6.2 and Table S6.1) which suggests a higher importance of the hydrogenotrophic activity during the degradation of unsaturated-LCFA.

Even though metaproteomics studies of complex microbial communities do not always allow a direct connection between particular members of the community and specific metabolic functions, they give information about the general activity of the community (VerBerkmoes et al., 2009). In this study metaproteomics analysis showed that LCFA degrading communities have their metabolism centered in energy production, lipid and methane metabolisms. Differences in LCFA consumers activities based on metaproteomics results were not clear between incubations even though microbial communities composition of saturated- and unsaturated-LCFA microcosms were dissimilar. It is of utmost importance to gather more genome data from syntrophic LCFA-degraders in databases in order to fully explore the metaproteome of LCFA-degrading microbial communities.

Chapter 7

Comparative proteomics of *Syntrophomonas zehnderi* and *Methanobacterium formicicum* growing on stearate and oleate

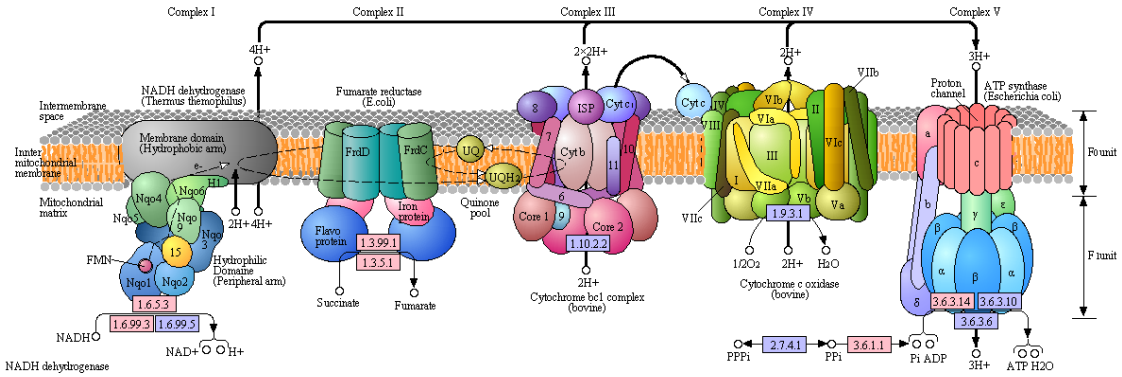

A co-culture of *Syntrophomonas zehnderi* and *Methanobacterium formicicum* were incubated with saturated- and monounsaturated-LCFAs with 18 carbon atoms. The degradation of stearate (C18:0) and oleate (C18:1) by *S. zehnderi* was followed by methane production by *M. formicicum*. The protein pool expressed by both microorganisms under those conditions was analyzed by a shotgun proteomics approach coupling high performance liquid chromatography to mass spectrometry. Mass spectra obtained were used for peptides identification and finally for proteins identification by searching against *Syntrophomonadacea*, *Clostridiales*, *Firmicutes* and *Methanobacterium* protein databases. A total of 313 proteins could be identified using this approach. The majority of the proteins were assigned to *Methanobacterium* genus (90%) and only 10% were assigned to bacteria. Proteins expressed by *M. formicicum* and by *S. zehnderi* were distributed by 19 and 9 different COG functional categories, respectively. Better represented COG categories for both microorganisms were energy production and conversion, posttranslational modification, protein turnover, chaperones and translation, ribosomal structure and biogenesis. Proteins assigned to coenzyme transport and metabolism functional category, which comprises several proteins related to methanogenesis, were also very well represented, counting with 13% to 17% of the spectra used for *Methanobacterium* proteins identification. Key enzymes for the utilization of fatty acids and methane production could be identified. This study shows for the first time the proteome analysis of an LCFA-degrading syntrophic co-culture. Although differences between degradation of saturated- and unsaturated-LCFA degradation were not possible to address, due to the low level of proteins identification expressed by *S. zehnderi*, the most important occurring metabolic processes, namely fatty acid oxidation and methane production could be recognized.

7.1 Introduction

Syntrophomonas zehnderi is a long-chain fatty acid (LCFA) degrading bacterium that was isolated from an anaerobic granular sludge bed reactor treating an oleate-based effluent (Sousa et al., 2007c). *S. zehnderi* is an obligate syntrophic microorganism and can only degrade LCFA when working in cooperation with a hydrogenotrophic methanogen like *Methanobacterium formicicum* (Sousa et al., 2007c). During syntrophic conversions, the methanogen receives electrons from the bacteria by exchanging hydrogen or formate and this way hydrogen levels are kept low enough enabling the anaerobic oxidation of LCFA (McInerney et al., 2009; Sousa et al., 2009a; Zhao et al., 1993). Both organisms benefit from this interaction and the energy gained by fatty acids β-oxidation and methane formation reactions can be used in anabolic pathways and for increasing cell yield. There are few syntrophic LCFA β-oxidizers able to degrade unsaturated long-chain fatty acids. Up to date *Syntrophomonas curvata*, *Syntrophomonas sapovorans* and *Syntrophomonas zehnderi* are the only known syntrophs that are able to grow on unsaturated LCFA with 18 carbon atoms under mesophilic conditions (Roy et al., 1986; Sousa et al., 2009a; Zhang et al., 2004). Additionally, two thermophilic microorganisms, *Thermosyntropha lipolytica* and *Thermosyntropha tengcongensis* also have the ability to degrade unsaturated-LCFA with 18 carbon atoms in syntrophy with *Methanothermobacter thermautotrophicus* (Sousa et al., 2009a; Svetlitshnyi et al., 1996; Zhang et al., 2012). The diversity of anaerobic communities seems to diverge if degrading saturated- or unsaturated-LCFA and this suggests that different microorganisms and probably different mechanisms are associated with the degradation of LCFAs with different degree of saturation (Sousa et al., 2007b). The enzymology and regulation of anaerobic LCFA β-oxidation pathway in *E. coli* is reported but there are no studies in syntrophic LCFA oxidizing bacteria (Campbell et al., 2003; Fujita et al., 2007). *S. zehnderi* is a good

candidate for investigating the possible differences between the degradation of saturated- and unsaturated-LCFA. In this study, co-cultures of *S. zehnderi* and *M. formicicum* were incubated with oleate (C18:1) or stearate (C18:0) and the proteins expressed in both conditions were analyzed by using a shotgun proteomics approach.

7.2 Materials and methods

7.2.1 Source of microorganisms and growth conditions

A co-culture of *Syntrophomonas zehnderi* (DSM 17840^T) and *Methanobacterium formicicum* (DSM 1535^T) was used in this study. Co-culture was grown at 37 ºC in sterile bicarbonate-buffered mineral salt medium supplemented with trace elements, vitamins and oleate (0.5 mM) or stearate (0.5 mM) as carbon source (Sousa et al., 2007b). Bottles headspace consisted of a mixture of N_2/CO_2 (80:20; $1.7x10^5$ Pa). Medium was reduced prior inoculation with 0.8 mM sodium sulfide ($Na_2S.xH_2O$, x=7-9). Growth was monitored by measuring methane production and also phase contrast microscopic observation. Early exponential phase *S. zenhderi* co-cultures, growing on oleate or stearate, were sampled for protein extraction. Methane analysis was performed as described in section 5.2.2.

7.2.2 Preparation of protein extracts from *S. zehnderi* co-cultures

Cells from 500 mL of *S. zehnderi* co-culture grown to early stationary phase, with oleate or stearate as sole carbon source, were harvested by centrifugation (3,219 xg, 4ºC, 10 min). Cells were resuspended in PBS buffer with 1 mM of PMSF and frozen at -80ºC until protein extraction. Proteins were extracted, purified and quantified as decribed in section 6.2.5.

7.2.3 SDS-PAGE protein electrophoresis and LC-MS/MS analysis

Proteins were separated by SDS-PAGE electrophoresis using NuPAGE Novex Bis-Tris Mini Gels (Invitrogen). Approximately 10 ug of total protein extracted were loaded in the

SDS-PAGE gel. A minimum of 12 gel fractions were collected along the protein profile (12 fractions in the case of the sample incubated with oleate and 24 fractions in the case of the sample incubated with stearate) and were subsequently digested with trypsin prior to liquid chromatography coupled to tandem mass spectrometry (LC-MS/MS) analysis. LC-MS/MS analysis was performed with an Ultimate 3000 LC system (Dionex) connected by a nanoelectrospray interface to a linear ion trap mass spectrometer coupled to an Orbitrap detector (LTQ-Orbitrap, Thermo Fisher, Waltham, MA, USA; PAPPSO proteomic platform, INRA, Jouy-en-Josas) as described elsewhere (Ibrahim et al., 2007).

7.2.4 Database searching, protein identification and functional annotation

Protein identification was made by matching tandem mass spectra against model spectra created from each peptide present in a protein database by using X!Tandem software (Craig and Beavis, 2004). Two protein databases, one specific for *Methanobacterium* genus (taxon: 2160, entries: 7507, downloaded on 10/12/2012) and another specific for *Syntrophomonadaceae* family (taxon: 68298, entries: 7954, downloaded on 19/01/2012) were downloaded from the Uniprot website (http://www.uniprot.org) and combined prior to analysis of MS/MS spectra with X!Tandem. Scaffold software (version 4.0.4) (Searle, 2010) was used to group, visualize and validate the identified proteins. Peptide and protein probability thresholds were set to higher than 95% and 99%, respectively, with at least 2 identified peptides per protein. Searches against *Clostridiales* (taxon: 186802, entries: 904195, downloaded on 29/05/2013) plus *Methanobacterium* and *Firmicutes* (taxon: 1239, entries: 5600462, downloaded on 29/05/2013) plus *Methanobacterium* protein databases were also performed aiming to increase the number of proteins retrieved. Functional annotation of proteins was obtained by scanning protein sequences against the Cluster of Orthologous Groups database (COG database) (http://www.ncbi.nlm.nih.gov/Structure/cdd/wrpsb.cgi) (Marchler-Bauer et al., 2011). The relative abundance of proteins was estimated based on the total number of spectra

assigned to each protein. Proteins which have EC number (Enzyme Commission Number) were mapped into KEGG metabolic pathways using the pathway mapping tool available in Kegg Pathway Database website (http://www.genome.jp/kegg/pathway.html).

7.3 Results

7.3.1 Proteins identified in *S. zehnderi* co-cultures

S. zehnderi cells (in co-culture with *M. formicicum*) were harvested during the exponential phase of growth on oleate or stearate, which occurred approximately 2 weeks after co-culture inoculation. The concentration of proteins extracted from the co-culture growing on stearate (5 ug/L) was about 3 times higher than the one obtained for the co-culture growing on oleate (1.7 ug/L). Differences could be detected between SDS-PAGE protein profiles obtained when the co-culture was incubated with stearate or with oleate (Figure S7.1). A total of 313 proteins were identified in the experiment, 261 of which were expressed by cultures growing with both oleate and stearate (Figure 7.1). Nevertheless, 34 proteins were only identified in the sample where oleate was the added substrate and other 18 proteins were only detected in stearate incubation.

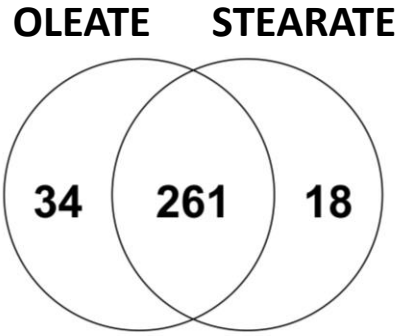

Figure 7.1 Venn diagram summarizing the similarities and differences between the proteins expressed during the conversion of oleate and stearate to methane by *S. zehnderi* and *M. formicicum*.

7.3.2 Proteins matching *Syntrophomonadaceae*, *Clostridiales* and *Firmicutes* protein databases

Syntrophomonas zehnderi proteome information is not available in public databases so far, thus it was not possible to perform the identification of proteins expressed by this bacterium based on a database specific for *S. zehnderi*. Therefore, proteins were identified by comparison with those present in the *Syntrophomonadaceae* protein database. This database includes proteins from *Dethiobacter alkaliphilus* AHT 1, *Syntrophothermus lipocalidus* TGB-C1 and from several microorganisms belonging to *Syntrophomonas* genus, from which only *Syntrophomonas wolfei* has its entire proteome available. Proteins identified by matching MS/MS mass spectra towards the *Syntrophomonadaceae* protein database are listed in Table 7.1.

Despite the higher protein concentration determined for stearate incubation compared with oleate incubation, more proteins assigned to *Syntrophomonadaceae* could be detected in the latter (Table 7.1). Eleven proteins were identified in stearate sample and their relative abundance was variable. COGs functional category C (Energy production and conversion) counts with 70 % of the assigned spectra, category O (Posttranslational modification, protein turnover, chaperones) and category J (Translation, ribosomal structure and biogenesis) each one with 10 % and category I (Lipid transport and metabolism) with 5 % of the assigned spectra matching *Syntrophomonadaceae* protein database. Protein "UPF0296 protein Swol_1238" is not classified in any COGs category and is represented by 5% of the assigned spectra in stearate incubation and 2% in oleate incubation. During oleate degradation the distribution of bacterial proteins over the several functional categories was different from that obtained for stearate incubation. The 32 proteins identified in oleate incubation were distributed by 5 additional functional categories namely Nucleotide transport and metabolism (category F), Transcription

(category K), Signal transduction mechanisms (category T), General function prediction only (category R) and Function unknown (category S).

Acyl-CoA dehydrogenase (Uniprot ID: D7CLS6 from *Syntrophothermus lipocalidus*) was found in both stearate and oleate incubations. This enzyme catalyzes the first step in each cycle of fatty acid beta-oxidation. Searches against protein databases specific for order *Clostridiales* and phylum *Firmicutes* did not increase the number of new COG functional categories but allowed the identification of more proteins assigned to category I (Lipid metabolism). Searches against general protein databases (e.g. the complete Uniprot protein database and the *Bacteria* protein database, Uniprot taxon ID 2) were also performed but no extra protein functions were identified.

Proteins related to fatty acid catabolism detected in this study are listed in Table 7.2. Databases that include proteins found in more than one microorganism, as it is the case of all the protein databases used in this work, comprise several proteins with the same function which belong to different microorganisms, and as a consequence the proteins identifications in the experiment might be redundant. For example in Table 7.2, from the 10 proteins identified only 4 different protein functions could be recognized. For instance, acyl-CoA dehydrogenase was identified three times when the data was searched independently against the three protein databases (*Syntrophomonadaceae*, *Clostridiales* and *Firmicutes* protein databases). The EC number (1.3.99.3) for acyl-CoA dehydrogenase does no longer exist and was transferred to 1.3.8.7, 1.3.8.8 and 1.3.8.9 if the acyl-CoA dehydrogenase is specific for medium-chain, long-chain or very-long-chain fatty acids, respectively. In Table 7.2 the old EC number is given but in Figure 7.2 the EC numbers specific for medium- and long-chain fatty acids are the ones represented in the fatty acid β-oxidation pathway.

Despite the low number of bacterial proteins identified in this study, the results showed that the metabolism of *Syntrophomonas zehnderi* is centered in energy production and

fatty acid metabolism. In Figure 7.2 the bacterial proteins involved in fatty acid oxidation that could be detected using this proteomics approach are highlighted (red boxes).

Table 7.1 Identification and functional assignment of proteins assigned to *Syntrophomonadaceae* family when *S. zehnderi* co-culture was incubated with stearate (ST) and oleate (OL). Relative abundance of each one of the proteins identified is given in percentage.

				Abundance (% of spectra)	
COG Functional Category	**Protein name**	**Uniprot ID**	**Organism**	**LCFA**	**OL**	**ST**
Energy production and conversion					52	70
	Acetate kinase	Q0AYW5	*Syntrophomonas wolfei subsp. wolfei*		4	0
	ATP synthase subunit alpha	Q0AUD1	*Syntrophomonas wolfei subsp. wolfei*		8	15
	ATP synthase subunit beta	Q0AUD3	*Syntrophomonas wolfei subsp. wolfei*		8	20
	ATP synthase subunit beta	D7CJR8	*Syntrophothermus lipocalidus*		8	5
	ATP synthase subunit alpha	D7CJS0	*Syntrophothermus lipocalidus*		5	20
	ATP synthase gamma chain	Q0AUD2	*Syntrophomonas wolfei subsp. wolfei*		3	5
	NADH dehydrogenase (Quinone)	Q0AY72	*Syntrophomonas wolfei subsp. wolfei*		2	0
	Phosphotransacetylase	Q0AYW6	*Syntrophomonas wolfei subsp. wolfei*		4	0
	Electron transfer flavoprotein, alpha subunit	Q0AZ33	*Syntrophomonas wolfei subsp. wolfei*		3	0
	Formate dehydrogenase alpha subunit	Q0AYT4	*Syntrophomonas wolfei subsp. wolfei*		2	0
	NADH dehydrogenase (Quinone)	Q0AY66	*Syntrophomonas wolfei subsp. wolfei*		2	5
	Electron transfer flavoprotein, beta subunit	Q0AZ34	*Syntrophomonas wolfei subsp. wolfei*		5	0
Posttranslational modification, protein turnover, chaperones					15	10
	60 kDa chaperonin	Q0AVV1	*Syntrophomonas wolfei subsp. wolfei*		2	10
	ATPase AAA-2 domain protein	C0GF50	*Dethiobacter alkaliphilus AHT 1*		2	0
	Putative ATPase with chaperone activity	Q0AZM6	*Syntrophomonas wolfei subsp. wolfei*		2	0
	Chaperone protein DnaK	Q0AZM9	*Syntrophomonas wolfei subsp. wolfei*		2	0
	Chaperone protein DnaK	Q0AWM3	*Syntrophomonas wolfei subsp. wolfei*		2	0
	ATPases with chaperone activity	Q0AUE8	*Syntrophomonas wolfei subsp. wolfei*		2	0
	Alkyl hydroperoxide reductase	Q0AUY1	*Syntrophomonas wolfei subsp. wolfei*		5	0
Translation, ribosomal structure and biogenesis					11	10
	Elongation factor Tu 2	Q0AUG3	*Syntrophomonas wolfei subsp. wolfei*		5	5
	50S ribosomal protein L6	Q0AUJ5	*Syntrophomonas wolfei subsp. wolfei*		2	0
	30S ribosomal protein S3	Q0AUI6	*Syntrophomonas wolfei subsp. wolfei*		2	0
	Translation elongation factor G	Q0AXU2	*Syntrophomonas wolfei subsp. wolfei*		3	5
Lipid transport and metabolism					4	5
	Acyl-CoA dehydrogenase domain protein	D7CLS6	*Syntrophothermus lipocalidus*		4	5
Nucleotide transport and metabolism					2	0
	Inosine-5'-monophosphate dehydrogenase	D7CMA3	*Syntrophothermus lipocalidus*		2	0
Transcription					8	0
	DNA-directed RNA polymerase subunit beta	Q0AUH2	*Syntrophomonas wolfei subsp. wolfei*		5	0
	DNA-directed RNA polymerase subunit beta	Q0AUH3	*Syntrophomonas wolfei subsp. wolfei*		2	0
	30S ribosomal protein S8	Q0AUJ4	*Syntrophomonas wolfei subsp. wolfei*		2	0
Signal transduction mechanisms					2	0
	Response regulator receiver protein	Q0AYM3	*Syntrophomonas wolfei subsp. wolfei*		2	0
General function prediction only					2	0
	CBS domain protein	Q0AWT7	*Syntrophomonas wolfei subsp. wolfei*		2	0
Function unknown					2	0
	Stage V sporulation protein S	D7CM97	*Syntrophothermus lipocalidus*		2	0
No COG					2	5
	UPF0296 protein Swol_1238	Q0AXK7	*Syntrophomonas wolfei subsp. wolfei*		2	5

Table 7.2 Identification of bacterial proteins involved in fatty acid metabolism that were assigned to phylum *Firmicutes*, order *Clostridiales* or family *Syntrophomonadaceae*.

Target protein database	Protein name	Uniprot ID	EC number	Microorganism
Syntrophomonadaceae	Acyl-CoA dehydrogenase domain protein	D7CLS6	1.3.99.3	*Syntrophothermus lipocalidus*
Clostridiales	Acyl-CoA dehydrogenase domain protein	B8FXG7	1.3.99.3	*Desulfitobacterium hafniense* (strain DCB-2)
Clostridiales and *Firmicutes*	Acyl-CoA dehydrogenase, N-terminal domain protein	G2FP38	1.3.99.3	*Desulfosporosinus* sp. OT
Clostridiales and *Firmicutes*	Enoyl-CoA hydratase/carnithine racemase	H5XUU6	4.2.1.17	*Desulfosporosinus youngiae* DSM 17734
Clostridiales and *Firmicutes*	Acetyl-CoA acetyltransferase	D7CLS5	2.3.1.9	*Syntrophothermus lipocalidus*
Clostridiales and *Firmicutes*	Acetyl-CoA acetyltransferase	Q0AVM3	2.3.1.9	*Syntrophomonas wolfei*
Clostridiales	Acetyl-CoA acetyltransferase	D4J7N8	2.3.1.9	*Coprococcus catus* GD/7
Clostridiales and *Firmicutes*	Acetyl-CoA acetyltransferase	F4A727	2.3.1.9	*Clostridium botulinum* BKT015925
Clostridiales	ThlA2	A5N3I6	2.3.1.9	*Clostridium kluyveri (strain ATCC 8527)*
Firmicutes	3-ketoacyl-CoA thiolase	F7TPZ1	2.3.1.16	*Brevibacillus laterosporus* LMG 15441

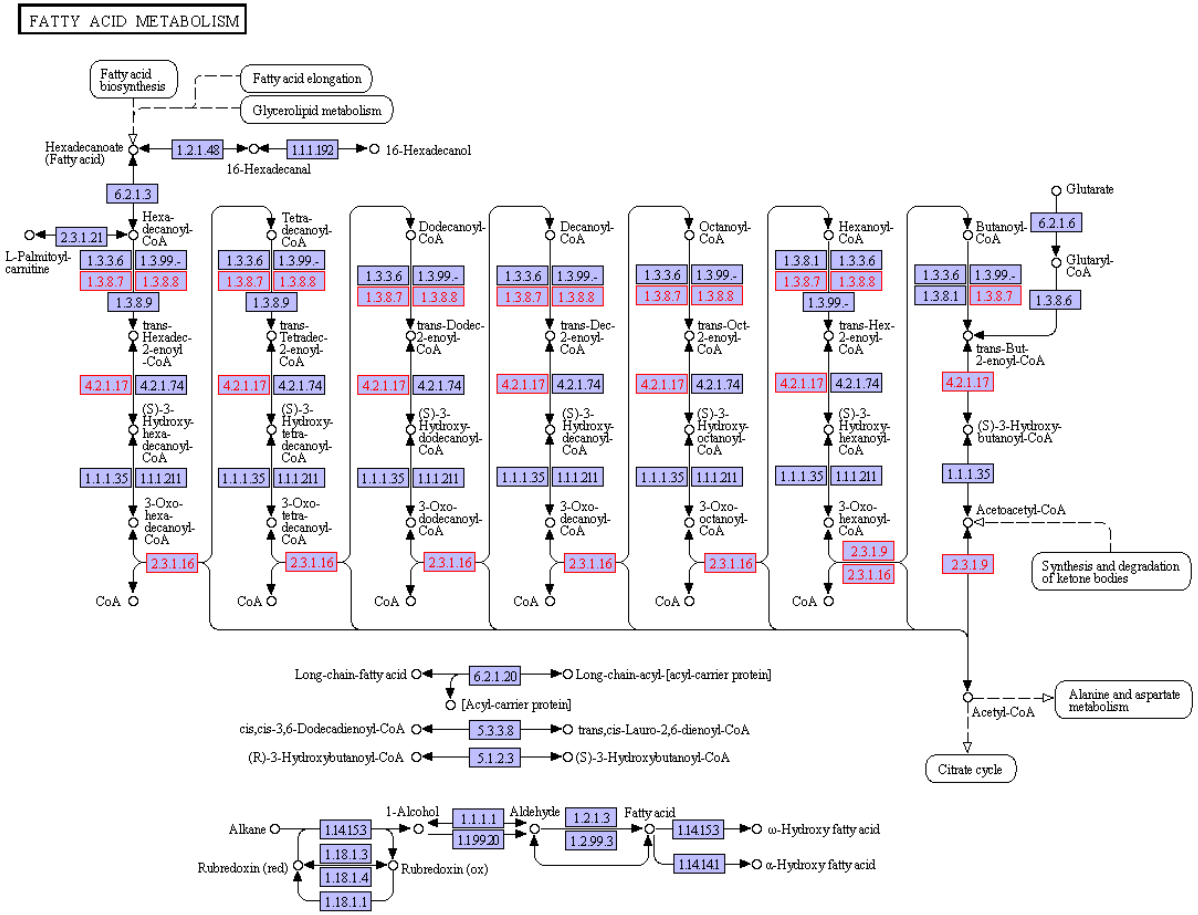

Figure 7.2 Representation of proteins matching *Syntrophomonadaceae*, *Clostridiales* and *Firmicutes* protein databases and identified in the experiment (red boxes) that are involved in fatty acid metabolism.

7.3.3 Proteins matching the *Methanobacterium* protein database

A total of 281 proteins assigned to *Methanobacterium* genus could be identified by peptide fingerprinting mass spectrometry. Few proteins from *Methanobacterium formicicum* DSM 1535, *Methanobacterium sp.* strain SWAN-1 and strain AL-21could be identified and the majority of proteins were assigned to *Methanobacterium formicicum* DSM 3637. Only 15 proteins from *M. formicicum* DSM 1535 are available in Uniprot database (Table S7.1) which explains why the proteins identified were assigned to *M. formicicum* DSM 3637 (that in contrast has 2519 protein entries in Uniprot database). Among those 15 proteins belonging to *M. formicicum* DSM 1535, five proteins were detected in the incubations with LCFA namely formate dehydrogenase subunit alpha and subunit beta, archaeal histone A1, methyl-coenzyme M reductase alpha subunit and methyl-coenzyme M reductase II alpha subunit (Table S7.1). Table 7.3 shows the relative abundance and the number of assigned spectra to COG functional categories identified in the experiment. *Methanobacterium* proteins were distributed by 19 COG functional categories and about 1% did not match to any category. Approximately 3% and 2% of the spectra were assigned to proteins with unknown function in oleate and stearate incubations, respectively. The majority of spectra (~30%) were used to identify proteins from category C (Energy production and conversion). Nevertheless, many abundant proteins were assigned to categories J (Translation, ribosomal structure and biogenesis) (about 13%) and H (Coenzyme transport and metabolism) (about 13% in oleate and 17% in stearate incubations). Nonetheless, remain COG categories were also very well represented including proteins belonging to several subcategories (Table 7.3).

Table 7.3 COG functional assignment of proteins from *Methanobacterium* genus when *S. zehnderi* co-cultures were incubated with stearate (ST) and oleate (OL). The number of assigned spectra to COG functional categories and their relative abundance (given by the percentage of spectra assigned) are represented.

	Number of Assigned Spectra			Abundance (% spectra)	
COG Functional Category	**LCFA**	**OL**	**ST**	**OL**	**ST**
C - Energy production and conversion		596	343	33,1	31,1
COG0039 Malate/lactate dehydrogenases		2	0	0,1	0,0
COG0045 Succinyl-CoA synthetase, beta subunit		2	3	0,1	0,3
COG0243 Anaerobic dehydrogenases, typically selenocysteine-containing		35	13	1,9	1,2
COG0644 Dehydrogenases (flavoproteins)		0	2	0,0	0,2
COG0674 Pyruvate:ferredoxin oxidoreductase and related 2-oxoacid:ferredoxin oxidoreductases, alpha subunit		7	4	0,4	0,4
COG0680 Ni,Fe-hydrogenase maturation factor		3	2	0,2	0,2
COG1013 Pyruvate:ferredoxin oxidoreductase and related 2-oxoacid:ferredoxin oxidoreductases, beta subunit		3	2	0,2	0,2
COG1014 Pyruvate:ferredoxin oxidoreductase and related 2-oxoacid:ferredoxin oxidoreductases, gamma subunit		12	7	0,7	0,6
COG1035 Coenzyme F420-reducing hydrogenase, beta subunit		36	23	2,0	2,1
COG1036 Archaeal flavoproteins		8	0	0,4	0,0
COG1142 Fe-S-cluster-containing hydrogenase components 2		4	2	0,2	0,2
COG1146 Ferredoxin		0	3	0,0	0,3
COG1148 Heterodisulfide reductase, subunit A and related polyferredoxins		62	52	3,4	4,7
COG1150 Heterodisulfide reductase, subunit C		11	3	0,6	0,3
COG1151 6Fe-6S prismane cluster-containing protein		2	9	0,1	0,8
COG1152 CO dehydrogenase/acetyl-CoA synthase alpha subunit		3	5	0,2	0,5
COG1155 Archaeal/vacuolar-type H+-ATPase subunit A		14	7	0,8	0,6
COG1156 Archaeal/vacuolar-type H+-ATPase subunit B		32	23	1,8	2,1
COG1229 Formylmethanofuran dehydrogenase subunit A		2	3	0,1	0,3
COG1390 Archaeal/vacuolar-type H+-ATPase subunit E		8	3	0,4	0,3
COG1394 Archaeal/vacuolar-type H+-ATPase subunit D		8	5	0,4	0,5
COG1456 CO dehydrogenase/acetyl-CoA synthase gamma subunit (corrinoid Fe-S protein)		3	5	0,2	0,5
COG1592 Rubrerythrin		2	1	0,1	0,1
COG1880 CO dehydrogenase/acetyl-CoA synthase epsilon subunit		6	0	0,3	0,0
COG1908 Coenzyme F420-reducing hydrogenase, delta subunit		9	3	0,5	0,3
COG1927 Coenzyme F420-dependent N(5),N(10)-methenyltetrahydromethanopterin dehydrogenase		19	11	1,1	1,0
COG1941 Coenzyme F420-reducing hydrogenase, gamma subunit		24	13	1,3	1,2
COG2037 Formylmethanofuran:tetrahydromethanopterin formyltransferase		8	2	0,4	0,2
COG2048 Heterodisulfide reductase, subunit B		22	3	1,2	0,3
COG2069 CO dehydrogenase/acetyl-CoA synthase delta subunit (corrinoid Fe-S protein)		3	2	0,2	0,2
COG2141 Coenzyme F420-dependent N5,N10-methylene tetrahydromethanopterin reductase and related flavin-dependent oxidoreductases		186	57	10,3	5,2
COG2218 Formylmethanofuran dehydrogenase subunit C		3	2	0,2	0,2
COG3259 Coenzyme F420-reducing hydrogenase, alpha subunit		52	69	2,9	6,3
COG3260 Ni,Fe-hydrogenase III small subunit		5	4	0,3	0,4

Table 7.3 (continued)

	Number of Assigned Spectra			Abundance (% spectra)	
COG Functional Category	**LCFA**	**OL**	**ST**	**OL**	**ST**
O - Posttranslational modification, protein turnover, chaperones		163	105	9,1	9,5
COG0071 Molecular chaperone (small heat shock protein)		2	3	0,1	0,3
COG0330 Membrane protease subunits, stomatin/prohibitin homologs		4	3	0,2	0,3
COG0378 Ni2+-binding GTPase involved in regulation of expression and maturation of		7	10	0,4	0,9
COG0396 ABC-type transport system involved in Fe-S cluster assembly, ATPase component		5	3	0,3	0,3
COG0443 Molecular chaperone		29	27	1,6	2,4
COG0459 Chaperonin GroEL (HSP60 family)		71	36	3,9	3,3
COG0464 ATPases of the AAA+ class		3	1	0,2	0,1
COG0638 20S proteasome, alpha and beta subunits		17	9	0,9	0,8
COG0652 Peptidyl-prolyl cis-trans isomerase (rotamase) - cyclophilin family		2	0	0,1	0,0
COG0719 ABC-type transport system involved in Fe-S cluster assembly, permease component		5	5	0,3	0,5
COG1047 FKBP-type peptidyl-prolyl cis-trans isomerases 2		10	5	0,6	0,5
COG1222 ATP-dependent 26S proteasome regulatory subunit		6	3	0,3	0,3
COG1973 Hydrogenase maturation factor		2	0	0,1	0,0
J - Translation, ribosomal structure and biogenesis		235	153	13,1	13,9
COG0013 Alanyl-tRNA synthetase		0	2	0,0	0,2
COG0017 Aspartyl/asparaginyl-tRNA synthetases		4	8	0,2	0,7
COG0023 Translation initiation factor 1 (eIF-1/SUI1) and related proteins		2	0	0,1	0,0
COG0048 Ribosomal protein S12		11	3	0,6	0,3
COG0051 Ribosomal protein S10		4	1	0,2	0,1
COG0052 Ribosomal protein S2		7	10	0,4	0,9
COG0072 Phenylalanyl-tRNA synthetase beta subunit		2	4	0,1	0,4
COG0080 Ribosomal protein L11		8	1	0,4	0,1
COG0093 Ribosomal protein L14		4	0	0,2	0,0
COG0096 Ribosomal protein S8		3	3	0,2	0,3
COG0097 Ribosomal protein L6P/L9E		5	5	0,3	0,5
COG0098 Ribosomal protein S5		6	5	0,3	0,5
COG0100 Ribosomal protein S11		16	7	0,9	0,6
COG0124 Histidyl-tRNA synthetase		1	2	0,1	0,2
COG0154 Asp-tRNAAsn/Glu-tRNAGln amidotransferase A subunit and related amidases		2	0	0,1	0,0
COG0244 Ribosomal protein L10		3	1	0,2	0,1
COG0423 Glycyl-tRNA synthetase (class II)		1	2	0,1	0,2
COG0480 Translation elongation factors (GTPases)		57	61	3,2	5,5
COG0689 RNase PH		6	1	0,3	0,1
COG1096 Predicted RNA-binding protein (consists of S1 domain and a Zn-ribbon domain)		3	2	0,2	0,2
COG1097 RNA-binding protein Rrp4 and related proteins (contain S1 domain and KH domain)		4	5	0,2	0,5
COG1471 Ribosomal protein S4E		3	2	0,2	0,2
COG1500 Predicted exosome subunit		3	0	0,2	0,0
COG1890 Ribosomal protein S3AE		11	1	0,6	0,1
COG2051 Ribosomal protein S27E		2	5	0,1	0,5
COG2058 Ribosomal protein L12E/L44/L45/RPP1/RPP2		3	1	0,2	0,1
COG2125 Ribosomal protein S6E (S10)		3	0	0,2	0,0
COG5256 Translation elongation factor EF-1alpha (GTPase)		61	18	3,4	1,6
COG5257 Translation initiation factor 2, gamma subunit (eIF-2gamma; GTPase)		0	3	0,0	0,3

Table 7.3 (continued)

	Number of Assigned Spectra			Abundance (% spectra)	
COG Functional Category	**LCFA**	**OL**	**ST**	**OL**	**ST**
F - Nucleotide transport and metabolism		48	35	2,7	3,2
COG0034 Glutamine phosphoribosylpyrophosphate amidotransferase		0	2	0,0	0,2
COG0046 Phosphoribosylformylglycinamidine (FGAM) synthase, synthetase domain		4	4	0,2	0,4
COG0047 Phosphoribosylformylglycinamidine (FGAM) synthase, glutamine amidotransferase domain		7	1	0,4	0,1
COG0104 Adenylosuccinate synthase		4	5	0,2	0,5
COG0105 Nucleoside diphosphate kinase		5	2	0,3	0,2
COG0504 CTP synthase (UTP-ammonia lyase)		0	5	0,0	0,5
COG0516 IMP dehydrogenase/GMP reductase		7	5	0,4	0,5
COG0717 Deoxycytidine deaminase		7	2	0,4	0,2
COG0856 Orotate phosphoribosyltransferase homologs		9	6	0,5	0,5
COG1328 Oxygen-sensitive ribonucleoside-triphosphate reductase		0	2	0,0	0,2
COG2019 Archaeal adenylate kinase		5	1	0,3	0,1
K – Transcription		58	32	3,2	2,9
COG0085 DNA-directed RNA polymerase, beta subunit/140 kD subunit		2	0	0,1	0,0
COG0086 DNA-directed RNA polymerase, beta' subunit/160 kD subunit		9	7	0,5	0,6
COG0195 Transcription elongation factor		2	2	0,1	0,2
COG0202 DNA-directed RNA polymerase, alpha subunit/40 kD subunit		0	2	0,0	0,2
COG0250 Transcription antiterminator		4	1	0,2	0,1
COG0464 ATPases of the AAA+ class		14	4	0,8	0,4
COG1095 DNA-directed RNA polymerase, subunit E'		2	0	0,1	0,0
COG1396 Predicted transcriptional regulators		2	0	0,1	0,0
COG1405 Transcription initiation factor TFIIIB, Brf1 subunit/Transcription initiation factor TFIIB		1	2	0,1	0,2
COG1522 Transcriptional regulators		4	1	0,2	0,1
COG1958 Small nuclear ribonucleoprotein (snRNP) homolog		3	1	0,2	0,1
COG2101 TATA-box binding protein (TBP), component of TFIID and TFIIIB		13	12	0,7	1,1
COG2524 Predicted transcriptional regulator, contains C-terminal CBS domains		2	0	0,1	0,0

Table 7.3 (continued)

	Number of Assigned Spectra			Abundance (% spectra)	
COG Functional Category	**LCFA**	**OL**	**ST**	**OL**	**ST**
E - Amino acid transport and metabolismo		66	49	3,7	4,4
COG0028 Thiamine pyrophosphate-requiring enzymes		2	3	0,1	0,3
COG0031 Cysteine synthase		0	2	0,0	0,2
COG0059 Ketol-acid reductoisomerase		1	2	0,1	0,2
COG0066 3-isopropylmalate dehydratase small subunit		4	5	0,2	0,5
COG0069 Glutamate synthase domain 2		4	6	0,2	0,5
COG0075 Serine-pyruvate aminotransferase/archaeal aspartate aminotransferase		9	4	0,5	0,4
COG0076 Glutamate decarboxylase and related PLP-dependent proteins		1	2	0,1	0,2
COG0112 Glycine/serine hydroxymethyltransferase		0	2	0,0	0,2
COG0119 Isopropylmalate/homocitrate/citramalate synthases		2	0	0,1	0,0
COG0133 Tryptophan synthase beta chain		0	2	0,0	0,2
COG0137 Argininosuccinate synthase		4	2	0,2	0,2
COG0174 Glutamine synthetase		1	3	0,1	0,3
COG0252 L-asparaginase/archaeal Glu-tRNAGln amidotransferase subunit D		0	2	0,0	0,2
COG0289 Dihydrodipicolinate reductase		3	2	0,2	0,2
COG0329 Dihydrodipicolinate synthase/N-acetylneuraminate lyase		2	0	0,1	0,0
COG0436 Aspartate/tyrosine/aromatic aminotransferase		0	2	0,0	0,2
COG0458 Carbamoylphosphate synthase large subunit (split gene in MJ)		6	2	0,3	0,2
COG0498 Threonine synthase		5	1	0,3	0,1
COG0527 Aspartokinases		3	0	0,2	0,0
COG1364 N-acetylglutamate synthase (N-acetylornithine aminotransferase)		5	3	0,3	0,3
COG1465 Predicted alternative 3-dehydroquinate synthase		4	0	0,2	0,0
COG1812 Archaeal S-adenosylmethionine synthetase		8	4	0,4	0,4
COG4992 Ornithine/acetylornithine aminotransferase		2	0	0,1	0,0
I - Lipid transport and metabolism		33	17	1,8	1,5
COG0183 Acetyl-CoA acetyltransferase		11	4	0,6	0,4
COG0365 Acyl-coenzyme A synthetases/AMP-(fatty) acid ligases		1	2	0,1	0,2
COG0439 Biotin carboxylase		1	3	0,1	0,3
COG1028 Dehydrogenases with different specificities (related to short-chain alcohol dehydrogenases)		2	1	0,1	0,1
COG1260 Myo-inositol-1-phosphate synthase		2	2	0,1	0,2
COG1924 Activator of 2-hydroxyglutaryl-CoA dehydratase (HSP70-class ATPase domain)		3	0	0,2	0,0
COG3425 3-hydroxy-3-methylglutaryl CoA synthase		13	5	0,7	0,5
G - Carbohydrate transport and metabolism		34	16	1,9	1,4
COG0057 Glyceraldehyde-3-phosphate dehydrogenase/erythrose-4-phosphate dehydrogenase		4	2	0,2	0,2
COG0126 3-phosphoglycerate kinase		2	0	0,1	0,0
COG0148 Enolase		5	4	0,3	0,4
COG0149 Triosephosphate isomerase		2	2	0,1	0,2
COG1109 Phosphomannomutase		3	2	0,2	0,2
COG1363 Cellulase M and related proteins		5	2	0,3	0,2
COG1830 DhnA-type fructose-1,6-bisphosphate aldolase and related enzymes		5	3	0,3	0,3
COG1980 Archaeal fructose 1,6-bisphosphatase		8	1	0,4	0,1

Table 7.3 (continued)

	Number of Assigned Spectra			Abundance (% spectra)	
COG Functional Category	**LCFA**	**OL**	**ST**	**OL**	**ST**
V - Defense mechanisms		10	2	0,6	0,2
COG1136 ABC-type antimicrobial peptide transport system, ATPase component		10	2	0,6	0,2
H - Coenzyme transport and metabolism		225	185	12,5	16,8
COG0007 Uroporphyrinogen-III methylase		4	0	0,2	0,0
COG0108 3,4-dihydroxy-2-butanone 4-phosphate synthase		2	1	0,1	0,1
COG0111 Phosphoglycerate dehydrogenase and related dehydrogenases		4	3	0,2	0,3
COG0163 3-polyprenyl-4-hydroxybenzoate decarboxylase		3	2	0,2	0,2
COG0214 Pyridoxine biosynthesis enzyme		4	0	0,2	0,0
COG0422 Thiamine biosynthesis protein ThiC		5	5	0,3	0,5
COG0499 S-adenosylhomocysteine hydrolase		1	2	0,1	0,2
COG1541 Coenzyme F390 synthetase		0	3	0,0	0,3
COG1635 Flavoprotein involved in thiazole biosynthesis		0	2	0,0	0,2
COG1962 Tetrahydromethanopterin S-methyltransferase, subunit H		12	10	0,7	0,9
COG3252 Methenyltetrahydromethanopterin cyclohydrolase		12	6	0,7	0,5
COG4054 Methyl coenzyme M reductase, beta subunit		76	59	4,2	5,3
COG4055 Methyl coenzyme M reductase, subunit D		5	1	0,3	0,1
COG4057 Methyl coenzyme M reductase, gamma subunit		11	2	0,6	0,2
COG4058 Methyl coenzyme M reductase, alpha subunit		82	89	4,6	8,1
COG4059 Tetrahydromethanopterin S-methyltransferase, subunit E		4	0	0,2	0,0
M - Cell wall/membrane/envelope biogenesis		6	5	0,3	0,5
COG0449 Glucosamine 6-phosphate synthetase, contains amidotransferase and phosphosugar isomerase domains		0	3	0,0	0,3
COG1210 UDP-glucose pyrophosphorylase		2	1	0,1	0,1
COG1088 dTDP-D-glucose 4,6-dehydratase		4	1	0,2	0,1
P - Inorganic ion transport and metabolism		8	4	0,4	0,4
COG1528 Ferritin-like protein		2	0	0,1	0,0
COG0605 Superoxide dismutase		2	0	0,1	0,0
COG1117 ABC-type phosphate transport system, ATPase component		2	2	0,1	0,2
COG0226 ABC-type phosphate transport system, periplasmic component		2	2	0,1	0,2
D - Cell cycle control, cell division, chromosome partitioning		35	16	1,9	1,4
COG0206 Cell division GTPase		9	6	0,5	0,5
COG1077 Actin-like ATPase involved in cell morphogenesis		23	7	1,3	0,6
COG0455 ATPases involved in chromosome partitioning		3	3	0,2	0,3
T - Signal transduction mechanisms		39	28	2,2	2,5
COG0467 RecA-superfamily ATPases implicated in signal transduction		3	3	0,2	0,3
COG0589 Universal stress protein UspA and related nucleotide-binding proteins		5	1	0,3	0,1
COG3848 Phosphohistidine swiveling domain		29	23	1,6	2,1
COG3920 Signal transduction histidine kinase		2	1	0,1	0,1
U - Intracellular trafficking, secretion, and vesicular transport		3	3	0,2	0,3
COG4962 Flp pilus assembly protein, ATPase CpaF		3	3	0,2	0,3

Table 7.3 (continued)

	Number of Assigned Spectra			Abundance (% spectra)	
COG Functional Category	**LCFA**	**OL**	**ST**	**OL**	**ST**
L - Replication, recombination and repair		47	22	2,6	2,0
COG0178 Excinuclease ATPase subunit		2	1	0,1	0,1
COG0358 DNA primase (bacterial type)		12	6	0,7	0,5
COG0468 RecA/RadA recombinase		20	4	1,1	0,4
COG0592 DNA polymerase sliding clamp subunit (PCNA homolog)		5	2	0,3	0,2
COG1241 Predicted ATPase involved in replication control, Cdc46/Mcm family		0	3	0,0	0,3
COG1599 Single-stranded DNA-binding replication protein A (RPA), large (70 kD) subunit and related ssDNA-binding proteins		5	5	0,3	0,5
COG2812 DNA polymerase III, gamma/tau subunits		3	1	0,2	0,1
B - Chromatin structure and dynamics		7	1	0,4	0,1
COG2036 Histones H3 and H4		7	1	0,4	0,1
R - General function prediction only		117	61	6,5	5,5
COG0073 EMAP domain		0	4	0,0	0,4
COG0312 Predicted Zn-dependent proteases and their inactivated homologs		3	0	0,2	0,0
COG0491 Zn-dependent hydrolases, including glyoxylases		18	10	1,0	0,9
COG0517 FOG: CBS domain		21	5	1,2	0,5
COG0535 Predicted Fe-S oxidoreductases		2	1	0,1	0,1
COG0673 Predicted dehydrogenases and related proteins		2	2	0,1	0,2
COG0824 Predicted thioesterase		3	2	0,2	0,2
COG1094 Predicted RNA-binding protein (contains KH domains)		3	0	0,2	0,0
COG1123 ATPase components of various ABC-type transport systems, contain duplicated ATPase		13	7	0,7	0,6
COG1350 Predicted alternative tryptophan synthase beta-subunit (paralog of TrpB)		5	9	0,3	0,8
COG1545 Predicted nucleic-acid-binding protein containing a Zn-ribbon		3	0	0,2	0,0
COG1707 ACT domain-containing protein		3	1	0,2	0,1
COG1712 Predicted dinucleotide-utilizing enzyme		3	1	0,2	0,1
COG1964 Predicted Fe-S oxidoreductases		0	8	0,0	0,7
COG2018 Uncharacterized distant relative of homeotic protein bithoraxoid		3	0	0,2	0,0
COG2085 Predicted dinucleotide-binding enzymes		2	0	0,1	0,0
COG2403 Predicted GTPase		1	2	0,1	0,2
COG2768 Uncharacterized Fe-S center protein		2	0	0,1	0,0
COG3269 Predicted RNA-binding protein, contains TRAM domain		5	3	0,3	0,3
COG3576 Predicted flavin-nucleotide-binding protein structurally related to pyridoxine 5'-phosphate oxidase		10	2	0,6	0,2
COG4026 Uncharacterized protein containing TOPRIM domain, potential nuclease		6	1	0,3	0,1
COG4747 ACT domain-containing protein		7	1	0,4	0,1
COG5643 Protein containing a metal-binding domain shared with formylmethanofuran dehydrogenase subunit E		2	2	0,1	0,2

Table 7.3 (continued)

	Number of Assigned Spectra			Abundance (% spectra)	
COG Functional Category	**LCFA**	**OL**	**ST**	**OL**	**ST**
S - Function unknown		58	18	3,2	1,6
COG0393 Uncharacterized conserved protein		15	2	0,8	0,2
COG0599 Uncharacterized homolog of gamma-carboxymuconolactone decarboxylase subunit		2	1	0,1	0,1
COG1417 Uncharacterized conserved protein		4	2	0,2	0,2
COG1432 Uncharacterized conserved protein		2	2	0,1	0,2
COG1627 Uncharacterized protein conserved in archaea		3	0	0,2	0,0
COG1690 Uncharacterized conserved protein		0	2	0,0	0,2
COG1701 Uncharacterized protein conserved in archaea		2	0	0,1	0,0
COG1704 Uncharacterized conserved protein		2	2	0,1	0,2
COG1795 Uncharacterized conserved protein		5	4	0,3	0,4
COG1873 Uncharacterized conserved protein		14	2	0,8	0,2
COG1891 Uncharacterized protein conserved in archaea		3	0	0,2	0,0
COG3367 Uncharacterized conserved protein		2	1	0,1	0,1
COG3874 Uncharacterized conserved protein		4	0	0,2	0,0
No COG		12	9	0,7	0,8
No COG		12	9	0,7	0,8

The most abundant COG subcategory was COG2141 designated by "Coenzyme F420-dependent N5,N10-methylene tetrahydromethanopterin reductase and related flavin-dependent oxidoreductases" but others were also very abundant as it is the case of COG4054 and COG4058 which refers to methyl coenzyme M reductase, another important protein involved in methane metabolism. Proteins expressed by *Methanobacterium formicicum,* with an EC number attributed, and that are involved in methanogenesis are represented in Figure 7.3. No major differences in protein expression between samples incubated with saturated- and unsaturated-LCFA could be detected. Fewer spectra were used for proteins identification in the sample incubated with stearate but the distribution of those spectra by each group of proteins was quite similar to what was observed with the sample incubated with oleate.

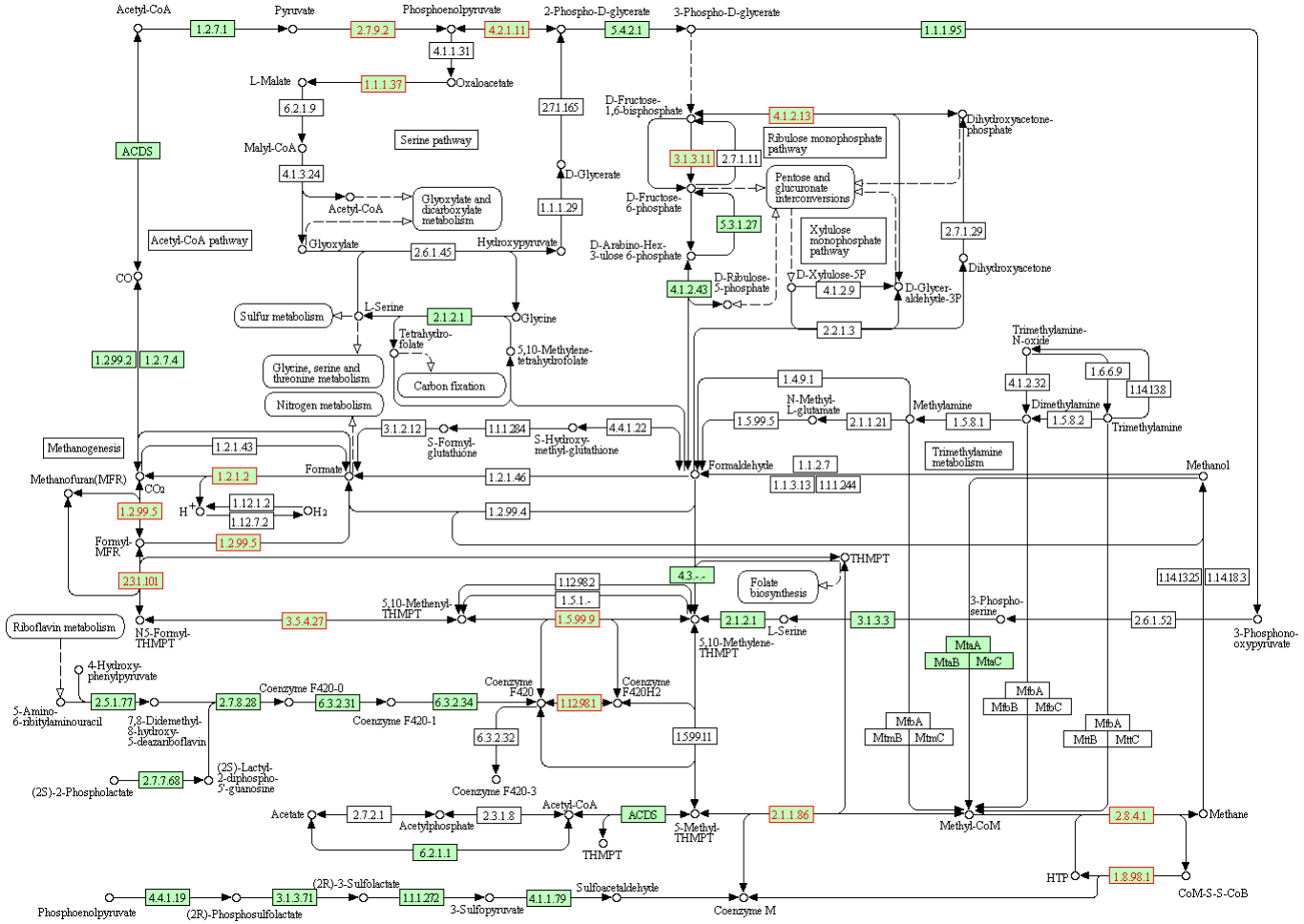

Figure 7.3 Representation of the identified archaeal proteins involved in methane metabolism that were expressed by *M. formicicum*, (red boxes).

7.4 Discussion

Peptides and consequently proteins identification relies on the direct match between predicted peptides and those present in target databases, and consequently differences in only one amino acid can prevent peptide identification in a way that most cross-species identifications are avoided (VerBerkmoes et al., 2009).

In this study, a minimum of 2 peptides were used to validate the identification of a protein in order to avoid incorrect protein assignments. When strict parameters are used to allow proteins identification (note that protein and peptide probability thresholds were set at 99% and 95%, respectively) and when non-specific databases are utilized for matching mass spectra identifications, as it was the case of this study (for the identification of *S. zehnderi* proteins), few proteins are expected to be identified. Due to the poor protein identification it was not possible to establish relevant differences on protein expression between oleate and stearate incubations. Nevertheless in the present approach, using family, order or even phylum specific databases, a small number of proteins were obtained but enzymes involved in important metabolic pathways could be identified. During oleate syntrophic degradation two enzymes assigned to COG "Energy production and conversion" could be detected, acetate kinase and phosphotransacetylase (Table 7.1), suggesting that substrate level phosphorylation is a mechanism of ATP synthesis performed by *S. zehnderi*, like it is in other members of *Syntrophomonadaceae* family (Wofford et al., 1986; Zhao et al., 1993). Phosphotransacetylase catalyzes the reverse reaction in which one molecule of acetyl-CoA (that in this case could result from the β-oxidation of LCFA) and one phosphate can be converted to acetylphosphate and CoA and then acetate kinase can use it to produce acetate and release ATP. Another

enzyme assigned to *Syntrophomonadaceae* family detected in oleate incubation was formate dehydrogenase. Besides, several spectra were assigned to formate dehydrogenase from *M. formicicum* (DSM 1535) during exposure to both stearate and oleate (Table S7.2). These results suggest that formate might be an important interspecies electron carrier between *S. zehnderi* and *M. formicicum* when converting LCFA to methane. However, the presence of formate in previous studies during LCFA degradation was never detected (Sousa et al., 2007b). Proteins that might be directly related with beta-oxidation of fatty acids were also identified. Acyl-CoA dehydrogenase catalyzes the first dehydrogenation that occurs in each β-oxidation cycle after CoA activation of fatty acids. The product of acyl-CoA enzymatic activity can be the substrate for enoyl-CoA hydratase (EC 4.2.1.17) that was also detected in this study. Another protein which participates in fatty acid β-oxidation is 3-ketoacyl-CoA thiolase (EC 2.3.1.16) that catalyzes the final step of each cycle producing one molecule of an acyl-CoA and an acetyl-CoA. These last two enzymes were only detected in the sample collected from the co-culture when incubated with oleate but not with stearate. On the other hand, acetyl-CoA acetyltransferase (EC 2.3.1.9) was detected in both incubations. Acetyl-CoA acetyltransferase catalyzes the reverse reaction of two molecules of acetyl-CoA to CoA and acetoacetyl-CoA, and operates at the final steps of beta-oxidation of fatty acids (Figure 7.2). Some of these proteins could only be identified in proteomes of bacterial phylogenetically distant (i.e. *Desulfosporosinus youngiae* from *Peptococcaceae* family and *Brevibacillus laterosporus* from *Paenibacillaceae* family). This is probably a consequence of the lack of proteomic information on syntrophic LCFA degraders, whose genomes are not sequenced so far. One advantage of this approach is that the spectra obtained can be re-analyzed anytime using more recent

and specific databases and which should increase the number of proteins identified. Like this, when *S. zehnderi* genomic and proteomic information is available it will be possible to draw more conclusions about differences on the degradation of saturated and unsaturated-LCFA. A good example of how different can the results be when searching against more or less specific databases is the case of the identification of proteins expressed by *M. formicicum* DSM 1535 in this study. The proteomic information from *M. formicicum* DSM 3637 was recently available in the Uniprot database (Gutierrez, 2012). In the present study, the 281 proteins identified were already obtained by searching against *Methanobacterium* database containing the proteomic data from *M. formicicum* DSM 3637. Before, when *Methanobacterium* sp. strains were the most closely related species to *M. formicicum* DSM 1535 with proteomic data available in databases, only 71 proteins (several of those redundant) could be identified (data not shown). Concerning *M. formicicum* results several protein functions could be identified, from energy production related mechanisms to maintenance and regulation, and most abundant proteins and functional categories were related to energy production and coenzyme transport that were directly related to methane metabolism (Table 7.3). Up to date only one proteomic study on fatty acid syntrophic microorganism is known (Schmidt et al., 2013). Those authors studied the proteome of *Syntrophomonas wolfei* in co-culture with *Methanospirillum hungatei*, whose genomes have been sequenced, during butyrate oxidation and the results enabled to build an electron flow scheme for syntrophic butyrate oxidation.

In this work, key enzymes involved in fatty acid metabolism and methane metabolism which are the central pathways for energy generation by the syntrophic

co-culture of *S. zehnderi* and *M. formicicum* growing on C18-LCFA were identified by a shotgun proteomics approach.

Chapter 8

General conclusions and suggestions for future work

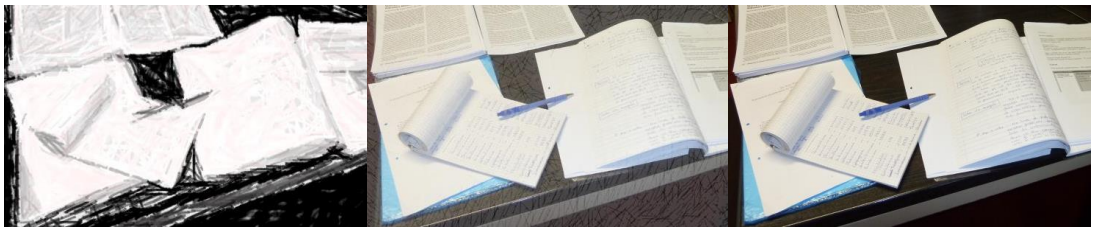

8.1 General conclusions

The work presented in this thesis contributed to get more insights on anaerobic microbial communities degrading LCFA.

Composition of microbial communities in contact with saturated- or unsaturated-LCFA is different both in anaerobic bioreactors and enrichment cultures (Sousa et al., 2007a; Sousa et al., 2007b). In Chapter 6 a biomass with no previous contact with LCFA was incubated with saturated- or unsaturated-LCFA: divergence of microbial communities was observed just after five days of incubation, indicating that adaptation of microbial consortia to specific LCFA is a rapid phenomenon. In Chapter 5, inhibition of aceticlastic methanogens by oleate is shown, both at activity and cellular levels. Unlike aceticlastic, hydrogenotrophic methanogenesis was not affected in any of the incubations unless when methanogens were grew in pure culture (Chapter 4), showing that behavior and endurance of individual species in pure culture or in complex communities can be completely different. Pure cultures of *M. formicicum* are less sensitive than pure cultures of *M. hungatei* to the presence of LCFA, although methanogenic activity of both is negatively affected by palmitate, stearate and oleate, with oleate exerting the most adverse effect (Chapter 4). Effect of oleate was also reflected in the protein pool expressed by the entire community with more proteins associated to hydrogenotrophic methanogenesis in oleate incubation when compared with stearate incubation.

In bioreactor systems, methanogens were able to adapt to high oleate concentrations (Chapter 3). Both hydrogenotrophic and acetoclastic methanogenesis were maintained in a bioreactor gradually acclimated to oleate. Predominant microrganisms in this system were closely related to *Methanobacterium* and *Methanosaeta*. *Syntrophomonas zehnderi*, a known syntrophic LCFA-degrading

bacterium, was identified as a key microorganism degrading oleate in methanogenic and also in non-methanogenic enrichments (Chapter 5). A syntrophic cooperation has been established not only with *M. formicicum* but also with other hydrogen- and formate-utilizing methanogens, namely *Methanobacterium beijingense* and *Methanoculleus bourgensis* which could be detected in oleate methanogenic enrichment culture. However, microbial relationships under non-methanogenic conditions were less clear: physiological results pointed out for the occurrence of homoacetogenic activity in one of the non-methanogenic enrichments, but no known homoacetogenic bacteria could be detected by cloning and sequencing analysis of 16S rRNA genes; *Desulfovibrio* species were predominant in non-methnogenic enrichments but their specific role in this ecosystem remains unclear. Formate is probably an interspecies electron carrier during oleate and stearate conversion to methane by the co-culture *S. zehnderi* and *M. formicicum* given by the number of spectra that could be assigned to formate dehydrogenases expressed by both microorganisms (Chapter 7).

8.2 Suggestions for future work

Anaerobic LCFA-degrading microbial communities merit further attention. A number of research questions regarding the microbiology of LCFA anaerobic conversion can be pointed out:

1) Why acetoclastic methanogens are more affected by the presence of oleate than palmitate?

2) Many microorganisms apparently not related with LCFA degradation can persist in LCFA-degrading environments. Which could be their function in these communities?

3) How do microbes interact in non-methanogenic LCFA-degrading enrichments? Is the conversion of unsaturated LCFA independent of syntrophic relations?

4) Why palmitate accumulates transiently during oleate degradtion by complex microbial communities?

The utilization of isotopically labeled substrates may help to understand better both main players and physiological properties of anaerobic LCFA degradation. Coupling stable isotope probing with community DNA and RNA or even protein analysis might help us to distinguish between the most and the less active microorganisms in LCFA-degrading communities. Proteomics approaches are also useful to investigate metabolic pathways and activities in complex microbial communities but the only way of retrieving more and better information from these studies is by increasing genomic information about the microorganisms commonly found in these communities. Using metagenomics approaches and sequencing the genomes of known LCFA-degraders would allow a much better interpretation of anaerobic LCFA-degrading environments in the future.

References

Abram,F., Enright,A.-M., O'Reilly,J., Botting,C.H., Collins,G., and O'Flaherty,V. (2011) A metaproteomic approach gives functional insights into anaerobic digestion. *J Appl Microbiol* **110**: 1550-1560.

Ahmadian,A., Ehn,M., and Hober,S. (2006) Pyrosequencing: history, biochemistry and future. *Clin Chim Acta* **363**: 83-94.

Altschul,S.F., Gish,W., Miller,W., Meyers,E.W., and Lipman,D.J. (1990) Basic local alignment search tool. *J Mol Biol* **215**: 403-410.

Alves,M.M., Pereira,M.A., Sousa,D.Z., Cavaleiro,A.J., Picavet,M., Smidt,H., and Stams,A.J.M. (2009) Waste lipids to energy: how to optimize methane production from long-chain fatty acids. *Microb Biotechnol* **2**: 538-550.

Alves,M.M., Picavet,M., Pereira,M.A., Cavaleiro,A.J., and Sousa,D.Z. Novel anaerobic reactor for the removal of long chain fatty acids from fat containing wastewater. [WO 2007058557]. 2007.

Alves,M.M., Vieira,J.A., Pereira,R.M., Pereira,M.A., and Mota,M. (2001) Effects of lipids and oleic acid on biomass development in anaerobic fixed-bed reactors. Part II: Oleic acid toxicity and biodegradability. *Water Res* **35**: 264-270.

Amann,R. and Ludwig,W. (2000) Ribosomal RNA-targeted nucleic acid probes for studies in microbial ecology. *FEMS Microbiol Rev* **24**: 555-565.

Angelidaki,I. and Ahring,B.K. (1992) Effects of free long-chain fatty acids on thermophilic anaerobic digestion. *Appl Microbiol Biotechnol* **37**: 808-812.

Angelidaki,I. and Ahring,B.K. (1995) Establishment and characterization of an anaerobic thermophilic (55°C) enrichment culture degrading long-chain fatty acids. *Appl Environ Microbiol* **61**: 2442-2445.

Ashelford,K.E., Chuzhanova,N.A., Fry,J.C., Jones,A.J., and Weightman,A.J. (2005) At least 1 in 20 16S rRNA sequence records currently held in public repositories is estimated to contain substantial anomalies. *Appl Environ Microbiol* **71**: 7724-7736.

Ashelford,K.E., Chuzhanova,N.A., Fry,J.C., Jones,A.J., and Weightman,A.J. (2006) New screening software shows that most recent large 16S rRNA gene clone libraries contain chimeras. *Appl Environ Microbiol* **72**: 5734-5741.

Balch,W.E., Fox,G.E., Magrum,L.J., Woese,C.R., and Wolfe,R.S. (1979) Methanogens: reevaluation of a unique biological group. *Microbiol Rev* **43**: 260–296.

Balgley,B.M., Laudeman,T., Yang,L., Song,T., and Lee,C.S. (2007) Comparative evaluation of tandem MS search algorithms using a target-decoy search strategy. *Mol Cell Proteomics* **6**: 1599–1608.

Baloch,M.I., Akunna,J.C., Kierans,M., and Collier,P.J. (2008) Structural analysis of anaerobic granules in a phase separated reactor by electron microscopy. *Bioresour Technol* **99**: 922–929.

Baserba,M.G., Angelidaki,I., and Karakashev,D. (2012) Effect of continuous oleate addition on microbial communities involved in anaerobic digestion process. *Bioresour Technol* **106**: 74–81.

Bertin,L., Colao,M.C., Ruzzi,M., and Fava,F. (2004) Performances and microbial features of a granular activated carbon packed-bed biofilm reactor capable of an efficient anaerobic digestion of olive mill wastewaters. *FEMS Microbiol Ecol* **48**: 413–423.

Beveridge,T.J., Sprott,G.D., and Whippey,P. (1991) Ultrastructure, inferred porosity, and gram-staining character of *Methanospirillum hungatei* filament termini describe a unique cell permeability for this archaeobacterium. *J Bacteriol* **173**: 130–140.

Biavati,B., Vasta,M., and Ferry,J.G. (1988) Isolation and characterization of "*Methanosphaera cuniculi*" sp. nov. *Appl Environ Microbiol* **54**: 768–771.

Black,P.N. and DiRusso,C.C. (2003) Transmembrane movement of exogenous long-chain fatty acids: proteins, enzymes, and vectorial esterification. *Microbiol Mol Biol Rev* **67**: 454–472.

Boone,D., Whitman,W., and Rouvi+¿re,P. (1993b) Diversity and Taxonomy of Methanogens. In *Methanogenesis*. Ferry,J. (ed). Springer US, pp. 35–80.

Boone,D.R. and Baker,C.C. (2001) Genus VI *Methanosalsum* gen. nov. In *Bergey's Manual of Systematic Bacteriology*. D.R.Boone,R.W.C.G.M.G. (ed). New York: Springer, pp. 287–289.

Boone,D.R., Mathrani,I.M., Liu,Y., Menaia,J.A., Mah,R.A., and Boone,J.E. (1993a) Isolation and Characterization of *Methanohalophilus portucalensis* sp. nov. and DNA Reassociation Study of the Genus *Methanohalophilus*. *Int J Syst Bacteriol* **43**: 430–437.

Brambilla,E., Djao,O.D.N., Daligault,H., Lapidus,A., Lucas,S., Hammon,N. et al. (2010) Complete genome sequence of *Methanoplanus petrolearius* type strain (SEBR 4847). *Standards in genomic sciences* **3**: 203-211.

Brauer,S.L., Cadillo-Quiroz,H., Ward,R.J., Yavitt,J.B., and Zinder,S.H. (2011) *Methanoregula boonei* gen. nov., sp. nov., an acidiphilic methanogen isolated from an acidic peat bog. *Int J Syst Evol Microbiol* **61**: 45-52.

Broughton,M.J., Thiele,J.H., Birch,E.J., and Cohen,A. (1998) Anaerobic batch digestion of sheep tallow. *Water Res* **32**: 1423-1428.

Cadillo-Quiroz,H., Yavitt,J.B., and Zinder,S.H. (2009) *Methanosphaerula palustris* gen. nov., sp. nov., a hydrogenotrophic methanogen isolated from a minerotrophic fen peatland. *Int J Syst Evol Microbiol* **59**: 928-935.

Campbell,J.W., Morgan-Kiss,R.M., and Cronan,J.E. (2003) A new *Escherichia coli* metabolic competency: growth on fatty acids by a novel anaerobic β-oxidation pathway. *Mol Microbiol* **47**: 793-805.

Canas,B., Pineiro,C., Calvo,E., Lopez-Ferrer,D., and Gallardo,J.M. (2007) Trends in sample preparation for classical and second generation proteomics. *J Chromatogr A* **1153**: 235-258.

Caporaso,J.G., Kuczynski,J., Stombaugh,J., Bittinger,K., Bushman,F.D., Costello,E.K. et al. (2010) QIIME allows analysis of high-throughput community sequencing data. *Nature methods* **7**: 335-336.

Cardinale,M., Brusetti,L., Quatrini,P., Borin,S., Puglia,A.M., Rizzi,A. et al. (2004) Comparison of different primer sets for use in automated ribosomal intergenic spacer analysis of complex bacterial communities. *Appl Environ Microbiol* **70**: 6147-6156.

Carepo,M., Baptista,J.F., Pamplona,A., Fauque,G., Moura,J.J.G., and Reis,M.A.M. (2002) Hydrogen metabolism in *Desulfovibrio desulfuricans* strain New Jersey (NCIMB 8313)-comparative study with *D. vulgaris* and *D. gigas* species. *Anaerobe* **8**: 325-332.

Cavaleiro,A.J., Pereira,M.A., and Alves,M. (2008) Enhancement of methane production from long chain fatty acid based effluents. *Bioresour Technol* **99**: 4086-4095.

Cavaleiro,A.J., Salvador,A.F., Alves,J.I., and Alves,M. (2009) Continuous high rate anaerobic treatment of oleic acid based wastewater is possible after a step feeding start-up. *Environ Sci Technol* **43**: 2931-2936.

Chen,K. and Pachter,L. (2005) Bioinformatics for whole-genome shotgun sequencing of microbial communities. *PLoS computational biology* **1**: 106-112.

Cheng,L., Qiu,T.L., Yin,X.B., Wu,X.L., Hu,G.Q., Deng,Y., and Zhang,H. (2007) *Methermicoccus shengliensis* gen. nov., sp. nov., a thermophilic, methylotrophic methanogen isolated from oil-production water, and proposal of Methermicoccaceae fam. nov. *Int J Syst Evol Microbiol* **57**: 2964-2969.

Christophersen,C.T., Morrison,M., and Conlon,M.A. (2011) Overestimation of the abundance of sulfate-reducing bacteria in human feces by quantitative PCR targeting the *Desulfovibrio* 16S rRNA gene. *Appl Environ Microbiol* **77**: 3544-3546.

Cole,J.R., Chai,B., Marsh,T.L., Farris,R.J., Wang,Q., Kulam,S.A. et al. (2003) The Ribosomal Database Project (RDP-II): previewing a new autoaligner that allows regular updates and the new prokaryotic taxonomy. *Nucleic Acids Res* **31**: 442-443.

Craig,R. and Beavis,R.C. (2003) A method for reducing the time required to match protein sequences with tandem mass spectra. *Rapid Commun Mass Spectrom* **17**: 2310-2316.

Craig,R. and Beavis,R.C. (2004) TANDEM: matching proteins with tandem mass spectra. *Bioinformatics* **20**: 1466-1467.

Delong,E.F. and Pace,N.R. (2001) Environmental diversity of bacteria and archaea. *Syst Biol* **50**: 470-478.

Demeyer,D.I. and Henderic,H.K. (1967) Effect of C18 unsaturated fatty acids on methane production in vitro by mixed rumen bacteria. *Biochim Biophys Acta* **137**: 484-497.

Desbois,A.P. and Smith,V.J. (2010) Antibacterial free fatty acids: activities, mechanisms of action and biotechnological potential. *Appl Microbiol Biotechnol* **85**: 1629-1642.

Diekert,G. and Wohlfarth,G. (1994) Metabolism of homoacetogens. *Antonie Van Leeuwenhoek* **66**: 209-221.

DiRusso,C.C. and Nystrom,T. (1998) The fats of *Escherichia coli* during infancy and old age: regulation by global regulators, alarmones and lipid intermediates. *Mol Microbiol* **27**: 1-8.

DiRusso,C.C., Black,P.N., and Weimar,J.D. (1999) Molecular inroads into the regulation and metabolism of fatty acids, lessons from bacteria. *Prog Lipid Res* **38**: 129-197.

Edgar,R.C. (2010) Search and clustering orders of magnitude faster than BLAST. *Bioinformatics* **26**: 2460-2461.

Enoki,M., Shinzato,N., Sato,H., Nakamura,K., and Kamagata,Y. (2011) Comparative proteomic analysis of *Methanothermobacter themautotrophicus* DeltaH in pure culture and in co-culture with a butyrate-oxidizing bacterium. *Plos One* **6**: e24309.

Ferry,J.G., Smith,P.H., and Wolfe,R.S. (1974) *Methanospirillum*, a new genus of methanogenic bacteria, and characterization of *Methanospirillum hungatii* sp. nov. *Int J Syst Bacteriol* **24**: 465-469.

Field,H.I., Fenyo,D., and Beavis,R.C. (2002) RADARS, a bioinformatics solution that automates proteome mass spectral analysis, optimises protein identification, and archives data in a relational database. *Proteomics* **2**: 36-47.

Fricke,W.F., Seedorf,H., Henne,A., Kruer,M., Liesegang,H., Hedderich,R. et al. (2006) The genome sequence of *Methanosphaera stadtmanae* reveals why this human intestinal archaeon is restricted to methanol and H2 for methane formation and ATP synthesis. *J Bacteriol* **188**: 642-658.

Frimmer,U. and Widdel,F. (1989) Oxidation of ethanol by methanogenic bacteria. *Arch Microbiol* **152**: 479-483.

Fujita,Y., Matsuoka,H., and Hirooka,K. (2007) Regulation of fatty acid metabolism in bacteria. *Mol Microbiol* **66**: 829-839.

Garcia,J.L., Patel,B.K., and Ollivier,B. (2000) Taxonomic, phylogenetic, and ecological diversity of methanogenic *Archaea*. *Anaerobe* **6**: 205-226.

Garcia-Martinez,J. and Rodriguez-Valera,F. (2000) Microdiversity of uncultured marine prokaryotes: the SAR11 cluster and the marine *Archaea* of Group I. *Mol Ecol* **9**: 935-948.

Grabowski,A., Blanchet,D., and Jeanthon,C. (2005) Characterization of long-chain fatty-acid-degrading syntrophic associations from a biodegraded oil reservoir. *Res Microbiol* **156**: 814-821.

Grosskopf,R., Janssen,P.H., and Liesack,W. (1998) Diversity and structure of the methanogenic community in anoxic rice paddy soil microcosms as examined by cultivation and direct 16S rRNA gene sequence retrieval. *Appl Environ Microbiol* **64**: 960-969.

Gunnigle,E., McCay,P., Fuszard,M., Botting,C.H., Abram,F., and O'Flaherty,V. (2013) A functional approach to uncover the low-temperature adaptation strategies of the archaeon *Methanosarcina barkeri*. *Appl Environ Microbiol* **79**: 4210-4219.

Gutierrez,G. (2012) Draft genome sequence of *Methanobacterium formicicum* DSM 3637, an Archaebacterium isolated from the methane producer amoeba *Pelomyxa palustris*. *J Bacteriol* **194**: 6967-6968.

Hanaki,K., Nagase,M., and Matsuo,T. (1981) Mechanism of inhibition caused by long-chain fatty acids in anaerobic digestion process. *Biotechnol Bioeng* **23**: 1591-1610.

Handelsman,J. (2004) Metagenomics: application of genomics to uncultured microorganisms. *Microbiol Mol Biol Rev* **68**: 669-685.

Handl,S., Dowd,S.E., Garcia-Mazcorro,J.F., Steiner,J.M., and Suchodolski,J.S. (2011) Massive parallel 16S rRNA gene pyrosequencing reveals highly diverse fecal bacterial and fungal communities in healthy dogs and cats. *FEMS Microbiol Ecol* **76**: 301-310.

Hane,B.G., Jager,K., and Drexler,H.G. (1993) The Pearson product-moment correlation coefficient is better suited for identification of DNA fingerprint profiles than band matching algorithms. *Electrophoresis* **14**: 967-972.

Hanreich,A., Heyer,R., Benndorf,D., Rapp,E., Pioch,M., Reichl,U., and Klocke,M. (2012) Metaproteome analysis to determine the metabolically active part of a thermophilic microbial community producing biogas from agricultural biomass. *Can J Microbiol* **58**: 917-922.

Hatamoto,M., Imachi,H., Fukayo,S., Ohashi,A., and Harada,H. (2007a) *Syntrophomonas palmitatica* sp. nov., an anaerobic, syntrophic, long-chain fatty-acid-oxidizing bacterium isolated from methanogenic sludge. *Int J Syst Evol Microbiol* **57**: 2137-2142.

Hatamoto,M., Imachi,H., Ohashi,A., and Harada,H. (2007b) Identification and cultivation of anaerobic, syntrophic long-chain fatty acid-degrading microbes from mesophilic and thermophilic methanogenic sludges. *Appl Environ Microbiol* **73**: 1332-1340.

Hatamoto,M., Imachi,H., Yashiro,Y., Ohashi,A., and Harada,H. (2007c) Diversity of anaerobic microorganisms involved in long-chain fatty acid degradation in methanogenic sludges as revealed by RNA-based stable isotope probing. *Appl Environ Microbiol* **73**: 4119-4127.

Hernandez-Eugenio,G., Fardeau,M.-L., Cayol,J.-L., Patel,B.K.C., Thomas,P., Macarie,H. et al. (2002) *Sporanaerobacter acetigenes* gen. nov., sp. nov., a novel acetogenic, facultatively sulfur-reducing bacterium. *Int J Syst Evol Microbiol* **52**: 1217-1223.

Hook,S.E., Wright,A.D., and McBride,B.W. (2010) Methanogens: methane producers of the rumen and mitigation strategies. *Archaea* **2010**: 945785.

Hwu,C.-S. and Lettinga,G. (1997) Acute toxicity of oleate to acetate-utilizing methanogens in mesophilic and thermophilic anaerobic sludges. *Enzyme Microb Technol* **21**: 297-301.

Hwu,C.-S., Donlon,B., and Lettinga,G. (1996) Comparative toxicity of long-chain fatty acid to anaerobic sludges from various origins. *Water Sci Technol* **34**: 351-358.

Hwu,C.-S., Tseng,S.K., Yuan,C.Y., Kulik,Z., and Lettinga,G. (1998) Biosorption of long-chain fatty acids in UASB treatment process. *Water Res* **32**: 1571-1579.

Ibrahim,M., Nicolas,P., Bessieres,P., Bolotin,A., Monnet,V., and Gardan,R. (2007) A genome-wide survey of short coding sequences in streptococci. *Microbiology* **153**: 3631-3644.

Imachi,H., Sakai,S., Sekiguchi,Y., Hanada,S., Kamagata,Y., Ohashi,A., and Harada,H. (2008) *Methanolinea tarda* gen. nov., sp. nov., a methane-producing archaeon isolated from a methanogenic digester sludge. *Int J Syst Evol Microbiol* **58**: 294-301.

Ince,B., Ince,O., and Ayman Oz,N. (2003) Changes in Acetoclastic Methanogenic Activity and Microbial Composition in an Upflow Anaerobic Filter. *Water, Air, & Soil Pollution* **144**: 301-315.

Jackson,B.E., Bhupathiraju,V.K., Tanner,R.S., Woese,C.R., and McInerney,M.J. (1999) *Syntrophus aciditrophicus* sp. nov., a new anaerobic bacterium that degrades fatty acids and benzoate in syntrophic association with hydrogen-using microorganisms. *Arch Microbiol* **171**: 107-114.

Jarrell,K.F., Saulnier,M., and Ley,A. (1987) Inhibition of methanogenesis in pure cultures by ammonia, fatty acids, and heavy metals, and protection against heavy metal toxicity by sewage sludge. *Can J Microbiol* **33**: 551-554.

Jetten,M.S.M., Stams,A.J.M., and Zehnder,A.J.B. (1992) Methanogenesis from acetate: a comparison of the acetate metabolism in *Methanothrix soehngenii* and *Methanosarcina* spp. *FEMS Microbiol Rev* **88**: 181-197.

Jiang,B., Parshina,S.N., van,D.W., Lomans,B.P., and Stams,A.J. (2005) *Methanomethylovorans thermophila* sp. nov., a thermophilic, methylotrophic methanogen from an anaerobic reactor fed with methanol. *Int J Syst Evol Microbiol* **55**: 2465-2470.

Kenny,J.G., Ward,D., Josefsson,E., Jonsson,I.M., Hinds,J., Rees,H.H. et al. (2009) The Staphylococcus aureus response to unsaturated long chain free fatty acids: survival mechanisms and virulence implications. *Plos One* **4**: e4344.

Khalsa-Moyers,G. and McDonald,W.H. (2006) Developments in mass spectrometry for the analysis of complex protein mixtures. *Brief Funct Genomic Proteomic* **5**: 98-111.

Kim,S.H., Han,S.K., and Shin,H.S. (2004) Two-phase anaerobic treatment system for fat-containing wastewater. *J Chem Technol Biotechnol* **79**: 63-71.

Koga,Y. and Morii,H. (2005) Recent advances in structural research on ether lipids from archaea including comparative and physiological aspects. *Biosci Biotechnol Biochem* **69**: 2019-2034.

Koga,Y., Morii,H., Akagawa-Matsushita,M., and Ohga,M. (1998) Correlation of Polar Lipid Composition with 16S rRNA Phylogeny in Methanogens. Further Analysis of Lipid Component Parts. *Biosci Biotechnol Biochem* **62**: 230-236.

Koga,Y., Nishihara,M., Morii,H., and Akagawa-Matsushita,M. (1993) Ether polar lipids of methanogenic bacteria: structures, comparative aspects, and biosyntheses. *Microbiol Rev* **57**: 164-182.

Kohler,T., Weidenmaier,C., and Peschel,A. (2009) Wall teichoic acid protects Staphylococcus aureus against antimicrobial fatty acids from human skin. *J Bacteriol* **191**: 4482-4484.

Kosaka,T., Uchiyama,T., Ishii,S., Enoki,M., Imachi,H., Kamagata,Y. et al. (2006) Reconstruction and regulation of the central catabolic pathway in the thermophilic propionate-oxidizing syntroph Pelotomaculum thermopropionicum. *J Bacteriol* **188**: 202-210.

Koster,I.W. (1987) Abatement of long-chain fatty acid inhibition of methanogenesis by calcium addition. *Biol Waste* **22**: 295-301.

Koster,I.W. and Cramer,A. (1987) Inhibition of methanogenesis from acetate in granular sludge by long-chain fatty acids. *Appl Environ Microbiol* **53**: 403-409.

Kuang,Y., Pullammanappallil,P., Lepesteur,M., and Ho,G.E. (2006) Recovery of oleate-inhibited anaerobic digestion by addition of simple substrates. *J Chem Technol Biotechnol* **81**: 1057-1063.

Kurr,M., Huber,R., König,H., Jannasch,H., Fricke,H., Trincone,A. et al. (1991) *Methanopyrus kandleri*, gen. and sp. nov. represents a novel group of hyperthermophilic methanogens, growing at 110°C. *Arch Microbiol* **156**: 239-247.

Lai,M.C., Chen,S.C., Shu,C.M., Chiou,M.S., Wang,C.C., Chuang,M.J. et al. (2002) *Methanocalculus taiwanensis* sp. nov., isolated from an estuarine environment. *Int J Syst Evol Microbiol* **52**: 1799-1806.

Lai,M.C., Lin,C.C., Yu,P.H., Huang,Y.F., and Chen,S.C. (2004) *Methanocalculus chunghsingensis* sp. nov., isolated from an estuary and a marine fishpond in Taiwan. *Int J Syst Evol Microbiol* **54**: 183-189.

Lalman,J.A. and Bagley,D.M. (2000) Anaerobic degradation and inhibitory effects of linoleic acid. *Water Res* **34**: 4220-4228.

Lalman,J.A. and Bagley,D.M. (2001) Anaerobic degradation and methanogenic inhibitory effects of oleic and stearic acids. *Water Res* **35**: 2975-2983.

Lane,D.J. (1991) 16S/23S rRNA sequencing. In *Nucleic acid techniques in bacterial systematics*. Stackebrandt,E. and Goodfellow,M. (eds). Chichester: John Wiley & Sons.

Lay,J.J., Li,Y.Y., and Noike,T. (1998) Mathematical model for methane production from landfill bioreactor. *Journal of Environmental Engineering-Asce* **124**: 730-736.

Leclerc,M., Delgenes,J.P., and Godon,J.J. (2004) Diversity of the archaeal community in 44 anaerobic digesters as determined by single strand conformation polymorphism analysis and 16S rDNA sequencing. *Environ Microbiol* **6**: 809-819.

Liesack,W., Weyland,H., and Stackebrandt,E. (1991) Potential risks of gene amplification by PCR as determined by 16S rDNA analysis of a mixed-culture of strict barophilic bacteria. *Microb Ecol* **21**: 191-198.

Lomans,B.P., Maas,R., Luderer,R., Op den Camp,H.J., Pol,A., Van Der Drift,C., and Vogels,G.D. (1999) Isolation and characterization of *Methanomethylovorans hollandica* gen. nov., sp. nov., isolated from freshwater sediment, a methylotrophic methanogen able to grow on dimethyl sulfide and methanethiol. *Appl Environ Microbiol* **65**: 3641-3650.

Long,F., Rouquette-Loughlin,C., Shafer,W.M., and Yu,E.W. (2008) Functional cloning and characterization of the multidrug efflux pumps NorM from Neisseria gonorrhoeae and YdhE from Escherichia coli. *Antimicrob Agents Chemother* **52**: 3052-3060.

Lorowitz,W.H., Zhao,H.X., and Bryant,M.P. (1989) *Syntrophomonas wolfei* subsp *saponavida* subsp. nov., a long chain fatty-acid degrading, anaerobic, syntrophic bacterium - *Syntrophomonas wolfei* subsp *wolfei* subsp. nov. - and emended descriptions of the genus and species. *Int J Syst Bacteriol* **39**: 122-126.

Loy,A., Lehner,A., Lee,N., Adamczyk,J., Meier,H., Ernst,J. et al. (2002) Oligonucleotide microarray for 16S rRNA gene-based detection of all recognized lineages of sulfate-reducing prokaryotes in the environment. *Appl Environ Microbiol* **68**: 5064-5081.

Ludwig,W., Strunk,O., Westram,R., Richter,L., Meier,H., Yadhukumar et al. (2004) ARB: a software environment for sequence data. *Nucleic Acids Res* **32**: 1363-1371.

Luton,P.E., Wayne,J.M., Sharp,R.J., and Riley,P.W. (2002) The mcrA gene as an alternative to 16S rRNA in the phylogenetic analysis of methanogen populations in landfill. *Microbiology* **148**: 3521-3530.

Maestrojuán,G.M. and Boone,D.R. (1991) Characterization of *Methanosarcina barkeri* MST and *227*, *Methanosarcina mazei* S-6T, and *Methanosarcina vacuolata* Z-76IT. *Int J Syst Bacteriol* **41**: 267-274.

Marchler-Bauer,A., Lu,S., Anderson,J.B., Chitsaz,F., Derbyshire,M.K., DeWeese-Scott,C. et al. (2011) CDD: a Conserved Domain Database for the functional annotation of proteins. *Nucleic Acids Res* **39**: D225-D229.

Martinez,E., Estupinan,M., Pastor,F.I., Busquets,M., Diaz,P., and Manresa,A. (2013) Functional characterization of ExFadLO, an outer membrane protein required for exporting oxygenated long-chain fatty acids in *Pseudomonas aeruginosa*. *Biochimie* **95**: 290-298.

McInerney,M.J., Sieber,J.R., and Gunsalus,R.P. (2009) Syntrophy in anaerobic global carbon cycles. *Curr Opin Biotechnol* **20**: 623-632.

McInerney,M.J., Struchtemeyer,C.G., Sieber,J., Mouttaki,H., Stams,A.J.M., Schink,B. et al. (2008) Physiology, ecology, phylogeny, and genomics of microorganisms capable of syntrophic metabolism. *Incredible Anaerobes: from Physiology to Genomics to Fuels* **1125**: 58-72.

Men,Y., Feil,H., Verberkmoes,N.C., Shah,M.B., Johnson,D.R., Lee,P.K. et al. (2012) Sustainable syntrophic growth of *Dehalococcoides ethenogenes* strain 195 with *Desulfovibrio vulgaris* Hildenborough and *Methanobacterium congolense*: global transcriptomic and proteomic analyses. *ISME J* **6**: 410-421.

Menes,R.J., Fernandez,A., and Muxi,L. (2001) Physiological and molecular characterisation of an anaerobic thermophilic oleate-degrading enrichment culture. *Anaerobe* **7**: 17-24.

Muyzer,G., de Waal,E.C., and Uitterlinden,A.G. (1993) Profiling of complex microbial populations by denaturing gradient gel electrophoresis analysis of polymerase chain reaction-amplified genes coding for 16S rRNA. *Appl Environ Microbiol* **59**: 695-700.

Neves,L., Pereira,M.A., Mota,M., and Alves,M.M. (2009) Detection and quantification of long chain fatty acids in liquid and solid samples and its relevance to understand anaerobic digestion of lipids. *Bioresour Technol* **100**: 91-96.

Nicolaisen,M.H. and Ramsing,N.B. (2002) Denaturing gradient gel electrophoresis (DGGE) approaches to study the diversity of ammonia-oxidizing bacteria. *J Microbiol Methods* **50**: 189-203.

Novak,J.T. and Carlson,D.A. (1970) Kinetics of anaerobic long chain fatty acid degradation. *J Water Pollut Control Fed* **42**: 1932-1943.

Nübel,U., Engelen,B., Felske,A., Snaidr,J., Wieshuber,A., Amann,R.I. et al. (1996) Sequence heterogeneities of genes encoding 16S rRNAs in *Paenibacillus polymyxa* detected by temperature gradient gel electrophoresis. *J Bacteriol* **178**: 5636-5643.

Ollivier,B., Fardeau,M.L., Cayol,J.L., Magot,M., Patel,B.K., Prensier,G., and Garcia,J.L. (1998) *Methanocalculus halotolerans* gen. nov., sp. nov., isolated from an oil-producing well. *Int J Syst Bacteriol* **48 Pt 3**: 821-828.

Palatsi,J., Illa,J., Prenafeta-Boldu,F.X., Laureni,M., Fernandez,B., Angelidaki,I., and Flotats,X. (2010) Long-chain fatty acids inhibition and adaptation process in anaerobic thermophilic digestion: batch tests, microbial community structure and mathematical modelling. *Bioresour Technol* **101**: 2243-2251.

Patel,G.B. and Sprott,G.D. (1990) *Methanosaeta concilii* gen. nov. sp. nov. (*"Methanothrix concilii"*) and *Methanosaeta thermoacetophila* nom. rev., comb. nov. *Int J Syst Bacteriol* **40**: 79-82.

Pereira,M.A., Pires,O.C., Mota,M., and Alves,M.M. (2002a) Anaerobic degradation of oleic acid by suspended and granular sludge: identification of palmitic acid as a key intermediate. *Water Sci Technol* **45**: 139-144.

Pereira,M.A., Pires,O.C., Mota,M., and Alves,M.M. (2005) Anaerobic biodegradation of oleic and palmitic acids: evidence of mass transfer limitations caused by long chain fatty acid accumulation onto the anaerobic sludge. *Biotechnol Bioeng* **92**: 15-23.

Pereira,M.A., Roest,K., Stams,A.J.M., Mota,M., Alves,M., and Akkermans,A.D.L. (2002b) Molecular monitoring of microbial diversity in expanded granular sludge bed (EGSB) reactors treating oleic acid. *FEMS Microbiol Ecol* **41**: 95-103.

Pereira,M.A., Sousa,D.Z., Mota,M., and Alves,M.M. (2004) Mineralization of LCFA associated with anaerobic sludge: kinetics, enhancement of methanogenic activity, and effect of VFA. *Biotechnol Bioeng* **88**: 502-511.

Perkins,D.N., Pappin,D.J., Creasy,D.M., and Cottrell,J.S. (1999) Probability-based protein identification by searching sequence databases using mass spectrometry data. *Electrophoresis* **20**: 3551-3567.

Perle,M., Kimchie,S., and Shelef,G. (1995) Some biochemical aspects of the anaerobic degradation of dairy wastewater. *Water Res* **29**: 1549-1554.

Prakash,T. and Taylor,T.D. (2012) Functional assignment of metagenomic data: challenges and applications. *Brief Bioinform* **13**: 711-727.

Prins,R.A., van Nevel,C.J., and Demeyer,D.I. (1972) Pure culture studies of inhibitors for methanogenic bacteria. *Antonie Van Leeuwenhoek* **38**: 281-287.

Ren,Y., Aguirre,J., Ntamack,A.G., Chu,C.H., and Schulz,H. (2004) An alternative pathway of oleate β-oxidation in *Escherichia coli* involving the hydrolysis of a dead end intermediate by a thioesterase. *J Biol Chem* **279**: 11042-11050.

Rinzema,A., Boone,M., van Knippenberg,K., and Lettinga,G. (1994) Bactericidal effect of long chain fatty acids in anaerobic digestion. *Wat Environ Res* **66**: 40-49.

Rizzi,A., Zucchi,M., Borin,S., Marzorati,M., Sorlini,C., and Daffonchio,D. (2006) Response of methanogen populations to organic load increase during anaerobic digestion of olive mill wastewater. *J Chem Technol Biotechnol* **81**: 1556-1562.

Romesser,J.A., Wolfe,R.S., Mayer,F., Spiess,E., and Walther-Mauruschat,A. (1979) *Methanogenium*, a new genus of marine methanogenic bacteria, and characterization of *Methanogenium cariaci* sp. nov. and *Methanogenium marisnigri* sp. nov. *Arch Microbiol* **121**: 147-153.

Ronaghi,M. (2001) Pyrosequencing sheds light on DNA sequencing. *Genome Res* **11**: 3-11.

Ros,A., Faupel,M., Mees,H., Oostrum,J., Ferrigno,R., Reymond,F. et al. (2002) Protein purification by Off-Gel electrophoresis. *Proteomics* **2**: 151-156.

Roy,F., Albagnac,G., and Samain,E. (1985) Influence of calcium addition on growth of highly purified syntrophic cultures degrading long-chain Fatty acids. *Appl Environ Microbiol* **49**: 702-705.

Roy,F., Samain,E., Dubourguier,H.C., and Albagnac,G. (1986) *Synthrophomonas sapovorans* sp. nov., a new obligately proton reducing anaerobe oxidizing saturated and unsaturated long-chain fatty acids. *Arch Microbiol* **145**: 142-147.

Rustan,A.C. and Drevon,C.A. (2005) Fatty Acids: Structures and Properties. Encyclopedia of life sciences.

Saitou,N. and Nei,M. (1987) The neighbor-joining method: a new method for reconstructing phylogenetic trees. *Mol Biol Evol* **4**: 406-425.

Salvador,A.F., Cavaleiro,A.J., Sousa,D.Z., Alves,M.M., and Pereira,M.A. (2013) Endurance of methanogenic archaea in anaerobic bioreactors treating oleate-based wastewater. *Appl Microbiol Biotechnol*.

Sanguinetti,C.J., Dias Neto,E., and Simpson,A.J. (1994) Rapid silver staining and recovery of PCR products separated on polyacrylamide gels. *BioTechniques* **17**: 914-921.

Schielke,S., Schmitt,C., Spatz,C., Frosch,M., Schubert-Unkmeir,A., and Kurzai,O. (2010) The transcriptional repressor FarR is not involved in meningococcal fatty acid resistance mediated by the FarAB efflux pump and dependent on lipopolysaccharide structure. *Appl Environ Microbiol* **76**: 3160-3169.

Schink,B. (1997) Energetics of syntrophic cooperation in methanogenic degradation. *Microbiol Mol Biol Rev* **61**: 262-280.

Schink,B. and Stams,A.J.M. (2006) Syntrophism among prokaryotes. In *The Prokaryotes: an evolving electronic resource for the microbiological community*. Dworkin,M., Falkow,S., Rosenberg,E., Schleifer,K.-H., and Stackebrandt,E. (eds). New York: Springer-Verlag, pp. 309-335.

Schmidt,A., Muller,N., Schink,B., and Schleheck,D. (2013) A Proteomic View at the Biochemistry of Syntrophic Butyrate Oxidation in *Syntrophomonas wolfei*. *Plos One* **8**: e56905.

Schmidt,A., Muller,N., Schink,B., and Schleheck,D. (2013) A Proteomic View at the Biochemistry of Syntrophic Butyrate Oxidation in *Syntrophomonas wolfei*. *Plos One* **8**: e56905.

Schneider,T. and Riedel,K. (2010) Environmental proteomics: analysis of structure and function of microbial communities. *Proteomics* **10**: 785-798.

Searle,B.C. (2010) Scaffold: a bioinformatic tool for validating MS/MS-based proteomic studies. *Proteomics* **10**: 1265-1269.

Sharma,V.K., Kumar,N., Prakash,T., and Taylor,T.D. (2012) Fast and accurate taxonomic assignments of metagenomic sequences using MetaBin. *Plos One* **7**: e34030.

Sheu,C.W. and Freese,E. (1973) Lipopolysaccharide layer protection of gram-negative bacteria against inhibition by long-chain fatty acids. *J Bacteriol* **115**: 869-875.

Shigematsu,T., Tang,Y., Mizuno,Y., Kawaguchi,H., Morimura,S., and Kida,K. (2006) Microbial diversity of mesophilic methanogenic consortium that can degrade long-chain fatty acids in chemostat cultivation. *J Biosci Bioeng* **102**: 535-544.

Shin,H.S., Kim,S.H., Lee,C.Y., and Nam,S.Y. (2003) Inhibitory effects of long-chain fatty acids on VFA degradation and β-oxidation. *Water Sci Technol* **47**: 139-146.

Sieber,J.R., McInerney,M.J., and Gunsalus,R.P. (2012) Genomic insights into syntrophy: the paradigm for anaerobic metabolic cooperation. *Annu Rev Microbiol* **66**: 429-452.

Sieber,J.R., Sims,D.R., Han,C., Kim,E., Lykidis,A., Lapidus,A.L. et al. (2010) The genome of Syntrophomonas wolfei: new insights into syntrophic metabolism and biohydrogen production. *Environ Microbiol* **12**: 2289-2301.

Siggins,A., Enright,A.M., Abram,F., Botting,C., and O'Flaherty,V. (2012a) Impact of trichloroethylene exposure on the microbial diversity and protein expression in anaerobic granular biomass at 37°C and 15°C. *Archaea* **2012**: 940159.

Siggins,A., Gunnigle,E., and Abram,F. (2012b) Exploring mixed microbial community functioning: recent advances in metaproteomics. *FEMS Microbiol Ecol* **80**: 265-280.

Silhavy,T.J., Kahne,D., and Walker,S. (2010) The bacterial cell envelope. *Cold Spring Harbor perspectives in biology* **2**: a000414.

Simon,C. and Daniel,R. (2011) Metagenomic analyses: past and future trends. *Appl Environ Microbiol* **77**: 1153-1161.

Singh,N., Kendall,M.M., Liu,Y., and Boone,D.R. (2005) Isolation and characterization of methylotrophic methanogens from anoxic marine sediments in Skan Bay, Alaska: description of *Methanococcoides alaskense* sp. nov., and emended description of *Methanosarcina baltica*. *Int J Syst Evol Microbiol* **55**: 2531-2538.

Smith,D.M., Snow,D.E., Rees,E., Zischkau,A.M., Hanson,J.D., Wolcott,R.D. et al. (2010) Evaluation of the bacterial diversity of pressure ulcers using bTEFAP pyrosequencing. *BMC medical genomics* **21**: 41.

Smith,D.R., Doucette-Stamm,L.A., Deloughery,C., Lee,H., Dubois,J., Aldredge,T. et al. (1997) Complete genome sequence of *Methanobacterium thermoautotrophicum* deltaH: functional analysis and comparative genomics. *J Bacteriol* **179**: 7135-7155.

Smith,K.S. and Ingram-Smith,C. (2007) *Methanosaeta*, the forgotten methanogen? *Trends Microbiol* **15**: 150-155.

Soliva CR, Bucher S, Meile L, and Kreuzer M . Methanogenesis archaea: conditions for inhibitory action of four saturated fatty acids when added to pure cultures. Conference Series: Earth and Environmental Science. abstr 242039. 2009.

Soliva,C.R., Meile,L., Cieslak,A., Kreuzer,M., and Machmuller,A. (2004a) Rumen simulation technique study on the interactions of dietary lauric and myristic acid supplementation in suppressing ruminal methanogenesis. *Br J Nutr* **92**: 689-700.

Soliva,C.R., Meile,L., Hindrichsen,I.K., Kreuzer,M., and Machmuller,A. (2004b) Myristic acid supports the immediate inhibitory effect of lauric acid on ruminal methanogens and methane release. *Anaerobe* **10**: 269-276.

Sousa,D.Z., Alves,J.I., Alves,M.M., Smidt,H., and Stams,A.J.M. (2009c) Effect of sulfate on methanogenic communities that degrade unsaturated and saturated long-chain fatty acids (LCFA). *Environ Microbiol* **11**: 68-80.

Sousa,D.Z., Cavaleiro,A.J., Stams,A.J.M., and Alves,M.M. Non-syntrophic oleate to palmitate conversion in anaerobic bioreactors. Proceedings of FEMS - 3rd Congress of European Microbiologists, Gothenburg, Sweden, 28 Jun-2 July. 2009b.

Sousa,D.Z., Pereira,M.A., Alves,J.I., Smidt,H., Stams,A.J.M., and Alves,M.M. (2008) Anaerobic microbial LCFA degradation in bioreactors. *Water Sci Technol* **57**: 439-444.

Sousa,D.Z., Pereira,M.A., Smidt,H., Stams,A.J.M., and Alves,M.M. (2007a) Molecular assessment of complex microbial communities degrading long chain fatty acids in methanogenic bioreactors. *FEMS Microbiol Ecol* **60**: 252-265.

Sousa,D.Z., Pereira,M.A., Stams,A.J.M., Alves,M.M., and Smidt,H. (2007b) Microbial communities involved in anaerobic degradation of unsaturated or saturated long chain fatty acids (LCFA). *Appl Environ Microbiol* **73**: 1054-1064.

Sousa,D.Z., Salvador,A.F., Ramos,J., Guedes,A.P., Barbosa,S., Stams,A.J.M. et al. (2013) Activity and viability of methanogens in anaerobic digestion of unsaturated and saturated long-chain fatty acids. *Appl Environ Microbiol.*, 79 (14):4239-45

Sousa,D.Z., Smidt,H., Alves,M.M., and Stams,A.J.M. (2007c) *Syntrophomonas zehnderi* sp. nov., an anaerobe that degrades long chain fatty acids in co-culture with *Methanobacterium formicicum*. *Int J Syst Evol Microbiol* **57**: 609-615.

Sousa,D.Z., Smidt,H., Alves,M.M., and Stams,A.J.M. (2009a) Ecophysiology of syntrophic communities that degrade saturated and unsaturated long-chain fatty acids. *FEMS Microbiol Ecol* **68**: 257-272.

Sprenger,W.W., van Belzen,M.C., Rosenberg,J., Hackstein,J.H., and Keltjens,J.T. (2000) *Methanomicrococcus blatticola* gen. nov., sp. nov., a methanol- and methylamine-reducing methanogen from the hindgut of the cockroach Periplaneta americana. *Int J Syst Evol Microbiol* **50** Pt 6: 1989-1999.

Sprott,G.D., Shaw,K.M., and Jarrell,K.F. (1983) Isolation and chemical composition of the cytoplasmic membrane of the archaebacterium *Methanospirillum hungatei*. *J Biol Chem* **258**: 4026-4031.

Stams,A.J. and Plugge,C.M. (2009) Electron transfer in syntrophic communities of anaerobic bacteria and archaea. *Nat Rev Microbiol* **7**: 568-577.

Stams,A.J.M., Sousa,D.Z., Kleerebezem,R., and Plugge,C.M. (2012) Role of syntrophic microbial communities in high-rate methanogenic bioreactors. *Water Sci Technol* **66**: 352-362.

Stams,A.J.M., van Dijk,J.B., Dijkema,C., and Plugge,C.M. (1993) Growth of syntrophic propionate-oxidizing bacteria with fumarate in the absence of methanogenic bacteria. *Appl Environ Microbiol* **59**: 1114-1119.

Svetlitshnyi,V., Rainey,F., and Wiegel,J. (1996) *Thermosyntropha lipolytica* gen. nov., sp. nov., a lipolytic, anaerobic, alkalitolerant, thermophilic bacterium utilizing short- and long-chain fatty acids in syntrophic coculture with a methanogenic archaeum. *Int J Syst Bacteriol* **46**: 1131-1137.

Swoboda,J.G., Campbell,J., Meredith,T.C., and Walker,S. (2010) Wall teichoic acid function, biosynthesis, and inhibition. *Chembiochem* **11**: 35-45.

Takai,K. and Horikoshi,K. (2000) Rapid detection and quantification of members of the archaeal community by quantitative PCR using fluorogenic probes. *Appl Environ Microbiol* **66**: 5066-5072.

Thauer,R.K., Jungermann,K., and Decker,K. (1977) Energy conservation in chemotropic anaerobic bacteria. *Bacteriol Rev* **41**: 100-180.

Tyson,G.W., Chapman,J., Hugenholtz,P., Allen,E.E., Ram,R.J., Richardson,P.M. et al. (2004) Community structure and metabolism through reconstruction of microbial genomes from the environment. *Nature* **428**: 37-43.

Valenzuela,L., Chi,A., Beard,S., Orell,A., Guiliani,N., Shabanowitz,J. et al. (2006) Genomics, metagenomics and proteomics in biomining microorganisms. *Biotechnol Adv* **24**: 197-211.

Venter,J.C., Remington,K., Heidelberg,J.F., Halpern,A.L., Rusch,D., Eisen,J.A. et al. (2004) Environmental genome shotgun sequencing of the Sargasso Sea. *Science* **304**: 66-74.

VerBerkmoes,N.C., Denef,V.J., Hettich,R.L., and Banfield,J.F. (2009) Functional analysis of natural microbial consortia using community proteomics. *Nature reviews Microbiology* **7**: 196-205.

Walker,C.B., He,Z., Yang,Z.K., Ringbauer,J.A.J., He,Q., Zhou,J. et al. (2009) The electron transfer system of syntrophically grown Desulfovibrio vulgaris. *J Bacteriol* **191**: 5793-5801.

Wang,Q., Garrity,G.M., Tiedje,J.M., and Cole,J.R. (2007) Naive Bayesian classifier for rapid assignment of rRNA sequences into the new bacterial taxonomy. *Appl Environ Microbiol* **73**: 5261-5267.

Weng,C. and Jeris,J.S. (1976) Biochemical mechanisms in methane fermentation of glutamic and oleic acids. *Water Res* **10**: 9-18.

Whitman,W., Bowen,T., and Boone,D. (2006) The Methanogenic Bacteria. In *The Prokaryotes*. Dworkin,M., Falkow,S., Rosenberg,E., Schleifer,K.H., and Stackebrandt,E. (eds). Springer New York, pp. 165-207.

Willumsen,P., Karlson,U., Stackebrandt,E., and Kroppenstedt,R.M. (2001) *Mycobacterium frederiksbergense* sp. nov., a novel polycyclic aromatic hydrocarbon-degrading Mycobacterium species. *Int J Syst Evol Microbiol* **51**: 1715-1722.

Wilmes,P. and Bond,P.L. (2004) The application of two-dimensional polyacrylamide gel electrophoresis and downstream analyses to a mixed community of prokaryotic microorganisms. *Environ Microbiol* **6**: 911-920.

Wilmes,P. and Bond,P.L. (2009) Microbial community proteomics: elucidating the catalysts and metabolic mechanisms that drive the Earth's biogeochemical cycles. *Curr Opin Microbiol* **12**: 310-317.

Wofford,N.Q., Beaty,P.S., and McInerney,M.J. (1986) Preparation of cell-free extracts and the enzymes involved in fatty-acid metabolism in *Syntrophomonas wolfei*. *J Bacteriol* **167**: 179-185.

Wooley,J.C., Godzik,A., and Friedberg,I. (2010) A primer on metagenomics. *PLoS Comput Biol* **6**: e1000667.

Wu,C., Liu,X., and Dong,X. (2006b) *Syntrophomonas erecta* subsp. *sporosyntropha* subsp. nov., a spore-forming bacterium that degrades short chain fatty acids in co-culture with methanogens. *Syst Appl Microbiol* **29**: 457-462.

Wu,C.G., Dong,X.Z., and Liu,X.L. (2007) *Syntrophomonas wolfei* subsp. *methylbutyratica* subsp. nov., and assignment of *Syntrophomonas wolfei* subsp. *saponavida* to *Syntrophomonas saponavida* sp. nov comb. nov. *Syst Appl Microbiol* **30**: 376-380.

Wu,C.G., Liu,X.L., and Dong,X.Z. (2006a) *Syntrophomonas cellicola* sp. nov., a spore-forming syntrophic bacterium isolated from a distilled-spirit-fermenting cellar, and assignment of *Syntrophospora bryantii* to *Syntrophomonas bryantii* comb. nov. *Int J Syst Evol Microbiol* **56**: 2331-2335.

Wu,J.-H., Wu,F.-Y., Chuang,H.-P., Chen,W.-Y., Huang,H.-J., Chen,S.-H., and Liu,W.-T. (2013) Community and proteomic analysis of methanogenic consortia degrading terephthalate. *Appl Environ Microbiol* **79**: 105-112.

Yates,J.R., III (1998) Database searching using mass spectrometry data. *Electrophoresis* **19**: 893-900.

Zellner,G., Messner,P., Winter,J., and Stackebrandt,E. (1998) *Methanoculleus palmolei* sp. nov., an irregularly coccoid methanogen from an anaerobic digester treating wastewater of a palm oil plant in North-Sumatra, Indonesia. *Int J Syst Bacteriol* **48**: 1111-1117.

Zhang,C.Y., Liu,X.L., and Dong,X.Z. (2004) *Syntrophomonas curvata* sp. nov., an anaerobe that degrades fatty acids in co-culture with methanogens. *Int J Syst Evol Microbiol* **54**: 969-973.

Zhang,F., Liu,X., and Dong,X. (2012) *Thermosyntropha tengcongensis* sp. nov., a thermophilic bacterium that degrades long-chain fatty acids syntrophically. *Int J Syst Evol Microbiol* **62**: 759-763.

Zhang,G., Jiang,N., Liu,X., and Dong,X. (2008) Methanogenesis from methanol at low temperatures by a novel psychrophilic methanogen, "*Methanolobus psychrophilus*" sp. nov., prevalent in Zoige wetland of the Tibetan plateau. *Appl Environ Microbiol* **74**: 6114-6120.

Zhao,H., Yang,D., Woese,C.R., and Bryant,M.P. (1993) Assignment of fatty acid-β-oxidizing syntrophic bacteria to *Syntrophomonadaceae* fam. nov. on the basis of 16S rRNA sequence analysis. *Int J Syst Bacteriol* **43**: 278-286.

Zhao,H.X., Yang,D.C., Woese,C.R., and Bryant,M.P. (1990) Assignment of *Clostridium bryantii* to *Syntrophospora bryantii* gen. nov., comb. nov. on the basis of a 16S ribosomal-RNA sequence analysis of its crotonate-grown pure culture. *Int J Syst Bacteriol* **40**: 40-44.

Zhou,X., Meile,L., Kreuzer,M., and Zeitz,J.O. (2013) The effect of saturated fatty acids on methanogenesis and cell viability of *Methanobrevibacter ruminantium*. *Archaea* **2013**: 106916.

Zinder,S.H., Anguish,T., and Cardwell,S.C. (1984) Selective inhibition by 2-bromoethanesulfonate of methanogenesis from acetate in a thermophilic anaerobic digestor. *Appl Environ Microbiol* **47**: 1343-1345.

Zoetendal,E.G., Akkermans,A.D.L., Akkermans van Vliet,W.M., de Visser,J.A.G.M., and de Vos,W.M. (2001) The host genotype affects the bacterial community in the human gastrointestinal tract. *Microb Ecol Health Dis* **13**: 129-134.

Scientific output

The work presented in this PhD thesis originated the following publications:

PAPERS IN JOURNALS WITH PEER REVIEW:

Salvador, **A**. **F**., Sousa, D. Z., Ramos, J., Guedes, A. P., Barbosa, S., Stams, A. J. M., Alves, M. M. and Pereira, M. A. (2013) Activity and viability of methanogens in anaerobic digestion of unsaturated and saturated long-chain fatty acids. Applied and Environmental Microbiology, 79 (14): 4239-45.

Salvador, **A**. **F**. Cavaleiro, A. J., Sousa, D. Z., Alves, M. M., Pereira, M. A. (2013) Endurance of methanogenic archaea in anaerobic bioreactors treating oleate-based wastewater. Applied Microbiology and Biotechnology, 97:2211-2218.

PAPERS IN PREPARATION FOR SUBMISSION TO PEER REVIEWED JOURNALS:

Salvador, **A**. **F**., Bize, A., Alves, M. M., Bouchez, T., Sousa, D. Z. Comparative metaproteomics and diversity of LCFA-degrading microbial communities.

Cavaleiro, A. J., **Salvador**, **A**. **F**., Silva, S., Guedes, A. P., Pereira, M. A., Alves, M. M., Sousa, D. Z. Methanogenic and non-methanogenic oleate-degrading enrichment cultures: syntrophic associations for acetate production.

PUBLICATIONS IN CONFERENCE PROCEEDINGS:

Salvador, **A**. **F**., Bize, A., Alves, M. M., Bouchez, T., Sousa, D. Z. (2013) Metaproteomics of anaerobic microbial communities degrading long-chain fatty acids. AD 13 – 13th World Congress on Anaerobic Digestion, Santiago de Compostela, Spain, 25-28 June, 2013. *Platform presentation.*

Salvador, **A**. **F**., Pereira, M. A., Alves, M. M., Sousa D. Z. 2011. Assessment of methanogen survival in anaerobic enrichment cultures degrading long-chain fatty acids. Proceedings of FEMS – 4th Congress of European Microbiologists, Geneva, Switzerland, 26-30 Jun. *Special poster presentation.*

ABSTRACTS AND POSTERS IN CONFERENCES:

Sousa, D. Z., **Salvador**, **A**. **F**., Ramos, J., Guedes, A. P., Barbosa, S., Stams, A. J. M., Alves, M. M. and Pereira, M. A. Effect of long-chain fatty acids (LCFA) on the prevalence and viability of hydrogenotrophic methanogens. AD 13 – 13th World Congress on Anaerobic Digestion, Santiago de Compostela, Spain, 25-28 June, 2013.

Salvador, **A**. **F**., Bize, A., Alves, M. M., Bouchez, T., Sousa, D. Z. Diversity and proteomic characterization of saturated and unsaturated LCFA anaerobic degrading

communities. ISME14 - 14th International Symposium on Microbial Ecology, Copenhagen, Denmark, 19-24 August, 2012.

Cavaleiro, A. J., **Salvador**, **A**. **F**., Silva, S., Pereira, M. A., Sousa, D. Z., Alves, M. M. New strategies for optimal methane production from long chain fatty acids. ecoSTP – EcoTechnologies for Wastewater Treatment, Technical, Enviromental & Economic Challenges Conference, Santiago de Compostela, Spain, 25-27 June, 2012.

Salvador, **A**. **F**., Pereira, M. A., Stams, A. J. M., Alves, M. M., Sousa D. Z. Microbial diversity and methanogen survival in anaerobic communities degrading long-chain fatty acids. 1st International Conference on Biogas Microbiology, Leipzig, Germany, 14-16 September, 2011.

Salvador, **A**. **F**., Pereira, M. A., Alves, M. M., Sousa D. Z. Assessment of methanogen survival in anaerobic enrichment cultures degrading long-chain fatty acids. Proceedings of FEMS – 4th Congress of European Microbiologists, Geneva, Switzerland, 26-30 June, 2011.

Salvador, **A**. **F**., Cavaleiro, A. J., Pereira, M. A., Alves, M. M. Molecular profiling of microbial communities in anaerobic bioreactors treating oleic acid rich wastewater. Proceedings of MicroBiotec'09- Vilamoura, Portugal, 28-30 November, 2009.

Salvador, **A**. **F**., Cavaleiro, A. J., Pereira, M. A., Alves, M. M. Molecular profiling of microbial communities developed in high-rate anaerobic treatment of oleic acid rich wastewater. Proceedings of FEMS – 3rd Congress of European Microbiologists (Posters), 356, Gothenburg, Sweden, 28 Jun-2 July, 2009.

Supplementary Material

Chapter 4

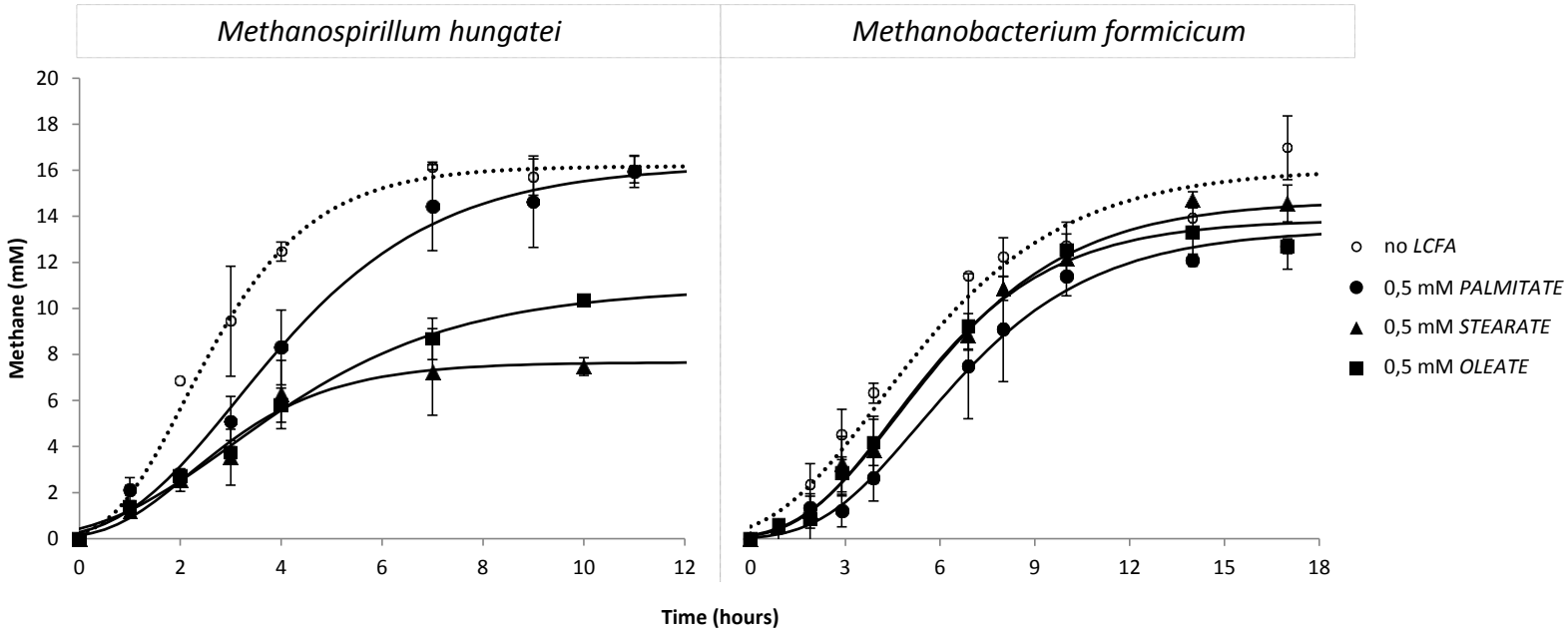

Figure S4.1 Methane production by pure cultures of *M. hungatei* and *M. formicicum* growing on H_2/CO_2, without LCFA addition and in the presence of 0.5 mM LCFA.

Chapter 6

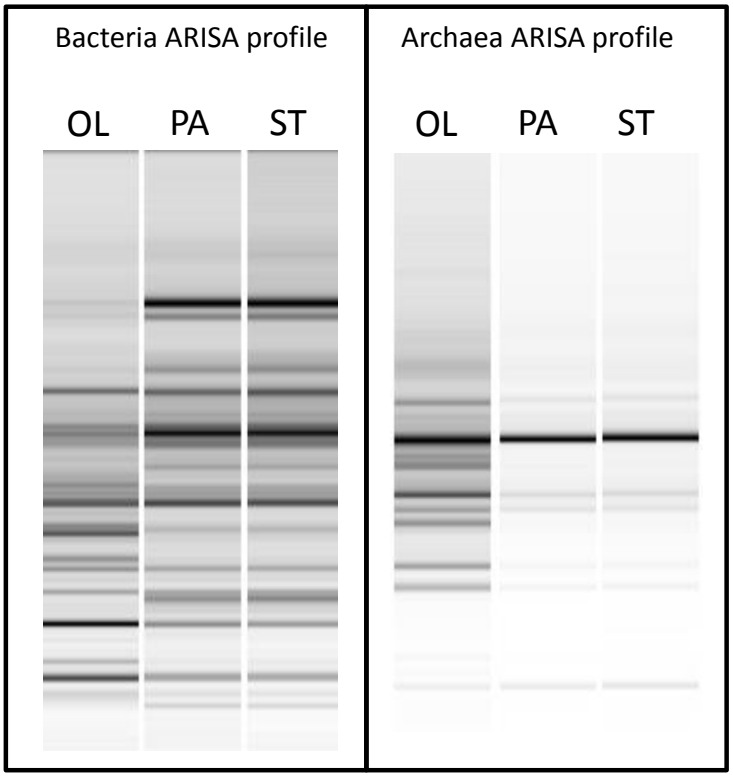

Figure S6.1 ARISA fingerprinting of bacterial and archaeal communities developed in PA, ST and OL incubations.

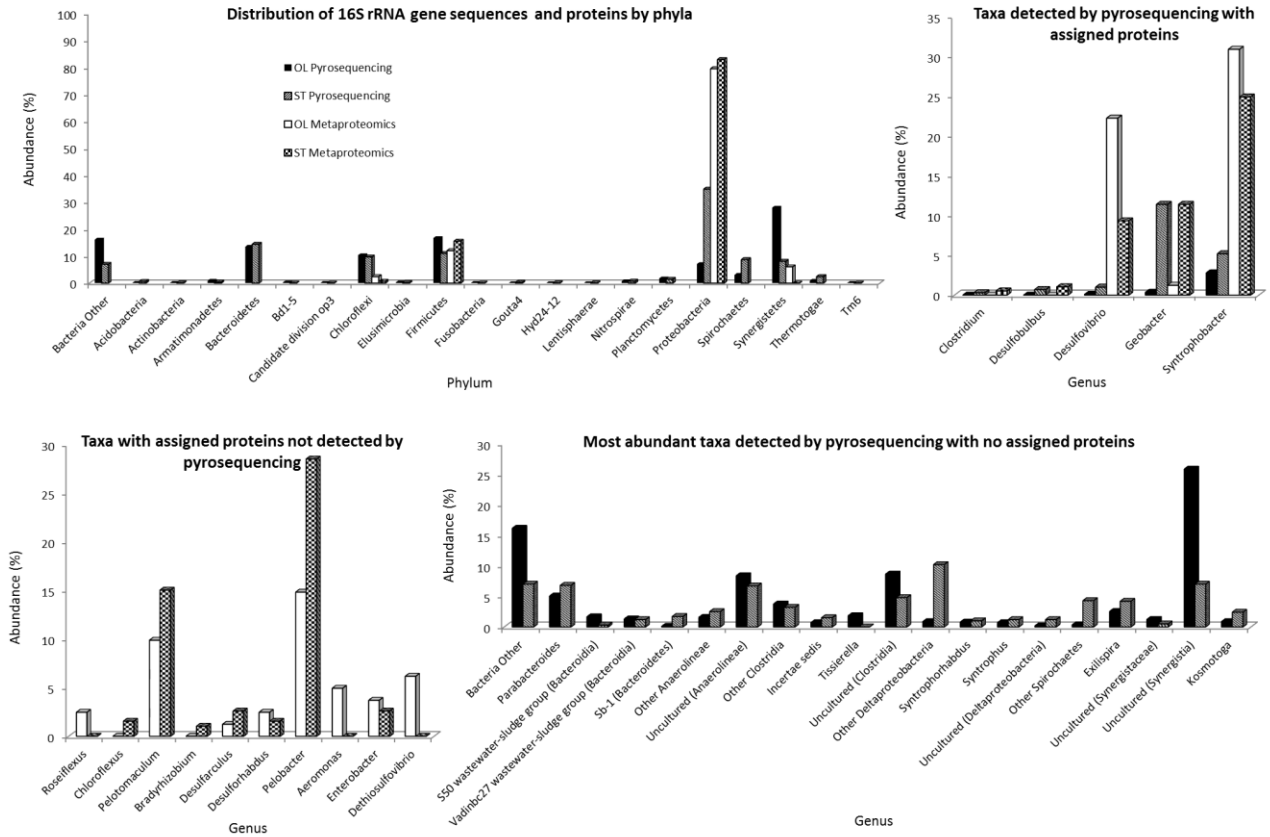

Figure S6.2 Distribution of 16S rRNA gene sequences and proteins by phyla and genera.

Table S6.1 Identification, functional assignment and relative abundance of archaeal proteins identified in PA, ST and OL incubations.

				Normalized Spectrum Counts			
COG Functional Category	**Protein name**	**Uniprot ID**	**Organism**	**LCFA**	**PA**	**ST**	**OL**
Energy production and conversion					722	758	674
	Acetyl-CoA decarbonylase/synthase complex subunit alpha	P26692	*Methanosaeta concilii* (strain GP-6)		138	166	158
	CO dehydrogenase/acetyl-CoA synthase E	E5KJT6	*Methanosaeta harundinacea*		3	11	6
	V-type ATP synthase beta chain	E5KJX1	*Methanosaeta harundinacea*		25	25	1
	5,10-methylenetetrahydromethanopterin reductase	G6FHR7	*Methanolinea tarda* NOBI-1		3	3	1
	Manganese-dependent inorganic pyrophosphatase	F4BW56	*Methanosaeta concilii* (strain GP-6)		4	5	1
	V-type ATP synthase alpha chain	F4BZ02	*Methanosaeta concilii* (strain GP-6)		100	77	63
	Acetyl-CoA decarbonylase/synthase complex subunit delta	F4C0K4	*Methanosaeta concilii* (strain GP-6)		39	16	14
	Acetyl-CoA decarbonylase/synthase complex subunit alpha	F4C0K8	*Methanosaeta concilii* (strain GP-6)		136	168	164
	V-type ATP synthase subunit I	F4BZ07	*Methanosaeta concilii* (strain GP-6)		1	3	9
	Acetyl-CoA decarbonylase/synthase complex subunit epsilon	F4C0K7	*Methanosaeta concilii* (strain GP-6)		13	13	9
	V-type ATP synthase subunit D	F4BZ00	*Methanosaeta concilii* (strain GP-6)		2	2	4
	CoB--CoM heterodisulfide reductase iron-sulfur subunit D	F4BVR1	*Methanosaeta concilii* (strain GP-6)		7	7	2
	V-type proton ATPase subunit E	F4BZ05	*Methanosaeta concilii* (strain GP-6)		1	2	2
	V-type ATP synthase subunit F	F4BZ03	*Methanosaeta concilii* (strain GP-6)		4	0	12
	Pyruvate oxidoreductase subunit alfa	F4BTC1	*Methanosaeta concilii* (strain GP-6)		1	2	4
	Flavodoxin domain protein	F4C0K0	*Methanosaeta concilii* (strain GP-6)		1	1	3
	Acetyl-CoA decarbonylase/synthase complex subunit beta	F4C0K6	*Methanosaeta concilii* (strain GP-6)		80	78	65
	CO dehydrogenase/acetyl-CoA synthase complex, subunit gamma	F4C0K3	*Methanosaeta concilii* (strain GP-6)		39	44	41
	F420H2 dehydrogenase, subunit B	F4BTJ6	*Methanosaeta concilii* (strain GP-6)		3	4	2
	V-type ATP synthase beta chain	F4BZ01	*Methanosaeta concilii* (strain GP-6)		70	75	61
	V-type ATP synthase subunit C	F4BZ04	*Methanosaeta concilii* (strain GP-6)		8	10	5
	Sulfite reductase, assimilatory-type	F4C004	*Methanosaeta concilii* (strain GP-6)		6	8	5
	F420H2 dehydrogenase, subunit D	F4BTJ7	*Methanosaeta concilii* (strain GP-6)		2	1	1
	5,10-methylenetetrahydromethanopterin reductase	B8GJQ5	*Methanosphaerula palustris* (strain E1-9c)		2	3	0
	Methyl-viologen-reducing hydrogenase delta subunit	F0T8S8	*Methanobacterium* sp. (strain AL-21)		0	0	3
	5,10-methylenetetrahydromethanopterin reductase	F0T9L4	*Methanobacterium* sp. (strain AL-21)		1	3	4
	Acetyl-CoA decarbonylase/synthase complex subunit alpha	A0B5W5	*Methanosaeta thermophila* (strain PT)		17	21	13
	Methyl-viologen-reducing hydrogenase delta subunit	F6D2B7	*Methanobacterium* sp. (strain SWAN-1)		0	0	3
	5,10-methylenetetrahydromethanopterin reductase	F6D5U5	*Methanobacterium* sp. (strain SWAN-1)		2	3	8
	5,10-methylenetetrahydromethanopterin reductase	Q2FTS9	*Methanospirillum hungatei* (strain JF-1)		3	1	1
	Acetyl-CoA decarbonylase/synthase complex subunit alpha	G7WKX9	*Methanosaeta harundinacea* (strain 6Ac)		10	9	9

Table S6.1 (continued)

COG Functional Category	Protein name	Uniprot ID	Organism	Normalized Spectrum Counts			
				LCFA	PA	ST	OL
Posttranslational modification, protein turnover, chaperones					35	38	56
	Thermosome subunit gamma	F4BUS8	*Methanosaeta concilii* (strain GP-6)		0	0	2
	AAA family ATPase, CDC48 subfamily	F4BV79	*Methanosaeta concilii* (strain GP-6)		2	1	1
	Thermosome subunit delta	F4BSZ0	*Methanosaeta concilii* (strain GP-6)		10	15	21
	Chaperone protein DnaK (HSP70)	F4BZ87	*Methanosaeta concilii* (strain GP-6)		6	4	7
	Peptidyl-prolyl cis-trans isomerase	F4BZH8	*Methanosaeta concilii* (strain GP-6)		0	0	2
	Proteasome subunit beta	F4C0P1	*Methanosaeta concilii* (strain GP-6)		9	11	12
	Thermosome subunit alfa	F4BUI2	*Methanosaeta concilii* (strain GP-6)		3	4	6
	Proteasome subunit alpha	A0B8W6	*Methanosaeta thermophila* (strain PT)		5	3	5
Translation, ribosomal structure and biogenesis					31	39	17
	30S ribosomal protein S24e	F4BU96	*Methanosaeta concilii* (strain GP-6)		3	1	2
	Probable exosome complex exonuclease 1	F4BTR2	*Methanosaeta concilii* (strain GP-6)		3	1	1
	Elongation factor 2 (EF-2)	F4BU76	*Methanosaeta concilii* (strain GP-6)		7	6	2
	Acidic ribosomal protein P0 homolog (L10E)	F4C0T3	*Methanosaeta concilii* (strain GP-6)		0	0	3
	Elongation factor 1-alpha	F4BU75	*Methanosaeta concilii* (strain GP-6)		18	24	10
	Elongation factor 1-alpha	D1YXX5	*Methanocella paludicola* (strain SANAE)		0	7	0
Nucleotide transport and metabolismo					9	9	11
	Putative thymidine phosphorylase	F4BX26	*Methanosaeta concilii* (strain GP-6)		0	1	2
	Nucleoside diphosphate kinase	F4BUT2	*Methanosaeta concilii* (strain GP-6)		2	3	3
	Adenylosuccinate synthetase	F4BX03	*Methanosaeta concilii* (strain GP-6)		3	2	4
	PyrE-like protein	F4BWV2	*Methanosaeta concilii* (strain GP-6)		1	0	2
	Adenylate kinase	F4BWP7	*Methanosaeta concilii* (strain GP-6)		3	4	0
Transcription					49	21	8
	V-type ATP synthase alpha chain	A0B9K2	*Methanosaeta thermophila* (strain PT)		37	14	0
	Putative nickel-responsive regulator	F4BU36	*Methanosaeta concilii* (strain GP-6)		2	3	3
	Uncharacterized protein	F4BWQ0	*Methanosaeta concilii* (strain GP-6)		2	1	3
	TATA-box-binding protein	F4BWT3	*Methanosaeta concilii* (strain GP-6)		4	3	2
	Uncharacterized protein	F4BUI1	*Methanosaeta concilii* (strain GP-6)		3	0	0

Table S6.1 (continued)

COG Functional Category	Protein name	Uniprot ID	Organism	Normalized Spectrum Counts			
				LCFA	PA	ST	OL
Amino acid transport and metabolism					17	7	28
	Extracellular solute-binding protein, family 5	F4BYH7	*Methanosaeta concilii* (strain GP-6)		0	0	2
	Histidinol dehydrogenase	F4BY85	*Methanosaeta concilii* (strain GP-6)		0	0	1
	Glutamate dehydrogenase	F4BUZ5	*Methanosaeta concilii* (strain GP-6)		1	0	1
	Oligopeptide ABC transporter, solute-binding protein	F4BXJ2	*Methanosaeta concilii* (strain GP-6)		0	1	4
	Soluble hydrogenase small subunit	F4BYZ7	*Methanosaeta concilii* (strain GP-6)		0	0	2
	Glutamine synthetase, type I	F4BUG1	*Methanosaeta concilii* (strain GP-6)		3	1	1
	3-isopropylmalate dehydratase small subunit	F4C0F9	*Methanosaeta concilii* (strain GP-6)		0	0	2
	Amino acid-binding ACT domain protein	F4BY88	*Methanosaeta concilii* (strain GP-6)		0	0	3
	Aspartate-semialdehyde dehydrogenase	F4C036	*Methanosaeta concilii* (strain GP-6)		1	3	1
	Extracellular solute-binding protein, family 5	F4BVQ8	*Methanosaeta concilii* (strain GP-6)		1	1	1
	Ketol-acid reductoisomerase	F4BWF4	*Methanosaeta concilii* (strain GP-6)		7	3	7
	ABC transporter, extracellular solute-binding protein, family 5	F4BWL4	*Methanosaeta concilii* (strain GP-6)		1	0	3
	S-adenosylmethionine synthase	F4C0D6	*Methanosaeta concilii* (strain GP-6)		3	0	1
Lipid transport and metabolismo					245	204	177
	Acetyl-coenzyme A synthetase	F4BX07	*Methanosaeta concilii* (strain GP-6)		103	85	77
	Acetyl-coenzyme A synthetase	F4BX08	*Methanosaeta concilii* (strain GP-6)		6	7	8
	Acetyl-coenzyme A synthetase	F4BX06	*Methanosaeta concilii* (strain GP-6)		74	61	63
	Acetyl-coenzyme A synthetase	F4C0Q1	*Methanosaeta concilii* (strain GP-6)		34	29	20
	Acetyl-coenzyme A synthetase	A0B8F2	*Methanosaeta thermophila* (strain PT)		29	22	9
Carbohydrate transport and metabolismo					14	10	16
	Uncharacterized protein	F4C0S9	*Methanosaeta concilii* (strain GP-6)		11	8	7
	Enolase	F4BUI5	*Methanosaeta concilii* (strain GP-6)		3	1	8
	Cellulase	F4BZI5	*Methanosaeta concilii* (strain GP-6)		0	1	1
Secondary metabolites biosynthesis, transport and catabolism					1	1	1
	Alkyl/aryl-sulfatase	F4BTL7	*Methanosaeta concilii* (strain GP-6)		1	1	1

Table S6.1 (continued)

				Normalized Spectrum Counts			
COG Functional Category	**Protein name**	**Uniprot ID**	**Organism**	**LCFA**	**PA**	**ST**	**OL**
Coenzyme transport and metabolismo					713	665	667
	Methyl-coenzyme M reductase subunit beta	P07955	*Methanosarcina barkeri* (strain Fusaro)		3	16	14
	Methyl-coenzyme M reductase I subunit beta	O27236	*Methanothermobacter thermautotrophicus*		0	0	2
	Methyl CoM reductase alpha subunit (Fragment)	B1GTB3	Uncultured methanogenic archaeon		9	2	5
	Methyl-coenzyme M reductase alpha subunit (Fragment)	A7Y3C6	Uncultured methanogenic archaeon		9	8	13
	Methyl coenzyme M reductase alpha subunit (Fragment)	A1XWG4	Uncultured methanogenic archaeon		43	33	16
	Methyl-coenzyme M reductase subunit A (Fragment)	Q49BZ8	Uncultured methanogenic archaeon		1	1	3
	Methyl-coenzyme M reductase, alpha subunit	J0SAE9	*Methanofollis liminatans*		1	2	1
	Methyl-coenzyme M reductase alpha subunit (Fragment)	D2KZW2	*Methanobacterium petrolearium*		1	2	9
	Methyl-coenzyme M reductase A	E5KJV1	*Methanosaeta harundinacea*		0	0	3
	Methyl-coenzyme M reductase B	E5KJV4	*Methanosaeta harundinacea*		0	11	0
	Methyl-coenzyme M reductase alpha subunit (Fragment)	E1ANS6	*Methanobacterium* sp. GH		1	1	5
	Methyl-coenzyme M reductase I, subunit beta	K2RAN9	*Methanobacterium formicicum* DSM 3637		2	0	7
	Methyl coenzyme M reductase I subunit alpha	K2QYM4	*Methanobacterium formicicum* DSM 3637		2	2	9
	Methyl-coenzyme M reductase alpha subunit (Fragment)	D2KZX2	*Methanobacterium subterraneum*		1	2	9
	Phosphoglycerate dehydrogenase	F4BVK8	*Methanosaeta concilii* (strain GP-6)		4	3	1
	Methyl-coenzyme M reductase, beta subunit	F4BXY4	*Methanosaeta concilii* (strain GP-6)		267	247	330
	Tetrahydromethanopterin S-methyltransferase, subunit A	F4BZJ2	*Methanosaeta concilii* (strain GP-6)		12	7	14
	Tetrahydromethanopterin S-methyltransferase subunit H	F4BZB0	*Methanosaeta concilii* (strain GP-6)		16	14	8
	Tetrahydromethanopterin S-methyltransferase subunit E	F4BZJ6	*Methanosaeta concilii* (strain GP-6)		5	2	7
	Tetrahydromethanopterin S-methyltransferase subunit B	F4BZJ3	*Methanosaeta concilii* (strain GP-6)		6	1	8
	Cobalt chelatase	F4BXX2	*Methanosaeta concilii* (strain GP-6)		0	0	1
	Tetrahydromethanopterin S-methyltransferase subunit C	F4BZJ4	*Methanosaeta concilii* (strain GP-6)		2	0	3
	Cobaltochelatase, CobN subunit	F4BXG6	*Methanosaeta concilii* (strain GP-6)		5	3	5
	Methyl-coenzyme M reductase, alpha subunit	F4BXY1	*Methanosaeta concilii* (strain GP-6)		158	134	123
	Methyl-coenzyme M reductase, gamma subunit	F4BXY2	*Methanosaeta concilii* (strain GP-6)		74	77	37
	Methyl-coenzyme M reductase, beta subunit	B8GE89	*Methanosphaerula palustris* (strain E1-9c)		2	4	9
	Methyl-coenzyme M reductase, alpha subunit, McrA	A5ULZ2	*Methanobrevibacter smithii* (strain PS)		0	1	2
	Methyl-coenzyme M reductase, gamma subunit	A0B6N7	*Methanosaeta thermophila* (strain PT)		3	8	0
	Methyl-coenzyme M reductase, alpha subunit	A0B6N6	*Methanosaeta thermophila* (strain PT)		11	7	0
	Tetrahydromethanopterin S-methyltransferase subunit A	A0B8Y2	*Methanosaeta thermophila* (strain PT)		6	2	0

Table S6.1 (continued)

COG Functional Category	Protein name	Uniprot ID	Organism	Normalized Spectrum Counts			
				LCFA	PA	ST	OL
Coenzyme transport and metabolism (cont.)					713	665	667
	Methyl-coenzyme M reductase, beta subunit	A0B6N9	*Methanosaeta thermophila* (strain PT)		53	54	7
	Tetrahydromethanopterin S-methyltransferase, subunit H	A0B8X9	*Methanosaeta thermophila* (strain PT)		5	7	0
	Oxidoreductase FAD/NAD(P)-binding domain protein	F2KRX4	*Archaeoglobus veneficus* (strain SNP6)		1	2	2
	Methyl-coenzyme M reductase, beta subunit	F6D2D7	*Methanobacterium sp.* (strain SWAN-1)		0	0	1
	Methyl-coenzyme M reductase, gamma subunit	Q2FSN1	*Methanospirillum hungatei* (strain JF-1)		3	1	1
	Methyl-coenzyme M reductase, beta subunit	Q2FSD8	*Methanospirillum hungatei* (strain JF-1)		2	4	8
	Methyl-coenzyme M reductase, alpha subunit	Q2FSN0	*Methanospirillum hungatei* (strain JF-1)		5	6	3
Cell wall/membrane/envelope biogenesis					13	8	34
	Cna B domain protein	F4BZ82	*Methanosaeta concilii* (strain GP-6)		13	8	32
	Fasciclin domain protein	F4BTZ6	*Methanosaeta concilii* (strain GP-6)		0	0	2
Inorganic ion transport and metabolism					12	11	34
	Sulfatase family protein	F4BZY1	*Methanosaeta concilii* (strain GP-6)		0	0	4
	Periplasmic binding protein	F4BXK3	*Methanosaeta concilii* (strain GP-6)		1	0	2
	Periplasmic binding protein	F4BXN7	*Methanosaeta concilii* (strain GP-6)		5	3	5
	ABC transporter, substrate-binding protein, aliphatic sulfonates family	F4C0D4	*Methanosaeta concilii* (strain GP-6)		0	1	2
	Uncharacterized protein	F4BXM7	*Methanosaeta concilii* (strain GP-6)		2	3	6
	Phosphate binding protein	F4BY48	*Methanosaeta concilii* (strain GP-6)		2	3	6
	Superoxide dismutase	F4BZF7	*Methanosaeta concilii* (strain GP-6)		1	2	0
	Periplasmic binding protein	F4BXW7	*Methanosaeta concilii* (strain GP-6)		0	0	1
	Periplasmic binding protein	F4BU58	*Methanosaeta concilii* (strain GP-6)		0	0	1
	Uncharacterized protein	F4BXK1	*Methanosaeta concilii* (strain GP-6)		0	0	2
	Periplasmic binding protein	F4BWK7	*Methanosaeta concilii* (strain GP-6)		1	0	4
	Periplasmic binding protein	F4BXG9	*Methanosaeta concilii* (strain GP-6)		0	0	2
Cell cycle control, cell division, chromosome partitioning					2	0	0
	Cell division protein FtsZ	F4BU02	*Methanosaeta concilii* (strain GP-6)		2	0	0
Intracellular trafficking, secretion, and vesicular transport					0	0	5
	WD40-like Beta Propeller Repeat protein	F4BY71	*Methanosaeta concilii* (strain GP-6)		0	0	5

Table S6.1 (continued)

				Normalized Spectrum Counts			
COG Functional Category	**Protein name**	**Uniprot ID**	**Organism**	**LCFA**	**PA**	**ST**	**OL**
Signal transduction mechanisms					34	38	86
	Universal stress protein	F4BUJ8	*Methanosaeta concilii* (strain GP-6)		2	3	2
	KaiC	F4BTD5	*Methanosaeta concilii* (strain GP-6)		6	3	3
	Universal stress protein	F4BZI6	*Methanosaeta concilii* (strain GP-6)		19	24	63
	Universal stress protein	F4BSY2	*Methanosaeta concilii* (strain GP-6)		6	6	12
	Universal stress protein	F4BZH5	*Methanosaeta concilii* (strain GP-6)		1	3	7
Replication, recombination and repair					3	5	1
	UPF0095 protein MCON_3176	F4BU89	*Methanosaeta concilii* (strain GP-6)		0	2	0
	DNA polymerase sliding clamp	F4BTF8	*Methanosaeta concilii* (strain GP-6)		3	3	1
General function prediction only					31	17	58
	Deoxyribonuclease/rho motif-related TRAM	K2QX04	*Methanobacterium formicicum* DSM 3637		3	0	3
	Methyl coenzyme M reductase system, component A2	F4BVZ3	*Methanosaeta concilii* (strain GP-6)		5	4	3
	Uncharacterized protein	F4BWL7	*Methanosaeta concilii* (strain GP-6)		2	1	7
	TPR-repeat protein	F4BWB0	*Methanosaeta concilii* (strain GP-6)		5	1	7
	Uncharacterized protein	F4BYH4	*Methanosaeta concilii* (strain GP-6)		0	0	5
	Pyridoxamine 5'-phosphate oxidase-related, FMN-binding protein	F4BWV6	*Methanosaeta concilii* (strain GP-6)		3	5	10
	UPF0278 protein	F4BX00	*Methanosaeta concilii* (strain GP-6)		0	2	0
	Formate dehydrogenase, alpha subunit	F4BUX7	*Methanosaeta concilii* (strain GP-6)		2	1	0
	TPR-repeat protein	F4BWB4	*Methanosaeta concilii* (strain GP-6)		2	0	6
	TPR-repeat protein	F4BWB5	*Methanosaeta concilii* (strain GP-6)		2	2	9
	Uncharacterized protein	F4BUT9	*Methanosaeta concilii* (strain GP-6)		4	0	6
	DJ-1/PfpI family/rubredoxin fusion protein	F4BVC1	*Methanosaeta concilii* (strain GP-6)		0	0	2
	Amino acid-binding ACT domain protein	F4BYA5	*Methanosaeta concilii* (strain GP-6)		3	0	0
Function unknown					10	8	29
	Uncharacterized protein	K2RRN0	*Methanobacterium formicicum* DSM 3637		1	2	3
	Carboxymuconolactone decarboxylase family protein	F4C0U6	*Methanosaeta concilii* (strain GP-6)		3	0	13
	Pentapeptide repeat protein	F4BVN7	*Methanosaeta concilii* (strain GP-6)		0	1	2
	Uncharacterized protein	F4BTC6	*Methanosaeta concilii* (strain GP-6)		3	1	7
	Uncharacterized protein	F4C022	*Methanosaeta concilii* (strain GP-6)		2	3	3
	Bifunctional enzyme fae/hps	F4BSV0	*Methanosaeta concilii* (strain GP-6)		1	1	1

Table S6.1 (continued)

COG Functional Category	Protein name	Uniprot	Organism	Normalized Spectrum Counts			
				LCFA	PA	ST	OL
No COG					144	119	263
	Uncharacterized protein	G6FHS2	*Methanolinea tarda* NOBI-1		1	2	3
	Uncharacterized protein	F4BXM4	*Methanosaeta concilii* (strain GP-6)		0	0	1
	Uncharacterized protein	F4BTY9	*Methanosaeta concilii* (strain GP-6)		4	2	10
	CARDB domain protein	F4C009	*Methanosaeta concilii* (strain GP-6)		2	0	1
	Uncharacterized protein	F4C0U0	*Methanosaeta concilii* (strain GP-6)		1	1	1
	S-layer-related duplication domain protein	F4BXZ6	*Methanosaeta concilii* (strain GP-6)		7	7	28
	Uncharacterized protein	F4BW14	*Methanosaeta concilii* (strain GP-6)		28	19	54
	Uncharacterized protein	F4BVY8	*Methanosaeta concilii* (strain GP-6)		4	1	8
	Polymorphic outer membrane protein	F4BXJ5	*Methanosaeta concilii* (strain GP-6)		0	0	1
	Uncharacterized protein	F4BTV3	*Methanosaeta concilii* (strain GP-6)		1	2	3
	Uncharacterized protein	F4BV37	*Methanosaeta concilii* (strain GP-6)		1	2	3
	Conserved repeat domain protein	F4BXV1	*Methanosaeta concilii* (strain GP-6)		0	0	4
	Uncharacterized protein	F4BUA8	*Methanosaeta concilii* (strain GP-6)		5	4	2
	Uncharacterized protein	F4BV04	*Methanosaeta concilii* (strain GP-6)		0	0	2
	Uncharacterized protein	F4BWF0	*Methanosaeta concilii* (strain GP-6)		1	1	1
	Uncharacterized protein	F4BVQ0	*Methanosaeta concilii* (strain GP-6)		0	0	1
	Uncharacterized protein	F4BXM0	*Methanosaeta concilii* (strain GP-6)		2	1	5
	Uncharacterized protein	F4BXM2	*Methanosaeta concilii* (strain GP-6)		0	0	1
	S-layer-related duplication domain protein	F4BZQ7	*Methanosaeta concilii* (strain GP-6)		48	42	83
	Cna protein B-type domain protein	F4BU06	*Methanosaeta concilii* (strain GP-6)		3	3	5
	Uncharacterized protein	F4BXL5	*Methanosaeta concilii* (strain GP-6)		7	1	6
	Uncharacterized protein	F4BXM5	*Methanosaeta concilii* (strain GP-6)		3	6	6
	Uncharacterized protein	F4BUT8	*Methanosaeta concilii* (strain GP-6)		5	3	3
	Uncharacterized protein	F4BXX8	*Methanosaeta concilii* (strain GP-6)		1	10	5
	Uncharacterized protein	F4BT26	*Methanosaeta concilii* (strain GP-6)		2	0	2
	Uncharacterized protein	Q2FTS3	*Methanospirillum hungatei* (strain JF-1)		7	6	12
	Uncharacterized protein	Q2FS26	*Methanospirillum hungatei* (strain JF-1)		9	5	11

Table S6.2 Relative abundance (%) of taxonomic groups of *Bacteria* in ST and OL incubations (based on pyrosequencing data).

Phylum	Class	Genus	Species	ST	OL
Other (Bacteria)	Other	Other	Other	6,99	16,13
Acidobacteria	*Acidobacteria*	Other	Other	0,10	0,09
Acidobacteria	*Acidobacteria*	*Bpc102*	Other	0,10	0,00
Acidobacteria	*Holophagae*	*Sja-36*	Uncultured bacterium	0,40	0,00
Actinobacteria	*Actinobacteria*	*Other*	Other	0,10	0,00
Actinobacteria	*Actinobacteria*	*Propionicicella*	Iron-reducing enrichment clone cl-a3	0,00	0,09
Armatimonadetes	Other	Other	Other	0,00	0,35
Armatimonadetes	Uncultured bacterium	*Armatimonadetes*	Uncultured bacterium	0,00	0,09
Armatimonadetes	Uncultured candidate division op10 bacterium	*Armatimonadetes*	Uncultured candidate division op10 bacterium	0,40	0,44
Bacteroidetes	Other	Other	Other	0,60	0,09
Bacteroidetes	*Bacteroidia*	Other	Other	0,50	0,96
Bacteroidetes	*Bacteroidia*	*Bacteroides*	Other	0,00	0,17
Bacteroidetes	*Bacteroidia*	*Bacteroides*	Iron-reducing enrichment clone cl-a12	0,10	0,87
Bacteroidetes	*Bacteroidia*	Blvii28 wastewater-sludge group	Other	0,10	0,00
Bacteroidetes	*Bacteroidia*	Blvii28 wastewater-sludge group	Bacteroidetes bacterium ppf50e2	0,20	0,00
Bacteroidetes	*Bacteroidia*	Blvii28 wastewater-sludge group	Uncultured bacterium	0,30	1,57
Bacteroidetes	*Bacteroidia*	Blvii28 wastewater-sludge group	Uncultured bacteroidetes/chlorobi group	0,00	0,17
Bacteroidetes	*Bacteroidia*	M2pb4-65 termite	Uncultured bacterium	0,20	0,00
Bacteroidetes	*Bacteroidia*	*Paludibacter*	Uncultured anaerobic	1,30	0,96
Bacteroidetes	*Bacteroidia*	*Paludibacter*	Uncultured bacterium	0,20	0,09
Bacteroidetes	*Bacteroidia*	*Parabacteroides*	Other	6,19	4,53
Bacteroidetes	*Bacteroidia*	*Parabacteroides*	*Bacteroides* sp. w7	0,10	0,09
Bacteroidetes	*Bacteroidia*	*Parabacteroides*	Uncultured bacteroides sp.	0,50	0,44
Bacteroidetes	*Bacteroidia*	*Proteiniphilum*	Other	0,00	0,09
Bacteroidetes	*Bacteroidia*	Rs-e47 termite group	Uncultured bacterium	0,10	0,00
Bacteroidetes	*Bacteroidia*	S50 wastewater-sludge group	Uncultured bacterium	0,30	1,66
Bacteroidetes	*Bacteroidia*	Vadinbc27 wastewater-sludge	Other	0,10	1,22
Bacteroidetes	*Bacteroidia*	Vadinbc27 wastewater-sludge	Bacterium enrichment culture clone dphb03	0,70	0,00
Bacteroidetes	*Bacteroidia*	Vadinbc27 wastewater-sludge	Uncultured bacterium	0,40	0,09
Bacteroidetes	*Sb-1*	*Sb-1*	Uncultured bacterium	1,70	0,09
Bacteroidetes	*Vadinha17*	*Vadinha17*	Other	0,50	0,44
Bacteroidetes	*Vadinha17*	*Vadinha17*	Uncultured bacterium	0,30	0,00
Bd1-5	Other	Other	Other	0,00	0,26
Candidate division op3	Uncultured banisveld landfill bacterium bvc56	*Candidate division op3*	Uncultured banisveld landfill bacterium bvc56	0,00	0,09

Table S6.2 (continued)

Phylum	Class	Genus	Species	ST	OL
Chloroflexi	Other	Other	Other	0,10	0,00
Chloroflexi	*Anaerolineae*	Other	Other	2,50	1,57
Chloroflexi	*Anaerolineae*	*Longilinea*	Uncultured bacterium	0,40	0,35
Chloroflexi	*Anaerolineae*	Uncultured	Other	2,50	3,40
Chloroflexi	*Anaerolineae*	Uncultured	Anaerobic bacterium mo-cfx1	0,00	0,17
Chloroflexi	*Anaerolineae*	Uncultured	Bacterium enrichment culture clone ba53	3,90	4,62
Chloroflexi	*Anaerolineae*	Uncultured	Uncultured longilinea sp.	0,30	0,17
Chloroflexi	*Sha-26*	*Sha-26*	Other	0,00	0,09
Elusimicrobia	*Elusimicrobia*	*Lineage i (endomicrobia)*	Other	0,20	0,26
Firmicutes	Other	Other	Other	0,30	0,09
Firmicutes	*Bacilli*	*Exiguobacterium*	Uncultured compost bacterium	0,10	0,00
Firmicutes	*Bacilli*	*Trichococcus*	Other	0,30	0,00
Firmicutes	*Clostridia*	Other	Other	3,20	3,75
Firmicutes	*Clostridia*	*Acetobacterium*	Other	0,00	0,09
Firmicutes	*Clostridia*	*Christensenella*	Other	0,10	0,00
Firmicutes	*Clostridia*	*Clostridium*	Other	0,20	0,00
Firmicutes	*Clostridia*	*Clostridium*	*Clostridium* sp. Strain p2	0,10	0,00
Firmicutes	*Clostridia*	*Fastidiosipila*	Other	0,00	0,44
Firmicutes	*Clostridia*	*Incertae sedis*	Other	1,00	0,44
Firmicutes	*Clostridia*	*Incertae sedis*	*Clostridium perfringens* cpe str. f4969	0,00	0,17
Firmicutes	*Clostridia*	*Incertae sedis*	*Clostridium* sp. 6-62	0,50	0,09
Firmicutes	*Clostridia*	*Oscillibacter*	*Clostridium* sp. Enrichment culture clone 7-14	0,20	0,00
Firmicutes	*Clostridia*	*Phascolarctobacterium*	Uncultured	0,00	0,09
Firmicutes	*Clostridia*	*Sporanaerobacter*	*Sporanaerobacter acetigenes*	0,00	0,87
Firmicutes	*Clostridia*	*Syntrophomonas*	Uncultured bacterium	0,10	0,26
Firmicutes	*Clostridia*	*Tissierella*	*Tissierella praeacuta*	0,00	1,83
Firmicutes	*Clostridia*	Uncultured	Other	0,80	3,31
Firmicutes	*Clostridia*	Uncultured	*Clostridium* sp. Enrichment culture clone vanctr93	0,10	0,00
Firmicutes	*Clostridia*	Uncultured	*Clostridium* sp. Enrichment culture clone vanctr97	3,60	4,97
Firmicutes	*Clostridia*	Uncultured	Iron-reducing bacterium enrichment culture clone hn109	0,10	0,00
Firmicutes	*Clostridia*	Uncultured	Iron-reducing bacterium enrichment culture clone hn117	0,10	0,17
Firmicutes	*Clostridia*	Uncultured	Uncultured bacterium hb69	0,10	0,09
Firmicutes	*Clostridia*	Uncultured	Uncultured clostridia bacterium	0,00	0,09
Firmicutes	*Clostridia*	*Veillonella*	Uncultured actinobacterium	0,10	0,00
Fusobacteria	*Fusobacteria*	Kd3-66	Uncultured bacterium	0,00	0,09
Gouta4	Other	Other	Other	0,30	0,00
Hyd24-12	Other	Other	Other	0,10	0,00
Lentisphaerae	*Lentisphaeria*	Bs5	Uncultured bacterium	0,10	0,00
Nitrospirae	*Nitrospira*	4-29	Other	0,10	0,00
Nitrospirae	*Nitrospira*	Opb95	Uncultured soil bacterium	0,10	0,00
Nitrospirae	*Nitrospira*	Uncultured	Other	0,10	0,00
Nitrospirae	*Nitrospira*	Uncultured	Uncultured bacterium	0,40	0,70

Table S6.2 (continued)

Phylum	Class	Genus	Species	ST	OL
Planctomycetes	*Phycisphaerae*	Other	Other	0,20	0,35
Planctomycetes	*Phycisphaerae*	Kclunmb-38-53	Uncultured bacterium	0,40	0,35
Planctomycetes	*Phycisphaerae*	Mle1-8	Uncultured bacterium	0,30	0,00
Planctomycetes	*Phycisphaerae*	Vadinba30 marine sediment group	Uncultured planctomycetales	0,40	1,05
Planctomycetes	Vadinha49	Vadinha49	Uncultured planctomycete	0,10	0,00
Proteobacteria	*Alphaproteobacteria*	Other	Other	0,20	0,09
Proteobacteria	*Alphaproteobacteria*	*Sphingopyxis*	Other	0,10	0,00
Proteobacteria	*Betaproteobacteria*	Other	Other	0,00	0,09
Proteobacteria	*Betaproteobacteria*	*Ottowia*	Unidentified	0,20	0,00
Proteobacteria	*Betaproteobacteria*	*Propionivibrio*	Uncultured bacterium	0,30	0,09
Proteobacteria	*Betaproteobacteria*	*Simplicispira*	Iron-reducing bacterium enrichment culture clone	0,30	0,00
Proteobacteria	*Deltaproteobacteria*	Other	Other	10,19	0,87
Proteobacteria	*Deltaproteobacteria*	*Desulfobulbus*	Other	0,30	0,00
Proteobacteria	*Deltaproteobacteria*	*Desulfobulbus*	Uncultured bacterium	0,40	0,00
Proteobacteria	*Deltaproteobacteria*	*Desulfomicrobium*	Other	0,10	0,00
Proteobacteria	*Deltaproteobacteria*	*Desulfomicrobium*	Uncultured bacterium	0,30	0,17
Proteobacteria	*Deltaproteobacteria*	*Desulfovibrio*	Other	0,70	0,09
Proteobacteria	*Deltaproteobacteria*	*Desulfovibrio*	*Desulfovibrio* sp. s14 pv	0,30	0,00
Proteobacteria	*Deltaproteobacteria*	*Geobacter*	Other	0,10	0,00
Proteobacteria	*Deltaproteobacteria*	*Geobacter*	Bacterium enrichment culture clone etoh-69	5,29	0,00
Proteobacteria	*Deltaproteobacteria*	*Geobacter*	Uncultured bacterium	5,99	0,35
Proteobacteria	*Deltaproteobacteria*	*Smithella*	Other	0,10	0,00
Proteobacteria	*Deltaproteobacteria*	*Smithella*	Uncultured syntrophus sp.	0,20	0,00
Proteobacteria	*Deltaproteobacteria*	*Syntrophobacter*	Uncultured bacterium	5,19	2,79
Proteobacteria	*Deltaproteobacteria*	*Syntrophorhabdus*	Other	0,40	0,61
Proteobacteria	*Deltaproteobacteria*	*Syntrophorhabdus*	Uncultured bacterium	0,20	0,17
Proteobacteria	*Deltaproteobacteria*	*Syntrophorhabdus*	Uncultured bacterium ta15	0,10	0,00
Proteobacteria	*Deltaproteobacteria*	*Syntrophorhabdus*	Uncultured syntrophorhabdaceae	0,30	0,00
Proteobacteria	*Deltaproteobacteria*	*Syntrophus*	Other	0,60	0,00
Proteobacteria	*Deltaproteobacteria*	*Syntrophus*	Uncultured bacterium	0,00	0,09
Proteobacteria	*Deltaproteobacteria*	*Syntrophus*	Uncultured delta proteobacterium	0,60	0,61
Proteobacteria	*Deltaproteobacteria*	Uncultured	Bacterium enrichment culture clone r4-74b	0,90	0,09
Proteobacteria	*Deltaproteobacteria*	Uncultured	Uncultured bacterium zdt-33i5	0,00	0,09
Proteobacteria	*Deltaproteobacteria*	Uncultured	Uncultured syntrophus sp.	0,30	0,00
Proteobacteria	*Epsilonproteobacteri*	*Sulfuricurvum*	Other	0,00	0,09
Proteobacteria	*Gammaproteobacte*	Other	Other	0,00	0,17
Proteobacteria	*Gammaproteobacte*	*Escherichia-*	Uncultured klebsiella sp.	0,10	0,00
Proteobacteria	*Gammaproteobacte*	*Escherichia-*	Uncultured shigella sp.	0,10	0,61
Proteobacteria	*Gammaproteobacte*	*Klebsiella*	Uncultured klebsiella sp.	0,10	0,00
Proteobacteria	*Gammaproteobacte*	*Pseudomonas*	*Pseudomonas putida*	0,70	0,00
Proteobacteria	*Gammaproteobacte*	*Pseudomonas*	*Pseudomonas* sp. hy-14	0,20	0,00
Spirochaetes	*Spirochaetia*	Other	Other	4,30	0,35
Spirochaetes	*Spirochaetia*	*Exilispira*	Uncultured bacterium	4,20	2,53
Spirochaetes	*Spirochaetia*	Gzkb75	Uncultured bacterium	0,00	0,09
Spirochaetes	*Spirochaetia*	Uncultured	Other	0,00	0,09
Spirochaetes	*Spirochaetia*	Uncultured	Uncultured leptospira sp.	0,20	0,00

Table S6.2 (continued)

Phylum	Class	Genus	Species	ST	OL
Synergistetes	*Synergistia*	Other	Other	0,30	0,44
Synergistetes	*Synergistia*	*Aminiphilus*	Other	0,30	0,44
Synergistetes	*Synergistia*	*Aminobacterium*	*Aminobacterium colombiense* dsm 12261	0,00	0,09
Synergistetes	*Synergistia*	*Synergistaceae*	Uncultured	0,50	1,22
Synergistetes	*Synergistia*	Uncultured	Other	4,10	19,70
Synergistetes	*Synergistia*	Uncultured	Bacterium enrichment culture clone ba27	0,30	0,35
Synergistetes	*Synergistia*	Uncultured	Bacterium enrichment culture clone pa10	1,40	3,40
Synergistetes	*Synergistia*	Uncultured	Synergistetes bacterium enrichment culture clone dhr^2/lm-f01	0,20	0,09
Synergistetes	*Synergistia*	Uncultured	Uncultured aminobacterium sp.	0,00	0,17
Synergistetes	*Synergistia*	Uncultured	Uncultured bacterium	0,00	0,09
Synergistetes	*Synergistia*	Uncultured	Uncultured deferribacter sp.	0,00	0,26
Synergistetes	*Synergistia*	Uncultured	Uncultured low g+c gram-positive bacterium	1,00	1,74
Thermotogae	*Thermotogae*	*Kosmotoga*	Other	2,30	0,70
Thermotogae	*Thermotogae*	*Kosmotoga*	Thermotogales bacterium enrichment culture clone vnc3b005	0,10	0,17
Tm6	Uncultured bacterium	*Tm6*	Uncultured bacterium	0,00	0,09

Table S6.3 Relative abundance (%) of taxonomic groups of *Archaea* in ST and OL incubations (based on pyrosequencing data).

Phylum	Class	Genus	Species	ST	OL
Other (Archaea)	Other	Other	Other	0,00	0,01
Crenarchaeota	Miscellaneous crenarchaeotic group	Miscellaneous crenarchaeotic group	Other	0,03	0,59
Crenarchaeota	Miscellaneous crenarchaeotic group	Miscellaneous crenarchaeotic group	Uncultured methanogenic archaeon	0,00	0,02
Euryarchaeota	Other	Other	Other	1,66	0,42
Euryarchaeota	*Methanobacteria*	Other	Other	0,01	0,03
Euryarchaeota	*Methanobacteria*	*Methanobacterium*	Other	0,53	7,33
Euryarchaeota	*Methanobacteria*	*Methanobacterium*	*Methanobacterium kanagiense*	0,09	0,13
Euryarchaeota	*Methanobacteria*	*Methanobacterium*	Uncultured archaeon	0,02	0,06
Euryarchaeota	*Methanobacteria*	*Methanobrevibacter*	Other	0,00	0,07
Euryarchaeota	*Methanobacteria*	*Methanobrevibacter*	Uncultured methanogenic	0,00	0,00
Euryarchaeota	*Methanomicrobia*	Other	Other	0,20	0,41
Euryarchaeota	*Methanomicrobia*	*Methanoculleus*	Other	0,00	0,00
Euryarchaeota	*Methanomicrobia*	*Methanofollis*	Methanomicrobiaceae archaeon 34am	0,00	0,00
Euryarchaeota	*Methanomicrobia*	*Methanolinea*	Other	0,02	0,05
Euryarchaeota	*Methanomicrobia*	*Methanolinea*	Uncultured archaeon	0,14	0,60
Euryarchaeota	*Methanomicrobia*	*Methanolinea*	Uncultured bacterium	0,77	4,86
Euryarchaeota	*Methanomicrobia*	*Methanomethylovorans*	Uncultured archaeon	0,02	0,09
Euryarchaeota	*Methanomicrobia*	*Methanoregula*	Other	0,02	0,23
Euryarchaeota	*Methanomicrobia*	*Methanosaeta*	Other	4,67	6,16
Euryarchaeota	*Methanomicrobia*	*Methanosaeta*	Uncultured archaeon	91,44	76,18
Euryarchaeota	*Methanomicrobia*	*Methanosaeta*	Uncultured methanogenic archaeon	0,01	0,02
Euryarchaeota	*Methanomicrobia*	*Methanosaeta*	Uncultured methanosaeta sp	0,03	0,03
Euryarchaeota	*Methanomicrobia*	*Methanosarcina*	Other	0,01	0,02
Euryarchaeota	*Methanomicrobia*	*Methanospirillum*	Other	0,20	1,12
Euryarchaeota	*Methanomicrobia*	*Methanospirillum*	*Methanospirillum hungatei* jf-1	0,03	0,13
Euryarchaeota	*Methanomicrobia*	*Methanospirillum*	Uncultured archaeon	0,00	0,00
Euryarchaeota	*Methanomicrobia*	Wcha2-08	Uncultured archaeon	0,02	0,05
Euryarchaeota	*Thermoplasmata*	Other	Other	0,00	0,02
Euryarchaeota	*Thermoplasmata*	2b5	Uncultured archaeon	0,00	0,03
Euryarchaeota	*Thermoplasmata*	Terrestrial miscellaneous gp(tmeg)	Other	0,02	0,67
Euryarchaeota	*Thermoplasmata*	Vadinca11 gut group	Other	0,00	0,06
Euryarchaeota	*Thermoplasmata*	Wcha1-57	Uncultured archaeon	0,04	0,62

Table S6.4 Abundance and number of proteins assigned to different bacteria. Proteins assigned to microorganisms capable of syntrophic interactions are highlighted.

	Normalized spectral abundance factor			
	PA	ST	OL	number of proteins
Aeromonas hydrophila subsp. hydrophila	0	0	1	1
Aeromonas veronii	0	0	1	1
Bradyrhizobium sp. (strain ORS278)	2	2	0	1
Chloroflexus aurantiacus	2	2	0	2
Clostridium perfringens C	2	1	0	1
Desulfarculus baarsii	2	3	1	1
Desulfobulbus propionicus	12	2	0	2
Desulforhabdus sp. DDT	7	2	2	1
Desulfovibrio desulfuricans	12	13	13	1
Desulfovibrio fructosovorans	1	2	1	1
Desulfovibrio salexigens	4	1	2	1
Dethiosulfovibrio peptidovorans	0	0	5	1
Enterobacter sp. (strain 638)	0	5	7	1
Geobacter bemidjiensis	2	2	0	1
Geobacter sulfurreducens	8	10	1	3
Geobacter uraniireducens	11	7	0	1
Halanaerobium hydrogeniformans	0	0	4	1
Pelobacter carbinolicus	9	13	0	2
Pelobacter propionicus	47	47	33	4
Pelotomaculum thermopropionicum	28	29	6	1
Roseiflexus sp. (strain RS-1)	1	0	1	1
Syntrophobacter fumaroxidans	42	43	21	10

Table S6.5 Identification, functional assignment and relative abundance of bacterial proteins identified in PA, ST and OL incubations with a minimum of one peptide to allow protein identification.

					Normalized Spectrum Counts			
COG	**Functional**	**Protein name**	**Uniprot ID**	**Organism**	**LCFA**	**PA**	**ST**	**OL**
Energy production and conversion						317	320	144
		ATP synthase subunit beta	A0LLF8	*Syntrophobacter fumaroxidans*		1	2	2
		Glycerol kinase	A9WJ21	*Chloroflexus aurantiacus*		2	1	0
		Glycerol kinase	A5UU55	*Roseiflexus sp.*		1	0	1
		Dissimilatory sulfite reductase alpha subunit (Fragment)	Q8VRQ8	*Desulfacinum infernum*		1	1	0
		Phosphate acetyltransferase	B0NB18	*Clostridium scindens*		0	1	0
		Putative uncharacterized protein	G9PSW0	*Synergistes sp.*		5	4	0
		AprA (Fragment)	A6YCY7	*Desulforhabdus sp.*		7	2	2
		AprA (Fragment)	A6YCW6	*Desulfocapsa thiozymogenes*		0	1	0
		NAD(P)-dependent iron-only hydrogenase diaphorase component iron-sulfur protein	E3CXT8	*Aminomonas paucivorans*		2	2	0
		Succinyl-CoA ligase [ADP-forming] subunit beta	H1I2U8	*Bacillus sp.*		1	0	0
		Aldehyde oxidase and xanthine dehydrogenase molybdopterin binding	E1JYE0	*Desulfovibrio fructosovorans JJ*		1	2	1
		Iron-containing alcohol dehydrogenase	E1K229	*Desulfovibrio fructosovorans JJ*		0	0	1
		Hydrolyase, tartrate beta subunit/fumarate domain protein, Fe-S type	A5ZJ83	*Bacteroides caccae*		3	1	1
		Alcohol dehydrogenase, class IV	I2Q2K9	*Desulfovibrio sp.*		1	1	0
		Phosphate butyryltransferase	D2Z7Z8	*Dethiosulfovibrio peptidovorans*		0	0	1
		Iron-containing alcohol dehydrogenase	E8RC61	*Desulfobulbus propionicus*		7	1	1
		Cytoplasmic [FeFe]-hydrogenase-associated NADPH oxidoreductase, major subunit	Q3A3H2	*Pelobacter carbinolicus*		2	1	0
		Pyruvate-flavodoxin oxidoreductase	A8MI59	*Alkaliphilus oremlandii*		0	2	0
		NADH dehydrogenase subunit F	A1AUT8	*Pelobacter propionicus*		0	1	0
		Aldehyde dehydrogenase, molybdenum-binding subunit apoprotein	A1AP96	*Pelobacter propionicus*		10	7	0
		NADH dehydrogenase subunit E	A1AUU0	*Pelobacter propionicus*		1	3	0
		Iron-containing alcohol dehydrogenase	A1AME6	*Pelobacter propionicus*		34	35	30
		Aldehyde oxidase and xanthine dehydrogenase molybdopterin binding	B8DK02	*Desulfovibrio vulgaris*		1	0	0
		Acetyl-CoA decarbonylase/synthase alpha subunit	A0LLE1	*Syntrophobacter fumaroxidans*		0	1	0
		Carbon-monoxide dehydrogenase, catalytic subunit	A0LLE2	*Syntrophobacter fumaroxidans*		1	1	0
		Flavodoxin/nitric oxide synthase	A0LF38	*Syntrophobacter fumaroxidans*		1	0	0
		Succinate dehydrogenase subunit A	A0LJT0	*Syntrophobacter fumaroxidans*		5	6	6
		Succinyl-CoA ligase [ADP-forming] subunit alpha	A0LIY7	*Syntrophobacter fumaroxidans*		11	11	4
		Adenylylsulfate reductase, beta subunit	A0LH39	*Syntrophobacter fumaroxidans*		1	1	0

Table S6.5 (continued)

COG	Functional	Protein name	Uniprot ID	Organism	Normalized Spectrum Counts LCFA	PA	ST	OL
Energy production and conversion (cont.)						138	161	67
		Methyl-viologen-reducing hydrogenase, delta subunit	A0LHS6	*Syntrophobacter fumaroxidans*		0	1	0
		NADH dehydrogenase (Quinone)	A0LLT9	*Syntrophobacter fumaroxidans*		1	0	0
		Pyruvate carboxylase subunit B	A0LFF9	*Syntrophobacter fumaroxidans*		3	5	0
		Succinate dehydrogenase subunit B	A0LJS9	*Syntrophobacter fumaroxidans*		1	1	1
		Glycerol kinase	F0RSJ9	*Sphaerochaeta globosa*		2	1	2
		Succinate dehydrogenase or fumarate reductase, flavoprotein subunit	C6BYJ6	*Desulfovibrio salexigens*		4	1	2
		Succinate dehydrogenase subunit B	E8RID1	*Desulfobulbus propionicus*		0	1	0
		Dissimilatory adenylylsulfate reductase alpha subunit	E8RDT8	*Desulfobulbus propionicus*		5	1	0
		NAD-dependent aldehyde dehydrogenase, CoA-acylating	Q3A0W4	*Pelobacter carbinolicus*		4	6	0
		Molybdopterin-binding aldehyde oxidoreductase	Q3A811	*Pelobacter carbinolicus*		5	7	0
		Succinate dehydrogenase and fumarate reductase iron-sulfur protein	B8J107	*Desulfovibrio desulfuricans*		2	3	3
		Succinate dehydrogenase or fumarate reductase, flavoprotein subunit	Q312T8	*Desulfovibrio desulfuricans*		12	12	13
		Aldehyde dehydrogenase, molybdenum-binding subunit apoprotein	A5GB32	*Geobacter uraniireducens*		11	7	0
		ATP synthase subunit beta	F6DP59	*Desulfotomaculum ruminis*		1	1	1
		Alcohol dehydrogenase	A5D4P0	*Pelotomaculum thermopropionicum*		29	29	6
Posttranslational modification, protein turnover, chaperones						19	27	17
		60 kDa chaperonin 1	A0LEH2	*Syntrophobacter fumaroxidans*		3	1	0
		60 kDa chaperonin 2	A0LKS4	*Syntrophobacter fumaroxidans*		1	2	0
		Chaperone protein DnaK (HSP70)	B5EC42	*Geobacter bemidjiensis*		2	2	0
		60 kDa chaperonin	D2Z8X1	*Dethiosulfovibrio peptidovorans*		0	0	5
		60 kDa chaperonin	D1B621	*Thermanaerovibrio acidaminovorans*		1	0	3
		60 kDa chaperonin	E8N0E4	*Anaerolinea thermophila*		1	1	0
		60 kDa chaperonin	E1QE82	*Desulfarculus baarsii*		2	3	1
		Chaperone protein DnaK (HSP70)	D7ALW9	*Geobacter sulfurreducens*		2	2	0
		60 kDa chaperonin	D7AG51	*Geobacter sulfurreducens*		8	11	1
		Thioredoxin	A4WG29	*Enterobacter sp.*		0	5	7

Table S6.5 (continued)

COG Functional	Protein name	Uniprot ID	Organism	Normalized Spectrum Counts LCFA	PA	ST	OL
Translation, ribosomal structure and biogenesis					0	6	1
	Elongation factor Tu	A9WFP3	*Chloroflexus aurantiacus*		0	1	0
	Elongation factor Tu	Q30X13	*Desulfovibrio desulfuricans*		0	1	1
	30S ribosomal protein S3	A5GAX1	*Geobacter uraniireducens*		0	2	0
	Elongation factor Tu	C4RXU4	*Yersinia bercovieri*		0	2	0
Transcription					10	9	2
	DNA-binding protein	D3A9W0	*Clostridium hathewayi*		10	9	2
Amino acid transport and metabolism					5	3	1
	Extracellular ligand-binding receptor	D1Y3L3	*Pyramidobacter piscolens*		0	0	1
	Nitrogen regulatory protein P-II	A1APM4	*Pelobacter propionicus*		1	0	0
	Extracellular ligand-binding receptor	A0LMX6	*Syntrophobacter fumaroxidans*		2	1	0
	Extracellular solute-binding protein, family 3	A0LQ70	*Syntrophobacter fumaroxidans*		0	1	0
	Ketol-acid reductoisomerase	D7AKA6	*Geobacter sulfurreducens*		2	1	0
Lipid transport and metabolismo					11	17	10
	Acetyl-coenzyme A synthetase	A3WRD2	*Nitrobacter sp.*		0	2	0
	Carboxyl transferase	A0LHL3	*Syntrophobacter fumaroxidans*		4	6	1
	Glutaconate CoA-transferase	A0LHC3	*Syntrophobacter fumaroxidans*		5	4	6
	Acyl CoA:acetate/3-ketoacid CoA transferase, alpha subunit	A5D0L9	*Pelotomaculum thermopropionicum*		1	4	3
Carbohydrate transport and metabolismo					5	3	2
	Enolase	Q3A578	*Pelobacter carbinolicus*		0	1	0
	Maltoporin	A0KHF6	*Aeromonas hydrophila*		0	0	1
	Pyruvate, phosphate dikinase	B1BIK5	*Clostridium perfringens C*		2	1	0
	Glyceraldehyde-3-phosphate dehydrogenase, type I	A5ZG57	*Bacteroides caccae*		1	0	1
	Pyruvate phosphate dikinase	A4YPR5	*Bradyrhizobium sp.*		2	2	0
	Enolase	E8MZM0	*Anaerolinea thermophila*		0	0	1
Coenzyme transport and metabolismo					0	1	0
	Bifunctional protein FolD	B5E7X9	*Geobacter bemidjiensis*		0	1	0

Table S6.5 (continued)

COG Functional	Protein name	Uniprot ID	Organism	Normalized Spectrum Counts LCFA	PA	ST	OL
Inorganic ion transport and metabolism					0	1	0
	Catalase-peroxidase	C6CDP7	*Dickeya dadantii*		0	1	0
Secondary metabolites biosynthesis, transport and catabolism					0	0	4
	Microcompartments protein	E4RM95	*Halanaerobium hydrogeniformans*		0	0	4
Cell wall/membrane/envelope biogenesis					0	0	1
	Omp38 protein	Q7X589	*Aeromonas veronii*		0	0	1
General function prediction only					15	12	3
	UPF0109 protein Sfum_2998	A0LMM0	*Syntrophobacter fumaroxidans*		1	2	0
	RNA-binding protein Hfq	A1AT91	*Pelobacter propionicus*		3	2	2
	ACT domain protein	A0LIW7	*Syntrophobacter fumaroxidans*		1	2	2
	Molybdopterin oxidoreductase Fe4S4 region	A0LJ81	*Syntrophobacter fumaroxidans*		1	1	0
	Molybdopterin oxidoreductase Fe4S4 region	A0LE81	*Syntrophobacter fumaroxidans*		9	4	0
No COG					4	1	3
	Putative uncharacterized protein	A0LJ30	*Syntrophobacter fumaroxidans*		1	0	0
	Selenoprotein B, glycine/betaine/sarcosine/D-proline reductase family	D5EG29	*Aminobacterium colombiense*		3	1	3

Table S6.6 List of primers used in Chapter 6.

Application	Primer	Sequence (5'–3')	Reference
PCR for ARISA (*Bacteria*)	ITSF	GTC GTA ACA AGG TAG CCG TA	Cardinale et al 2004
PCR for ARISA (*Bacteria*)	ITSR	GCC AAG GCA TCC ACC	Cardinale et al 2004
PCR for ARISA (*Archaea*)	1389F	CTT GCA CAC ACC GCC CGT C	Loy et al 2010
PCR for ARISA (*Archaea*)	71R	TCG CAG CTT RSC ACG YCC TTC	García-Martínez and Rodríguez-Valera 2000
Pyrosequencing (*Bacteria*)	28F	GAG TTT GAT CNT GGC TCA G	Liesack et al 1991
Pyrosequencing (*Bacteria*)	519R	TCT CAG GTN TTA CNG CGG CKG CTG	Handl et al 2011
Pyrosequencing (*Archaea*)	Arch349F	GYG CAS CAG KCG MGA AW	Takai and Horikoshi 2000
Pyrosequencing (*Archaea*)	Arch806R	GGA CTA CVS GGG TAT CTA AT	Takai and Horikoshi 2000

Chapter 7

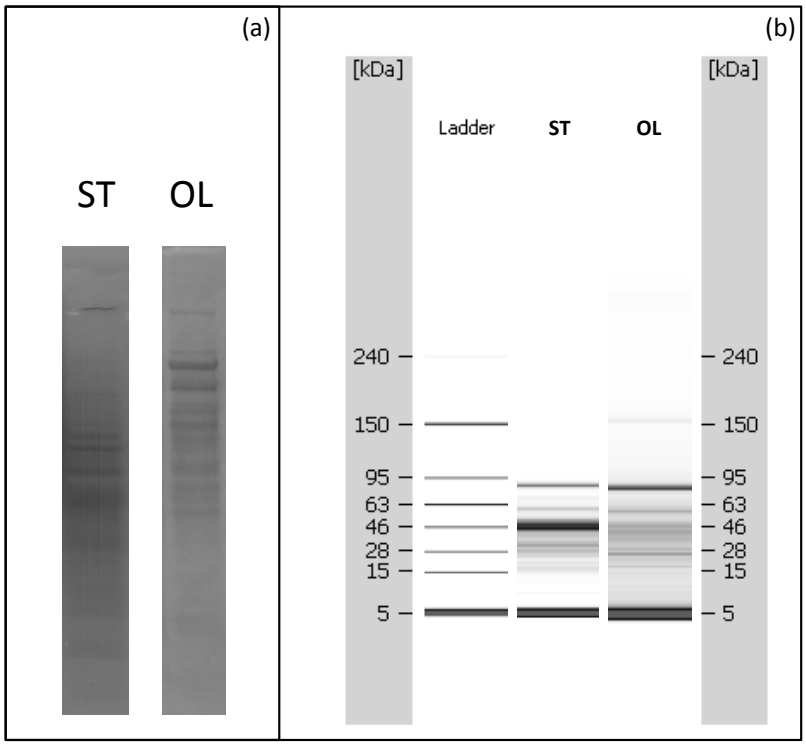

Figure S7.1 Protein profiles obtained by SDS-PAGE (a) and with Agilent 2100 Bioanalyzer (High Sensitivity Protein 250 Kit) (b) for proteins extracted from the co-culture of *S. zehnderi* growing on stearate (ST) and oleate (OL).

Table S7.1 List of proteins from *Methanobacterium formicicum* DSM 1535 in Uniprot database.

Protein	Uniprot ID
Formate dehydrogenase subunit alpha (EC 1.2.1.2)	P06131
Formate dehydrogenase subunit beta (EC 1.2.1.2)	P06130
Probable formate transporter	P35839
Glyceraldehyde-3-phosphate dehydrogenase (GAPDH) (EC 1.2.1.59)	P19315
Archaeal histone A1	P48782
Archaeal histone A2	P48783
Archaeal histone B	P48784
Methyl-coenzyme M reductase II alpha subunit (Fragment)	Q977F7
Methyl coenzyme M reductase (Fragment)	A4UNW7
Methyl-coenzyme M reductase alpha subunit (Fragment)	D2KZW8
Methyl-coenzyme M reductase II alpha subunit (Fragment)	D2KZX6
Methyl coenzyme M reductase (Fragment)	I7FEW7
Methyl coenzyme M reductase (Fragment)	A4UNX2
Methyl-coenzyme M reductase alpha subunit (Fragment)	Q977F8
Formate dehydrogenase (Fragment)	Q49167

Table S7.2 Identification and functional assignment of proteins assigned to *Methanobacterium* genus when the co-culture was incubated with stearate (ST) and oleate (OL).

				Number of assigned spectra	
COG	**Protein name**	**Uniprot ID**	**Organism**	**LCFA**	**OL**	**ST**
Energy production and conversion					596	343
	Formate dehydrogenase subunit alpha (EC 1.2.1.2)	P06131	*Methanobacterium formicicum*		35	13
	Formate dehydrogenase subunit beta (EC 1.2.1.2)	P06130	*Methanobacterium formicicum*		25	16
	Acetyl-CoA decarbonylase/synthase complex subunit gamma	K2RSU4	*Methanobacterium formicicum* DSM 3637		3	5
	V-type ATP synthase alpha chain (EC 3.6.3.14) (V-ATPase subunit A)	K2RBU1	*Methanobacterium formicicum* DSM 3637		14	7
	V-type ATP synthase beta chain (V-ATPase subunit B)	K2QZQ5	*Methanobacterium formicicum* DSM 3637		19	14
	Acetyl-CoA decarbonylase/synthase complex subunit alpha (EC 1.2.99.2)	K2RSU0	*Methanobacterium formicicum* DSM 3637		3	5
	V-type proton ATPase subunit E (V-ATPase subunit E)	K2R3I4	*Methanobacterium formicicum* DSM 3637		5	1
	Hydroxylamine reductase (EC 1.7.-.-) (Hybrid-cluster protein)	K2RTI3	*Methanobacterium formicicum* DSM 3637		2	9
	V-type ATP synthase subunit D (V-ATPase subunit D)	K2R3H7	*Methanobacterium formicicum* DSM 3637		8	5
	Rubrerythrin	K2RDI2	*Methanobacterium formicicum* DSM 3637		2	1
	Succinyl-CoA ligase [ADP-forming] subunit beta (EC 6.2.1.5)	K2R0S6	*Methanobacterium formicicum* DSM 3637		2	3
	Coenzyme F420-reducing hydrogenase subunit beta (EC 1.12.98.1)	K2R2M8	*Methanobacterium formicicum* DSM 3637		11	7
	NADH ubiquinone oxidoreductase 20 kDa subunit	K2RAQ4	*Methanobacterium formicicum* DSM 3637		11	6
	Acetyl-CoA decarbonylase/synthase complex subunit delta	K2RBZ2	*Methanobacterium formicicum* DSM 3637		3	2
	Methyl viologen-reducing hydrogenase subunit alpha	K2RRN3	*Methanobacterium formicicum* DSM 3637		41	46
	Pyruvate synthase	K2RT08	*Methanobacterium formicicum* DSM 3637		7	4
	Archaeoflavoprotein AfpA	K2RTG9	*Methanobacterium formicicum* DSM 3637		3	0
	5,10-methylenetetrahydromethanopterin reductase (EC 1.5.99.11)	K2R3X9	*Methanobacterium formicicum* DSM 3637		78	23
	Pyruvate ferredoxin oxidoreductase subunit beta	K2RC51	*Methanobacterium formicicum* DSM 3637		3	2
	Hydrogen dehydrogenase	K2QWH1	*Methanobacterium formicicum* DSM 3637		5	8
	NADH ubiquinone oxidoreductase 20 kDa subunit	K2QAU8	*Methanobacterium formicicum* DSM 3637		1	2
	Archaeoflavoprotein AfpA	K2RBN6	*Methanobacterium formicicum* DSM 3637		5	0
	Formylmethanofuran--tetrahydromethanopterin formyltransferase (EC 2.3.1.101)	K2R2E3	*Methanobacterium formicicum* DSM 3637		4	2
	NADH ubiquinone oxidoreductase 20 kDa subunit	K2R2B6	*Methanobacterium formicicum* DSM 3637		2	2
	NADH ubiquinone oxidoreductase 20 kDa subunit	K2R8L1	*Methanobacterium formicicum* DSM 3637		2	0
	Digeranylgeranylglycerophospholipid reductase (DGGGPL reductase) (EC 1.3.1.-)	K2QF23	*Methanobacterium formicicum* DSM 3637		0	2
	4Fe-4S ferredoxin	K2R6I7	*Methanobacterium formicicum* DSM 3637		43	32
	Coenzyme F420 hydrogenase subunit gamma	K2REI5	*Methanobacterium formicicum* DSM 3637		13	7
	Coenzyme F420-reducing hydrogenase subunit delta	K2RVK3	*Methanobacterium formicicum* DSM 3637		3	2
	Methyl-viologen-reducing hydrogenase subunit delta	K2QYN3	*Methanobacterium formicicum* DSM 3637		9	3
	Pyruvate ferredoxin oxidoreductase subunit gamma/delta	K2R3V7	*Methanobacterium formicicum* DSM 3637		6	5
	Acetyl-CoA decarbonylase/synthase complex subunit epsilon	K2QCS7	*Methanobacterium formicicum* DSM 3637		6	0
	Cob/CoM heterodisulfide reductase subunit C	K2RTF5	*Methanobacterium formicicum* DSM 3637		11	3
	4Fe-4S ferredoxin	K2QBS9	*Methanobacterium formicicum* DSM 3637		4	2
	F420-dependent methylenetetrahydromethanopterin dehydrogenase (EC 1.5.99.9)	K2R351	*Methanobacterium formicicum* DSM 3637		19	11
	Coenzyme F420 hydrogenase subunit alpha	K2QFA9	*Methanobacterium formicicum* DSM 3637		6	15
	2-oxoglutarate ferredoxin oxidoreductase subunit gamma (EC 1.2.7.3)	K2R4J0	*Methanobacterium formicicum* DSM 3637		6	2

Cob/CoM heterodisulfide reductase subunit B	K2RCN2	*Methanobacterium formicicum* DSM 3637	9	3
Formylmethanofuran dehydrogenase subunit A	F0T788	*Methanobacterium* sp. (strain AL-21)	2	3
Formylmethanofuran/tetrahydromethanopterin N-formyltransferase (EC 2.3.1.101)	F0T892	*Methanobacterium* sp. (strain AL-21)	4	0
V-type proton ATPase subunit E (V-ATPase subunit E)	F0T964	*Methanobacterium* sp. (strain AL-21)	3	2
Malate dehydrogenase (EC 1.1.1.37)	F0TA07	*Methanobacterium* sp. (strain AL-21)	2	0
CoB/CoM heterodisulfide reductase, subunit B (EC 1.8.98.1)	F0TAS6	*Methanobacterium* sp. (strain AL-21)	8	0
Formylmethanofuran dehydrogenase subunit C (EC 1.2.99.5)	F0T787	*Methanobacterium* sp. (strain AL-21)	3	2
5,10-methylenetetrahydromethanopterin reductase (EC 1.5.99.11)	F0T9L4	*Methanobacterium* sp. (strain AL-21)	50	17
4Fe-4S ferredoxin iron-sulfur binding domain-containing protein	F0T7S9	*Methanobacterium* sp. (strain AL-21)	19	20
V-type ATP synthase beta chain (V-ATPase subunit B)	F6D6U4	*Methanobacterium* sp. (strain SWAN-1)	13	9
CoB/CoM heterodisulfide reductase, subunit B (EC 1.8.98.1)	F6D1T9	*Methanobacterium* sp. (strain SWAN-1))	5	0
Archaeal glutamate synthase [NADPH] (EC 1.4.1.13)	F6D4E0	*Methanobacterium* sp. (strain SWAN-1)	0	3
5,10-methylenetetrahydromethanopterin reductase (EC 1.5.99.11)	F6D5U5	*Methanobacterium* sp. (strain SWAN-1)	58	17
Posttranslational modification, protein turnover, chaperones			163	105
ATPase AAA	K2QBV6	*Methanobacterium formicicum* DSM 3637	3	1
Uncharacterized protein	K2QF40	*Methanobacterium formicicum* DSM 3637	4	3
Chaperone protein DnaK (HSP70)	K2R6B2	*Methanobacterium formicicum* DSM 3637	29	27
Proteasome subunit beta (EC 3.4.25.1)	K2R289	*Methanobacterium formicicum* DSM 3637	8	8
ABC transporter	K2R2I4	*Methanobacterium formicicum* DSM 3637	5	3
Cobalamin synthesis protein P47K	K2R1Q9	*Methanobacterium formicicum* DSM 3637	3	2
Proteasome subunit alpha (EC 3.4.25.1) (20S proteasome alpha subunit)	K2R2T6	*Methanobacterium formicicum* DSM 3637	9	1
ABC transporter subunit Ycf24	K2QBS7	*Methanobacterium formicicum* DSM 3637	3	3
Cyclophilin type peptidyl-prolyl cis-trans isomerase	K2QFR6	*Methanobacterium formicicum* DSM 3637	2	0
Heat shock protein Hsp20	K2QCG1	*Methanobacterium formicicum* DSM 3637	2	3
Proteasome-activating nucleotidase (PAN) (Proteasomal ATPase)	K2RQX0	*Methanobacterium formicicum* DSM 3637	6	3
Hydrogenase nickel incorporation protein HypB	K2QXV0	*Methanobacterium formicicum* DSM 3637	4	8
Thermosome	K2QA50	*Methanobacterium formicicum* DSM 3637	30	12
AiR synthase-like protein domain-containing protein	K2RW71	*Methanobacterium formicicum* DSM 3637	2	0
Peptidyl-prolyl cis-trans isomerase	K2QWB3	*Methanobacterium formicicum* DSM 3637	10	5
Thermosome	K2QAH8	*Methanobacterium formicicum* DSM 3637	8	3
SufBD protein	F0T8S6	*Methanobacterium* sp. (strain AL-21)	2	2
Thermosome	F6D7T2	*Methanobacterium* sp. (strain SWAN-1)	33	21
Translation, ribosomal structure and biogenesis			235	153
Elongation factor 2 (EF-2)	K2RCU5	*Methanobacterium formicicum* DSM 3637	41	42
Histidine--tRNA ligase (EC 6.1.1.21) (Histidyl-tRNA synthetase)	K2RRY1	*Methanobacterium formicicum* DSM 3637	1	2
RNA-associated protein	K2QZ08	*Methanobacterium formicicum* DSM 3637	3	0
Glycyl-tRNA ligase (EC 6.1.1.14)	K2Q9Q5	*Methanobacterium formicicum* DSM 3637	1	2
Elongation factor 1-alpha (EF-1-alpha) (Elongation factor Tu)	K2RTM7	*Methanobacterium formicicum* DSM 3637	50	15
Translation initiation factor 2 subunit gamma (aIF2-gamma) (eIF-2-gamma)	K2RRW4	*Methanobacterium formicicum* DSM 3637	0	3
30S ribosomal protein S6e	K2QBZ5	*Methanobacterium formicicum* DSM 3637	3	0
Alanine--tRNA ligase (EC 6.1.1.7) (Alanyl-tRNA synthetase)	K2QY04	*Methanobacterium formicicum* DSM 3637	0	2
Probable exosome complex RNA-binding protein 1	K2RB40	*Methanobacterium formicicum* DSM 3637	4	5
50S ribosomal protein L6P	K2R086	*Methanobacterium formicicum* DSM 3637	5	5
Phenylalanine--tRNA ligase beta subunit (EC 6.1.1.20)	K2RUI1	*Methanobacterium formicicum* DSM 3637	2	4

30S ribosomal protein S11P	K2R401	*Methanobacterium formicicum* DSM 3637	8	3
50S ribosomal protein L11P	K2RA32	*Methanobacterium formicicum* DSM 3637	8	1
30S ribosomal protein S12	K2R4K4	*Methanobacterium formicicum* DSM 3637	11	3
30S ribosomal protein S10	K2QDP1	*Methanobacterium formicicum* DSM 3637	4	1
Acidic ribosomal protein P0 homolog (L10E)	K2QB40	*Methanobacterium formicicum* DSM 3637	3	1
30S ribosomal protein S3Ae	K2QB71	*Methanobacterium formicicum* DSM 3637	11	1
Aspartate--tRNA ligase (EC 6.1.1.12) (Aspartyl-tRNA synthetase)	K2R9F2	*Methanobacterium formicicum* DSM 3637	4	8
30S ribosomal protein S8	K2RCC4	*Methanobacterium formicicum* DSM 3637	3	3
RNA-binding protein	K2R2Q1	*Methanobacterium formicicum* DSM 3637	3	2
30S ribosomal protein S5	K2RCC0	*Methanobacterium formicicum* DSM 3637	6	5
30S ribosomal protein S2	K2R061	*Methanobacterium formicicum* DSM 3637	4	5
Protein translation factor SUI1 homolog	K2R420	*Methanobacterium formicicum* DSM 3637	2	0
30S ribosomal protein S4e	K2R415	*Methanobacterium formicicum* DSM 3637	3	2
Probable exosome complex exonuclease 1 (EC 3.1.13.-)	K2RS08	*Methanobacterium formicicum* DSM 3637	6	1
30S ribosomal protein S27e	K2REJ5	*Methanobacterium formicicum* DSM 3637	2	5
50S ribosomal protein L12P	K2R1S1	*Methanobacterium formicicum* DSM 3637	3	1
Glutamyl-tRNA(Gln) amidotransferase subunit A (Glu-ADT subunit A) (EC 6.3.5.-)	K2RW62	*Methanobacterium formicicum* DSM 3637	2	0
Ribosomal protein S11P	F0TBA7	*Methanobacterium* sp. (strain AL-21)	8	4
50S ribosomal protein L14P	F0TB85	*Methanobacterium* sp. (strain AL-21)	4	0
Elongation factor 1-alpha (EF-1-alpha) (Elongation factor Tu)	F0T6G8	*Methanobacterium* sp. (strain AL-21)	11	3
Elongation factor 2 (EF-2)	F6D1Z5	*Methanobacterium* sp. (strain SWAN-1)	16	19
30S ribosomal protein S2	F6D7A9	*Methanobacterium* sp. (strain SWAN-1)	3	5
Nucleotide transport and metabolism			48	35
Probable deoxycytidine triphosphate deaminase (dCTP deaminase) (EC 3.5.4.13)	K2R0H7	*Methanobacterium formicicum* DSM 3637	5	2
Nucleoside diphosphate kinase (NDK) (NDP kinase) (EC 2.7.4.6)	K2QYV5	*Methanobacterium formicicum* DSM 3637	5	2
Adenylosuccinate synthetase (AMPSase) (AdSS) (EC 6.3.4.4)	K2RC98	*Methanobacterium formicicum* DSM 3637	4	5
Adenylate kinase (AK) (EC 2.7.4.3) (ATP-AMP transphosphorylase)	K2RT60	*Methanobacterium formicicum* DSM 3637	5	1
CTP synthase (EC 6.3.4.2) (CTP synthetase) (UTP--ammonia ligase)	K2RQK4	*Methanobacterium formicicum* DSM 3637	0	3
DUTP diphosphatase	K2QBU9	*Methanobacterium formicicum* DSM 3637	2	0
Inosine-5'-monophosphate dehydrogenase (EC 1.1.1.205)	K2R5I3	*Methanobacterium formicicum* DSM 3637	7	5
Amidophosphoribosyltransferase (ATase) (EC 2.4.2.14)	K2QDY5	*Methanobacterium formicicum* DSM 3637	0	2
Phosphoribosylformylglycinamidine synthase 1 (EC 6.3.5.3)	K2RSD3	*Methanobacterium formicicum* DSM 3637	4	0
Phosphoribosylformylglycinamidine synthase 2 (EC 6.3.5.3)	K2RVU5	*Methanobacterium formicicum* DSM 3637	4	4
Anaerobic ribonucleoside-triphosphate reductase	K2R3C8	*Methanobacterium formicicum* DSM 3637	0	2
PyrE-like protein	K2QE46	*Methanobacterium formicicum* DSM 3637	9	6
Phosphoribosylformylglycinamidine synthase 1 (EC 6.3.5.3)	F0TBZ3	*Methanobacterium* sp. (strain AL-21)	3	1
CTP synthase (EC 6.3.4.2) (CTP synthetase) (UTP--ammonia ligase)	F6D3R6	*Methanobacterium* sp. (strain SWAN-1)	0	2
Transcription			58	32
AAA ATPase	K2R140	*Methanobacterium formicicum* DSM 3637	14	4
Transcriptional regulator	K2QYI1	*Methanobacterium formicicum* DSM 3637	4	1
Cupin	K2R0N3	*Methanobacterium formicicum* DSM 3637	2	0
DNA-directed RNA polymerase subunit A'' (EC 2.7.7.6)	K2RCU3	*Methanobacterium formicicum* DSM 3637	7	5
Putative signal transduction protein with CBS domains	K2QWZ8	*Methanobacterium formicicum* DSM 3637	2	0
Putative snRNP Sm-like protein	K2RD75	*Methanobacterium formicicum* DSM 3637	3	1

DNA-directed RNA polymerase subunit E (EC 2.7.7.6)	K2R2P8	*Methanobacterium formicicum* DSM 3637	2	0
Transcription elongation factor NusA-like protein	K2QDN6	*Methanobacterium formicicum* DSM 3637	2	2
DNA-directed RNA polymerase subunit B (EC 2.7.7.6)	K2QDN1	*Methanobacterium formicicum* DSM 3637	2	0
TATA-box-binding protein (Box A-binding protein)	K2R153	*Methanobacterium formicicum* DSM 3637	13	12
DNA-directed RNA polymerase subunit D (EC 2.7.7.6)	K2QD35	*Methanobacterium formicicum* DSM 3637	0	2
Transcription antitermination protein NusG	K2QXZ9	*Methanobacterium formicicum* DSM 3637	4	1
Transcription initiation factor IIB (TFIIB)	F0T642	*Methanobacterium* sp. (strain AL-21)	1	2
DNA-directed RNA polymerase (EC 2.7.7.6)	F6D1Y9	*Methanobacterium* sp. (strain SWAN-1)	2	2
Amino acid transport and metabolism			66	49
Threonine synthase (EC 4.2.3.1)	K2RRX2	*Methanobacterium formicicum* DSM 3637	5	1
4-hydroxy-tetrahydrodipicolinate reductase (HTPA reductase) (EC 1.17.1.-)	K2R951	*Methanobacterium formicicum* DSM 3637	3	2
Glutamine synthetase (EC 6.3.1.2)	K2QGC0	*Methanobacterium formicicum* DSM 3637	1	3
4-hydroxy-tetrahydrodipicolinate synthase (HTPA synthase) (EC 4.3.3.7)	K2RQ09	*Methanobacterium formicicum* DSM 3637	2	0
Serine--pyruvate transaminase	K2QBV4	*Methanobacterium formicicum* DSM 3637	9	4
Aspartokinase (EC 2.7.2.4)	K2QA54	*Methanobacterium formicicum* DSM 3637	3	0
Acetylornithine aminotransferase (ACOAT) (EC 2.6.1.11)	K2R308	*Methanobacterium formicicum* DSM 3637	2	0
Ketol-acid reductoisomerase (EC 1.1.1.86)	K2RW18	*Methanobacterium formicicum* DSM 3637	1	2
Arginine biosynthesis bifunctional protein ArgJ	K2QEI4	*Methanobacterium formicicum* DSM 3637	3	2
Cysteine synthase A	K2QAS2	*Methanobacterium formicicum* DSM 3637	0	2
Archaeal glutamate synthase [NADPH] (EC 1.4.1.13)	K2QYS6	*Methanobacterium formicicum* DSM 3637	1	4
Tryptophan synthase beta chain (EC 4.2.1.20)	K2RTW1	*Methanobacterium formicicum* DSM 3637	0	2
Argininosuccinate synthase (EC 6.3.4.5) (Citrulline--aspartate ligase)	K2QF10	*Methanobacterium formicicum* DSM 3637	4	2
3-isopropylmalate dehydratase small subunit (EC 4.2.1.33)	K2R6I1	*Methanobacterium formicicum* DSM 3637	4	5
Acetolactate synthase (EC 2.2.1.6)	K2R6X5	*Methanobacterium formicicum* DSM 3637	2	3
3-dehydroquinate synthase (DHQ synthase) (EC 1.4.1.24)	K2QAG2	*Methanobacterium formicicum* DSM 3637	4	0
Putative (R)-citramalate synthase CimA (EC 2.3.1.182)	K2RDA4	*Methanobacterium formicicum* DSM 3637	2	0
Archaeal glutamate synthase [NADPH] (EC 1.4.1.13)	K2R2B2	*Methanobacterium formicicum* DSM 3637	3	2
LL-diaminopimelate aminotransferase (DAP-AT) (EC 2.6.1.83)	K2R1V5	*Methanobacterium formicicum* DSM 3637	0	2
Glutamyl-tRNA(Gln) amidotransferase subunit D (EC 6.3.5.-)	K2R4F4	*Methanobacterium formicicum* DSM 3637	0	2
Serine hydroxymethyltransferase (SHMT) (Serine methylase) (EC 2.1.2.-)	K2R2T1	*Methanobacterium formicicum* DSM 3637	0	2
Carbamoyl-phosphate synthase large chain (EC 6.3.5.5)	K2QB20	*Methanobacterium formicicum* DSM 3637	2	0
S-adenosylmethionine synthase (AdoMet synthase) (EC 2.5.1.6)	K2R2X0	*Methanobacterium formicicum* DSM 3637	8	4
Glutamate decarboxylase	K2R3X6	*Methanobacterium formicicum* DSM 3637	1	2
Carbamoyl-phosphate synthase large chain (EC 6.3.5.5)	F0TCQ2	*Methanobacterium* sp. (strain AL-21)	4	2
Arginine biosynthesis bifunctional protein ArgJ	F6D694	*Methanobacterium* sp. (strain SWAN-1)	2	1
Lipid transport and metabolism			33	17
Pyruvate carboxylase subunit A (EC 6.4.1.1)	K2R0A4	*Methanobacterium formicicum* DSM 3637	1	3
UPF0219 protein A994_11482	K2QX31	*Methanobacterium formicicum* DSM 3637	13	5
Acetate/CoA ligase	K2RQD8	*Methanobacterium formicicum* DSM 3637	1	2
Uncharacterized protein	K2R158	*Methanobacterium formicicum* DSM 3637	2	1
Acetyl-CoA acetyltransferase (EC 2.3.1.9)	K2R947	*Methanobacterium formicicum* DSM 3637	8	2
Myo-inositol-1-phosphate synthase	F0T927	*Methanobacterium* sp. (strain AL-21)	2	2
Methanogenesis marker protein 15	F0TAR3	*Methanobacterium* sp. (strain AL-21)	3	0
Propanoyl-CoA C-acyltransferase (EC 2.3.1.176)	F6D254	*Methanobacterium* sp. (strain SWAN-1)	3	2

Carbohydrate transport and metabolism			34	16
Triosephosphate isomerase (TIM) (EC 5.3.1.1)	K2R0T1	*Methanobacterium formicicum* DSM 3637	2	2
Fructose-1,6-bisphosphatase	K2RAW4	*Methanobacterium formicicum* DSM 3637	6	1
Enolase (EC 4.2.1.11) (2-phospho-D-glycerate hydro-lyase)	K2RT51	*Methanobacterium formicicum* DSM 3637	5	4
Cellulase	K2R9L8	*Methanobacterium formicicum* DSM 3637	5	2
Glyceraldehyde-3-phosphate dehydrogenase (GAPDH) (EC 1.2.1.59)	K2R1B6	*Methanobacterium formicicum* DSM 3637	4	2
Bifunctional phosphomannomutase/phosphoglucomutase (EC 5.4.2.2)	K2R0M8	*Methanobacterium formicicum* DSM 3637	3	2
Phosphoglycerate kinase (EC 2.7.2.3)	K2RCT9	*Methanobacterium formicicum* DSM 3637	2	0
Fructose-bisphosphate aldolase (EC 4.1.2.13)	K2R160	*Methanobacterium formicicum* DSM 3637	5	3
Putative uncharacterized protein	F0TA10	*Methanobacterium* sp. (strain AL-21)	2	0
Defense mechanisms			10	2
ABC transporter	K2QXZ3	*Methanobacterium formicicum* DSM 3637	3	0
Phosphonate-transporting ATPase	K2QC42	*Methanobacterium formicicum* DSM 3637	7	2
Coenzyme transport and metabolism			225	185
Coenzyme F390 synthetase II	K2QED7	*Methanobacterium formicicum* DSM 3637	0	3
Methyl-coenzyme M reductase operon protein D	K2R615	*Methanobacterium formicicum* DSM 3637	2	0
Ribose 1,5-bisphosphate isomerase (EC 5.3.1.n2)	K2QAU0	*Methanobacterium formicicum* DSM 3637	0	2
Methyl-coenzyme M reductase I, subunit beta	K2RAN9	*Methanobacterium formicicum* DSM 3637	38	30
Methyl coenzyme M reductase I subunit alpha	K2QYM4	*Methanobacterium formicicum* DSM 3637	19	19
Adenosylhomocysteinase (EC 3.3.1.1) (S-adenosyl-L-homocysteine hydrolase)	K2RD34	*Methanobacterium formicicum* DSM 3637	1	2
D-3-phosphoglycerate dehydrogenase	K2RBW4	*Methanobacterium formicicum* DSM 3637	4	3
Phosphomethylpyrimidine synthase (EC 4.1.99.17)	K2RWC1	*Methanobacterium formicicum* DSM 3637	5	5
Pyridoxal biosynthesis lyase PdxS (EC 4.-.-.-)	K2QBW6	*Methanobacterium formicicum* DSM 3637	4	0
Uroporphyrin-III C-methyltransferase (EC 2.1.1.107)	K2RBJ6	*Methanobacterium formicicum* DSM 3637	2	0
Methyl-coenzyme M reductase subunit beta	K2QF15	*Methanobacterium formicicum* DSM 3637	29	27
Methyl-coenzyme M reductase operon protein D	K2RRL7	*Methanobacterium formicicum* DSM 3637	3	1
Methyl-coenzyme M reductase subunit gamma	K2R2D4	*Methanobacterium formicicum* DSM 3637	5	2
3,4-dihydroxy-2-butanone 4-phosphate synthase	K2R714	*Methanobacterium formicicum* DSM 3637	2	1
Tetrahydromethanopterin S-methyltransferase subunit E (EC 2.1.1.86)	K2RAP2	*Methanobacterium formicicum* DSM 3637	4	0
3-octaprenyl-4-hydroxybenzoate carboxy-lyase	K2R5H9	*Methanobacterium formicicum* DSM 3637	3	2
Methenyltetrahydromethanopterin cyclohydrolase (EC 3.5.4.27)	K2RQT5	*Methanobacterium formicicum* DSM 3637	12	6
Methyl coenzyme M reductase I subunit gamma	K2R2H1	*Methanobacterium formicicum* DSM 3637	6	0
Tetrahydromethanopterin S-methyltransferase subunit H (EC 2.1.1.86)	K2QBS0	*Methanobacterium formicicum* DSM 3637	12	10
Methyl-coenzyme M reductase subunit alpha	K2REA7	*Methanobacterium formicicum* DSM 3637	22	28
Methyl-coenzyme M reductase alpha subunit (Fragment)	D2KZW8	*Methanobacterium formicicum*	23	13
Methyl-coenzyme M reductase II alpha subunit (Fragment)	D2KZX6	*Methanobacterium formicicum*	18	29
Uroporphyrin-III C-methyltransferase (EC 2.1.1.107)	F0TBZ4	*Methanobacterium* sp. (strain AL-21)	2	0
Methyl-coenzyme M reductase, beta subunit (EC 2.8.4.1)	F6D2D7	*Methanobacterium* sp. (strain SWAN-1)	9	2
Cell wall/membrane/envelope biogenesis			6	5
Glutamine--fructose-6-phosphate aminotransferase [isomerizing] (EC 2.6.1.16)	K2QWN8	*Methanobacterium formicicum* DSM 3637	0	3
UTP-glucose-1-phosphate uridylyltransferase	K2RD62	*Methanobacterium formicicum* DSM 3637	2	1
dTDP-glucose 4,6-dehydratase	K2QDX9	*Methanobacterium formicicum* DSM 3637	4	1
Inorganic ion transport and metabolism			8	4

Ferritin	K2RDP5	*Methanobacterium formicicum* DSM 3637	2	0
Superoxide dismutase (EC 1.15.1.1)	K2R5G7	*Methanobacterium formicicum* DSM 3637	2	0
Phosphate ABC transporter ATP-binding protein	K2QCV3	*Methanobacterium formicicum* DSM 3637	2	2
Phosphate binding protein	K2R3R6	*Methanobacterium formicicum* DSM 3637	2	2
Cell cycle control, cell division, chromosome partitioning			35	16
Cell division protein FtsZ	K2QB36	*Methanobacterium formicicum* DSM 3637	9	6
Rod shape-determining protein MreB	K2QDL2	*Methanobacterium formicicum* DSM 3637	19	7
Cell shape determining protein MreB/Mrl	F0T6K9	*Methanobacterium* sp. (strain AL-21)	4	0
Site-determining protein	F0TAF5	*Methanobacterium* sp. (strain AL-21)	3	3
Signal transduction mechanisms			39	28
Signal transduction histidine kinase	K2R3L7	*Methanobacterium formicicum* DSM 3637	2	1
UspA domain-containing protein	K2QEE9	*Methanobacterium formicicum* DSM 3637	2	0
Circadian clock protein KaiC	K2R1C5	*Methanobacterium formicicum* DSM 3637	3	3
UspA domain-containing protein	K2QXY1	*Methanobacterium formicicum* DSM 3637	3	1
Phosphoenolpyruvate synthase (EC 2.7.9.2)	K2RSE0	*Methanobacterium formicicum* DSM 3637	22	18
Phosphoenolpyruvate synthase (EC 2.7.9.2)	F0T910	*Methanobacterium* sp. (strain AL-21)	3	1
Phosphoenolpyruvate synthase (EC 2.7.9.2)	F6D1W5	*Methanobacterium* sp. (strain SWAN-1)	4	4
Intracellular trafficking, secretion, and vesicular transport			3	3
Type ii secretion system protein E	K2QZV1	*Methanobacterium formicicum* DSM 3637	3	3
Replication, recombination and repair			47	22
MCM family protein	K2QYN6	*Methanobacterium formicicum* DSM 3637	0	3
UPF0095 protein A994_10158	K2R1Y1	*Methanobacterium formicicum* DSM 3637	12	6
Replication factor-A domain-containing protein	K2RVQ2	*Methanobacterium formicicum* DSM 3637	5	5
UvrABC system protein A (UvrA protein) (Excinuclease ABC subunit A)	K2QXK5	*Methanobacterium formicicum* DSM 3637	2	1
DNA repair and recombination protein RadA	K2QFI0	*Methanobacterium formicicum* DSM 3637	16	2
DNA polymerase sliding clamp (Proliferating cell nuclear antigen homolog)	K2R6E3	*Methanobacterium formicicum* DSM 3637	5	2
DNA repair and recombination protein RadA	F0T7T1	*Methanobacterium* sp. (strain AL-21)	4	2
Replication factor C small subunit (RFC small subunit)	F0TAD6	*Methanobacterium* sp. (strain AL-21)	3	1
Chromatin structure and dynamics			7	1
Archaeal histone A1	P48782	*Methanobacterium formicicum*	4	1
Transcription factor CBF/NF-Y/histone domain-containing protein	K2RQ61	*Methanobacterium formicicum* DSM 3637	3	0
General function prediction only			117	61
Beta-lactamase domain-containing protein	K2R057	*Methanobacterium formicicum* DSM 3637	2	2
Flavodoxin/nitric oxide synthase	K2R6S0	*Methanobacterium formicicum* DSM 3637	12	3
TOPRIM domain-containing protein	K2R511	*Methanobacterium formicicum* DSM 3637	6	1
Amino acid-binding ACT domain-containing protein	K2R8P4	*Methanobacterium formicicum* DSM 3637	3	1
Peptidase U62 modulator of DNA gyrase	K2QXB6	*Methanobacterium formicicum* DSM 3637	3	0
Phosphonate-transporting ATPase	K2R1S4	*Methanobacterium formicicum* DSM 3637	2	2
Uncharacterized protein	K2RBE1	*Methanobacterium formicicum* DSM 3637	2	2
CBS domain-containing membrane protein	K2RE52	*Methanobacterium formicicum* DSM 3637	2	1
NADPH-dependent F420 reductase	K2RRX7	*Methanobacterium formicicum* DSM 3637	2	0
Oxidoreductase domain-containing protein	K2RUC7	*Methanobacterium formicicum* DSM 3637	2	2
Probable L-aspartate dehydrogenase (EC 1.4.1.21)	K2R3L3	*Methanobacterium formicicum* DSM 3637	3	1
Putative signal transduction protein with CBS domains	K2RV17	*Methanobacterium formicicum* DSM 3637	14	3

RNA-processing protein	K2QDZ9	*Methanobacterium formicicum* DSM 3637	3	0
Amino acid-binding ACT domain-containing protein	K2RUL8	*Methanobacterium formicicum* DSM 3637	4	0
Radical SAM domain-containing protein	K2R998	*Methanobacterium formicicum* DSM 3637	0	8
Tryptophan synthase beta chain (EC 4.2.1.20)	K2R358	*Methanobacterium formicicum* DSM 3637	5	9
Methionine--tRNA ligase (EC 6.1.1.10) (Methionyl-tRNA synthetase)	K2RQB5	*Methanobacterium formicicum* DSM 3637	0	4
Uncharacterized protein	K2QFG2	*Methanobacterium formicicum* DSM 3637	3	0
Amino acid-binding ACT domain-containing protein	K2R290	*Methanobacterium formicicum* DSM 3637	3	1
Signal transduction protein with CBS domains	K2RA15	*Methanobacterium formicicum* DSM 3637	5	1
NIL domain-containing protein	K2QAC5	*Methanobacterium formicicum* DSM 3637	2	0
Pyridoxamine 5'-phosphate oxidase-like FMN-binding protein	K2QXU7	*Methanobacterium formicicum* DSM 3637	2	1
Thioesterase	K2Q9U2	*Methanobacterium formicicum* DSM 3637	3	2
Methyl coenzyme M reductase system, component A2	K2RBQ2	*Methanobacterium formicicum* DSM 3637	5	1
Roadblock/LC7 family protein	K2R8M5	*Methanobacterium formicicum* DSM 3637	3	0
Radical SAM domain-containing protein	K2QC15	*Methanobacterium formicicum* DSM 3637	2	1
Pyridoxamine 5'-phosphate oxidase-related FMN-binding protein	K2R248	*Methanobacterium formicicum* DSM 3637	4	1
Deoxyribonuclease/rho motif-related TRAM	K2QX04	*Methanobacterium formicicum* DSM 3637	5	3
Pyridoxamine 5'-phosphate oxidase-like FMN-binding protein	K2QAS9	*Methanobacterium formicicum* DSM 3637	4	0
Cyclic 2,3-diphosphoglycerate synthetase (cDPGS) (EC 6.5.-.-)	K2R171	*Methanobacterium formicicum* DSM 3637	1	2
KH-domain/beta-lactamase-domain-containing protein	K2QBJ4	*Methanobacterium formicicum* DSM 3637	0	3
Methyl coenzyme M reductase system, component A2 (EC 3.6.3.17)	F0T6L8	*Methanobacterium* sp. (strain AL-21)	6	4
Flavodoxin/nitric oxide synthase	F6D5Y7	*Methanobacterium* sp. (strain SWAN-1)	4	0
KH-domain/beta-lactamase-domain protein	F6D2X7	*Methanobacterium* sp. (strain SWAN-1)	0	2
Function unknown			58	18
PRC-barrel domain-containing protein	K2QZT1	*Methanobacterium formicicum* DSM 3637	4	1
Uncharacterized protein	K2RRN0	*Methanobacterium formicicum* DSM 3637	10	1
Uncharacterized protein	K2RPI6	*Methanobacterium formicicum* DSM 3637	2	1
Uncharacterized protein	K2QCM5	*Methanobacterium formicicum* DSM 3637	4	2
Uncharacterized protein	K2RTJ8	*Methanobacterium formicicum* DSM 3637	3	0
UPF0145 protein A994_06900	K2QZS6	*Methanobacterium formicicum* DSM 3637	11	2
Bifunctional enzyme fae/hps	K2R6Z7	*Methanobacterium formicicum* DSM 3637	5	4
Uncharacterized protein	K2R9W2	*Methanobacterium formicicum* DSM 3637	2	1
LemA family protein	K2RF48	*Methanobacterium formicicum* DSM 3637	2	2
UPF0264 protein A994_03308	K2R1T3	*Methanobacterium formicicum* DSM 3637	3	0
Sporulation protein YtfJ	K2RQ65	*Methanobacterium formicicum* DSM 3637	4	0
UPF0145 protein A994_05310	K2R1H2	*Methanobacterium formicicum* DSM 3637	4	0
Uncharacterized protein	K2RAU4	*Methanobacterium formicicum* DSM 3637	0	2
Putative uncharacterized protein	F6D3S0	*Methanobacterium* sp. (strain SWAN-1)	2	0
Putative uncharacterized protein	F6D7X0	*Methanobacterium* sp. (strain SWAN-1)	2	2
No COG			12	9
Uncharacterized protein	K2RPH4	*Methanobacterium formicicum* DSM 3637	6	2
Uncharacterized protein	K2QYT1	*Methanobacterium formicicum* DSM 3637	1	3
Uncharacterized protein	K2Q9P0	*Methanobacterium formicicum* DSM 3637	2	1
Uncharacterized protein	K2R0E9	*Methanobacterium formicicum* DSM 3637	2	1
Molybdopterin dinucleotide-binding region	F6D826	*Methanobacterium* sp. (strain SWAN-1)	1	2